



HAL
open science

Magnetic latex particles for bionanotechnology and biosensors

Talha Jamshaid

► **To cite this version:**

Talha Jamshaid. Magnetic latex particles for bionanotechnology and biosensors. Biotechnology. Université de Lyon, 2016. English. NNT : 2016LYSE1061 . tel-01430413

HAL Id: tel-01430413

<https://theses.hal.science/tel-01430413>

Submitted on 9 Jan 2017

HAL is a multi-disciplinary open access archive for the deposit and dissemination of scientific research documents, whether they are published or not. The documents may come from teaching and research institutions in France or abroad, or from public or private research centers.

L'archive ouverte pluridisciplinaire **HAL**, est destinée au dépôt et à la diffusion de documents scientifiques de niveau recherche, publiés ou non, émanant des établissements d'enseignement et de recherche français ou étrangers, des laboratoires publics ou privés.



N°d'ordre NNT : 2016LYSE1061

THESE de DOCTORAT DE L'UNIVERSITE DE LYON

Opérée au sein de
L'Université Claude Bernard Lyon 1

Ecole Doctorale N° ED 206
Ecole Doctorale de Chimie

Spécialité de doctorat : Biotechnologie et Pharmacotechnie

Soutenue publiquement le 24/05/2016, par :

Talha Jamshaid

Synthèse de latex magnétique submicronique et fonctionnalisé pour application
en Biocapteur

Devant le jury composé de :

Saidi Salima	Professeur	Université d'Oran	Rapporteur
Carbonnier Benjamin	Professeur	Université Paris-Es	Rapporteur
Laayoun Ali	Chercheur	BioMérieux,S.A Grenoble	Examineur
Chehimi Mohamed Mehdi	DR-CNRS	Université Paris-Est	Examineur
Briançon Stéphanie	Professeur	Université Lyon-1	Examinatrice
Elaissari, Abdelhamid	DR-CNRS	Université Lyon-1	Directeur de thèse
Errachid El-Salhi Abdelhamid	Professeur	ISA,Université Lyon-1	Co-directeur de thèse

UNIVERSITE CLAUDE BERNARD - LYON 1

Président de l'Université

Vice-président du Conseil d'Administration

Vice-président du Conseil des Etudes et de la Vie Universitaire

Vice-président du Conseil Scientifique

Directeur Général des Services

M. François-Noël GILLY

M. le Professeur Hamda BEN HADID

M. le Professeur Philippe LALLE

M. le Professeur Germain GILLET

M. Alain HELLEU

COMPOSANTES SANTE

Faculté de Médecine Lyon Est – Claude Bernard

Faculté de Médecine et de Maïeutique Lyon Sud – Charles
Mérieux

Faculté d'Odontologie

Institut des Sciences Pharmaceutiques et Biologiques

Institut des Sciences et Techniques de la Réadaptation

Département de formation et Centre de Recherche en Biologie
Humaine

Directeur : M. le Professeur J. ETIENNE

Directeur : Mme la Professeure C. BURILLON

Directeur : M. le Professeur D. BOURGEOIS

Directeur : Mme la Professeure C. VINCIGUERRA

Directeur : M. le Professeur Y. MATILLON

Directeur : Mme. la Professeure A-M. SCHOTT

COMPOSANTES ET DEPARTEMENTS DE SCIENCES ET TECHNOLOGIE

Faculté des Sciences et Technologies

Département Biologie

Département Chimie Biochimie

Département GEP

Département Informatique

Département Mathématiques

Département Mécanique

Département Physique

UFR Sciences et Techniques des Activités Physiques et Sportives

Observatoire des Sciences de l'Univers de Lyon

Polytech Lyon

Ecole Supérieure de Chimie Physique Electronique

Institut Universitaire de Technologie de Lyon 1

Ecole Supérieure du Professorat et de l'Education

Institut de Science Financière et d'Assurances

Directeur : M. F. DE MARCHI

Directeur : M. le Professeur F. FLEURY

Directeur : Mme Caroline FELIX

Directeur : M. Hassan HAMMOURI

Directeur : M. le Professeur S. AKKOUCHE

Directeur : M. le Professeur Georges TOMANOV

Directeur : M. le Professeur H. BEN HADID

Directeur : M. Jean-Claude PLENET

Directeur : M. Y. VANPOULLE

Directeur : M. B. GUIDERDONI

Directeur : M. P. FOURNIER

Directeur : M. G. PIGNAULT

Directeur : M. le Professeur C. VITON

Directeur : M. le Professeur A. MOUGNIOTTE

Directeur : M. N. LEBOISNE

Acknowledgements

First of all I am very thankful to my God who gives me this opportunity to achieve the desired goal. I would like to express my special appreciation and thanks to my supervisor **Dr. Abdelhamid Elaissari** *director of research at CNRS, vice director of LAGEP at Lyon, France and editor-in-chief of JOURNAL OF COLLOID SCIENCE AND BIOTECHNOLOGY*. He has been a tremendous mentor for me. I would like to thank you for encouraging my research and for allowing me to grow as a research scientist. His advices, on both researches as well as on my personal life have been priceless. I appreciate all his contributions regarding his precious time, ideas, and personal support to make my PhD experience productive and stimulating. The joy and enthusiasm he has for his research was contagious and motivational for me, even during tough times in the PhD pursuit. He is someone you will instantly love and never forget once you meet him. He's the funniest advisor and one of the smartest people I know. I hope that I could be as lively, enthusiastic, and energetic as Dr. Abdelhamid Elaissari. In addition to our academic collaboration, I greatly value the close personal rapport that he and I have forged over the years. And also I will not forget for whole my life at time when I was ill and he treated me more than like a father. I am also extremely indebted to my guide my **co-supervisor Professor Abdel Hamid Errachid El-Salhi** *full professor* at the University Claude Bernard-Lyon 1 and *head of the Micro/Nanotechnology group*, who provided me all necessary infrastructure and resources to accomplish my research work in his lab under his kind supervision and guidance. I would also like to thank Dr **Nadia Zine** who came time to time in my lab and guide me side by side.

I would like to thank some of my senior brothers which guided me from early days of my research period. Mohamed Eissa associate professor in Polymers Department, National Research Centre, Giza, Egypt, Ahmed Bitar ,Abdoullatif Baraket, Karim Miladi and Naveed Ahamed who encouraged me a lot for doing this research goal.

I appreciate the prompt response from technical engineering staff that assists me to solve my technical problems. I am grateful to Nadia Chapel (secretary to our lab's director) and Garrigues Olivier as my computer administrator for his cooperation in different administrative works and computer problems, also thanks to Geraldine Agusti for her kinds help regarding to TEM and TGA characterizations.

It's my fortune to gratefully acknowledge the support of Muhammad Ahasan Bashir for his support, generous care and the homely feeling at Lyon. He was always beside me during the happy and hard moments to push me and motivate me.

Last but not the least, I would like to thank my parents who raised me, supported me, taught me, and loved me. I would also like to thank my younger brother **Usama Jamsaid** who supported me in time of difficulties and encouraged me time to time.

I would also like to thanks my beloved wife **Nadiyah Zafar**, who took care of me in time of bad situations and helped me side by side. My deepest gratitude to the compassion extended by my mother-in-law, father-in-law and sister-in-law, who supported me throughout this journey.

I thank to my God and my good father **professor Dr.Muhammad Jamshaid** , for letting me through all the difficulties and my mother **Riffat Jamshaid** who

prayed all time to reach this goal. I have experienced your guidance day by day. You are the one who let me finish my degree. I will keep on trusting you for my future. Thanks to you dear father. To him I dedicate this thesis. Finally, I would like to thank my only paternal aunt, ***Tasneem Bibi***, who sacrificed her life for developing and building a good family. Her supportive, encouraging, patience and unconditional love and encouragement generously paved the way for development as a researcher family. We are all proud of her. God bless her and her family Ameen!. At end, I am thankful to *University of Lahore, Pakistan* for providing scholarship to complete my PhD goal.

Talha Jamshaid
Université Claude Bernard Lyon 1

France

Résumé

L'objectif de ce travail de recherche est de remplacer les procédés longs et fastidieux comme la filtration et la centrifugation qui sont généralement utilisées dans le diagnostic biomédical *in-vitro* par l'utilisation de particules de latex magnétique. Ces particules magnétiques après fonctionnalisation sont également utilisées non seulement comme support de biomolécules, mais aussi pour améliorer le signal lors d'utilisation en biocapteurs.

Les particules de latex magnétiques et submicroniques en taille sont préparées en utilisant une émulsion huile (ferrofluide organique) dans l'eau. La réalisation d'une étude systématique en fonction de la composition chimique (ratio styrène/ divinylbenzène, nature chimique d'amorceur) a conduit aux conditions d'obtention de particules à cœur magnétique et écorce polymère (morphologie core-shell). La fonctionnalisation de ces particules a été réalisée en utilisant soit un amorceur de polymérisation fonctionnel 4, 4'-azobis acide cyanopentanoïque (ACPA) ou à l'utilisation d'un monomère fonctionnel comme l'acide méthacrylique. Ces particules de latex magnétiques sont utilisées par la suite comme support de biomolécules chimiquement greffées.

Ces particules de latex magnétiques sont utilisées comme support de biomolécules après greffage sur un substrat aminé pour la détection de l'Ochratoxine A qui existe dans les produits alimentaires séchés. La détection a été mise en évidence en utilisant des anticorps anti-Ochratoxine A fluorescents. Les particules magnétiques sensibilisées par l'anticorps (Ab155) spécifique à l'antigène (SA2BSA) sont également utilisées pour augmenter la sensibilité du biocapteur spécifique à l'antigène préalablement greffé à la surface d'un substrat en Or.

TABLE OF CONTENTS

I.	General Introduction	1
II.	Bibliography	8
II.1.	Ferrofluids: From Preparation to Biomedical Applications	11
II.2.	Soft Hybrid Nanoparticles: from Preparation to Biomedical Application	30
II.3.	Characterization methodologies TGA and Magnetization	63
II.4.	Magnetic particles: From preparation to lab-on-a-chip, biosensor microsystems And microfluidics applications	76
III.	Experimental Part	99
III.1	Elaboration of submicron hybrid magnetic latex particles	102
III.2	Carboxylic magnetic latex particles and enhancement with Methacrylic acid	112
III.3	Ochratoxin A detection with Carboxylic magnetic latex particles	124
III.4	Magneto-biosensor for Sulfaperidine detection	144
IV.	Discussion and Conclusion	156
V.	Perspective	160
VI.	Publications	163

PART I
GENERAL INTRODUCTION

General Introduction and AIM

Nanotechnology is the scientific study of particles of a substance at the scale of one billionth of a meter (i.e., 10^{-9} m = 1 nm). In principle, it is the scientific discipline which deals with matter at the atomic and molecular levels. With the passage of time, nanotechnology has introduced several diversified fundamental and applied aspects, such as nanobiotechnology, bionanotechnology, surface-enhanced Raman scattering (SERS), quantum dots and applied microbiology, in materials science and engineering¹. Nanoparticle is a nano-sized entity which may be crystalline (a nanocrystal), amorphous or non-crystalline array (a cluster, such as a fullerene)². It is the integral component in the manufacture of a nanostructure. It is more infinitesimal than ordinary objects that are governed by Newton's laws of motion; however, larger than atoms or simple molecules that follow quantum mechanics. A nanoparticle is any sort of particle with at least one dimension less than 500 nm. Nanoparticles profoundly affect a number of areas encompassing pharmaceuticals, advanced materials, environmental detection and monitoring etc.

In general, nanoparticles can be categorized into two groups as engineered or nonengineered. Engineered nanoparticles are deliberately designed and manufactured with specific physical characteristics aimed to cater the requirements of particular applications. Such nanoparticles can be the end products of themselves, as in the case of pharmaceuticals or quantum dots, or they can be the substances later incorporated into other separate end products such as carbon black in rubber products. In any way, the physical characteristics of nanoparticles are of utmost significance to their performance and the working of any other product into which they are finally incorporated. In converse, nonengineered nanoparticles are naturally generated particles, for example, atmospheric nanoparticles created during combustion. Physical properties also have a significant role in the case of nonengineered nanoparticles as they determine whether or not ill effects will appear as a consequence of the existence of these nanoparticles. On the basis of application of interest, nanoparticles may possess several alternate and commercial names such as particulate matter, aerosols, colloids, nanocomposites, nanopowders and nanoceramics. On the basis of biomedical applications, nanoparticles can be grouped as organic and inorganic. Both of these classes include biodegradable and non-biodegradable nanoparticles. For instance, biodegradable organic nanoparticles consist of micelles, liposomes, lipid nanoparticles, polymeric nanoparticles etc. On the other hand, non-biodegradable organic nanoparticles consist of polymeric substances such as poly (styrene), poly (ethylene), poly (methyl methacrylate), polyamides etc. Likewise, biodegradable inorganic nanoparticles consist of iron oxide, magnetism, zinc oxide, calcium phosphate etc. while non-biodegradable inorganic nanoparticles consist of carbon nanotubes, quantum dots, gold, silver, nickel, aluminum, talc, cerium oxide, copper, manganese, bismuth and titanium etc. Nanoparticles have performed a substantial role in drug delivery, imaging, tissue engineering, detoxification and theranostics^{1,3}.

Colloidal particles offer very convenient diagnostic solutions, with consistent results through effective screening approaches for numerous maladies. These encompass cell sorting, immunoassay, nucleic acid capturing and detection etc⁴. During the last ten years, several colloidal particles have been fabricated and extensively investigated for medical purposes⁵. For instance, colloidal particles containing different functional groups, such as sulfhydryl

group (–SH), amine group (–NH₂), carboxylic group (–COOH) etc., and dendrimers have been developed to covalently bind biomolecules in order to be employed as a solid support for the specific capture of targets and imaging. This has enabled incorporation of diverse functionalities as well. Even though various types of particles have been embraced for their potential aptness in biomedical science, yet the most alluring of them are the hybrid particles containing both the magnetic attributes and the capability to functionalize with important functional groups on drug molecules and biomolecules. Such a functional colloidal particle usually reveals soft hybrid core-shell morphology, which is engineered in such a fashion that the core is made up of an inorganic substance whereas the peripheral shell consists of a soft organic material⁶. Moreover, gold nanoparticles can capture light over a broad spectral range, from the visible to near-infrared, and can be employed for diagnosis as optically tuneable carriers because of their shape and size⁷. Hybrid nanoparticles carry both organic and inorganic moieties simultaneously. They also exhibit interesting optical, magnetic and mechanical features^{8, 9}. Several techniques such as adsorption of polymers on colloidal particles¹⁰, adsorption of polymers via layer-by-layer self-assembly¹¹, adsorption of nanoparticles on colloidal particles¹², chemical grafting of preformed polymers¹³, polymerization from and on to colloidal particles¹³, click chemistry¹⁴, atomic-transfer radical polymerization (ATRP)¹⁵, reversible addition-fragmentation chain-transfer radical (RAFT) polymerization¹⁶, nitroxide-mediated polymerization (NMP)¹⁷ and conventional seed radical polymerization¹⁸ have been established for the fabrication and characterization of soft hybrid core-shell colloidal particles.

Since the last decade, magnetic nanoparticles (superparamagnetism) have played an imperative role in *in-vitro* and in *in-vivo* biomedical science. Synthetic methodologies, such as separation of iron salts from aqueous solutions by precipitation, thermal decomposition of iron precursors in organic or aqueous media and water-in-oil (w/o) microemulsion, have been engaged for the development of homogenous and monodisperse superparamagnetic iron oxide nanoparticles (SPION). In particular, magnetic colloidal particles have contributed remarkable applications in a number of biomedical and therapeutic diagnostic applications. These particles are employed as solid support for biomolecules such as bacteria, viruses etc. in order to improve the sensitivity of *in-vitro* biomedical diagnosis¹⁹.

On the basis of magnetic particles, bionanotechnology has various promising applications. In the past, magnetic particles have been exploited for their outstanding applications in different fields such as controlled drug delivery, catalysis, nucleic acid isolation, imaging, bacteria and viruses detection, sensing and targeted drug delivery, magnetic resonance imaging, cell sorting, recognition of fluorescent antibody, specific bacteria and viruses separation, determination of titer of nucleic acid, as a vaccine carrier and *in-vitro* diagnosis. The utilization of colloidal particles as a solid support demands several tedious and time consuming isolation techniques such as filtration and centrifugation which hinder the automation of diagnostic procedures resulting in prolonged diagnosis. On the other hand, magnetic particles provide advantage by circumventing these problems. The chief advantage provided by magnetic particles is associated with quick particle isolation upon applying even low magnetic field²⁰. Thus, the magnetic particles facilitate the process of automation, thereby, lessening time delays.

Now-a-days, the key emphasis in biomedical diagnosis is to improve the specificity and sensitivity and to minimize time consumption. One way to achieve this goal is to increase the

concentration of captured targets such as antigen, viruses, bacteria and nucleic acid prior to the detection step. In the previous decades, magnetic latex nanoparticles have been grabbing enormous attention owing to their superparamagnetic characteristics originating from their nano-sizes²¹. They have contributed several outstanding applications in different industrial and biomedical diagnostic fields, for instance, rapid separation upon applying even low magnetic field, purification and detection of biomolecules etc²⁰. A number of methodologies have been put forward for the fabrication of magnetic latex particles for diagnostic purposes. These methods are based on classical polymerization in dispersed media like emulsion²², suspension²³, miniemulsion²⁴, dispersion²⁵, combination of different polymer-based process²⁶ and inverse emulsion²⁷; however, all these techniques lead to unwanted limitations such as low magnetic content, heterogeneous distribution of magnetic nanoparticles, low magnetic separation under magnetic field etc²⁴. The pioneer work regarding the preparation of magnetic latexes and their use for biomedical diagnostic purposes was coined by Ugelstad²⁸. Recently, Montage et al²¹ has reported a process for obtaining highly magnetic submicron magnetic latex particles. This process is called seed emulsion polymerization. Previously, magnetic latex particles have been employed for capturing of biological samples, for nucleic acid extraction and purification, specific antigen detection, in monitoring of protein adsorption and desorption²⁹.

Microfluidic systems are devices that deal with sub-Nano liter volumes of fluids³⁰. These devices possess reduced dimensions and together with colloids play an important role in the development of monodispersed colloidal particles in a continuous mode³¹. Microfluidic reactors are employed for the formation of nanoparticles. The flow process has an important role in these devices. This flow can be regulated by the application of force motion of colloidal micro particles in micro-channel. Regarding biology of human body, the molecular events play a significant role in biomedical diagnosis³² which can be accomplished by executing various biological tests in specific laboratories. These tests involve multi-step and intricate processes, such as sample collection, preparation and specific identification of biomolecules, requiring both labor and prolonged duration.

In recent years, considerable advancement has been made in microfluidic technology. It possesses numerous promising applications in pharmaceutical industry, life science and chemical researches. It deals with miniaturization and combination of molecular-level biological tests into high-performance and ultrafine systems that can integrate miniaturized laboratory functions (such as separation and analysis of components of a mixture) on a single microprocessor chip using very minute fluid volumes from nanoliters to picoliters in an organized fashion. Based on microelectromechanical technology, microfluidic technology integrates and miniaturizes the separating reaction and mixing devices in general laboratories onto a very tiny chip called Lab-on-a-chip system also known as a micro-total-analytical system (μ TAS) or microfluidics device³³. These devices are very convenient due to their exclusive properties such as reduction of solvent, reduction of sample collection, improvement of mass and heat transfer owing to a high surface-to-volume ratio. These microdevices have certain merits, such as less time consumption, inexpensiveness and improved reproducibility, essential to routine biological samples³⁴.

Magnetic latex particles are generally used in microfluidics and for environmental content. Our aim is to investigate how these magnetic latex particles can be used to enhance sensitivity or how to functionalize surface of biosensor.

In order to target such objective our aim is to prepare submicron magnetic latex particles by using seed emulsion polymerization having magnetic core and polymer shell (core-shell) to protect iron oxide inside perfect polymer shell, with specific properties such as superparamagnetic in nature, high magnetic content, good colloidal stability, good chemical stability (there is no degradation of particles) and with almost narrow size distribution. Functionality of these particles was done with carboxylic groups for immunoassay.

This thesis is divided into two main parts. The first parts deals with the state of art or literature review. This literature survey is necessary to highlight in a comprehensive way. First review gives different preparation methodologies for ferrofluids and their applications in biomedical field. Second review gives information regarding development and preparation methods of soft hybrid particles especially their preparation with conventional seed radical polymerization and applications in biomedical field. Third review explains characterization properties to measure magnetic content and magnetization for magnetic hybrid particles. Fourth review provides the readers with encapsulation of magnetic particles, more interestingly their usage in lab-on-a-chip, microfluidics, microsystems and biosensors.

The second part of thesis deals with experimental studies. Firstly, different polymerization experiments are performed in order to get desired morphology with submicron magnetic latex particles. Secondly, functionalization and enhancement of these magnetic latex particles is done with carboxylic groups. Finally, these particles are used in biosensor to increase sensitivity and also for specific antibody detection.

References:

1. Aula, S. *et al.* Biophysical, biopharmaceutical and toxicological significance of biomedical nanoparticles. *RSC Adv.* **5**, 47830–47859 (2015).
2. Barnard, A. S. Modelling of nanoparticles: approaches to morphology and evolution. *Rep. Prog. Phys.* **73**, 086502 (2010).
3. Zafar, N., Fessi, H. & Elaissari, A. Colloidal particles containing labeling agents and cyclodextrins for theranostic applications. *Int. J. Pharm.* **472**, 118–129 (2014).
4. Gupta, A. K. & Gupta, M. Synthesis and surface engineering of iron oxide nanoparticles for biomedical applications. *Biomaterials* **26**, 3995–4021 (2005).
5. Mora-Huertas, C. E., Fessi, H. & Elaissari, A. Polymer-based nanocapsules for drug delivery. *Int. J. Pharm.* **385**, 113–142 (2010).
6. Hübner, E. *et al.* Synthesis of Polymer/Silica Hybrid Nanoparticles Using Anionic Polymerization Techniques. *Macromolecules* **43**, 856–867 (2010).
7. Loo, C., Lowery, A., Halas, N., West, J. & Drezek, R. Immunotargeted Nanoshells for Integrated Cancer Imaging and Therapy. *Nano Lett.* **5**, 709– 711 (2005).
8. Gravano, S. M., Dumas, R., Liu, K. & Patten, T. E. Methods for the surface functionalization of γ -Fe₂O₃ nanoparticles with initiators for atom transfer radical polymerization and the formation of core-shell inorganic-polymer structures. *J. Polym. Sci. Part Polym. Chem.* **43**, 3675–3688 (2005).
9. Bombalski, L., Dong, H., Listak, J., Matyjaszewsk, K. & Bockstaller, M. R. Null-Scattering Hybrid Particles Using Controlled Radical Polymerization. *Adv. Mater.*

- 19**, 4486–4490 (2007).
10. Bijsterbosch, H.D. Copolymer adsorption and the effect on colloidal stability
 11. Caruso, F. in *Colloid Chemistry II* (ed. Antonietti, P. D. M.) 14-168.
 12. Lansalot, M., Sabor, M., Elaissari, A. & Pichot, C. Elaboration of fluorescent and highly magnetic submicronic polymer particles via a stepwise heterocoagulation process. *Colloid Polym. Sci.* **283**, 1267–1277(2005).
 13. Charleux, B., D'Agosto, F. & Delaittre, G. in *Hybrid Latex Particles* (eds. Herk, A. M. van & Landfester, K.) 125–183 (Springer Berlin Heidelberg, 2010).
 14. Kolb, H. C., Finn, M. G. & Sharpless, K. B. Click Chemistry: Diverse Chemical Function from a Few Good Reactions. *Angew. Chem. Int. Ed.* **40**, 2004–2021 (2001).
 15. Von Werne, T. & Patten, T. E. Atom transfer radical polymerization from nanoparticles: a tool for the preparation of well-defined hybrid nanostructures and for understanding the chemistry of controlled/'living' radical polymerizations from surfaces. *J. Am. Chem. Soc.* **123**, 7497–7505 (2001).
 16. Moad, G., Rizzardo, E. & Thang, S. H. Radical addition–fragmentation chemistry in polymer synthesis. *Polymer* **49**, 1079–1131 (2008).
 17. Ladmiral, V., Morinaga, T., Ohno, K., Fukuda, T. & Tsujii, Y. Synthesis of monodisperse zinc sulfide particles grafted with concentrated polystyrene brush by surface-initiated nitroxide-mediated polymerization. *Eur. Polym. J.* **45**, 2788–2796 (2009).
 18. G. Pibre, L. Hakenholz, S. Braconnot, H. Mouaziz and A. Elaissari, *e-Polymers*, 2009, No. 139.
 19. Bitar, A. *et al.* Ferrofluids: From Preparation to Biomedical Applications. *J. Colloid Sci. Biotechnol.* **3**, 3–18 (2014).
 20. Elaissari, A. & Fessi, H. Reactive and Highly Submicron Magnetic Latexes for Bionanotechnology Applications. *Macromol. Symp.* **288**, 115–120 (2010).
 21. Montagne, F., Mondain-Monval, O., Pichot, C. & Elaissari, A. Highly magnetic latexes from submicrometer oil in water ferrofluid emulsions. *J. Polym. Sci. Part Polym. Chem.* **44**, 2642–2656 (2006).
 22. Yanase, N., Noguchi, H., Asakura, H. & Suzuta, T. Preparation of magnetic latex particles by emulsion polymerization of styrene in the presence of a ferrofluid. *J. Appl. Polym. Sci.* **50**, 765–776(1993).
 23. Daniel, J.-C., Schuppiser, J.-L. & deceased, M. T. Magnetic polymer latex and preparation process. (1982).
 24. Ramírez, L. P. & Landfester, K. Magnetic Polystyrene Nanoparticles with a High Magnetite Content Obtained by Miniemulsion Processes. *Macromol. Chem. Phys.* **204**, 22–31 (2003).
 25. Ding, X. B., Sun, Z. H., Wan, G. X. & Jiang, Y. Y. Preparation of thermosensitive magnetic particles by dispersion polymerization. *React. Funct. Polym.* **38**, 11–15 (1998).
 26. Elaissari, A. Magnetic Latex Particles in Nanobiotechnologies for Biomedical Diagnostic Applications: State of the Art. *Macromol. Symp.* **281**, 14–19 (2009).
 27. Dresco, P. A., Zaitsev, V. S., Gambino, R. J. & Chu, B. Preparation and Properties of Magnetite and Polymer Magnetite Nanoparticles. *Langmuir* **15**, 1945–1951 (1999).
 28. Ugelstad, J. *et al.* in *Molecular Interactions in Bioseparations* (ed. Ngo, T. T.) 229–244 (Springer US, 1993).
 29. Jamshaid, T. *et al.* in *Soft Nanoparticles for Biomedical Applications* (2014). at RSC.
 30. Minc, N. Microfluidic systems of self-assembled magnetic particles; application

- to DNA separation and protein digestion. *Houille Blanche-Rev. Int. Eau* 51–54 (2006).
31. Liu, Y., Hugentobler, C. P. & Shum, H. C. A Millifluidic Approach for Continuous Generation of Liquid Marbles. *J. Colloid Sci. Biotechnol.* **2**, 350– 354 (2013).
 32. Joo, J. *et al.* A facile and sensitive detection of pathogenic bacteria using magnetic nanoparticles and optical nanocrystal probes. *Analyst* **137**, 3609– 3612 (2012).
 33. Kuschel, M., Neumann, T., Barthmaier, P. & Kratzmeier, M. Use of lab-on- a-chip technology for protein sizing and quantitation. *J. Biomol. Tech. JBT* **13**, 172–178 (2002).
 34. Elaissari, A. *Colloidal Nanoparticles in Biotechnology*. (John Wiley & Sons, 2008).

PART II
BIBLIOGRAPHY

Introduction

In the past, colloidal particles have been utilized to furnish very useful diagnostic solutions and standardized results through effective screening methods for numerous diseases. Soft hybrid core-shell morphology bearing particles or hybrid particles are employed for optical examinations of biological interactions. Their other characteristics which affect these results considerably encompass super Para magnetism, fluorescence and biodegradability. A lot of techniques have been devised for the formation and characterization of soft hybrid core-shell colloidal particles. These include adsorption of polymers on colloidal particles, adsorption of polymers via layer-by-layer self-assembly, adsorption of nanoparticles on colloidal particles, chemical grafting of preformed polymers, polymerization from and on to colloidal particles, click chemistry, atomic-transfer radical polymerization (ATRP), reversible addition-fragmentation chain-transfer radical (RAFT) polymerization, nitroxide-mediated polymerization (NMP) and conventional seed radical. Soft hybrid nanoparticles have been fabricated to target specific biomedical applications and to accomplish required therapeutic or diagnostic functions. Since the last decade, a number of colloidal particles have been fabricated and thoroughly studied for medical purpose. Magnetically responsive hybrid iron oxide colloidal nanoparticles have super paramagnetic features and are extensively employed in bio-imaging to deliver high diagnostic accuracy in the detection of atherosclerosis, cancer, arthritis and various diseases.

On the basis of magnetic particles, bionanotechnology has various promising applications. In the past, magnetic particles have been exploited for their outstanding applications in different fields such as controlled drug delivery, catalysis, nucleic acid isolation, imaging, bacteria and viruses detection, sensing and targeted drug delivery, magnetic resonance imaging, cell sorting, recognition of fluorescent antibody, specific bacteria and viruses separation, determination of titer of nucleic acid, as a vaccine carrier and *in-vitro* diagnosis. The utilization of colloidal particles as a solid support demands several tedious and time consuming isolation techniques such as filtration and centrifugation which hinder the automation of diagnostic procedures resulting in prolonged diagnosis. On the other hand, magnetic particles provide advantage by circumventing these problems. The chief advantage provided by magnetic particles is associated with quick particle isolation upon applying even low magnetic field. Thus, the magnetic particles facilitate the process of automation, thereby, lessening time delays.

Now-a-days, the key importance in biomedical diagnosis is to improve the specificity and sensitivity and to reduce time consumption. One way to reach this goal is to increase the titer of captured targets such as antigen, viruses, bacteria and nucleic acid prior to the detection step. In the previous decades, magnetic latex nanoparticles (MNPs) have been grabbing enormous attention owing to their superparamagnetic characteristics originating from their nano-sizes. They have contributed several outstanding applications in different industrial and biomedical diagnostic fields, for instance, rapid separation upon applying even low magnetic field, purification and detection of biomolecules etc.

In recent years, considerable advancement has been made in microfluidic technology. It deals with miniaturization and combination of molecular-level biological tests into high-

Performance and ultrafine systems that can integrate miniaturized laboratory functions (such as separation and analysis of components of a mixture) on a single microprocessor chip using very minute fluid volumes from nanoliters to picoliters in an organized fashion. Based on microelectromechanical technology, microfluidic technology integrates and miniaturizes the separating reaction and mixing devices in general laboratories onto a very tiny chip called Lab-on-a-chip system also known as a micro-total-analytical system (microTAS) or microfluidics device. These devices are very convenient due to their exclusive properties such as reduction of solvent, reduction of sample collection, improvement of mass and heat transfer owing to a high surface-to-volume ratio. These microdevices have certain merits, such as less time consumption, inexpensiveness and improved reproducibility, essential to routine biological samples.

A number of methodologies have been put forward for the fabrication of magnetic latex particles for diagnostic purposes. These methods are based on classical polymerization in dispersed media like emulsion, suspension, miniemulsion, dispersion, combination of different polymer-based process and inverse emulsion; however, all these techniques lead to unwanted limitations such as low magnetic content, heterogenous distribution of magnetic nanoparticles, low magnetic separation under magnetic field etc. Submicron magnetic latex particles containing magnetic core and polymeric shell are obtained by forming a magnetic emulsion which is subsequently used as a seed in the process called seed emulsion polymerization. For rapid separation and biomedical applications, magnetic latex nanoparticles with high saturation magnetization are necessary; therefore, high magnetic content is desired. The magnetic latex particles have narrow size distribution (homogeneous) and provide high specific area for immobilization of large amount of biomolecules. These particles furnish surface functionality for covalent grafting of biomolecules and high iron oxide (super paramagnetic) content for rapid separation under applied magnetic field. The morphology of these magnetic latex nanoparticles significantly determines their ultimate utilization. The core-shell structure of the colloidal magnetic nanoparticles is the most appropriate for biomedical diagnosis. This morphology also prevents from modification of their biological properties. Surface modification or attachment of specific functional groups like sulfate, carboxyl, amine and hydroxyl is required to diversely utilize magnetic particles as carrier of biomolecules (e.g. antibody, antigen, virus, bacteria, etc.) and then to design a Lab-on-Chip system using the same magnetic latex particles and consequently exploring the immobilization of antibodies for diagnostic uses. Magnetic latex particles are employed efficiently as carrier of biomolecules in microsystem.

CHAPTER II.1

Ferrofluids: From Preparation to Biomedical Applications

Summary

Ferrofluids are stable magnetic dispersions comprised of ferromagnetic nanoparticles with approximately 10nm size dispersed in aqueous or organic medium. Preparation of these particles is performed at two levels that is synthesis of magnetic nanoparticles and their subsequent dispersion in aqueous or organic medium. The stabilization of ferromagnetic particles is done by two methods; either by using polymer or surfactant or by creating charges on surface of nanoparticles. The magnetization properties are related directly to their composition. In general, metallic particles at nanometric size range have a long range of magnetostatic interaction causing their agglomeration and sedimentation and hence necessitating their stabilization as described above. Currently, ferrofluids are available for various applications like magnetic inks, paints, and also in biomedical applications.

The preparation of ferrofluids involves maghemite and magnetite. Several methods have been used for their preparation include size reduction, chemical synthesis (co-precipitation, thermal decomposition and microemulsion methods) electrodecomposition techniques, evaporation of metal in liquids and carrier liquid exchange. Size reduction and Chemical Synthesis methods are frequently employed.

Properties of ferrofluids are a crucial area for their ultimate use in applications. Ferrites are iron oxides having spine type crystal structure. The crystallographic structure of the maghemite is identical to that of magnetite with the exception of certain deformities associated with oxidation reduction. Mossbauer spectroscopy is thus proved to be a method of choice to identify exact nature of iron oxides.

Morphology, Size and Size Distribution Analysis is done by using atomic force microscopy (AFM), scanning electron microscopy (SEM) and transmission electron microscopy (TEM). Morphology and shape of particles mainly depend upon preparation process.

With regards to electrokinetic properties, being amphoteric in nature, iron oxides possess negative charge in basic medium while they are positive in acidic medium. Therefore, their state of dispersion depends on the surface charge density. Several ligands have been studied resulting in stable ferrofluids at different pH ranges. Apart from mechanism of stabilization at specific pH, their stability depends largely on the nature of ligand functional groups involved in complexation reaction.

Colloidal stability is achieved by surfactant or polymer modification of the magnetic nanoparticles. Magnetic properties also are important determinant for their applications. Magnetic nanoparticle's response to applied magnetic field depends on the size of particles (typically between 10-20nm depending on the material) as well as its state.

Surface Functionalization is based on two main techniques i.e. physical chemistry based approach and chemistry based process. Physical chemistry based approaches include surface

Immobilization and polymers adsorption, while the most widely used chemistry based approach is silica coating of iron oxide nanoparticles.

Magnetic ferrofluids have been successfully tried in numerous applications including their use in industry, magnetic inks, sealing, paints for recording tapes and recently in biomedical applications like magnetic resonance imaging (MRI), bio-separation, diagnostics and as carrier for cancer chemotherapeutic agents. The magnetic properties of ferrofluids have been widely exploited in data storage like tapes for audio visual recording, magnetic cards, data storage devices and informatics. Furthermore, Magnetic particles possessing good stability have a promising role in catalysis and biocatalysis assisting separation of catalysts, nuclear wastes and biochemical products. Biocatalytic process often requires the full recovery of catalyst to gain economic benefits and to avoid waste disposal. Ferrofluids have been successfully tried to achieve this goal.

Functionalization of ferrofluids with suitable functional group to avoid bio-incompatibility has opened new avenues in biomedical applications. Their quick response to magnetic field enables them to act as excellent separation and extraction markers. The interaction between particles and target molecules (biomolecules, cells, bacteria and viruses) that are sensitive to environmental conditions like pH, salinity, and temperature can help adsorb and desorb these molecules. On the same lines, nucleic acids can be separated and extracted using ferrofluids making them excellent candidates in diagnostics possessing rapidity, sensitivity and sensibility. Ferrofluids have also been successfully employed as contrast agents for MRI. This application requires not only biosafety of nanoparticles but also their functionalization with specific target such as an antibody. Recent studies suggest their effectiveness in achieving these marks.

Hyperthermia using nanotechnology based nanoparticles has attracted significant attention recently in cancer therapy. Cancer is treated through magnetic field modulated cell membrane damage exploiting ferrofluids that emit heat upon exposure to altering external magnetic field. The produced heat can effectively kill cancer cell and spares the neighboring normal cells, a feature very much desired in cancer therapy. In cancer therapy, obtaining high specific loss power (SLP) is a necessity to ensure effectiveness of therapy and an area for further exploration. Significant work is required to address this hot area of research. Very recently, magnetic emulsions (a new form of ferrofluids) have been developed that hold great promise in further biomedical applications.



Ferrofluids: From Preparation to Biomedical Applications

Ahmad Bitar¹, Chariya Kaewsaneha^{1,2}, Mohamed M. Eissa^{1,4,*}, Talha Jamshaid¹,
Pramuan Tangboriboonrat², Duangporn Polpanich³, and Abdelhamid Elaissari¹

¹Université de Lyon, F-69622, Lyon, France; Université Lyon1, Villeurbanne, CNRS, UMR 5007,
Laboratoire d'Automatique et de Génie des Procédés, LAGEP-CPE-308G,
43 bd. 5 du 11 Nov.1918, F-69622, Villeurbanne, France

²Department of Chemistry, Faculty of Science, Mahidol University, Phyathai, Bangkok 10400, Thailand

³National Nanotechnology Center (NANOTEC), Thailand Science Park, PathumThani 12120, Thailand

⁴Polymers and Pigments Department, National Research Centre, Dokki, Giza 12622, Egypt

Discovery of the magnetic property (superparamagnetism) of ferrofluid (i.e., magnetic fluid) and its effects on the other materials open wide varieties of applications in human daily life. Continually, new applications require different forms of magnetic materials, which have significant attractions nowadays. This review highlights the ferrofluids synthesis methods. All known methods are cited, and a special interest is focused on the most commonly used methods for preparation, which depends on size reduction and chemical co-precipitation. Furthermore, the industrial and biomedical applications of ferrofluids and their based particles are discussed. Finally, the new water based dispersed ferrofluids particles “magnetic emulsion” is also introduced.

Keywords: Magnetic Nanoparticles, Ferrofluid, Synthesis, Applications.

Delivered by Publishing Technology to: University of Lyon-1
IP: 134.214.70.27 On: Tue, 04 Nov 2014 14:58:35
Copyright: American Scientific Publishers

CONTENTS

1. Introduction	3
2. Preparation Methods	5
2.1. Physical Based Method (Size Reduction)	6
2.2. Chemistry Based Processes	6
3. Properties	7
3.1. Chemical Structure Analysis (X-Ray, Mössbauer)	8
3.2. Morphology, Size and Size Distribution Analysis	9
3.3. Electrokinetic Properties	9
3.4. Colloidal Stability	10
3.5. Magnetic Properties	10
4. Surface Functionalization	11
4.1. Physical Chemistry Based Processes	11
4.2. Chemistry Based Approaches	12
5. Applications	12
5.1. Industrial Applications	12
5.2. Biocatalysis	13
5.3. Biomedical Applications	14
6. Conclusion	16
Acknowledgment	16
References and Notes	16

1. INTRODUCTION

Magnetization or magnetic susceptibility is a value which indicates the magnetization degree of a magnetic material under the effect of an external magnetic field. The material response to magnetic field depends on its size

meaning that there is difference between the magnetic behavior of bulk and nanoparticles under the magnetic field. Nanoparticles with a radius below 150 Å belong to “single domain particle,” which remains in a state of uniform magnetization at any magnetic field.¹ Moreover, both particle shape and size are greatly considerable factors when discussing the magnetic properties of particles.² Consequently, the nanoparticles have also paramagnetism property which means that they possess magnetic properties only when they are exposed to an external magnetic field. Iron oxide nanoparticles are found to have superparamagnetic properties, which allow using these nanoparticles for wide range of applications.

Ferrofluids are stable magnetic dispersions comprised of ferromagnetic nanoparticles with a diameter of approximately 10 nanometers dispersed in an aqueous or organic liquid carrier. Rosensweig has described them for the first time in 1966.³ The preparation of a magnetic fluid is generally performed in two main stages, including: (i) the synthesis of magnetic nanoparticles, and then (ii) the dispersion of these particles in a solvent or in a liquid phase by the aid of a surfactant capable of generating repulsive interactions between the particles. The stabilization of ferromagnetic particles in the continuous phase can be achieved by using two methods, in the first, the nanoparticles are stabilized by a surfactant or polymer, it is called ferrofluid nanoparticles bearing surfactant; in the second,

* Author to whom correspondence should be addressed.



Ahmad Bitar was born in 1977 in Idleb, Syria. He received his B.Sc. in 2000, third/one hundred and twenty students, from the university of Aleppo, Syria. He received his M.Sc. in 2010 from the University of Lyon1, Lyon, France. In July 2013, he received his Ph.D. in nanoparticles synthesis for biomedical diagnostic application, in Engineering Processes and Automatic Laboratory (LAGEP), university Lyon-1, Lyon, France. Currently, he is working as post-doc in the university Lyon1 on the synthesis of active-loaded particles for cosmetic applications.



Chariya Kaewsaneha was born in 1984. She received Ph.D. (Polymer Science and Technology) from Mahidol University, Bangkok, Thailand in 2014. With financial support from the RGJ-TRF and French government, she has collaborative research with LAGEP Laboratory, Claude Bernard University Lyon-1, Lyon, France.



Mohamed M. Eissa is Associate Professor in Polymers Department, National Research Centre, Giza, Egypt. He has got Bachelor (1991), Master (1999) and Ph.D. (2006) from Chemistry Department, Faculty of Science-Cairo University, Egypt. His work is focused on polymer synthesis, and preparation of polymer composites and their applications in the industrial and biomedical domains. He has got four post doc scholarships in the period 2010–2013 from the French government in the Engineering Processes and Automatic Laboratory (LAGEP-Lyon), France. Dr. Mohamed M. Eissa is Associate Editor in the Journal of Colloid Science and Biotechnology (JCSB) and he is a reviewer for many international Journals.



Talha Jamshaid is lecturer at the University of Lahore, Lahore, Pakistan. Currently, he is a Ph.D. scholar at LAGEP, University of Lyon-1, France. He received his first degree, Doctor of Pharmacy, from University of the Punjab, Lahore, Pakistan. He is doing research in the subject of Pharmaceutical Technology. He is particularly involved in the preparation of Magnetic latex particles to be used in microfluidic devices like Lab-on-a Chip, biosensors and microfluidics.



Pramuan Tangboriboonrat (Ph.D., Université de Haute Alsace, Ecole Nationale Supérieure de Chimie de Mulhouse, France in 1991) is full Professor at Department of Chemistry, Faculty of Science, Mahidol University. She experts in polymer colloids and surface modification of natural rubber latex.



Duangporn Polpanich was born in 1980. She received Ph.D. (Polymer Science and Technology) from Mahidol University, Thailand in 2007. She is currently a researcher at National Nanotechnology Center, National Science and Technology Development Agency, Thailand Science Park, Pathum Thani. Her research works focus on magnetic nanoparticles for biological applications.



Abdelhamid Elaissari is the Director of research at CNRS, received his undergraduate education from Agadir University, Morocco in 1988. He moved to the Louis Pasteur University (ICS), Strasbourg, France in which he received Ph.D. degree for polymers and colloids in 1991. He got a permanent position in CNRS in 1991 and then he joined CNRS-bioMerieux@ENS-Lyon laboratory, until 2007 in which he has developed colloids for biomedical applications including *in vivo*, *in vitro* and bionanotechnologies. In 2007, he moved to Engineering Processes and Automatic Laboratory (LAGEP@Lyon) in which he is acting not only as a director of research but also as the vice director of LAGEP.

the stabilization of nanoparticles is provided by creating charges on the surface of nanoparticles. This type of stabilization is obviously not possible in the aqueous medium, and the obtained dispersion is called “ionic ferrofluid.”

The originality of the ferrofluids is their behavior when subjected to a magnetic field. Indeed, the strong interaction between the nanoparticles and the solvent molecules provides a magnetic behavior for the entire fluid, which then acts as a “single phase” liquid. This unique property of the magnetic fluids can be exploited in many potential applications in various fields.

A magnetic fluid “ferrofluid” belongs to colloidal suspensions family and consists of stable colloidal fine nanoparticles in a carrier liquid. The magnetization properties are related to the nanoparticle composition, which is essentially consisting of iron oxides. As a general tendency, metallic particles at nanometric size possess a long-range of magnetostatic attraction leading to their agglomeration and sedimentation. Therefore, when the particle size is less than 10 nm, a stabilizing agent is required to enhance the colloidal stability by reducing the attractive forces and raising the repulsive forces between the particles. In this regards, oleic acid is widely used as a stabilizing agent and many carrier liquids are employed in order to achieve a stable ferrofluid. Nowadays, ferrofluids are commercially available to serve the different applications in several fields such as magnetic inks,^{4,5} paints,⁶ and more interestingly in biomedical applications.⁷

This review highlights the ferrofluids synthesis methods, emphasizing the two most important methods, the physical size reduction and chemical coprecipitation, as well as properties and the applications based

on ferrofluids. Industrial applications including magnetic recording media, magnetic inks and sealing by ferrofluids are described. More interestingly, the newly adapted *in vivo* and *in vitro* biomedical applications such as magnetic resonance imaging (MRI), therapeutic application, biological cells separation and nucleic acid extraction are reported. Moreover, the new form of ferrofluids, i.e., magnetic emulsion is also discussed.

2. PREPARATION METHODS

Magnetite (Fe_3O_4) and maghemite ($\gamma\text{-Fe}_2\text{O}_3$) are the most commonly ferrites used for preparation of ferrofluids. However, according to the magnetic properties desired, the ferrofluid can also consist of mixed oxides containing, iron, cobalt, manganese, barium or nickel. Magnetic fluid or ferrofluid could not be prepared by melting the ferromagnetic metals such as iron, cobalt and nickel, because the ferromagnetic materials lose their strong magnetic properties when heated above its Curie temperature. Moreover, for all known ferromagnetic materials this temperature is always below their melting points.⁸ Therefore, to prepare a good and useful ferrofluid, it is necessary to coat the synthesized fine ferromagnetic particles with a stabilizing layer of surfactant, followed by dispersion in a suitable liquid.

Regarding to preparation of magnetic nanoparticles, there are several methods (physical and chemical) used to produce ferromagnetic nanoparticles, e.g., size reduction, chemical synthesis (coprecipitation, thermal decomposition and microemulsion methods), electro-decomposition techniques, evaporation of metal in liquid, and carrier

liquid exchange.^{9,10} In the next section, size reduction and chemical synthesis methods are described in details.

2.1. Physical Based Method (Size Reduction)

Size reduction method is a physical based process related to grinding of the permanent magnets or ferromagnetic metals for more than 20 days in presence of oleic acid and organic solvent (heptane).¹¹ The obtained particles have an average size from 50 to 200 Å and such suspension is considered as an apparently magnetically responsive continuous liquid. Ostensibly, the ferrofluid is a homogenous liquid but in reality it is composed of very small magnetic particles suspended in a carrier solvent. Despite the long time and hard work needed by this technique it was widely used to synthesize ferrofluids. Rosensweig and coworkers used Papell's grinding method to prepare the ferrofluids and they extensively studied their physical, thermal and hydrodynamic properties.¹²⁻¹⁶ Kaiser et al.¹⁷ published his work on the preparation and the properties of stable ferrofluid prepared by the same technique. In this paper they cited the most important works described the grinding process to prepare ferrofluids. Furthermore, due to the importance and number of applications based on ferrofluids, the research and development in ferrofluids are drastically increased in this field as indicated from the number of papers and patents published (more than 1,000 patents and 1,900 papers) in the period of 1986–1990.¹⁸ The ferrofluids obtained by size reduction method have good colloidal stability in solvent carriers with fine particle size in the range of 150 Å. However, this technique requires very long time and consumes high energy. In addition, particle size and particle size distribution of the obtained magnetic particles are large as compared with those obtained by using other methods.

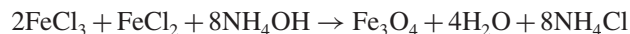
2.2. Chemistry Based Processes

Due to the considerable interest of ferrofluids and their wide applications, it is necessary to improve their synthesis methods. Thus, the chemical synthesis, including precipitation from iron salt solution and thermal decomposition of metal carbonyls, is considered as a good, fast, simple, cheap and controllable technique for ferrofluids production. Practically, ferrofluid preparation consists of two main steps: (i) nanoparticles preparation and (ii) their dispersion in a carrier liquid.

2.2.1. Coprecipitation Method

Chemical coprecipitation is the most conventional method used to prepare magnetic nanoparticles (MNPs). This can be attributed to the high yield of the magnetic ferrofluid which can be obtained; in addition to that this method is simple and cost-effective. Moreover, the reaction temperature and time consumed to complete the reaction are lower than other methods, e.g., thermal decomposition and hydrothermal techniques.

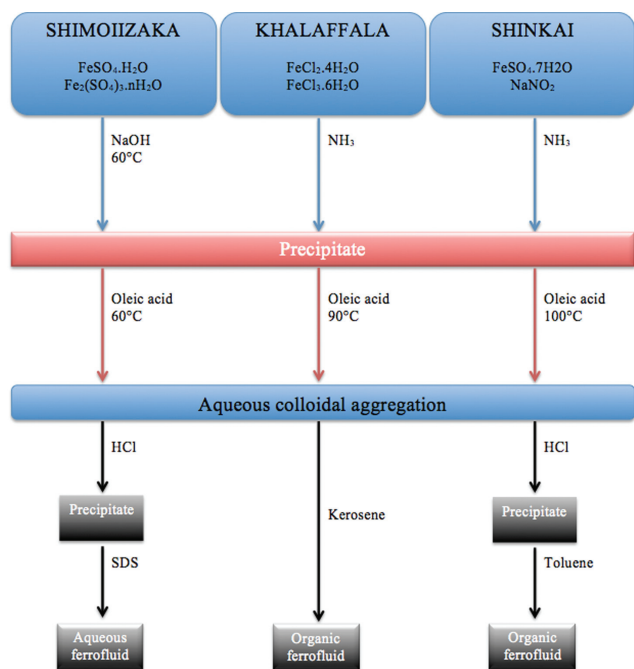
Generally, this procedure begins with a mixture of FeCl₃ and FeCl₂ solution in water and then coprecipitation is performed by the addition of a base, typically ammonium or sodium hydroxide. This reaction can be summarized as follow:



This process involves two stages: (i) a short burst of nucleation when the concentration of the species reaches critical supersaturation and (ii) a slow growth of the nuclei by diffusion of the solutes to the surface of the crystal. In order to produce monodisperse MNPs, the nucleation should be avoided during the period of growth.¹⁹ The coprecipitation is affected by different parameters such as the type and concentration of salts (e.g., chlorides, sulfates or nitrates), temperature, pH and the addition rate of the alkali solution.¹⁹⁻²² According to thermodynamics of this reaction, the precipitation of Fe₃O₄ should be performed at pH between 8 and 14 with a stoichiometric ratio (Fe³⁺:Fe²⁺) of 2:1 under inert atmosphere at room temperature or at elevated temperature. Usually, ferromagnetic particles produced by this technique have an average size larger than 20 nm and they are composed of mixture of γ-Fe₂O₃ and Fe₃O₄ depending on the reaction conditions.²³

Preparation of magnetic fluids by coprecipitation of ferric and ferrous salts in aqueous solution was first reported by Reimers et al.²⁴ The reactants ratio (FeCl₃:FeCl₂) was fixed at 2:1 and NH₄OH was used to precipitate the iron oxide nanoparticles. After the co-precipitation, the iron oxide nanoparticles were subjected to surfactant stabilization for improving their colloidal stability in the dispersion medium by using fatty acid derivatives to stabilize iron oxide nanoparticles either in organic or aqueous medium. Oleic acid (OA) is the most commonly dispersant agent used as water insoluble adsorption layer, thus OA-coated nanoparticles can be easily and highly dispersed in organic solvent.²⁵ At alkaline pH, the carboxyl groups at the chain end of oleic acid will be ionized enhancing its binding onto the nanoparticle surface, while the aliphatic chain forms the hydrophobic layer that helps the nanoparticles to disperse in non-polar solvent. Scheme 1 presents the main chemical reactions used to prepare ferrofluids.

To use the ferrofluid in hydrophilic media, one needs to coat the ferromagnetic nanoparticles by ionic layer. Massart et al.²⁶⁻²⁹ prepared aqueous ferrofluids without surfactants in acidic medium (nitric acid) to have ionic iron oxide nanoparticles. Furthermore, it was found that the size of precipitated particles can be controlled by adding the citrate ions or sodium dodecyl sulfate to the reaction medium.^{28,30} These ions, at a specific ratio, can control the particle size by inhibiting the growth process so raising the number of nucleation. It was also reported that the addition of chelating organic anion stabilizer and/or reducing agents (carboxyl or hydroxyl carboxylate ions,



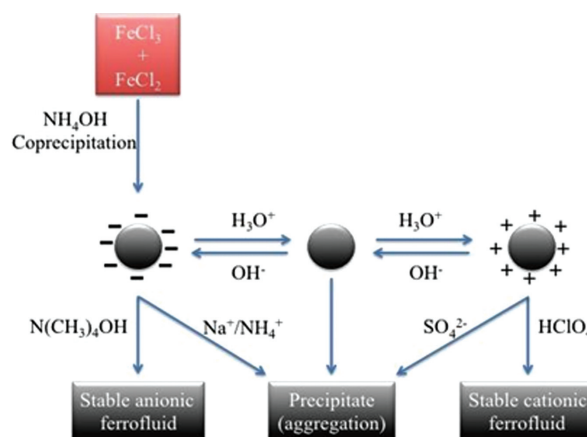
Scheme 1. Chemistry based ferrofluid preparation methods.³¹

e.g., citric, gluconic or oleic acid or polymer surface complexing agents (e.g., dextran, carboxydextran, poly(vinyl alcohol) or starch) during the formation of magnetite can help to control the size of nanoparticles.^{19,20} The chelation of organic ions on the magnetic particles surface either prevents nucleation and then leads to larger particles or inhibits the growth of crystal nuclei, leading to small nanoparticles.

However, the particles prepared by this technique tend to be polydisperse. The control of particle size distribution is quite limited because only kinetic factors affect the crystal growth.

In the case of ionic ferrofluids, the iron oxide nanoparticles are negatively or positively charged depending on the pH of the medium. The overall neutrality of the colloidal solution is provided by the counter-ion of the base used in the coprecipitation reaction. According to the polarizing counter-ion power, the dispersion of nanoparticles of iron oxide in water is more or less effective. For example, the synthesis of iron oxide in ammonia medium results in aggregated nanoparticles due to the high polarizing power of NH_4^+ cation which reduces interaction between water molecules and the particles. Then, it is necessary to substitute the ammonium cation in order to induce charges on the particles surface. The use of tetramethylammonium hydroxide ($\text{N}(\text{CH}_3)_4\text{OH}$) or perchloric acid (HClO_4) provides stable anionic or cationic ferrofluid, respectively as shown in Scheme 2.

Ionic ferrofluids can also consist of mixed oxides. Indeed, depending on the final properties desired for the ferrofluid, the magnetic nanoparticles might contain manganese (MnFe_2O_3), cobalt (CoFe_2O_4), or more complex



Scheme 2. Synthesis of ionic (cationic or anionic) ferrofluids via coprecipitation process. Adapted from [32], J. P. Jolivet, et al., *Nouv J. Chim.* 7, 325 (1983). © 1983.

alloys ($\text{Ni}_x\text{Zn}_y\text{Fe}_z\text{O}_4$, with $x + y + z = 3$). In this case, the preparation method remains similar, but the preparation of mixed oxides requires performing the coprecipitation reaction at higher temperatures.

2.2.2. Thermal Decomposition Method

To obtain MNPs with narrow size distribution, thermal decomposition is needed. Generally, thermal decomposition of organometallic compounds followed by oxidation in high-boiling temperature organic solvents containing stabilizing surfactants can lead to highly monodisperse MNPs. The process usually requires relatively higher temperatures and a complicated operation.^{20,33} The organometallic compounds include $\text{Fe}(\text{cup})_3$ (cup = *N*-nitrosophenylhydroxylamine),³⁴ $\text{Fe}(\text{acac})_3$ (acac; acetylacetonate),³⁵ or $\text{Fe}(\text{CO})_5$ (iron pentacarbonyl).³⁶ For instance, monodisperse $\gamma\text{-Fe}_2\text{O}_3$ nanocrystallites with size of 4–16 nm were prepared by thermal decomposition of $\text{Fe}(\text{CO})_5$ in the presence of oleic acid at 100 °C by controlling the experimental parameters.³⁶ The resulting iron nanoparticles were transferred to monodispersed $\gamma\text{-Fe}_2\text{O}_3$ nanocrystallites by controlling oxidation using trimethylamine oxide as a mild oxidant. Although ferrofluid MNPs with controlled size and shape are obtained by thermal decomposition method, the resulting nanoparticles are generally dissolved only in nonpolar solvents, which is the drawback of this method.

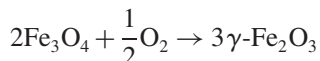
3. PROPERTIES

For the vast majority of ferrofluids, whether aqueous or organic, the magnetic properties are provided by ferrite nanoparticles. More rarely, magnetic fluids composed of metal nanoparticles are also found. This latter case will not be discussed in this review.

3.1. Chemical Structure Analysis (X-Ray, Mössbauer)

Ferrites are metal oxides, which have a crystal structure of spinel type and whose main component is iron. Ferrites MFe_2O_4 kind (where M is a divalent cation) belongs to the family of ferromagnetic compounds. In the spinel structure, the O^{2-} ions form a face-centered cubic lattice. The divalent cations (M^{2+}) and Fe^{3+} are located in the octahedral or tetrahedral cavities formed by the network of O^{2-} ions. It is the particular arrangement of ions that give the material its magnetic properties. The spinel type crystal structure is shown in Scheme 3. Half of the octahedral sites are occupied by Fe^{3+} cations (site B) and the eighth of the tetrahedral sites by M^{2+} cations (site A).

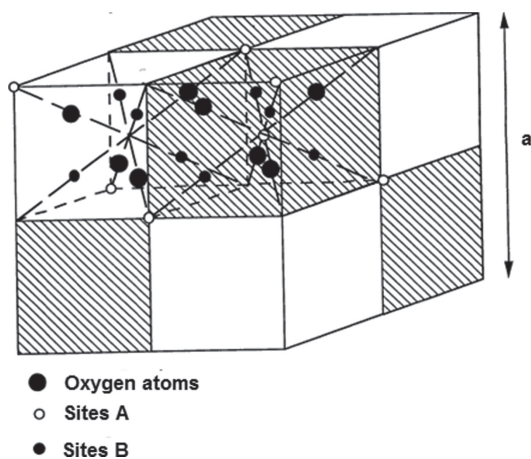
Magnetite (Fe_3O_4) is a mixed oxide of iron II and iron III, which has an inverse spinel structure. In this type of structure, a quarter of the octahedral sites are occupied by Fe^{3+} cations, another quarter is occupied by Fe^{2+} cations, and the eighth of the tetrahedral sites is occupied by Fe^{3+} cations. Maghemite ($\gamma-Fe_2O_3$) is formed by oxidation of magnetite according to the following reaction:



The crystallographic structure of the maghemite is identical to that of magnetite, with the exception of certain deficiencies caused by the iron oxidation reaction.

The crystallographic structure of iron oxide nanoparticles in its powder state was generally examined by X-ray diffraction technique. The typical spectrum of magnetite (Fe_3O_4) and maghemite ($\gamma-Fe_2O_3$) is shown in Figure 1. This spectrum shows six major diffraction peaks relatively well defined, suggesting the formation of highly crystalline iron oxide.^{37,38} The characteristic diffraction peaks of magnetite (Fe_3O_4) and maghemite ($\gamma-Fe_2O_3$) are also shown in the experimental spectrum.

To facilitate comparison with the more probable crystallographic structures of iron oxide, the experimental inter-reticular distances (d_{exp}) relating to different groups



Scheme 3. Crystallographic structure of iron oxide Fe_3O_4 .³¹

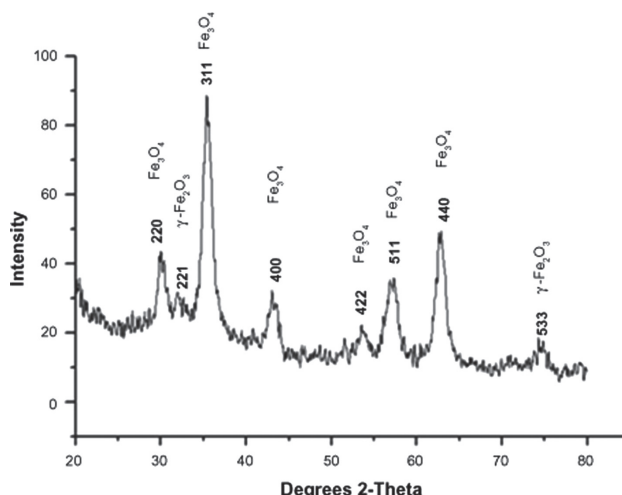


Fig. 1. X-ray diffraction pattern of synthesized nanoparticles confirms the existence of magnetite (Fe_3O_4) and maghemite $\gamma-Fe_2O_3$. Reproduced with permission from [38], N. Tran, et al., *Int. J. Nanomedicine* 5, 277 (2010). © 2010, Dove Medical Press Ltd.

of crystal planes $\{hkl\}$ are calculated from the Bragg's equation:

$$n\lambda = 2d \sin \theta$$

where n is an integer, λ is the wavelength of incident radiation ($CuK\alpha = 1.5418 \text{ \AA}$), d is the spacing between the planes in the atomic lattice, and θ is the angle between the incident ray and the scattering planes. The determined experimental distances (d_{exp}) are then compared with the values reported in the ASTM (American Society for Testing and Materials) for pure magnetite and maghemite, as represented in Table I.³¹

As clearly seen in Figure 1, the diffraction spectra of magnetite and maghemite are very close, since these two oxides have a crystallographic structure of inverse spinel. Furthermore, when the sample is composed of a heavy element such as iron, a portion of the incident radiation may be absorbed, which causes a shift of all the peaks of the spectrum. To confirm X-ray results, iron oxide was generally analyzed using Mössbauer spectroscopy. This technique allows measuring the hyperfine magnetic fields around iron cores. These fields are due to the electronic environment of the iron and thus to determine precisely the degree of oxidation. Indeed, in the maghemite, iron is

Table I. Comparison between the experimental distances (d_{exp}) of iron oxide nanoparticles derived from XRD with the standard data of magnetite and maghemite in the ASTM (American Society for Testing and Materials).

Plane $\{hkl\}$	d_{exp} (Å)	d (Fe_3O_4) (Å)	d ($\gamma-Fe_2O_3$) (Å)
(220)	2.955	2.967	2.953
(311)	2.522	2.532	2.518
(400)	2.091	2.099	2.089
(422)	1.706	1.714	1.704
(511)	1.608	1.616	1.607
(440)	1.478	1.484	1.476

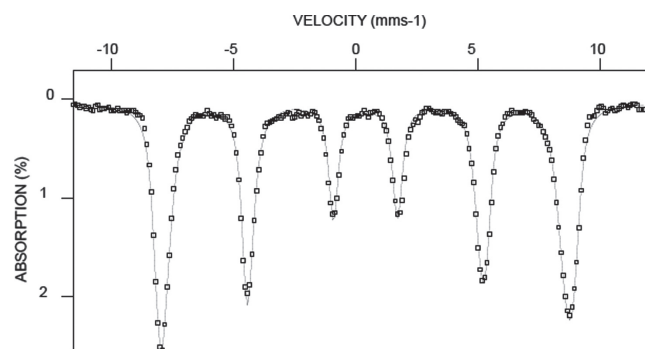


Fig. 2. Mössbauer spectrum of iron oxide nanoparticles: Experimental (\square) and calculated (line) at $T = 4.2$ K. Reproduced with permission from [37], F. Montagne, et al., *J. Magn. Magn. Mater.* 250, 302 (2002). © 2002, Elsevier.

present in the oxidation state (3) while it is in the oxidation state (8/3) in the magnetite. Therefore, this technique proves to be a method of choice to identify the exact nature of the iron oxide.

A typical Mössbauer spectrograph for iron oxide is presented in Figure 2. Mössbauer parameters are generally obtained using two methods of calculation; the first to determine the hyperfine parameters (δ , Γ and H) sites of iron. The values of isomer shifts δ are then used in a second calculation method (method of Hesse and Rübartsch) to determine the distribution of iron between the different sites in the crystallographic structure. The general Mössbauer experimental parameters are δ (the isomer shift), Γ (the width at half-height), H (the magnetic hyperfine field), and $S1$ and $S2$ (the two octahedral sites of the inverse spinel structure). The deep analysis of these parameters leads to confirm the exact crystallographic structure of the analyzed magnetic material.³⁷

3.2. Morphology, Size and Size Distribution Analysis

The morphology analysis of particles is generally investigated using various techniques such as atomic force microscopy (AFM), scanning electron microscopy (SEM) and transmission electron microscopy (TEM). In the case of iron oxide nanoparticles, the morphology and shape of the particles mainly depend on the preparation process. For instance, the coprecipitation process can be performed in batch continuous phase or in inverse microemulsion. In the case of inverse microemulsion, the morphology was found to be affected by the presence of polymer in the internal phase, whereas, in the case of classical coprecipitation process, the morphology of the obtained particles is not really spherical as illustrated by TEM image (Fig. 3).³⁷

By considering the particles spherical, the polydispersity index ($I_p = Dw/Dn$) can be calculated from the number average diameter (Dn) and the weight average diameter (Dw). Generally, it was found to be > 1 , revealing the polydispersity of the particles prepared by coprecipitation process.³⁸ As a general tendency, the hydrodynamic

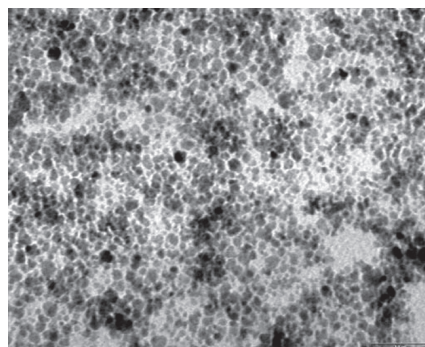


Fig. 3. Transmission electron microscopy image of iron oxide nanoparticles prepared via classical coprecipitation process. Reproduced with permission from [37], F. Montagne, et al., *J. Magn. Magn. Mater.* 250, 302 (2002). © 2002, Elsevier.

particle size is around 20 nm with large size distribution, as below illustrated in Figure 4.

3.3. Electrokinetic Properties

In the case of ionic ferrofluids prepared by Massart, the repulsive electrostatic interactions are derived from the nature and surface charges originating from oxygen atoms of the metal oxide. Iron oxides have an amphoteric behavior, they are negatively charged in basic medium (anionic ferrofluid) and positively charged (cationic ferrofluid) in the acidic medium (Fig. 5). Consequently, the state of dispersion depends on the charge density on the surface of the particles.

In a pH range between 6 and 10, the charge density is near to or equal to zero (at approximately pH 7.5), or at least not sufficient to ensure the stability of the ferrofluid particles leading to their flocculation. As an indication, approximately 2% of iron sites are protonated at pH 2.7; it is the iron present on the surface of nanoparticles. The zone of instability can be moved to low pH by changing the nature of the surface charges. Indeed, by replacing the hydroxyl groups with a ligand such as citric acid ($\text{HOOC-C(OH)-(CH}_2\text{-COOH)}_2$), the ferrofluid obtained is stable at $\text{pH} \geq 4$. Therefore, the pH range in which the ferrofluid become stable is a key element for any applications.

Several ligands have been studied (Table II) leading to stable ferrofluids at different pH ranges.³¹ These ligands are adsorbed on iron oxide nanoparticles in their protonated

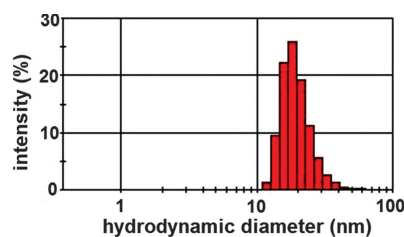


Fig. 4. Size distribution of iron oxide nanoparticles prepared via coprecipitation process. Reproduced with permission from [39], S. Ghoshal, et al., *Nanoscale Res. Lett.* 6, 540 (2011). © 2002, Springer.

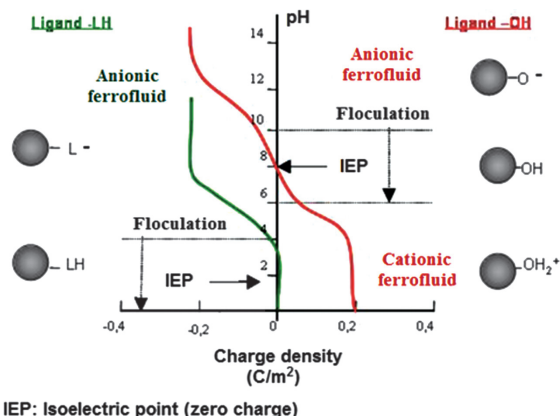


Fig. 5. Surface charge density of iron oxide nanoparticles as a function of pH of the dispersion medium. Adapted with permission from [40], J.-C. Bacri, et al., *J. Magn. Magn. Mater.* 85, 27 (1990). © 1990, Elsevier.

form (OH²⁺) leading to complexation reaction. The stability of the magnetic nanoparticles mainly depends on the nature of ligand functional groups (carboxylic, hydroxyl or thiol) involved in the complexation reaction, in addition to the mechanism of stabilization at a specific pH.

3.4. Colloidal Stability

Colloidal stability is an essential parameter to be taken into account for future applications of magnetic nanoparticles. For ferrofluids, the magnetic nanoparticles do not remain naturally dispersed but they tend to settle because of their high density (about 5 g/cm³) which is much higher than that of conventional solvents. Moreover, if the particles have sufficiently small size (about 10 nm), then Brownian motion maintains the homogeneity of the ferrofluid. Of course, the only thermal agitation is not sufficient to ensure the colloidal stability of the dispersion. In fact, it is also necessary to prevent the formation of aggregates, which enhance the settling phenomena and may cause irreversible stabilization of the dispersion. For the surfactant

Table II. Different types of ligands used to stabilize the ferrofluids in aqueous medium.

Ligand	Formula	Stability area
Tartaric acid	<chem>O=C(O)C(O)C(O)C(O)C(=O)O</chem>	pH > 4 (anionic ferrofluid)
Gluconic acid	<chem>O=C(O)C(O)C(O)C(O)C(O)C(O)C(O)C(O)C(=O)O</chem>	pH < 4 (cationic ferrofluid) pH > 7.5 (anionic ferrofluid)
Dimercaptosuccinic acid	<chem>OC(=O)C(S)C(S)C(=O)O</chem>	pH > 3 (anionic ferrofluid)
Arginine	<chem>NC(=N)NCCCNC(=O)O</chem>	pH < 8 (cationic ferrofluid) pH > 11 (anionic ferrofluid)

free ferrofluid dispersion, two types of attractive forces induce the formation of aggregates; the first is Van der Waals forces, which act at a short distance and are more important for particles with large size. The second is the attractive magnetic dipole-dipole interactions, which arise from the alignment of magnetic moments of the particles when a magnetic field is applied. In order to compensate the attractive forces and to avoid irreversible aggregation phenomena, it is necessary to introduce repulsive interactions between the particles. These repulsive (electrostatic or steric) interactions can be achieved by surfactant or polymer modification of the magnetic nanoparticles, as above discussed.

In the case of surfactant containing ferrofluids, the surfactant is adsorbed on the surface of the nanoparticles in the form of a single protective monolayer for organic ferrofluid dispersions and under double layer in the case of aqueous ferrofluid. In the latter case, the repulsive forces are electrosteric in nature. The electrostatic part arising from the polar heads of the surfactant, forming the second layer, is oriented towards the aqueous phase and also contributes to the stabilization of the dispersion.

3.5. Magnetic Properties

In the most of the great interest applications, the particles perform best when the size of the nanoparticles is below a critical value, which is typically around 10–20 nm depending on the material. Moreover, the MNPs response to an applied magnetic field depends on its state. The characteristics of MNPs are usually displayed as shown in Figure 6. The magnetization (*M*) of superparamagnetic material (curve 2) depends on the external or applied magnetic field (*H*), in addition to its remnant magnetization (*M_r*) (the residual magnetization after removing the magnetic field) and coercive force (the external field required to reduce the magnetization back to zero) (*H_c*) which are

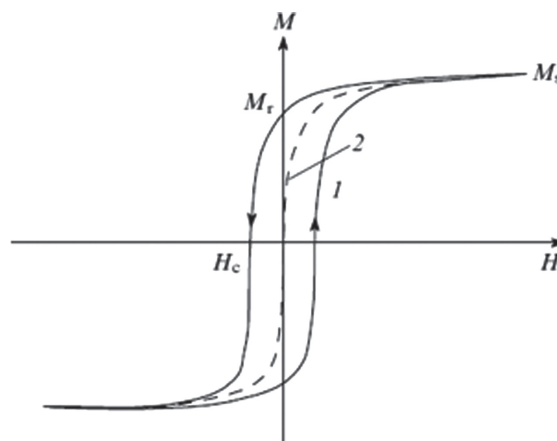


Fig. 6. Magnetization curves of (1) ferromagnetic and (2) superparamagnetic materials. *M_s* is saturation magnetization, *H_c* is coercive force, *H* is the applied magnetic field, *M* is induced magnetization, and *M_r* is remnant magnetization. Reproduced with permission from [41], U. Jeong, et al., *Adv. Mater.* 19, 33 (2007). © 2007, John Wiley and Sons.

negligible. The magnetization curve of this type of material lacks of the hysteresis loop. In addition, the magnetic moment of the particle in its superparamagnetic state reverses at time shorter than the experimental time scales. On contrary, the magnetic dipoles inside the ferromagnetic material always exist in absence and presence of an external field and produce a hysteresis loop (curve 1).⁴¹

Generally, the saturation magnetization (M_s) values found in nanostructured materials are usually smaller than the corresponding bulk phase, when assume that no change in ionic configuration occurs. Accordingly, experimental M_s value of ferromagnetic nanoparticles has been reported to span the 30–50 $\text{emu} \cdot \text{g}^{-1}$ range, lower than that of the bulk (90 $\text{emu} \cdot \text{g}^{-1}$).³³ In addition, an important parameter to describe superparamagnetic colloids is the blocking temperature, a transition point at which the thermal energy is comparable to the energy of magnetic anisotropy or the energy barrier for spin re-orientation. Below blocking temperature, the anisotropy of the particle blocks the free movement of the moment. Above the blocking temperature, the moment is free to align in an applied magnetic field and appears superparamagnetic. Figure 7 shows the behavior of ferrofluid in presence and absence of a magnetic field.³¹ Hyeon et al.⁴² reported the blocking temperature of the monodisperse $\gamma\text{-Fe}_2\text{O}_3$ nanocrystallites obtained by the thermal decomposition method which was 25, 185 and 290 K for particle diameter of 4, 13 and 16 nm, respectively. Mehdaoui et al.⁴³ synthesized cubic shape of Fe(0) ferromagnetic nanoparticles of particle diameters 16 and 11 nm. The M_s of bulk iron and iron nanoparticles were 200 ± 10 and 178 ± 9 $\text{emu} \cdot \text{g}^{-1}$ at 300 K, respectively. At 300 K, the H_c of the Fe(0) nanoparticles having particle diameter of 16 and 11 nm were 16 and 5 mT, respectively.

One interesting phenomenon is the generation of thermal energy when the magnetic nanoparticles (ferrofluid) is exposed to a fast switching (alternating) magnetic field.^{43–45} The frictions caused by the physical rotation of nanoparticles, Brownian relaxation, and magnetization reversal within nanoparticle (Neel relaxation) lead to the loss of magnetic energy and generation of thermal energy. The power released by the nanoparticles is assessed by their specific adsorption rate (SAR). The increase in SARs



Fig. 7. Behavior of the ferrofluid in absence (a) and presence (b) of a magnetic field.³¹

above $1 \text{ W} \cdot \text{g}^{-1}$ could be beneficial for several aspects of the hyperthermia applications.⁴⁵ The SAR measured on 16 and 11 nm nanocubes was $1,690 \pm 160$ and $1,320 \pm 140 \text{ W} \cdot \text{g}^{-1}$ at 300 kHz and 66 mT, respectively. Although very large SARs on ferromagnetic nanoparticles were obtained, the efficiency of magnetic nanocubes for hyperthermia applications was limited due to the presence of magnetic interactions.

4. SURFACE FUNCTIONALIZATION

Generally, the functionalization of magnetic nanoparticle's surfaces is based on two main approaches: (i) physical chemistry based approach and (ii) chemistry based process. These two processes are below described and illustrated and only the most used approaches are described.

4.1. Physical Chemistry Based Processes

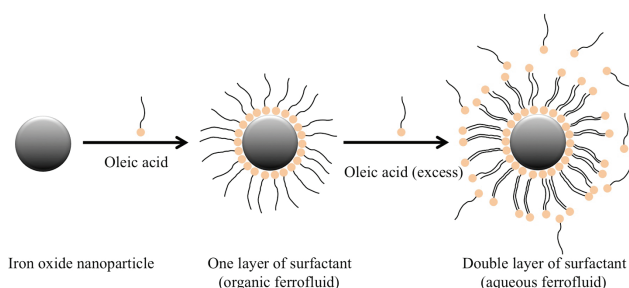
Physical chemistry based approach is basically related to surface modification of nanoparticles via adsorption process such as surfactant immobilization, polyelectrolytes adsorption or even small molecules immobilization. Then in this part, two processes will be presented; surfactant immobilization and polyelectrolyte's adsorption.

4.1.1. Surfactant Immobilization

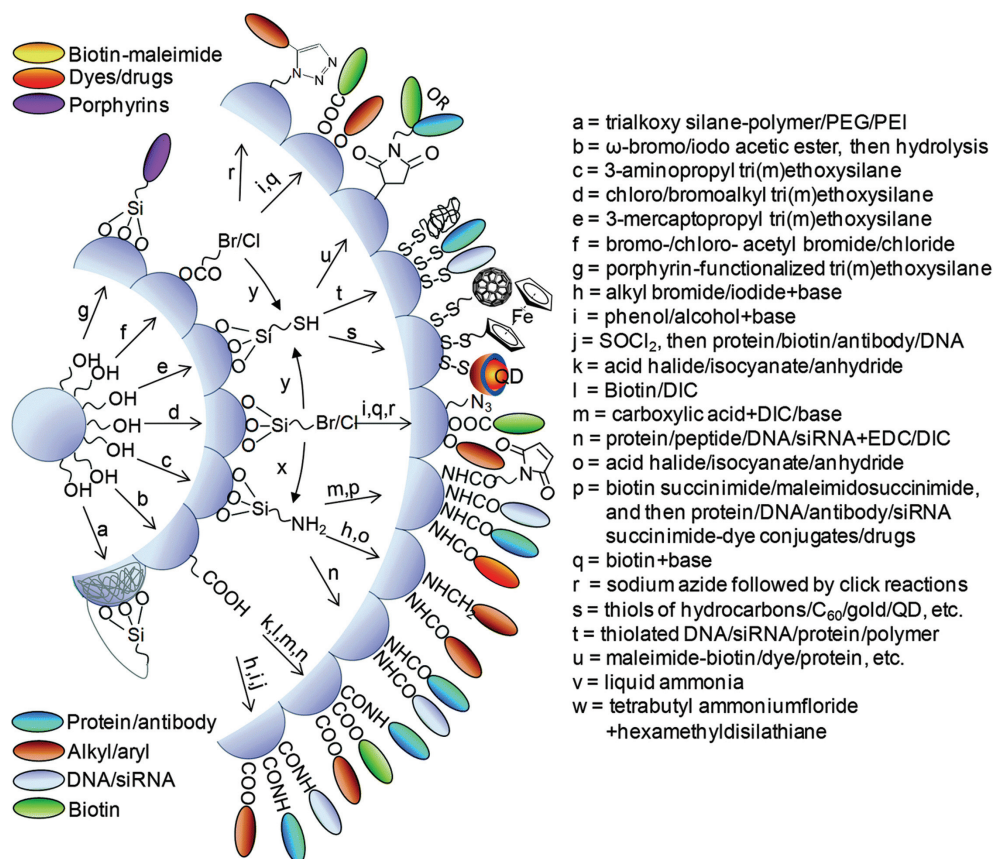
Oleic acid is the most commonly used surfactant for surface modification of iron oxide nanoparticles. The carboxylic groups of this surfactant are chemically complexed with iron oxide surface leading to the formation of non aqueous (hydrophobic) dispersible particles. That is why oleic acid has been widely used to prepare organic ferrofluid. However, the excess use of oleic acid leads to the formation of a double surfactant layer on the surface of iron oxide nanoparticles and then gives rise to water dispersible particles as below illustrated in Scheme 4.

4.1.2. Polymers Adsorption

Polymer adsorption onto solid surface has been largely examined and various adsorption mechanisms have been reported as a function of polymer properties, surface nature and adsorption medium. The most investigated system is based on attractive electrostatic interaction. Regarding



Scheme 4. Schematic illustration for surface modification of iron oxide nanoparticles via oleic acid layers adsorption.



Scheme 5. Most commonly used methods for functionalization and bioconjugation onto silica-coated magnetic nanoparticles. Reproduced with permission from [47], V. Biju, *Chem. Soc. Rev.* 43, 744 (2014). © 2014, Royal Society of Chemistry.

the surface modification of iron oxide nanoparticles, the adsorption of polyelectrolytes on oppositely charged iron oxide nanoparticles has been investigated as reported by Mouaziz et al.⁴⁶ In this work, the adsorption of amine containing dextran polymer on negatively charged iron oxide has been investigated. It has been reported that the adsorption process leads incontestably to aggregated particles and at the same time to positively charged modified nanoparticles. The reported aggregation has been attributed to bridging flocculation of the used polyelectrolyte. Such phenomena can be reduced when the adsorption is performed in highly diluted dispersion medium. The final cationic particles derived from this work have been used for non-specific nucleic acids adsorption.

4.2. Chemistry Based Approaches

The surface modification of iron oxide nanoparticles using supported chemistry has been investigated using various approaches. The most widely reported method is based on silica coating of iron oxide nanoparticles. The use of sol gel approach leads to well-defined magnetic core and silica shell. These silica particles can be easily removed by applying simple magnetic sorting. The obtained magnetic silica particles are then easy to be functionalized by inducing amine, carboxylic or any classical chemical group by using

well appropriate functional tetraethyl orthosilicate (TEOS) derivative,⁴⁷ as illustrated in Scheme 5.

5. APPLICATIONS

Ferrofluids and their synthesis techniques were the focus of attention of scientists soon after the first synthesis in 1960s. Few years later, in 1980s, all published papers and patents talked about the ferrofluids synthesis and properties.^{11, 14, 16, 17, 24, 26, 27, 48–50} The real applications of ferrofluids started in 1980s including magnetic inks,⁴ paints for recording taps,⁵¹ sealing,⁵² and more recently in biomedical applications⁴⁷ such as in bioseparation, magnetic resonance imaging (MRI),^{53, 54} and as therapeutic agents for cancer treatment.^{44, 55, 56}

5.1. Industrial Applications

The combination of liquid and magnetic properties expands the potential applications of ferrofluids in several different areas. Indeed, the work developed over the last twenty years leads nowadays to elaborate a wide range of magnetic fluids (aqueous, organic in various solvents and various chemical structures). The magnetic properties of ferrofluids were widely applied in data saving field, tapes for audio and video recording, magnetic cards, computer storage and informatics.^{51, 57} Primarily, magnetic pigments were produced using iron oxide^{58–60} and then magnetic

inks⁵ and paints were prepared from these pigments. The strong point in using magnetic inks is that the magnetic characters can be recognized digitally and magnetic ink character recognition (MICR) technology is adapted to read this type of characters.⁶¹ Consequently, using this technique provides a high secure environment of work especially for banking and magnetic cards uses. Moreover, it saves time and effort to transfer information into digital form. Recording media are mainly based on magnetic films techniques,⁶² which are produced from magnetic fluids to record and playback the information. Furthermore, the informatics developments nowadays need high capacity of storage and speed of data transfer, thus developing the magnetic recording media is drastically raised last years.^{63–65}

Sealing and bearing by using ferrofluids was invented by Furumura et al.⁵² It was depended on the filling of engraved grooves on the surface of cylindrical magnet by ferrofluid, which was retained in the gap between the magnet and rotary shaft. Then, the use of ferrofluids was commonly and extensively studied.^{66–71} Recently, this technique is widely applied in industrial pumps, vacuum systems, computer hard disk drives⁷¹ and as valves in microfluidics devices,⁷² in which an organic ferrofluid was used to generate up to 5 kPa in a device composed of a pump and two valves as shown in Figure 8.

5.2. Biocatalysis

Magnetic nanoparticles with good stability have promising future in catalysis and biocatalytic applications. Such magnetic nanoparticles can be very useful to assist an effective separation of catalysts, nuclear wastes, and biochemical products.⁷³ In pharmaceutical and chemical industries, biocatalytic processes often require a full recycling of biocatalysts to optimize economic benefits and minimize waste disposal. Immobilization of biocatalysts onto particulate carriers has been widely explored as an option to meet these requirements. More interestingly, the immobilization

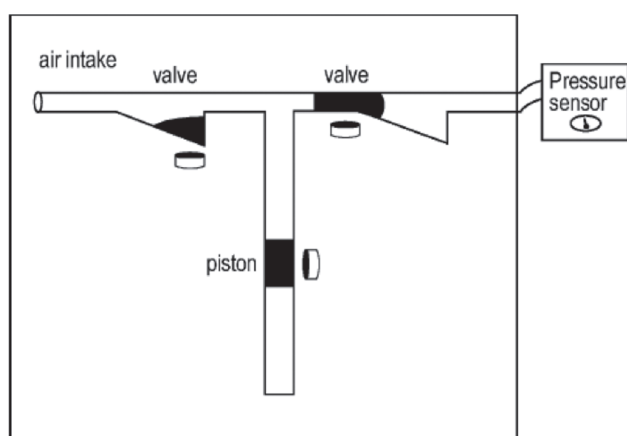


Fig. 8. Pumping system used ferrofluid and permanent magnets as a pump and valves. Adapted with permission from [72], H. Hartshorne, et al., *Sensors Actuators B Chem.* 99, 592 (2004). © 2004, Elsevier.

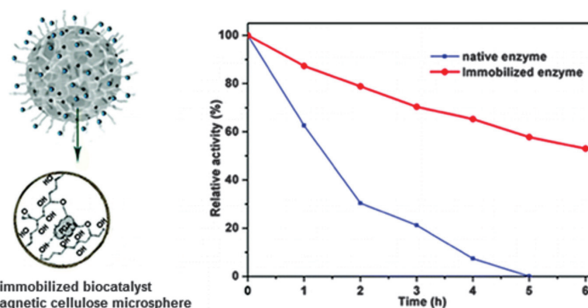


Fig. 9. Catalytic activity of penicillin *G* acylase (PGA) immobilized on magnetic cellulose porous microspheres. Reproduced with permission from [76], X. Luo and L. Zhang, *Biomacromolecules* 11, 2896 (2010). © 2010, American Chemical Society.

of these active species on solid magnetic support make the recovery of catalysts in a liquid-phase reaction by an external magnet much easier than by cross-flow filtration and centrifugation, especially when the catalysts are in the sub-micrometer size range. Consequently, such small and magnetically separable catalysts could combine the advantages of high dispersion and reactivity with easy separation.^{74, 75}

In pharmaceutical industries, for instance, Penicillin *G* acylase (PGA) is a major industrial biocatalyst used in the enzymatic production of 6-aminopenicillanic acid (6-APA), which is world widely used for production of antibiotics. Luo and Zhang have reported the immobilization of penicillin *G* acylase (PGA) in the magnetic cellulose porous microspheres for production of 6-APA.⁷⁶ The immobilized PGA exhibited highly effective catalytic activity (Fig. 9), thermal stability, and enhanced tolerance to pH variations. Furthermore, the cellulose microspheres loaded with this enzyme could be removed and recovered easily by introducing a magnetic field, leading to an acceptable reusability.

Recently, magnetite nanoparticles, prepared through coprecipitation method, were coated with alkyl silanes of different alkyl chain lengths to modulate their surface hydrophobicity. *Candida rugosa* lipase was then directly immobilized onto the modified nanoparticles through hydrophobic interaction. Enzyme activity was assessed by catalytic hydrolysis of *p*-nitrophenyl acetate. The activity of immobilized lipase was found to increase with increasing chain length of the alkyl silane. After 7 recycles, the activity of the lipase immobilized on C18 modified nanoparticles retained 65%, indicating significant enhancement of lipase stability through hydrophobic interaction. In addition, the alkyl silane modified magnetite nanoparticles exhibited high efficiency for enzyme immobilization enabling efficient enzyme recovery and recycling.⁷⁷

Furthermore, Karaoğlu et al. have prepared piperidine-4-carboxylic acid (PPCA) functionalized Fe₃O₄ nanoparticles as a novel organic–inorganic hybrid heterogeneous catalyst.⁷⁸ The catalytic activity of Fe₃O₄–PPCA was probed through one-pot synthesis of nitro alkenes through Knoevenagel reaction in CH₂Cl₂ at room temperature

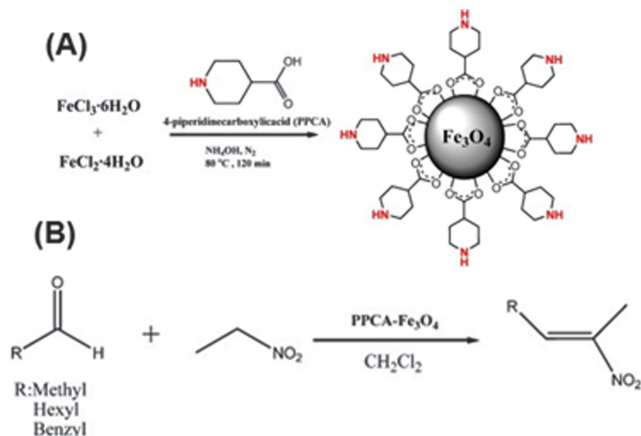


Fig. 10. Schematic representation for (A) Preparation of Fe₃O₄-PPCA nanoparticles, (B) Nitro-aldol condensation reaction using Fe₃O₄-PPCA nanoparticles as magnetically separable catalyst. Reproduced with permission from [78], E. Karaoğlu, et al. *Mater. Res. Bull.* 47, 2480 (2012). © 2012, Elsevier.

(Fig. 10). The heterogeneous catalyst showed very high conversion rates (97%) and could be magnetically recovered easily and reused many times without significant loss of its catalytic activity.

5.3. Biomedical Applications

Nanotechnology is drastically developed in the last decade and it is widely applied in biomedical fields, especially for diagnosis and hyperthermia. On the other hand, the techniques of molecular biology are well known and developed. Thus the association between the nanotechnology and molecular biology created high preferment nanostructures that show characteristics improvement such as rapidity, specificity and sensibility.

Ferrofluids, at their industrial form, are not tolerant to be in contact with biological systems due to the cytotoxicity of magnetic fluids.⁷⁹ Therefore, coating of the magnetic nanoparticle surfaces with biocompatible polymers or biomolecules, e.g., dextran⁸⁰⁻⁸² or albumin,⁸³⁻⁸⁵ were applied to expand their use borders in the biomedical domain.

5.3.1. In Vitro

Ferrofluids are characterized by their speed response to the magnetic field and this property satisfies the exigency of separation and extraction makers. Biomolecules extraction and separation, which based on the classical methods such as DNA and RNA extraction by phenol-chloroform, was too difficult, and consumed long time. In addition, the use of high quantities of organic solvents is against the environmental concerns. Nowadays, magnetic fluids with numerous types of micro- and nanostructures act as magnetic responsive solid supports to create biomolecules extraction and separation tools.⁸⁶ MNPs were also used as solid support for enzymes⁸⁷ and antibodies⁸⁸ in immunoassay. As a general method for these applications, MNPs

were coated with molecules that can interact with bimolecular targets, like antibodies or anti-bacteria to catch the bacteria. Then, MNPs were separated by an external magnetic field with captured targets, which can be separated from MNPs by changing the pH or ionic strength of the dispersion medium. Furthermore, MNPs can be coated by fluorophores that can emit fluorescence in case of contact with the target molecules.

5.3.1.1. Cell and Bacteria Separations. This technique used submicron magnetic structures that can adsorb and desorb the biomolecules, cells, bacteria and viruses.⁸³ The key of this technique is the interaction between particles and target molecules, which is sensitive to the environmental conditions such as pH, salinity and temperature. Superparamagnetic particles are prepared and then biotinylated for specific cells sorting.⁸⁹ Likewise, Sestier et al.⁹⁰ prepared MNPs coupled with enzymes or antibodies and measured the particles electrophoretic mobility by laser-Doppler velocimetry, as a technique to follow the charge surface modifications. Bacteria can be also captured and magnetically separated by using functionalized MNPs.⁹¹ FePt nanoparticles attached with the vancomycin (Van), a spectrum antibiotic, can bind to the terminal peptide D-Ala-D-Ala on the cell wall of gram-positive bacterium via hydrogen bonds. Figure 11 illustrates the bacteria separation using Van-coated MNPs.

More recently, Joo et al.⁹² reported a sensitive method to separate and quantify the pathogenic bacteria (*salmonella*). They used antibody-conjugated magnetic nanoparticles (MNPs) and antibody-immobilized TiO₂ nanocrystals. The first MNPs for capturing and magnetically separating the bacteria and TiO₂ nanocrystals to quantify the bacteria number by UV spectrophotometry (Fig. 12). The detection limit of *salmonella* in milk was found to be more than 100 cfu ml⁻¹.

5.3.1.2. Nucleic Acid Extraction and Separation. Extraction of nucleic acids (DNA and RNA) based on MNPs realized for the first time by Uhlen.⁹³ The

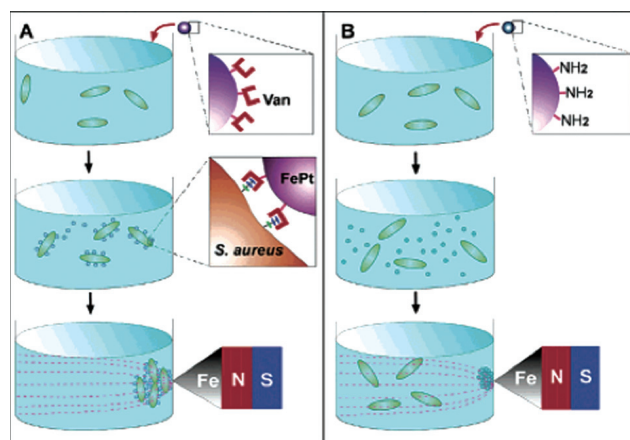


Fig. 11. Capture and separation of gram-positive bacteria by using Van-coated MNPs. Reproduced with permission from [91], H. Gu, et al., *J. Am. Chem. Soc.* 125, 15702 (2003). © 2003, American Chemical Society.

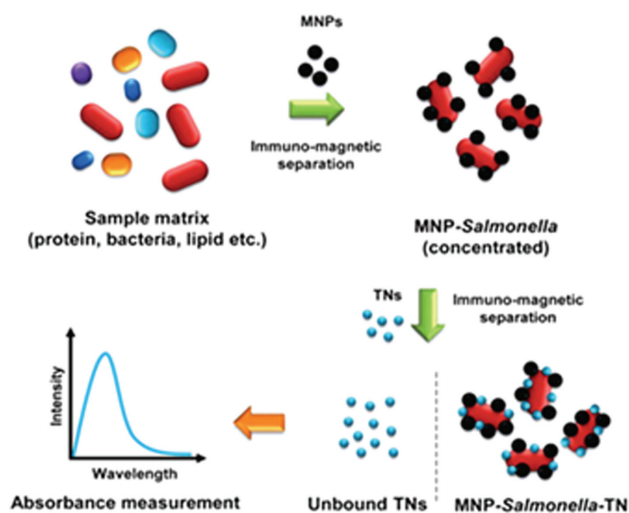


Fig. 12. Schematic illustration for separation and detection of the pathogenic bacteria using magnetic nanoparticles and optical nanoprobes. Reproduced with permission from [92], J. Joo, et al., *Analyst* 137, 3609 (2012). © 2012, Royal Society of Chemistry.

particles need a surface treatment step before nucleic acid extraction.⁹⁴ Since the interaction between the particles and nucleic acids is typically electrostatic, thus the particle surface should have an opposite charge to the DNA and RNA molecules. Since silica nanoparticles can reversibly adsorb/desorb DNA,⁹⁵ silica-coated MNPs are created and applied for extraction and separation of nucleic acids.^{96–103} In addition, another treatment for magnetic particles to be suitable for nucleic acids separation is based on the polymerization; the magnetic fluids were coated by a polymer shell, magnetic latex,^{104–108} and used to extract DNA and RNA.^{109–112} Moreover, magnetic latex based on ferrofluids was used also for *in vitro* proteins separation.^{113,114}

5.3.2. In Vivo Applications

5.3.2.1. In Vivo Diagnostic. To apply the magnetic nanoparticles for *in vivo* diagnosis, such as MRI contrast agents,^{115–119} a special attention for the synthesis to reduce the nanoparticles toxicity to the lowest level is

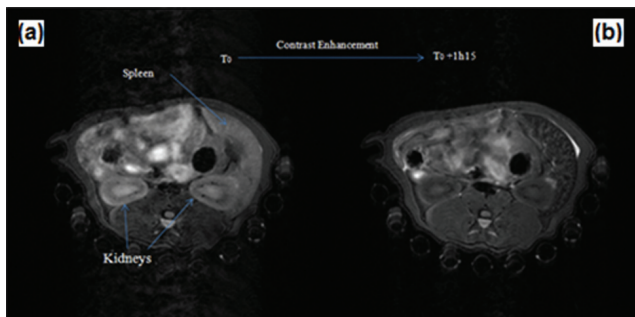


Fig. 13. T_2 enhancement of contrast in kidneys and spleen of Sprague dawley rats (a) MR image before and (b) after 1 hour and 15 min of injection of magnetic iron oxide emulsion. Reproduced with permission from [122], N. Ahmed, et al., *J. Biomed. Nanotechnol.* 9, 1579 (2013). © 2013, American Scientific Publishers.

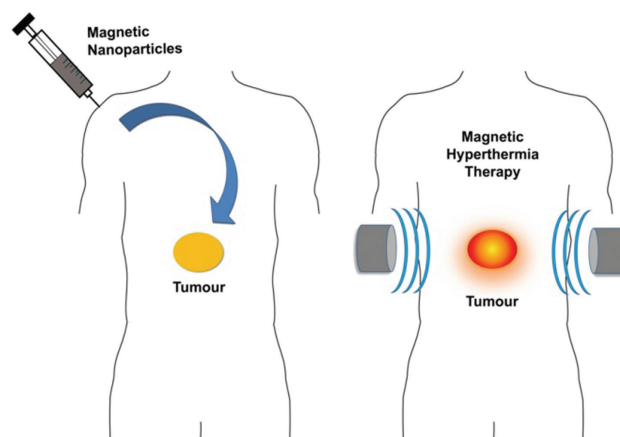


Fig. 14. Hyperthermia of tumor cells using magnetic iron oxide nanoparticles under the effect of an alternating external magnetic field. Reproduced with permission from [123], A. Andrade, et al., *Biomedical Engineering-Frontiers and Challenges*, edited by R. Fazel, InTech (2011). © 2011, InTech.

needed. In addition, surface functionalization of the MRI contrast agents with a specific target such as an antibody is required.^{85,120,121} Weissleder et al.¹¹⁷ reported the trans-gene expression *in vivo* by MRI in which MNPs were synthesized and coated with dextran and transferrin. The engineered transferrin receptor (ETR) was used to study gene focusing on its over expression accompanied with more uptakes of nanoparticles by cells.

In a recent study, o/w magnetic emulsion of colloidal particle size 250 nm stabilized by poly(ethylene oxide) surfactant was highly diluted and administered intravenously to the Sprague dawley rats to be tested as contrast agent for *in vivo* MRI. In this preliminary study, MRI images showed significant enhancement in contrast, especially for T_2 (relaxation time) contrast enhancement, indicating the distribution of magnetic colloidal nanoparticles within organs, like liver, spleen and kidneys of the Sprague dawley rats (Fig. 13). In addition, it was found that 500 μL of the highly diluted magnetic emulsion (0.05 wt.%) was found to be adequate for MR imaging.¹²²

5.3.2.2. In Vivo Therapeutic. Cancer treatment by magnetic fluid (hyperthermia) is one of the innovative applications of the ferrofluid in medicine. The cancer cell treatment by ferrofluid is achieved through magnetic field modulated cell membrane damage. Upon exposure to an alternating external magnetic field, the magnetic nanoparticles continuously emit heat.^{44,55} The produced heat is sufficient to kill tumor cells, which are highly sensitive to the increase in temperature, as compared with its surrounding normal cells (Fig. 14).¹²³

The therapeutic effect mainly depends on two mechanisms; the compromised integrity of the cell membrane and promoted apoptosis. These mechanisms are in contrast with the more common magneto-thermal effect, which requires a high-frequency oscillating magnetic field

(52 kA · m⁻¹) to achieve high magnetic saturation. For practical therapeutic applications with minimized side effects, it is critically important to obtain optimum heating efficiency to reach the desired hyperthermia temperature at 41–46 °C during a few hours. In this regard, it was reported that the use of (Zn_{0.4}Mn_{0.6})-Fe₂O₄ nanoparticles with high specific loss power (SLP) in cancer cell treatment led to the death of 84.4% of HeLa cells after the application of the AC magnetic field for 10 min. As compared with the conventional treating agent Feridex (dextran-coated MNPs), 13.5% of those cells were died.⁵⁶ In cancer cell treatment, the nanometer size ferrofluid provided high penetration depth. Such therapeutic capability is dependent on the SLP. The strategy for enhancing SLP has been important, since high SLP can bring better efficacy with a lower dosage level of magnetic nanoparticles.

6. CONCLUSION

Magnetic fluids or ferrofluids are stable dispersion of MNPs in organic or aqueous media. Synthesis of ferrofluids have been extensively studied and developed. Chemical coprecipitation is the commonly used method to synthesize ferrofluids. The obtained nanoparticles have average diameter varied from 3 to 20 nm, in addition to the superparamagnetic properties and high colloidal stability in aqueous and organic media, which are highly need for various industrial and biomedical applications.

For industrial applications, ferrofluids are widely used in magnetic recording media, which highly answer the daily increasing in electronic data size in the internet and informatics sciences. Furthermore, they were applied in magnetic paints and inks that provided high-speed reading, treatment and archiving the information. In the biomedical field, ferrofluids have found promising *in vivo* applications as MRI contrast agents and in chemotherapy. In addition, they were used *in vitro*, especially for separation, extraction and reconcentration of biomolecules, bacteria and viruses. More recently, a new form of ferrofluids (water stable dispersion) called “magnetic emulsions” has a significant attraction in the future applications.

Acknowledgment: The authors thank and appreciate the research grant (RTA5480007) from The Thailand Research Fund (TRF)/Commission on Higher Education to Pramuan Tangboriboonrat, and the scholarship from TRF, Mahidol University and French Government through the Royal Golden Jubilee Ph.D. Program (Grant No. PHD/0174/2552) to the Ph.D. student Chariya Kaewsaneha.

References and Notes

- C. P. Bean and J. D. Livingston, *J. Appl. Phys.* 30 S120 (1959).
- J. Popplewell and L. Sakhini, *J. Magn. Magn. Mater.* 149, 72 (1995).
- R. E. Rosensweig, *AIAA J.* 4, 1751 (1966).
- S. W. Charles, *J. Magn. Magn. Mater.* 65, 350 (1987).
- E. Papirer, E. Walter, A. Vidal, B. Siffert, and H. Jakusch, *J. Colloid Interface Sci.* 193, 291 (1997).
- M. Murphy, *Met. Finish.* 98, 9 (2000).
- Y. Sahoo, A. Goodarzi, M. T. Swihart, T. Y. Ohulchanskyy, N. Kaur, E. P. Furlani, and P. N. Prasad, *J. Phys. Chem. B* 109, 3879 (2005).
- S. W. Charles and J. Popplewell, *Endeavour* 6, 153 (1982).
- E. Blüms, A. Cebers, T. A. O. Sebers, and M. M. Maiorov, *Magnetic Fluids*, Walter de Gruyter, Berlin, New York (1997), p. 416.
- S. W. Charles, *Ferrofluids*, edited by S. Odenbach, Springer, Berlin Heidelberg (2012), Vol. 594, pp. 3–18.
- S. S. Papell, US Patent 3,215,575 (1965).
- A. G. Boudouvis, J. L. Puchalla, L. E. Scriven, and R. E. Rosensweig, *J. Magn. Magn. Mater.* 65 307 (1987).
- R. E. Rosensweig, *J. Magn. Magn. Mater.* 252, 370 (2002).
- R. Rosensweig, R. Kaiser, and G. Miskolczy, *J. Colloid Interface Sci.* 29, 680 (1969).
- R. E. Rosensweig, J. Popplewell, and R. J. Johnston, *J. Magn. Magn. Mater.* 85, 171 (1990).
- J. L. Neuringer and R. E. Rosensweig, *Phys. Fluids* 7, 1927 (1964).
- R. Kaiser and G. Miskolczy, *J. Appl. Phys.* 41, 1064 (1970).
- E. Blüms, R. Ozols, and R. E. Rosensweig, *J. Magn. Magn. Mater.* 85, 303 (1990).
- S. Laurent, D. Forge, M. Port, A. Roch, C. Robic, V. L. Elst, and R. N. Muller, *Chem. Rev.* 108, 2064 (2008).
- A.-H. Lu, E. L. Salabas, and F. Schüth, *Angew. Chem. Int. Ed.* 46, 1222 (2007).
- A. K. Gupta and M. Gupta, *Biomaterials* 26, 3995 (2005).
- M. Faraji, Y. Yamini, and M. Rezaee, *J. Iran. Chem. Soc.* 7, 1 (2010).
- C.-L. Lin, C.-F. Lee, and W.-Y. Chiu, *J. Colloid Interface Sci.* 291, 411 (2005).
- G. W. Reimers and G. W. Reimers, *Production of Magnetic Fluids by Peptization Techniques*, October (1974), Vol. 3843540.
- R. Tadmor, R. E. Rosensweig, J. Frey, and J. Klein, *Langmuir* 16, 9117 (2000).
- R. Massart. Préparation de ferrofluides aqueux en l'absence desurfactant: comportement en fonction du pH et de la nature des ions présentes en solution. *C. R. Acad. Sc. Paris* (1980).
- R. Massart, *IEEE Trans. Magn.* 17, 1247 (1981).
- A. Bee, R. Massart, and S. Neveu, *J. Magn. Magn. Mater.* 149, 6 (1995).
- R. Massart, E. Dubois, V. Cabuil, and E. Hasmonay, *J. Magn. Magn. Mater.* 149, 1 (1995).
- N. Moumen and M. P. Pileni, *J. Phys. Chem.* 100, 1867 (1996).
- F. Montagne, *Elaboration de latex magnétique a partir d'émulsions directes de ferrofluides*, claude bernard-lyon1 (2002).
- J. P. Jolivet, R. Massart, and J.-M. Fruchart, *Nouv J Chim.* 7, 325 (1983).
- W. Wu, Q. He, and C. Jiang, *Nanoscale Res. Lett.* 3, 397 (2008).
- J. Rockenberger, E. C. Scher, and A. P. Alivisatos, *J. Am. Chem. Soc.* 121, 11595 (1999).
- S. Sun, H. Zeng, D. B. Robinson, S. Raoux, P. M. Rice, S. X. Wang, and G. Li, *J. Am. Chem. Soc.* 126, 273 (2004).
- T. Hyeon, S. S. Lee, J. Park, Y. Chung, and H. B. Na, *J. Am. Chem. Soc.* 123, 12798 (2001).
- F. Montagne, O. Mondain-Monval, C. Pichot, H. Mozzanega, and A. Elaassari, *J. Magn. Magn. Mater.* 250, 302 (2002).
- N. Tran, A. Mir, D. Mallik, A. Sinha, S. Nayar, and T. J. Webster, *Int. J. Nanomedicine* 5, 277 (2010).
- S. Ghoshal, A. A. Ansar, S. O. Raja, A. Jana, N. R. Bandyopadhyay, A. K. Dasgupta, and M. Ray, *Nanoscale Res Lett.* 6, 540 (2011).

40. J.-C. Bacri, R. Perzynski, D. Salin, V. Cabuil, and R. Massart, *J. Magn. Magn. Mater.* 85, 27 (1990).
41. U. Jeong, X. Teng, Y. Wang, H. Yang, and Y. Xia, *Adv. Mater.* 19, 33 (2007).
42. T. Hyeon, S. S. Lee, J. Park, Y. Chung, and H. B. Na, *J. Am. Chem. Soc.* 123, 12798 (2001).
43. B. Mehdaoui, A. Meffre, L.-M. Lacroix, J. Carrey, S. Lachaize, M. Gougeon, M. Respaud, and B. Chaudret, *J. Magn. Magn. Mater.* 322, L49 (2010).
44. D. Yoo, J.-H. Lee, T.-H. Shin, and J. Cheon, *Accounts Chem. Res.* 44, 863 (2011).
45. R. Hergt and S. Dutz, *J. Magn. Magn. Mater.* 311, 187 (2007).
46. H. Mouaziz, R. Veyret, A. Theretz, F. Ginot, and A. Elaissari, *J. Biomed. Nanotechnol.* 5, 172 (2009).
47. V. Biju, *Chem. Soc. Rev.* 43, 744 (2014).
48. S. Khalafalla, *Chem. Tech.* 5, 540 (1975).
49. A. Tari, R. W. Chantrell, S. W. Charles, and J. Popplewell, *Phys. BC* 97, 57 (1979).
50. S. Khalafalla and G. Reimers, *Magn. IEEE Trans.* 16, 178 (1980).
51. A. Nakayama, K. Nakamura, K. Hata, and M. Yamamoto, *Magnetic Paint for Magnetic Recording Media* 4594174, June (1986).
52. K. Furumura, H. Sugi, Y. Murakami, and H. Asai, Sealing and Bearing Means by Use of Ferrofluid, 4598914, July (1986).
53. A. Halbreich, J. Roger, J. N. Pons, D. Geldwerth, M. F. Da Silva, M. Roudier, and J. C. Bacri, *Biochimie* 80, 379 (1998).
54. J. Lu, S. Yang, K. M. Ng, C.-H. Su, C.-S. Yeh, Y.-N. Wu, and D.-B. Shieh, *Nanotechnology* 17, 5812 (2006).
55. D. Ho, X. Sun, and S. Sun, *Accounts Chem. Res.* 44, 875 (2011).
56. J. Jang, H. Nah, J.-H. Lee, S. H. Moon, M. G. Kim, and J. Cheon, *Angew. Chem. Int. Ed.* 48, 1234 (2009).
57. Y. V. Gulyaev, A. N. Kalinkin, A. Y. Mityagin, and B. V. Khlopov, *Inorg. Mater.* 46, 1403 (2010).
58. E. Schonafinger, *Iron Oxide Magnetic Pigments for the Production of Magnetic Coatings* November (1981).
59. J. Meng, G. Yang, L. Yan, and X. Wang, *Dyes Pigments* 66, 109 (2005).
60. X. Wang, G. Yang, Z. Zhang, L. Yan, and J. Meng, *Dyes Pigments* 74, 269 (2007).
61. Van Nostrand's Scientific Encyclopedia, John Wiley & Sons, Inc. (2005).
62. H. Hibst, *J. Magn. Magn. Mater.* 74, 193 (1988).
63. D. Speliotis, M. Dugas, J. Humenansky, K. L. Babcock, and K. Peter, *J. Appl. Phys.* 81, 3830 (1997).
64. P. R. Bissell, *Encyclopedia of Materials: Science and Technology*, 2nd edn., edited by K. H. J. Buschow, R. W. Cahn, M. C. Flemings, B. Iltschner (print), E. J. Kramer, S. Mahajan, P. Veysseyre (updates), Elsevier, Oxford (2001), pp. 4889.
65. B. Terris, *Encyclopedia of Materials: Science and Technology*, 2nd edn., edited by K. H. Jürgen Buschow Robert W. Cahn, Merton C. Flemings, Bernard Iltschner (print), Edward J. Kramer, Subhash Mahajan, Patrick Veysseyre (updates), Elsevier, Oxford (2011), pp. 1–6.
66. H. L. Gowda, C. J. Cheever, and F. Bloom, Ferrofluid seal for a stationary shaft and a rotating hub. 4694213, September (1987).
67. C. S. Hajec, Electric motor with ferrofluid bearing. 4734606, March (1988).
68. T. J. B. Jr, Ferrofluid exclusion seal and method of assembly. 4817964, April (1989).
69. J. E. Leland, Ferrofluid piston pump for use with heat pipes or the like. 5005639, April (1991).
70. W. Ochoński, *Wear* 130, 261 (1989).
71. R. Currie, *Seal. Technol.* 2002, 6 (2002).
72. H. Hartshorne, C. J. Backhouse, and W. E. Lee, *Sensors Actuators B Chem.* 99, 592 (2004).
73. R. Veyret, T. Delair, and A. Elaissari, *J. Magn. Magn. Mater.* 293, 171 (2005).
74. N. Miletić, A. Nastasović, and K. Loos, *Bioresour. Technol.* 115, 126 (2012).
75. M. M. Rahman, hasan. Ahmad, and M. M. Islam, *J. Colloid Sci. Biotechnol.* 2, 171 (2013).
76. X. Luo and L. Zhang, *Biomacromolecules* 11, 2896 (2010).
77. J. Wang, G. Meng, K. Tao, M. Feng, X. Zhao, Z. Li, H. Xu, D. Xia, and J. R. Lu, *PLoS ONE* 7, e43478 (2012).
78. E. Karaoğlu, A. Baykal, M. Şenel, H. Sözeri, M. S. Toprak, *Mater. Res. Bull.* 47, 2480 (2012).
79. I. Hilger, S. Frühauf, W. Linß, R. Hiergeist, W. Andrä, R. Hergt, W. A. Kaiser, *J. Magn. Magn. Mater.* 261, 7 (2003).
80. hasegawa, masakatsu; hokkoku, syusaburo. Magnetic iron oxide-dextran complex and process for its production. 4,101,435, July 18, (1978).
81. L. M. Lacava, Z. G. M. Lacava, M. F. Da Silva, O. Silva, S. B. Chaves, R. B. Azevedo, F. Pelegrini, C. Gansau, N. Buske, D. Sabolovic, and P. C. Morais, *Biophys. J.* 80, 2483 (2001).
82. L. M. Lacava, V. A. P. Garcia, S. Kückelhaus, R. B. Azevedo, Z. G. M. Lacava, O. Silva, F. Pelegrini, C. Gansau, N. Buske, and P. C. Morais, *J. Appl. Phys.* 93, 7563 (2003).
83. A. E. Senyei and K. J. Widder, Method of magnetic separation of cells and the like, and microspheres for 4230685, October (1980).
84. C. C. Berry, S. Wells, S. Charles, and A. S. G. Curtis, *Biomaterials* 24, 4551 (2003).
85. D. Horák, Z. Svobodová, J. Autebert, B. Coudert, Z. Plichta, K. Královce, Z. Bílková, and J.-L. Viovy, *J. Biomed. Mater. Res. A* 101A, 23 (2013).
86. O. Olsvik, T. Popovic, E. Skjerve, K. S. Cudjoe, E. Hornes, J. Ugelstad, and M. Uhlén, *Clin. Microbiol. Rev.* 7, 43 (1994).
87. J.-L. Guesdon and S. Avrameas, *Immunochemistry* 14, 443 (1977).
88. Z.-M. Liu, H.-F. Yang, Y.-F. Li, Y.-L. Liu, G.-L. Shen, and R.-Q. Yu, *Sensors Actuators B Chem.* 113, 956 (2006).
89. S. Miltényi, W. Müller, W. Weichel, and A. Radbruch, *Cytometry* 11, 231 (1990).
90. C. Sestier, M. F. Da-Silva, D. Sabolovic, J. Roger, and J. N. Pons, *Electrophoresis* 19, 1220 (1998).
91. H. Gu, P.-L. Ho, K. W. T. Tsang, L. Wang, and B. Xu, *J. Am. Chem. Soc.* 125, 15702 (2003).
92. J. Joo, C. Yim, D. Kwon, J. Lee, H. H. Shin, H. J. Cha, and S. Jeon, *Analyst* 137, 3609 (2012).
93. M. Uhlen, Publ. Online 31 August 1989 Doi101038340733a0 340, 733 (1989).
94. J. Prodralová, B. Rittich, A. Spanová, K. Petrová, and M. J. Benes, *J. Chromatogr. A* 1056, 43 (2004).
95. M. Strege and A. Lagu, *Anal. Chem.* 63, 1233 (1991).
96. P. Ashtari, X. He, K. Wang, and P. Gong, *Talanta* 67, 548 (2005).
97. Z. Zhang, L. Zhang, L. Chen, L. Chen, and Q. Wan, *Biotechnol. Prog.* 22, 514 (2006).
98. Y. Liang, J.-L. Gong, Y. Huang, Y. Zheng, J.-H. Jiang, G.-L. Shen, and R.-Q. Yu, *Talanta* 72, 443 (2007).
99. M. Park and J. Chang, *Mater. Sci. Eng. C* 27, 1232 (2007).
100. X. He, H. Huo, K. Wang, W. Tan, P. Gong, and J. Ge, *Talanta* 73, 764 (2007).
101. K. Kang, J. Choi, J. H. Nam, S. C. Lee, K. J. Kim, S.-W. Lee, and J. H. Chang, *J. Phys. Chem. B* 113, 536 (2009).
102. X. Li, J. Zhang, and H. Gu, *Langmuir* 27, 6099 (2011).
103. J. Zhang, W. Sun, L. Bergman, J. M. Rosenholm, M. Lindén, G. Wu, H. Xu, and H. Gu, *Mater. Lett.* 67, 379 (2012).
104. A. Elaissari, *Tech. Ingénieur J* 2 275 (2008).
105. J.-C. Daniel, J.-L. Schuppiser, and M. Tricot, deceased. Magnetic polymer latex and preparation process. 4358388, November (1982).
106. F. Montagne, O. Mondain-Monval, C. Pichot, and A. Elaissari, *J. Polym. Sci. Part Polym. Chem.* 44, 2642 (2006).
107. S. Braconnot, C. Hoang, H. Fessi, and A. Elaissari, *Mater. Sci. Eng. C* 29, 624 (2009).

108. J. Dou, Q. Zhang, L. Jian, and J. Gu, *Colloid Polym. Sci.* 288, 1751 (2010).
109. A. Elaissari, M. Rodrigue, F. Meunier, and C. Herve, *J. Magn. Magn. Mater.* 225, 127 (2001).
110. A. Elaissari, *Macromol. Symp.* 281, 14 (2009).
111. A. Elaissari and H. Fessi, *Macromol. Symp.* 288, 115 (2010).
112. M. M. Rahman and A. Elaissari, *J. Colloid Sci. Biotechnol.* 1, 3 (2012).
113. A. Elaissari and V. Bourrel, *J. Magn. Magn. Mater.* 225, 151 (2001).
114. Z.-A. Lin, J.-N. Zheng, F. Lin, L. Zhang, Z. Cai, and G.-N. Chen, *J. Mater. Chem.* 21, 518 (2010).
115. S. Saini, J. Sullivan, J. T. Ferrucci Jr., D. D. Stark, and J. Wittenberg, *Magn. Reson. Imaging* 4, 179 (1986).
116. D. Pouliquen, J. J. Le Jeune, R. Perdrisot, A. Ermias, and P. Jallet, *Magn. Reson. Imaging* 9, 275 (1991).
117. R. Weissleder, A. Moore, U. Mahmood, R. Bhorade, H. Benveniste, E. A. Chiocca, and J. P. Bacion, *Nat. Med.* 6, 351 (2000).
118. J. W. M. Bulte and D. L. Kraitchman, *NMR Biomed.* 17, 484 (2004).
119. H. Lee, H. Shao, Y. Huang, and B. Kwak, *Magn. IEEE Trans.* 41, 4102 (2005).
120. J. R. McCarthy and R. Weissleder, *Adv. Drug Deliv. Rev.* 60, 1241 (2008).
121. M.-S. Martina, J.-P. Fortin, C. Ménager, O. Clément, G. Barratt, C. Grabielle-Madelmont, F. Gazeau, V. Cabuil, and S. Lesieur, *J. Am. Chem. Soc.* 127, 10676 (2005).
122. N. Ahmed, C. Jaafar-Maalej, M. M. Eissa, H. Fessi, and A. Elaissari, *J. Biomed. Nanotechnol.* 9, 1579 (2013).
123. A. Andrade, R. Ferreira, J. Fabris, and R. Domingues, *Biomedical Engineering-Frontiers and Challenges*, edited by R. Fazel, InTech (2011).

Received: 27 March 2014. Accepted: 15 May 2014.

Delivered by Publishing Technology to: University of Lyon-1
IP: 134.214.70.27 On: Tue, 04 Nov 2014 14:58:35
Copyright: American Scientific Publishers

CHAPTER II.2

Soft Hybrid Nanoparticles:fromPreparation to Biomedical Applications

Summary

Hybrid particles are a class of materials that include both organic and inorganic moieties at the same time and also possess interesting magnetic, optical and mechanical properties. Other properties that make them suitable for plethora of biomedical applications are superparamagnetism, biodegradability and fluorescence. Extensive research efforts are undergoing to explore the effectiveness of these particles for not only in therapeutics but also in diagnostic technology. Although, variety of nanoparticles have been employed for their potential applications in biomedical field, yet most interesting of them are the hybrid particles having both the magnetic properties and the ability to functionalize with important drug moieties and biomolecules. Many methods have been developed for the synthesis and characterization of soft hybrid core-shell colloidal particles including polymer immobilization on preformed particles, adsorption of polymers on colloidal particles, adsorption of polymers via layer-by-layer self-assembly, adsorption of nanoparticles on colloidal particles, chemical grafting of preformed polymers, polymerization from and on to colloidal particles, click chemistry, atomic-transfer radical polymerization (ATRP), reversible addition-fragmentation chain-transfer radical (RAFT) polymerization, nitroxide-mediated polymerization (NMP) and conventional seed radical polymerization.

In order to develop and find uses for soft hybrid core-shell colloidal particles, there is always a need to incorporate certain characteristics to meet the specific demands of desirable biomedical application. Each method and technique has its own merits that are mainly dependent on the nature of particles, safety considerations, composition, size distribution etc. The softness of such nanoparticles is attributed mainly to the soft polymer shell. Such materials can be prepared using different processes starting from easy to more complex approaches. The first and easiest method is basically the adsorption of polymer layers on hybrid nanoparticles. The adsorption can be performed in one step or multiple steps such as random sequential adsorption of oppositely charged polymers. It is interesting that the adsorption process leads to the presence of some aggregated particles due to the bridging flocculation phenomenon. Consequently, this adsorption approach was discarded. Chemical grafting has been widely studied to avoid the problems associated with adsorption. This is done by using batch grafting of reactive polymers, 'grafting from' or 'grafting to'. The chemical grafting approach involves the immobilization of preformed polymers or using chemical synthesis approaches, including mainly conventional seeded polymerization process "from" or "onto" the colloidal particles. However, conventional polymerization leads to layers of heterogeneous thickness and to an uncontrolled degree of polymerization of the formed brush soft layer.

Polymerization methods such as ATRP, RAFT and NMP have been studied to control the microstructure and the soft shell part. Another interesting polymerization based on click chemistry has also been investigated and showed promising results but RAFT polymerization remains the most credible approach and leads to a well-controlled soft layer.

Soft hybrid colloidal particles are designed to control surface functionality, morphology and chemical composition to evaluate them in variety of medical fields at different levels. For example, they have been examined as a solid support for sample preparation and in biotechnology as in rapid diagnostics. Newer diagnostic techniques require minute samples and are also required to be less invasive, safe, quick and with the highest possible accuracy in terms of detection. Soft hybrid colloidal particles have showed significant promise in this regard. Hairy- like colloidal particles bearing end chains and containing desired functional groups (mainly carboxylic acid groups in the surface) are generally being utilized for chemical grafting of biomolecules in order to enhance the capture efficiency of a target analyte. In this regards, these particles have been extensively and successfully examined.

Highly charged tentacles on the surface of these particles are effectively being exploited for the extraction of biomolecule via adsorption, The main purpose of biomedical applications is to enhance sensitivity and specificity, but in the area of nucleic acid probes, problems such as level of sensitivity is the most encountered issue and can be efficiently solved using soft hybrid nanoparticles. Extraction of nucleic acids can be done either by non-specific capture or by specific capture. On the same lines, proteins have been extracted from the given samples using soft hybrid nanoparticles and this provides a great mean for the quick and efficient diagnosis of variety of diseases and biomarkers. For protein denaturation and irreversible adsorption, polystyrene has been used as a solid phase when applied in diagnostic field. The use of thermosensitive microgel particles with low critical solution temperature (LCST) is of great interest in the biomedical field, because their physicochemical properties and the adsorption of proteins can be controlled by changing pH, the salinity of the medium and the temperature.

The extraction of hemorrhagic viruses such as Lassa and Ebola is a recent diagnostic method for developing countries. Soft hybrid nanoparticles owing to their characteristic properties showed a significant promise for not only the detection but quantification of the viruses for the diagnosis of diseases. Colloidal particles and especially the soft hybrid nanoparticles have potential and promising applications, particularly in the biomedical diagnostic domain. The fascinating features of such colloidal particles make them good and suitable candidate for rapid conjugation and sensitive detection of various biomolecules even with minute volume of analytes.

Functionalized soft nanoparticles are used for sample preparation in which the extraction of biomolecules such as proteins, nucleic acids, viruses and bacteria are of paramount importance in order to enhance the sensitivity of *in-vitro* medical diagnostics. Since, the discovery of biotechnology, special attention has been dedicated to the elaboration of multifunctionalized and stimuli-responsive soft hybrid nanoparticles for use not only as solid supports for the immobilization of biomolecules, but also for transport and even detection in microsystems combining microfluidic and lab-on-a-chip technology.

CHAPTER 9

Soft Hybrid Nanoparticles: from Preparation to Biomedical Applications

TALHA JAMSHAD,^{a,b} MOHAMED EISSA,^{a,c} NADIA ZINE,^b
ABDELHAMID ERRACHID EL-SALHI,^b NASIR M. AHMAD^d AND
ABDELHAMID ELAISSARI*^a

^a University of Lyon, 69622 Lyon, France; University of Lyon-1, Villeurbanne, CNRS, UMR-5007, LAGEP-CPE; 43 boulevard 11 Novembre 1918, 69622 Villeurbanne, France; ^b Institut des Sciences Analytiques (ISA), Université Lyon, Université Claude Bernard Lyon-1, UMR-5180, 5 rue de la Doua, 69100 Villeurbanne, France; ^c Polymers and Pigments Department, National Research Centre, Dokki, Giza 12622, Egypt; ^d Polymer and Surface Engineering Laboratory, Department of Materials Engineering, School of Chemical and Materials Engineering (SCME), National University of Sciences and Technology (NUST), Islamabad-44000, Pakistan
*Email: elaissari@lagep.univ-lyon1.fr

9.1 Introduction

Colloidal particles provide highly useful diagnostic solutions and standardized results through efficient screening processes for several diseases.^{1–6} Furthermore, newer diagnostic techniques require minute samples and also need to be less invasive, safe and quick and with the highest possible accuracy in terms of detection.⁷ In this context, various types of functional

RSC Nanoscience & Nanotechnology No. 34

Soft Nanoparticles for Biomedical Applications

Edited by José Callejas-Fernández, Joan Estelrich, Manuel Quesada-Pérez and Jacqueline Forcada

© The Royal Society of Chemistry 2014

Published by the Royal Society of Chemistry, www.rsc.org

colloidal particles have been developed and explored for their biomedical applications. Among the key features of such functional colloidal particles are their soft hybrid core-shell structures, which are engineered in such a way that the core consists of an inorganic material whereas the shell is composed of a soft organic substance.⁸ In other words, hybrid particles are a class of materials that include both organic and inorganic moieties at the same time and also possess interesting magnetic, optical and mechanical properties.^{9,10} These particles are used for optical investigations of biological interactions and their other significant properties such as superparamagnetism, biodegradability and fluorescence.¹¹ These particles also have the ability to occupy space much more efficiently, allowing the dispersed phase to reach much higher volume fractions than random close packing of spheres.¹² These materials have potential applications in areas such as gas separation, catalysis, storage and, most importantly, biomaterials for diverse biomedical applications. Their unique characteristics make them suitable materials for developing desirable patterns or functions by exploiting nanoscale phenomena through build-up *via* atom-by-atom or molecule-by-molecule methods (top-down) or through self-organization (bottom-up).¹³

Extensive research efforts are being made to develop and explore the biomedical applications of soft hybrid nanoparticles.¹⁻⁶ In addition, numerous types of the soft hybrid nanoparticles have been developed to target specific biomedical applications and to perform desirable diagnostics or therapeutic functions. For example, with current rapid advances in nanomedicine, colloiddally engineered particles are gaining immense importance in biomedical fields such as cancer and gene therapy,¹⁴⁻¹⁷ disease diagnosis¹⁸ and bioimaging.¹⁹⁻²¹ During the past decade, numerous colloidal particles have been created and widely investigated for medical use.²²⁻²⁵ Innovations in development have been able to incorporate diverse functionalities, and colloidal particles bearing reactive groups (*e.g.* -COOH, -NH₂, -SH) and dendrimers have been developed for the covalent binding of biomolecules in order to be used as a solid support for the specific capture of targets and imaging. Colloidal particles are also designed in such a way that they have suitable particle size, hydrophilic-lipophilic balance (HLB), size distribution and surface reactive groups for the target diagnosis.²⁶ The attachment of many macromolecules (*e.g.* polysaccharides, proteins, lecithins, antibodies, glycoproteins) can be non-covalent and generally probes such as gold acquire the properties of attached macromolecules. Their stability upon storage is also very good.²⁷ Furthermore, gold nanoparticles can absorb light over a wide spectral range, from the visible to near-infrared, and can be used for diagnosis as optically tuneable carriers because of their shape and size.²⁸ Soft hybrid nanoparticles of calcium phosphate/hydroxyapatite and mesoporous silica particles have been employed to carry drugs and DNA to intracellular organelles by interaction with cells.²⁹⁻³¹ Polymer-based latexes have been widely used as carriers for antigen and antibody reactions in immunoagglutination assays and were first used to detect rheumatoid

factor.³² Various other core materials have also been employed for diagnostics and bioimaging, such as quantum dots (QDs), silver nanorods to separate viruses, bacteria and microscopic components of blood samples (allowing the identification of these parameters in less than 1 h) and carbon nanotubes (CNTs), which are used in sensors to detect proteins specific to oral cancer.³³ Other very interesting types of colloidal particles are based on magnetically active inorganic particles in the core to introduce magnetic properties, which enhances the concentration of the targeted biomolecules and consequently the sensitivity of the biomedical diagnostic. Magnetically responsive hybrid iron oxide colloidal nanoparticles have superparamagnetic properties and are extensively used in bioimaging to provide high diagnostic accuracy in the detection of atherosclerosis, cancer, arthritis and many other diseases.^{34–36} Owing to their magnetic character, which can be controlled through the application of an external magnetic field, magnetic particles and latexes are extensively used in biomedical diagnosis such as in molecular biology, bacteria and virus isolation, immunoassays, nucleic acid extraction (NAE) and cell sorting.³⁷ Dual magnetic and luminescent properties which help in different types of diagnosis and the incorporation of functional groups on soft hybrid colloidal nanoparticles have also been developed and many biomolecules have been immobilized for selective organelle labelling used in the detection of polynucleotides^{12,38} (DNA, RNA).

9.2 Development of Soft Hybrid Core-Shell Nanoparticles

Many methods and techniques have been developed to synthesize and characterize soft hybrid core-shell colloidal particles, as discussed elsewhere.^{1,2,5,34} Each method and technique has its own merits that are mainly dependent on the nature of the particles, safety considerations, composition, size distribution, *etc.* Keeping in mind the importance of developing soft hybrid nanoparticles, a few important methods are discussed below to provide an overview of the state of the art in this important area.

9.2.1 Polymer Immobilization on Preformed Particles

In order to develop and find uses for soft hybrid core-shell colloidal particles, there is always a need to incorporate certain characteristics to meet the specific demands of desirable biomedical applications. These characteristics include a certain degree of hydrophilicity, composition, architecture, surface energy and stimuli-responsive character. For this purpose, the immobilization of polymers provides perhaps the most powerful tool for tuning the surface properties of the shell without much affecting the characteristics of the core particles. In this direction, extensive research work has been carried out and an attempt is made below to outline concisely some of these techniques.

9.2.2 Adsorption of Polymers on Colloidal Particles

Adsorption is a process that mostly occurs at the surface of an adsorbent.³⁹ In the case of polymers, when these interact with colloidal particles, their adsorption on the surface of particles takes place through specific interactions of functional groups present in the chains. The stabilization of colloidal particles can be controlled through various parameters at the solid/liquid interface.^{40,41} A scheme of the adsorption of polymer chains on colloidal particles is illustrated in Figure 9.1. Adsorption of polymers on solid particle surfaces takes place because of either electrostatic (Coulombic) interactions or others, such as polar or non-polar forces or weaker van der Waals forces.⁴² It is also possible that weaker or incomplete adsorption leads to the aggregation of particles. Colloidal dispersions are generally stable only if there is no aggregation and this stability develops only in the presence of some repulsive forces, the nature of which can be electrostatic or steric. Particles having surface charges play an important role in electrostatic stabilization. Diffuse adsorbed layers that start to overlap induce an electrostatic repulsive force and produce stable dispersions because the range of this repulsive force is greater than the van der Waals attraction.

Polymer adsorption on the particle surface plays an important role in steric stabilization because the thickness of the polymer layer protects particles from aggregation due to van der Waals forces. Adsorbed polymer chains have part of their segments in contact with the surface, but they do not constitute rigid structures and continually change their conformation. When polymer chains change the relative position of their adsorbed segments, they retain a large degree of their conformational freedom. In other words, the segments in contact with the surface continually exchange their position with non-adsorbed segments. Two surfaces with adsorbed polymers tend to confine these polymers in approaching each other, so this process is not entropically favourable and can eventually cause repulsion between

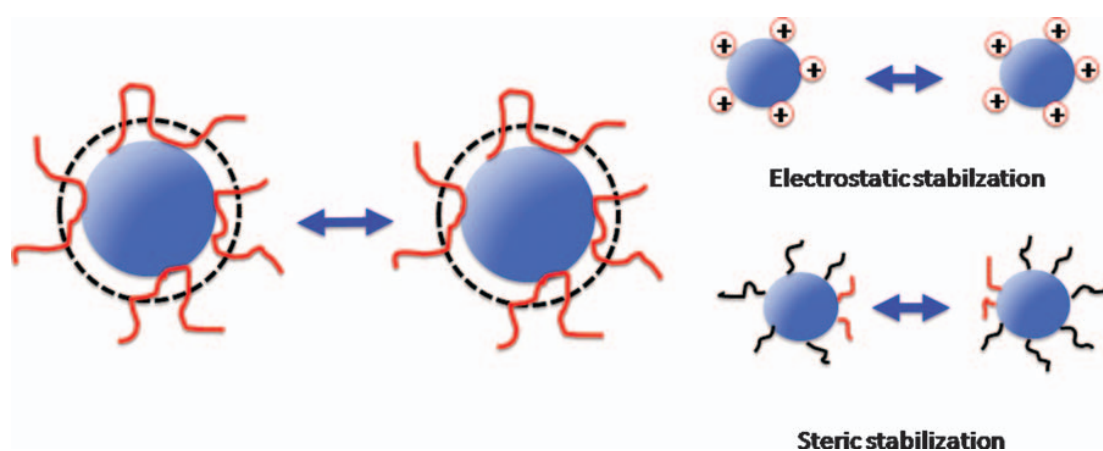


Figure 9.1 Top: electrostatic contribution to colloid stability, two like-charged particles repelling each other. Bottom: steric contribution to colloid stability, polymer chains being pushed together and confined are repelled owing to the unfavourable decrease in entropy.

them. Among the various polymers, perhaps diblock copolymers are the most widely used owing to the different advantages of steric stabilization. In fact, steric stabilization offers more advantages than charge stabilization.⁴³ Hence the use of adsorbed polymers either to stabilize or to flocculate plays an important role in applications such as colloidal stabilization, lubrication and adhesion.^{44–46}

9.2.3 Adsorption of Polymers *via* Layer-by-Layer Self-Assembly

This method provides a versatile approach to tuning the properties of colloidal particles by adsorption of polyelectrolytes.⁴⁷ The adsorption generally takes place through electrostatic Coulombic interactions between oppositely charged polyelectrolytes and colloidal particles. Generally, irreversible electrostatic attraction helps polyelectrolyte adsorption at supersaturating bulk concentrations. There are also other types of interaction that can be utilized for assembly in layer-by-layer (LBL) systems, namely van der Waals and hydrophobic interactions and hydrogen bonding. The important features that need to be considered in the LBL method include control of the number of layers, thickness, functionalities, roughness, morphology, composition, surface energy and many more. Furthermore, desirable surface properties on the colloidal particles or templates of almost any topography (spherical or others) can be incorporated by simply varying different parameters such as pH, salt concentration, type of polyelectrolyte (weak or strong) and solvent.^{3,48} The formed polyelectrolyte-coated colloidal particles can be further adsorbed with additional oppositely charged nanoparticles of various types including gold and molecular precursors to give ultrathin multilayers films of molecular precursor layer and nanoparticles,⁴⁸ as shown in Figure 9.2.⁴⁹ Similarly, by employing the LBL technique, oil-in-water submicron magnetic emulsions have also been obtained, as presented in Figure 9.2(iii).⁵⁰

9.2.4 Adsorption of Nanoparticles on Colloidal Particles

There are many techniques that can be employed to adsorb polymer nanoparticles including (but not limited to) various polymerization methods, physiochemical LBL methods and stepwise heterocoagulation.^{51–53} In the stepwise heterocoagulation method, electrostatic interactions are exploited to induce the coating of relatively small particles on the larger ones. One of the pioneering examples included the adsorption of small polystyrene (PS) particles with cationic charges particles on large PS particles with anionic charges.⁵¹ The heterocoagulation driven by electrostatic interaction produces a monolayer of smaller particles on the larger particles through an adsorption process resulting in the formation of core-shell colloidal particles. By applying the heterocoagulation method, several types of soft core-shell colloidal particles with well-controlled morphologies have

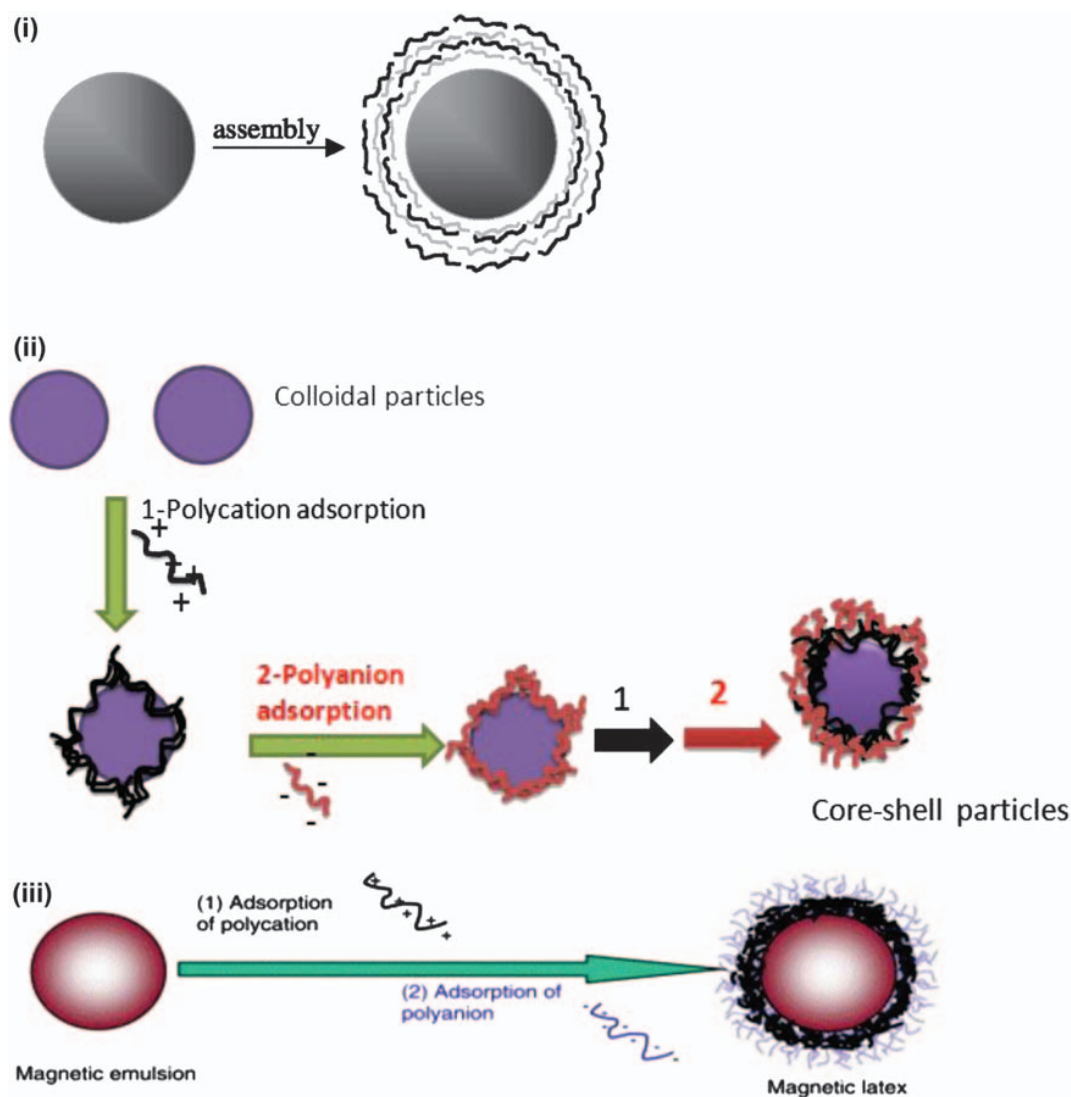


Figure 9.2 (i) Schematic illustration of LBL adsorption on a particle surface through self-assembly. (ii) Polyelectrolyte multilayers *via* LBL adsorption. (iii) LBL adsorption on a magnetic emulsion using a polycation and a polyanion.

been reported, including the adsorption of magnetic nanoparticles on sub-micron-sized PS latex particles.⁵¹ In order to stop any release of magnetic nanoparticles, the encapsulation of the magnetic layer can be carried out *via* polymerization to form a cross-linked shell.⁵¹ In order to overcome low sedimentation rates and specific areas for non-specific or specific binding with biomolecules for such larger sized particles, various modifications to the stepwise heterocoagulation have been proposed. For example, sub-micron highly magnetic particles and also fluorescent polymer particles were designed based on innovative stepwise heterocoagulation processes, as shown in Figure 9.3. The synthesis of polymer core-shell particles by stepwise heterocoagulation has typically used smaller coating particles with low glass transition temperatures, T_g . This low T_g was exploited and used as a model to develop the heterocoagulates, which were obtained by heating at a temperature

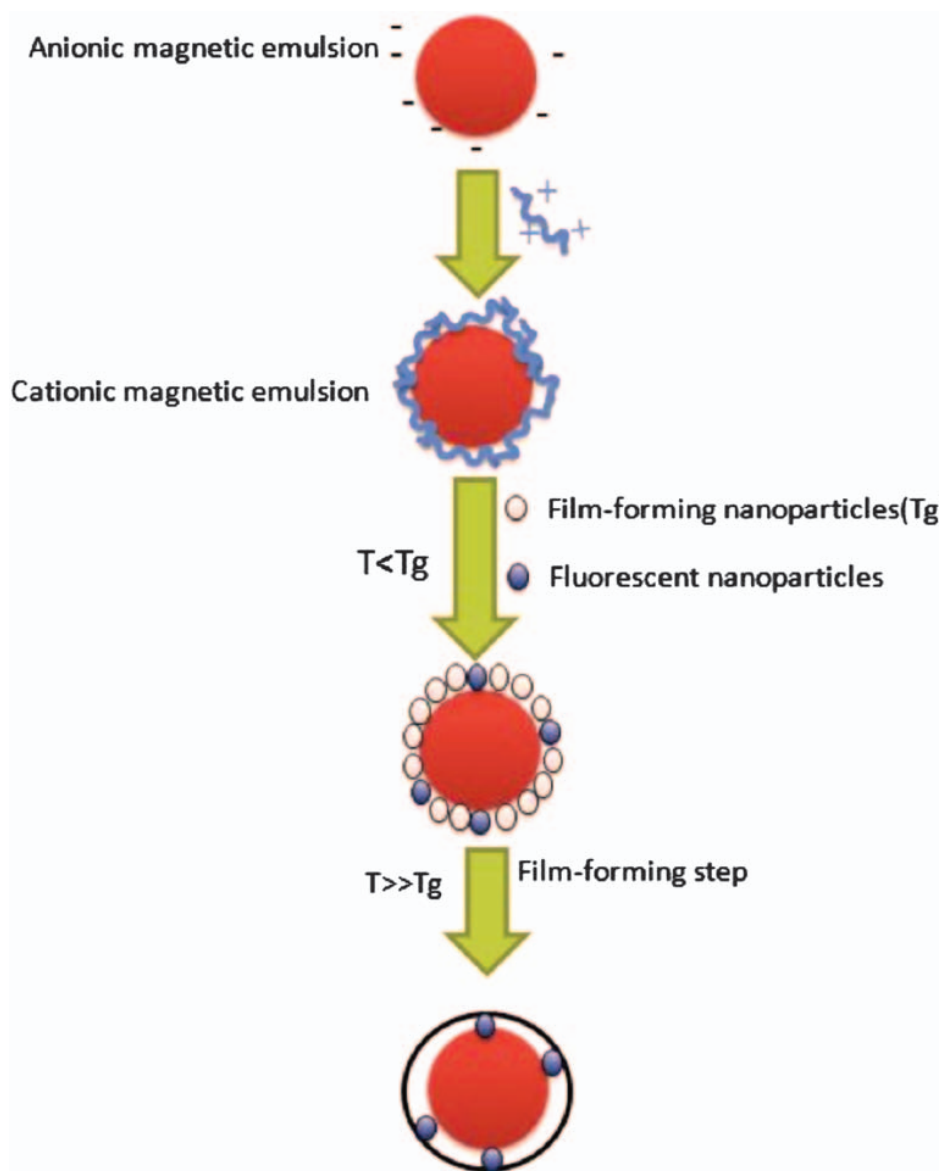


Figure 9.3 Stepwise heterocoagulation processes to form magnetic particles. Adapted from Refs. 54 and 55.

lower than the T_g of the larger particles, but above the T_g of the smaller film-forming nanolatex particles to form a homogeneous polymer shell.⁵² Therefore, such a process does not require any additional (or final) polymerization step to encapsulate the adsorbed nanoparticles *via* polymerization.^{54,55}

9.2.5 Chemical Grafting of Preformed Polymers

Grafting, in the context of polymer chemistry, refers to the addition of polymer chains to a surface.^{56,57} The grafting is a useful tool for altering the physical and/or chemical activity or interaction of the surface through processes of grafting 'to' and 'from'. Ultrathin (end-) grafted polymer layers are well known to affect dramatically the surface properties of substrates such as adhesion, lubrication, wettability, friction and biocompatibility. The layers are frequently used to modulate the surface properties of various materials,

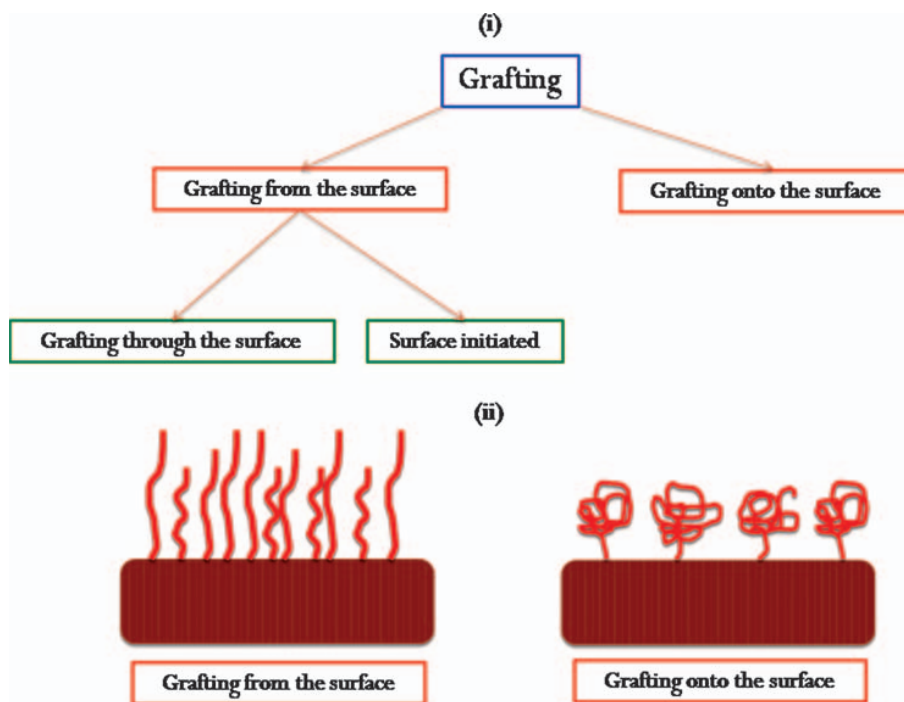


Figure 9.4 Grafting processes: (i) an overview of the grafting process; (ii) ‘grafting from’ and ‘grafting to’ a surface.

including colloidal particles, without altering their bulk performance. The chemical grafting of polymers can be accomplished by ‘grafting to’ or ‘grafting from’ methods. According to the ‘grafting to’ technique, end-functionalized polymer molecules react with complementary functional groups located on the surface to form tethered chains. The ‘grafting from’ technique utilizes the polymerization initiated from the substrate surface by initiating groups usually attached by covalent bonds. Most of the grafting methods developed – ‘to’ and ‘from’ – require the attachment of (end-) functionalized polymers or low molecular weight substances (*e.g.* initiators) to the substrate for the synthesis of the polymer brush. Usually the coupling methods are relatively complex and specific for certain substrate–(macro) molecule combinations.

A schematic overview of these two different grafting processes is presented in Figure 9.4 and discussed below.

9.2.6 Polymerization from and on to Colloidal Particles

Soft hybrid core-shell colloidal materials can be made by either the ‘grafting to’ or the ‘grafting from’ mechanism.⁵⁸ The mechanisms and advantages of these grafting processes are different and widely used to prepare colloidal particles bearing a polymer shell as shown in Figures 9.5 and 9.6. These two processes adopt two possible conformations known commonly as mushroom and polymer brush.

In the ‘grafting to’ mechanism, a preformed polymer chain is adsorbed on a surface from solution. Because prepolymerized chains used in this

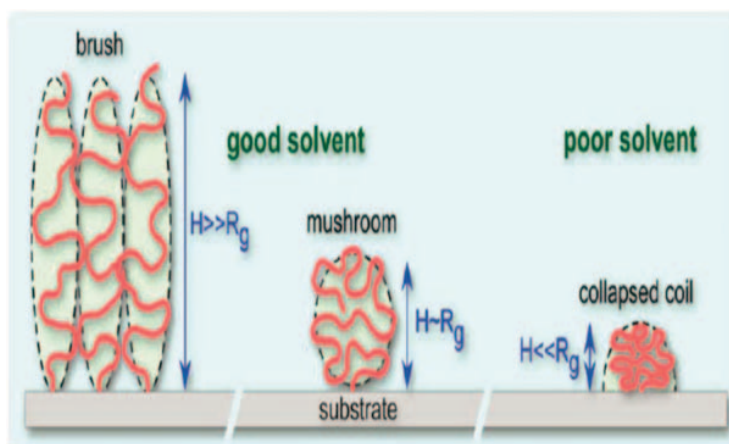


Figure 9.5 Possible conformations of 'grafted from' polymers from a surface in brush form and surface grafted in the mushroom shape in a good solvent. The conformation of 'grafted to' polymer in a poor solvent is also shown. R_g is the radius of gyration of the polymer chain and H is its thickness.⁵⁹

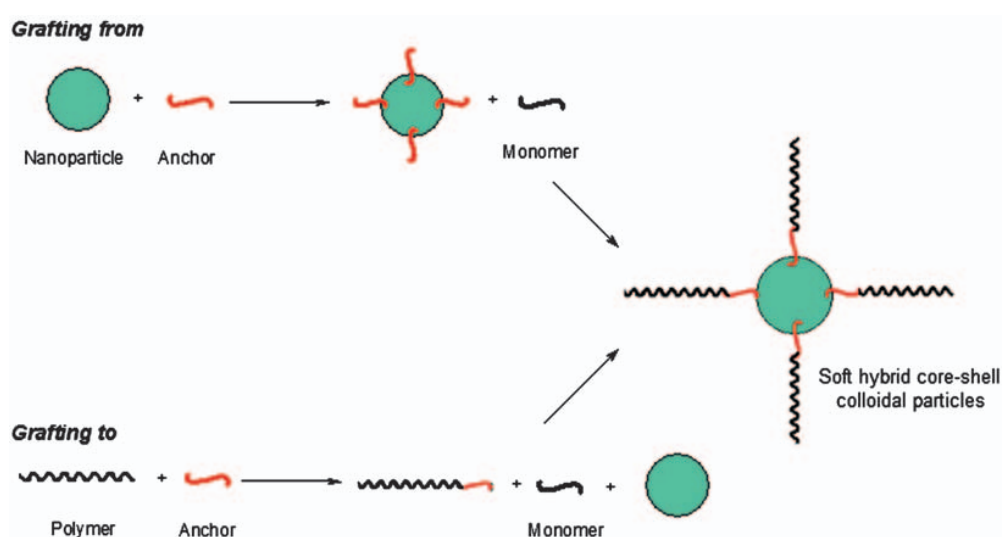


Figure 9.6 Schematic representation of the 'grafting from' and 'grafting to' systems to form a shell on the core surface to develop soft hybrid core-shell colloidal particles.⁵⁶

mechanism have a thermodynamically favoured conformation in solution (an equilibrium hydrodynamic volume), their adsorption density is self-limiting. The radius of gyration of the coil polymer chain is therefore the limiting factor in the number of polymer chains that can reach the surface and adhere. In the 'grafting from' mechanism, an initiator is adsorbed on the surface followed by initiation of the chain and propagation of monomer *via* surface-initiated polymerization. As shown in Figure 9.7, various polymerization methods have been developed to carry out the 'grafting from' process. Specifically, these include various control radical polymerization (CRP) techniques such as atom-transfer radical polymerization (ATRP), reversible addition-fragmentation chain-transfer polymerization (RAFT) and

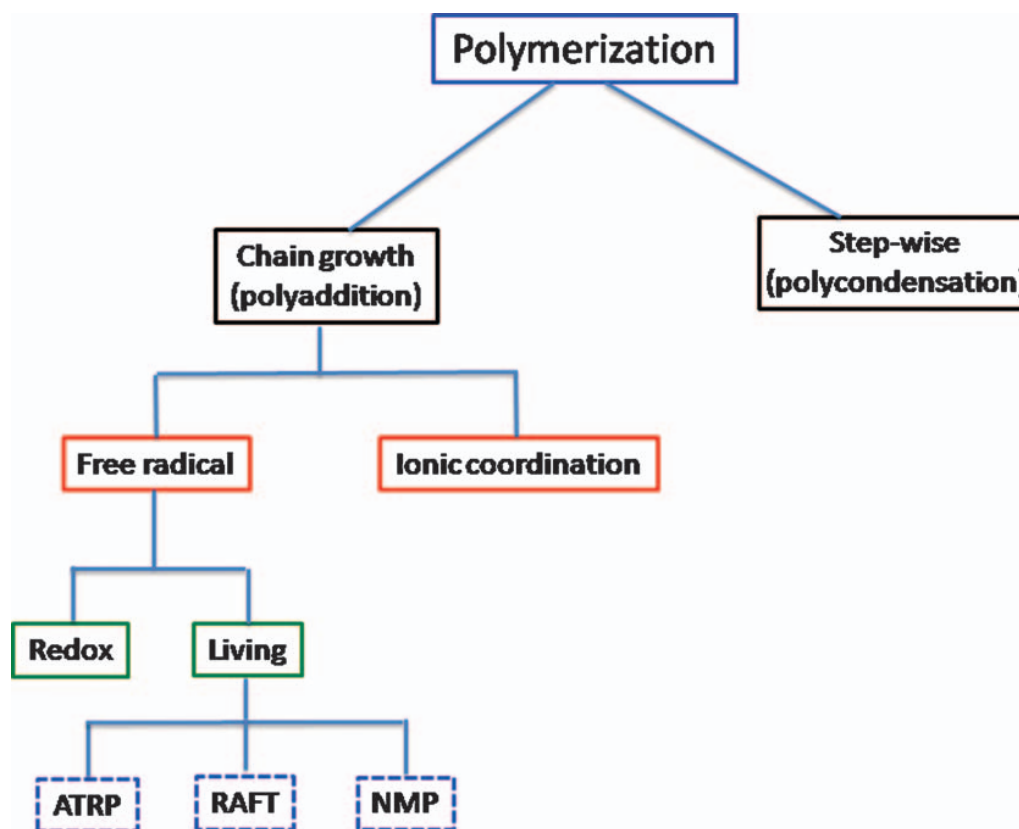


Figure 9.7 Various polymerization methods that can be used to form a shell on the core of different materials including colloidal particles to develop soft hybrid core-shell colloidal particles.

nitroxide-mediated radical polymerization (NMP). The CRP techniques have attracted much attention as they represent a facile approach to making end-grafted polymers with flexibility on the surface of various nanoparticles. Currently, CRP is regarded as the essential means to synthesize polymers with well-controlled functionality, composition, structure and architecture.

The ‘grafting from’ method has the advantage of allowing higher grafting densities than the ‘grafting to’ process. As shown in Figures 9.5 and 9.6, the ‘grafting to’ mechanism generally results in a ‘mushroom regime,’ to adhere to the surface of either a droplet or bead in solution. Owing to the larger volume of the coiled polymer and the steric hindrance that this causes, the grafting density is lower for ‘grafting to’ than for ‘grafting from.’ In contrast, the ‘extended conformation’ of the polymerized monomers from the surface of the bead means that the monomer must be in the solution and therefore be lyophilic in nature. This results in a polymer that has favourable interactions with the solution, allowing the polymer to form a more linear structure. ‘Grafting from’ therefore has a higher grafting density since there is greater access to chain ends. Peptide synthesis provides an example of a ‘grafting from’ synthetic process. In this approach, an amino acid chain is grown by a series of condensation reactions from a polymer bead surface. This grafting technique allows excellent control over the peptide composition as the bonded chain can be washed without desorption from the

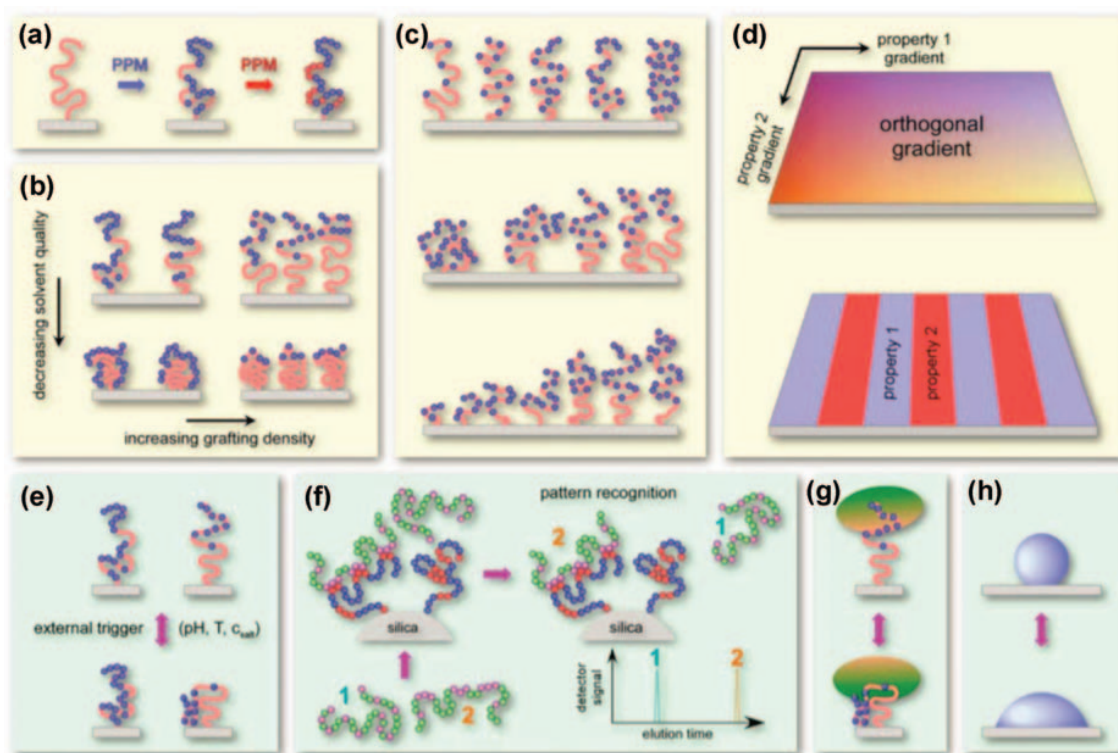


Figure 9.8 Schematic representing the formation (a–d) and function (e–h) of surface-grafted polymer systems generated by post-polymerization modification (PPM) protocols.⁵⁹

polymer. Polymeric coatings are another area of application of grafting techniques. In the formulation of water-borne paints, latex particles are often surface modified to control particle dispersion and thus coating characteristics such as viscosity, film formation and environmental stability (UV exposure and temperature variations). Owing to such unique characteristics, grafting processes have been extensively applied to tune the surface properties of materials without much influencing the bulk characteristics. The grafting systems of both ‘grafting from’ and ‘grafting to’ have found extensive applications in various important areas, as shown in Figure 9.8.

9.2.7 Click Chemistry

Click chemistry can be defined as a concept of reactions for the rapid synthesis of new compounds through heteroatom links (C–X–C).⁶⁰ Typical examples of click chemistry include the Cu(I)-catalysed azide–alkyne–‘click’ (CuAAC) reaction between terminal azides and alkynes,^{61–68} cycloaddition click reactions⁶⁹ and the thiol–ene click reactions.⁷⁰ Two approaches in click chemistry involve ‘grafting to’ and ‘grafting from’ mechanisms. In the ‘grafting to’ method, the azide- or alkyne-functionalized polymer is grafted to the corresponding functionalized nanoparticles (NPs).^{71–75} For example, SiO₂ NPs have been modified with PS and polyacrylamide through the CuAAC reaction using the ‘grafting to’ method, as shown in Figure 9.9.⁷⁶

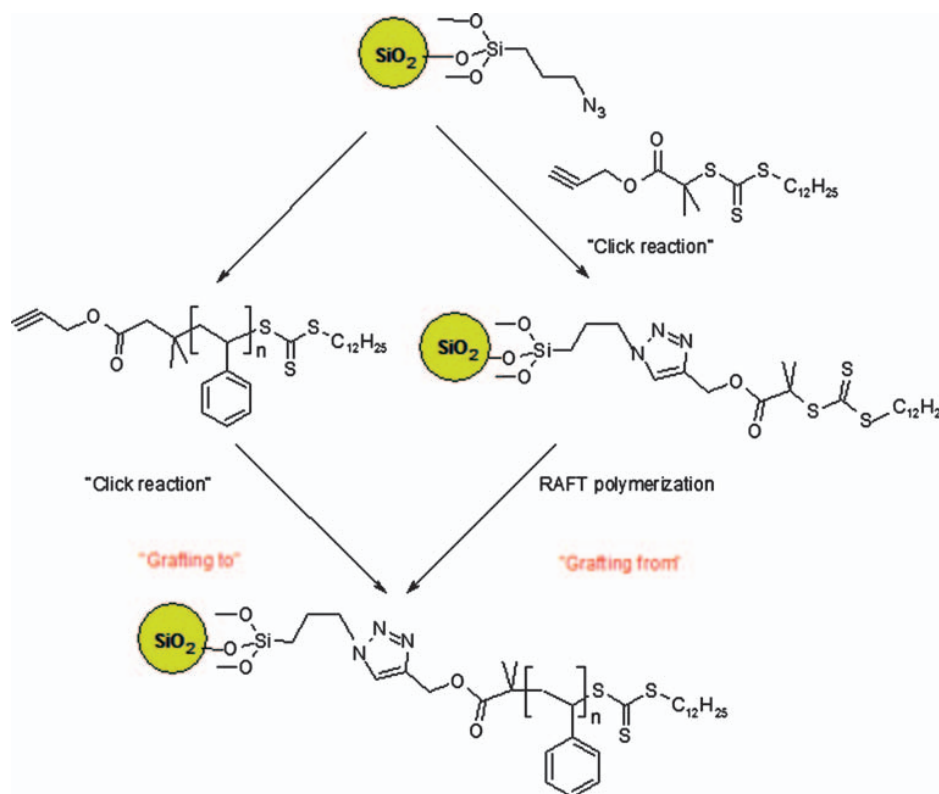


Figure 9.9 Modification of SiO₂ NPs with polystyrene *via* 'grafting to'⁷¹ and 'grafting from'^{80,81} methods based on click chemistry employing RAFT polymerization. Adapted from Ref. 76.

Other NPs such as Fe₂O₃,⁷⁷ Pt⁷⁸ and Au⁷⁹ have also been grafted with various polymers. In this direction, the 'grafting from' approach has found useful applications.^{80,81} For example, first a RAFT initiator clicked on the surface of SiO₂ NPs and polymerization was initiated, as shown in Figure 9.10. Low molecular weight monomers having high diffusibility and high grafting density are used in the 'grafting from' method, whereas, the 'grafting to' approach involves the use of the preformed high molecular weight whole polymer chain that restricts the polymer diffusibility.⁷⁶

9.2.8 Atom-Transfer Radical Polymerization (ATRP)

Different methods have been used for grafting polymers to various substrates.^{82–99} To tune the properties of core-shell colloidal particles, surface-initiated polymerization *via* the 'grafting from' approach is the most widely employed technique owing to its capability to impart good functionality control, molecular weight of polymer brushes and grafting density.¹⁰⁰ Furthermore, among the various polymerization methods, ATRP has been used extensively to modify the properties of various substrates.^{85–99} ATRP has also been used to produce hydrophilic polymer layers having remarkable thickness and surface density.^{95–99} Similarly, various functional and stimuli-responsive polymers have also been incorporated on particle surfaces using

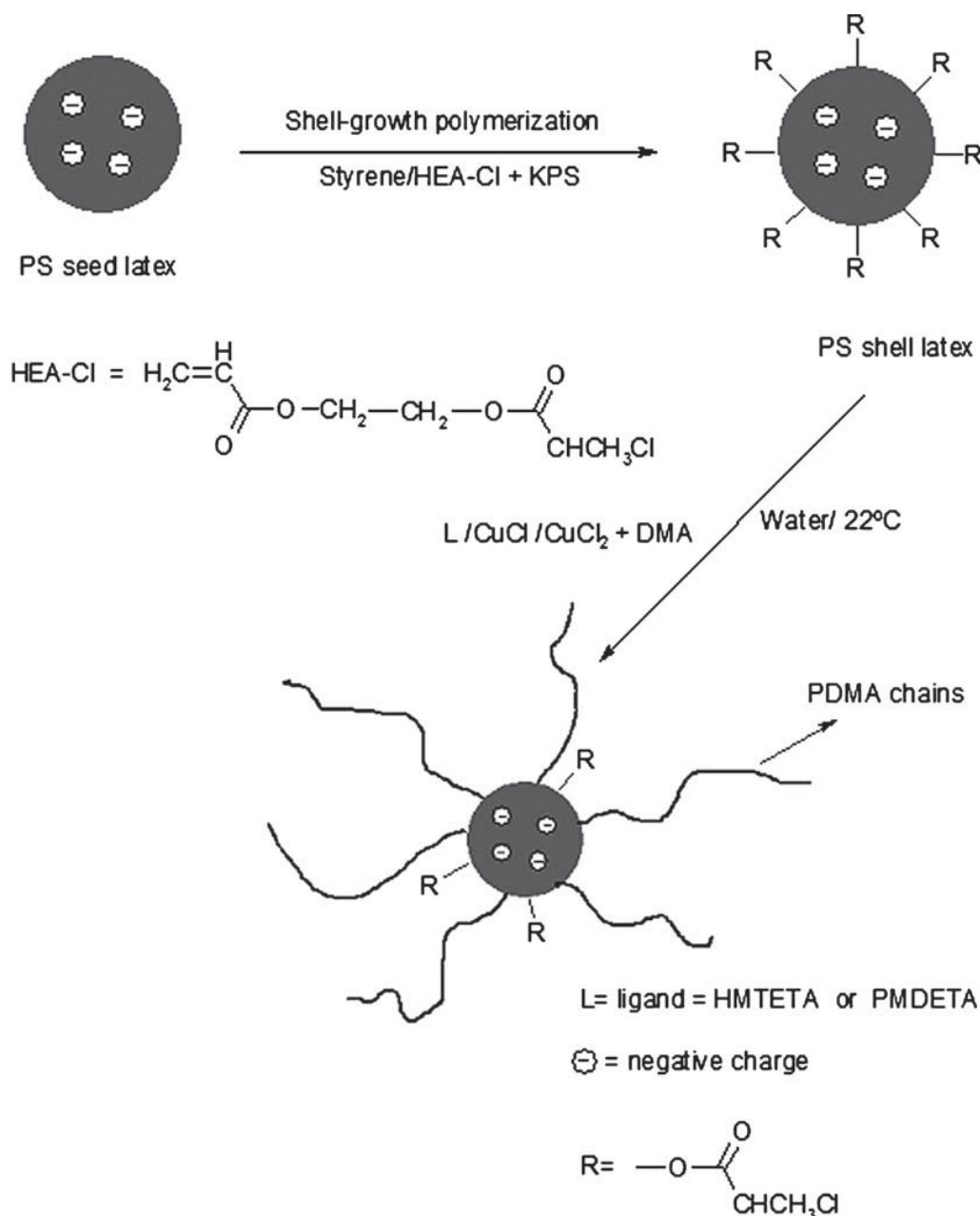


Figure 9.10 Graft polymerization of *N,N*-dimethylacrylamide (DMA) from PS particle surface based on the aqueous ATRP. Adapted from Ref. 101.

ATRP. For example, in an interesting study, a controlled synthesis of poly(*N*-isopropylacrylamide) (PNIPAM) brushes was carried out from a PS particle surface using ATRP (see Figure 9.10).¹⁰¹

This process is based on several steps. First, PS latex particles were synthesized through surfactant-free emulsion polymerization of styrene monomer. Second, by the use of potassium persulfate (KPS) as an initiator, the polymerization of styrene and (2,2'-chloropropionato)ethyl acrylate (HEA-Cl) was performed to form the shell on the core PS seed particles. Third, aqueous ATRP polymerization of *N*-isopropylacrylamide (NIPAM) monomer from the preformed seed latex particle in the presence of

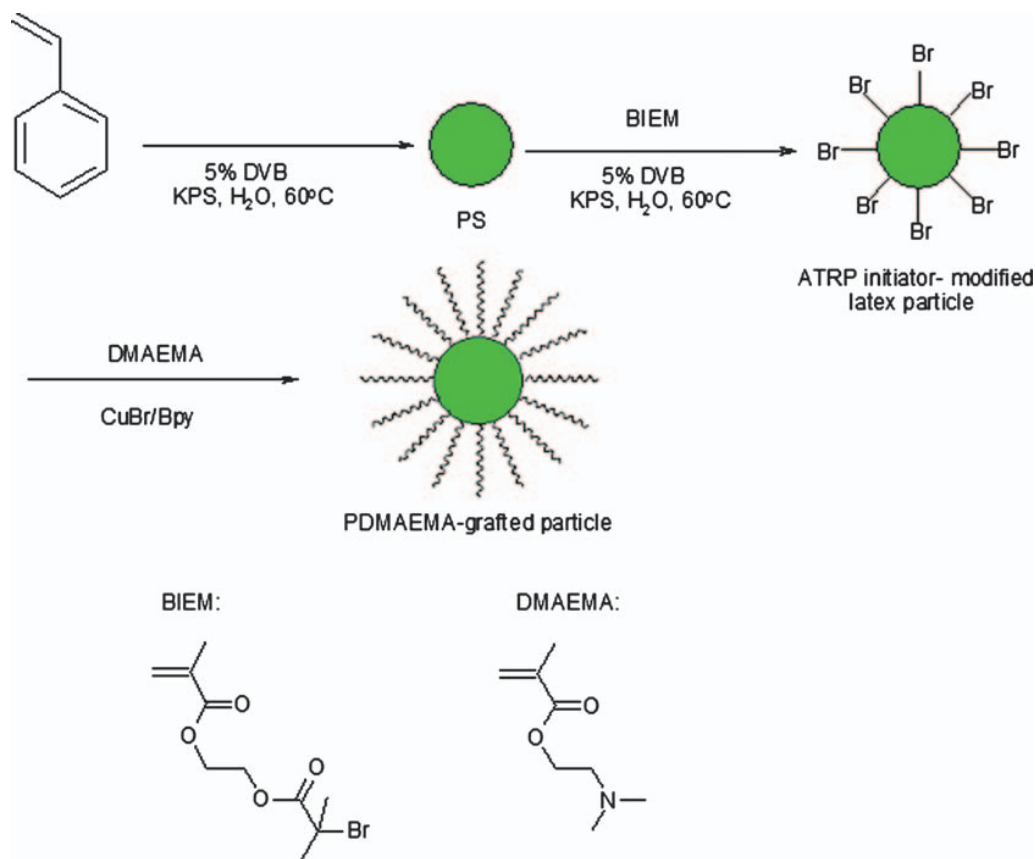


Figure 9.11 Formation of poly[2-(dimethyl amino)ethyl methacrylate] (PDMAEMA) brushes on the surface of colloid particles by employing ATRP. Adapted from Ref. 104.

1,1,4,7,10,10-hexamethyltriethylenetetramine (HMTETA)–CuCl–CuCl₂ powder under continuous stirring at room temperature was carried out. Similarly, different temperature-sensitive brushes such as PNIPAM, PMEA-*b*-PNIPAM, poly(*N,N*-dimethylacrylamide)^{102,103} and poly[2-(dimethylamino)ethyl methacrylate] (PDMAEMA) (see Figure 9.11) have been also grafted on the surface of colloidal particles.¹⁰⁴ Such grafting *via* ATRP clearly demonstrates the potential of this polymerization technique to confer desirable characteristics on the hybrid soft core-shell colloidal particles.

9.2.9 Reversible Addition–Fragmentation Chain-Transfer Radical (RAFT) Polymerization

RAFT polymerization is among the most widely used controlled radical polymerization techniques. In RAFT processes, the polymerization conditions are similar to those in conventional radical polymerization except that they involve the addition of a specific chain-transfer agent (CTA).^{105–109} RAFT polymerization employs a CTA in the form of a RAFT agent based on thiocarbonylthio compounds such as dithioesters, xanthates and thio-carbamates to mediate the polymerization. A typical CTA generally used in RAFT processes is shown in Figure 9.12.¹¹⁰ Here the Z group serves to

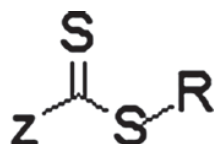


Figure 9.12 Chain-transfer agents used in RAFT polymerization. R and Z groups are described in the text.

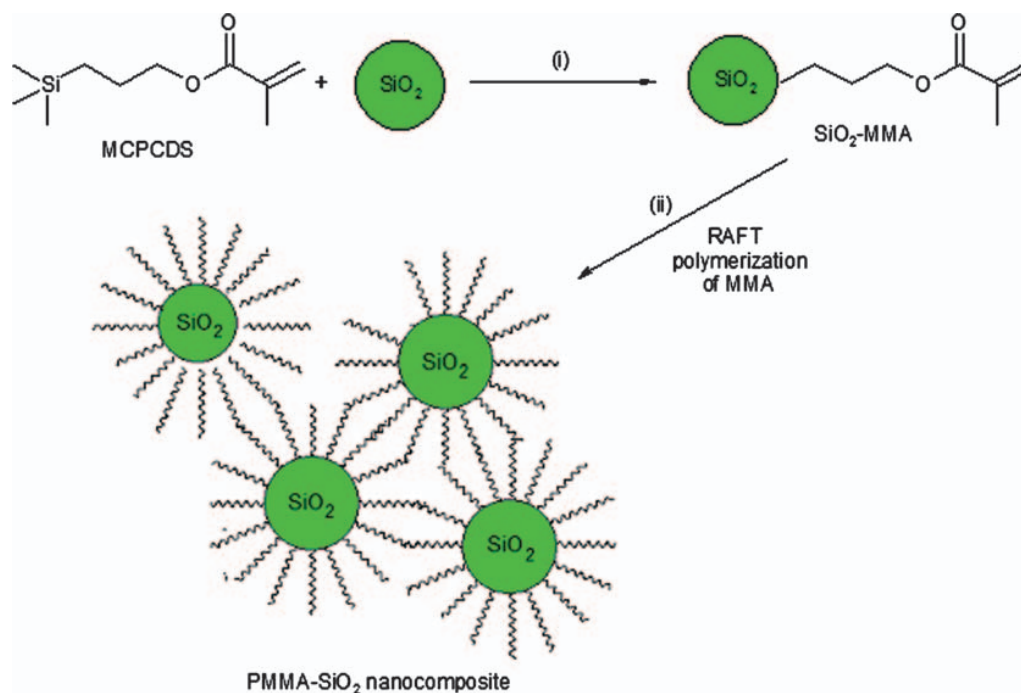


Figure 9.13 Grafting a polymer to the surface of silica by the ‘grafting through’ method using RAFT polymerization. Adapted from Ref. 118.

activate or deactivate the reactivity of the C=S bond towards the addition reaction and the R group forms a stable free radical. RAFT polymerization *via* a reversible chain-transfer process is capable of generating polymer particles with low polydispersity indexes and a prechosen molecular weight during the free-radical polymerization.

Among the distinctive features of RAFT polymerization is its tolerance to different kinds of reaction conditions such as a large range of solvents including water in a wide temperature range. It is also suitable for different functional monomers and does not require highly rigorous removal of oxygen and other impurities.^{106,108,111–113} Owing to such advantages, RAFT polymerizations can be used to design polymers of complex architectures, such as linear block copolymers, comb-like and star polymers, dendrimers and also polymer brushes. In the last case, RAFT polymerization has been employed to graft polymers to the surface of various substrates, including colloidal particles. For example, RAFT polymerization was used to graft polymers to silica particles by using either ‘grafting to’^{114,115} or ‘grafting from’^{116,117} methods. In a more recent study, a new ‘grafting through’ method was used to graft polymer chains to the surface of silica by using

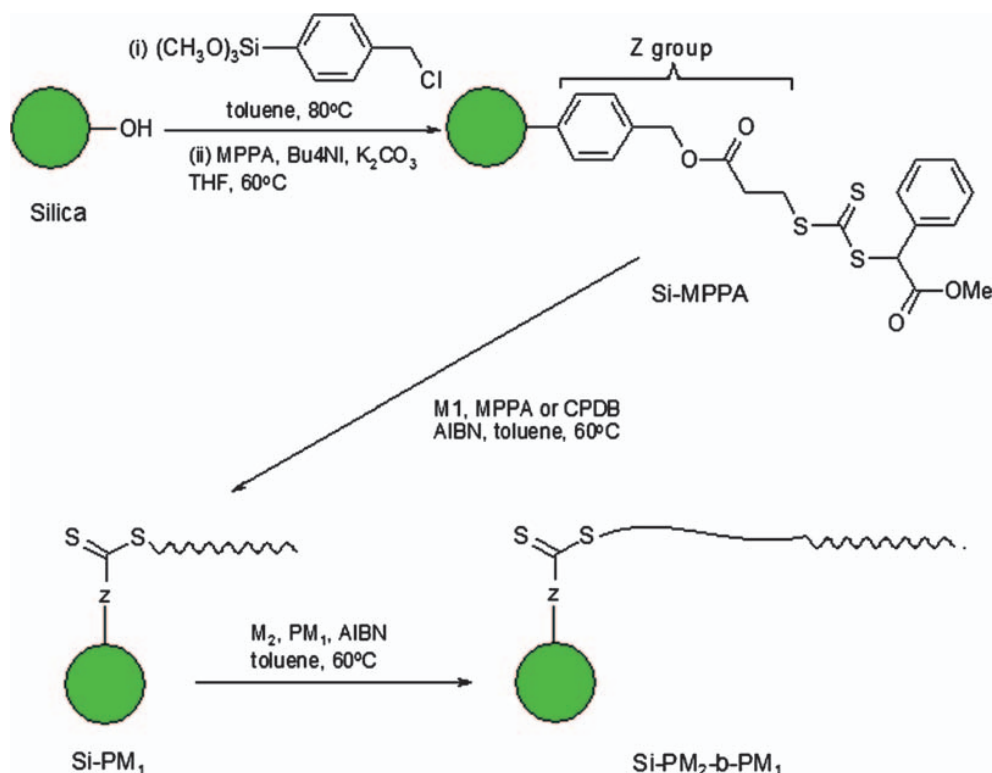


Figure 9.14 Synthetic route to polymer-grafted silica particles using the Z group by RAFT polymerization. Adapted from Ref. 124.

RAFT polymerization as illustrated in Figure 9.13.¹¹⁸ This method has also been used to graft a polymer on silica without the use of RAFT polymerization.^{119–123} However, the ‘grafting from’ approach has been widely used to synthesize silica nanocomposites by employing different types of RAFT agents that utilized the Z group to attach the RAFT agent to the silica surface, as shown in Figure 9.14,¹²⁴ and other typical RAFT methods used the R group by attaching the RAFT agent to the surface of a substrate.^{116,117}

9.2.10 Nitroxide-Mediated Polymerization (NMP)

NMP is another controlled living free radical polymerization process like ATRP and RAFT polymerization. NMP makes use of a compound known as an alkoxyamine initiator, which is viewed as an alcohol bound to a secondary amine by an N-O single bond as shown in Figure 9.15.¹²⁵

The typical NMP reaction is controlled by reversible capping and decapping of growing (radical) polymer chains by the nitroxide radical. This results in a decrease in the concentration of growing radicals and also slows the polymerization. Consequently, the radical chain grows at a controlled rate to generate polymers of well-defined molecular weight, polydispersity index and architecture. The NMP process allows a relative lack of true termination, which in turn allows polymerization to continue as long as there is available monomer. Because of this, the NMP is said to be ‘living’ in

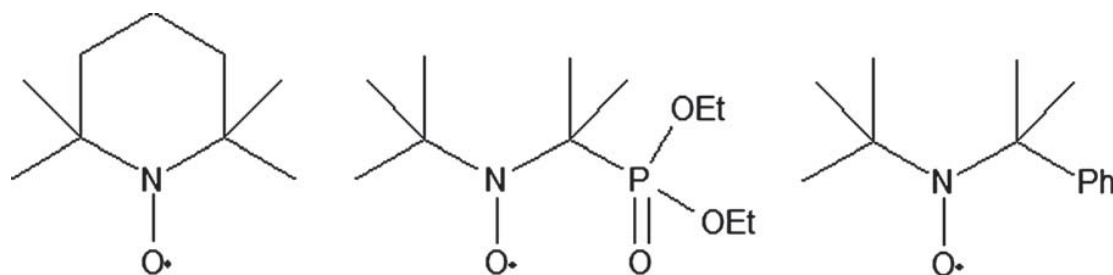


Figure 9.15 Commonly used alkoxyamine nitroxide initiating agents for NMP.¹²⁵

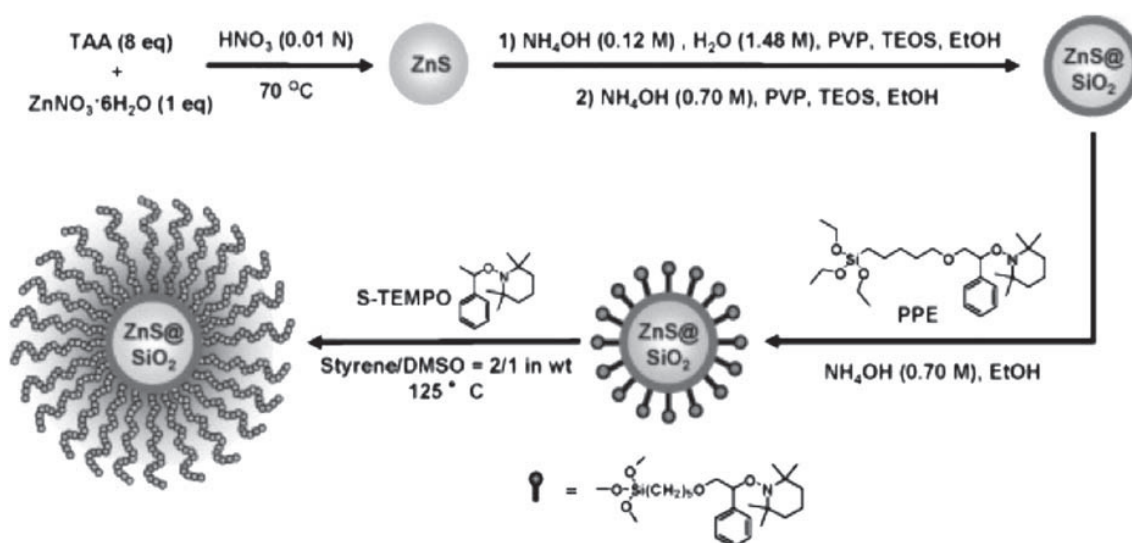


Figure 9.16 Synthesis of ZnS@SiO₂-PS particles by a surface-initiated nitroxide-mediated polymerization process.¹²⁶

nature and almost all of the growing chains are ‘capped’ by a mediating nitroxide. This consequently results in the dissociation and growth of chains at very similar rates to generate a largely uniform polymer chain length and structure. Because of such unique characteristics, the NMP process has been successfully employed to carry out surface-initiated polymerization (SIP) to alter the characteristics of particle surfaces. For example, a fairly recent study involved the synthesis of hybrid colloidal ZnS@SiO₂-PS particles by surface-initiated nitroxide-mediated polymerization as shown in Figure 9.16.¹²⁶ Here the procedure involved various steps including the synthesis of monodisperse ZnS particles by a homogeneous precipitation–aggregation process and then covering through uniform layer formation of SiO₂ particles. These ZnS@SiO₂ particles were subsequently functionalized with alkoxyamine moieties to initiate the surface polymerization *via* the NMP process. The SIP *via* NMP of styrene in DMSO solvent using S-TEMPO as sacrificial initiator was achieved with relatively good control over the molecular weight and molecular weight distribution of the grafted polymer, and polymer brushes of various molecular weights and high graft density were synthesized.

9.2.11 Conventional Seed Radical Polymerization

The conventional seed radical polymerization process offers another versatile approach to developing soft hybrid core-shell colloidal particles. In this method, free-radical polymerization of the desired monomer from the core or seed particles is carried out. One of the main advantages is that monomers with multiple functionalities can be polymerized from the surface of the seed particles. This is important since there has not been much work reporting the elaboration of core-shell particles grafted with functional polymers that possess hydrophilic and particularly temperature-sensitive magnetic latexes. In one of this studies, the elaboration of thermally sensitive magnetic latexes using a stepwise approach to obtain submicron composite particles was reported.⁵⁵ The inverse microemulsion polymerization process has also been studied to obtain hydrophilic nanoparticles of low magnetic content and narrow size distribution.¹²⁷⁻¹²⁹

In another interesting study, latex particles with different magnetic contents were prepared using conventional seed radical polymerization of functional monomers.¹³⁰ This study was focused on the elaboration of hydrophilic cationic and thermally sensitive magnetic latexes from an oil-in-water magnetic emulsion. To achieve such objective, two-stage polymerization processes were used: (i) the elaboration of seed magnetic latex particles and (ii) the functionalization of the seed by using water-soluble monomers. The cationic character was induced by using an amino-containing monomer. The encapsulation was performed using water-soluble reactants and the functionalization was induced by using the amino-containing monomer. Thermal sensitivity was induced by the use of NIPAM. The use of a large amount of functional monomer leads to high water-soluble polymer formation and highly cationic particles. Through this method, colloidal particles with different functionalization and applications can be prepared. For example, for the elaboration of hairy soft hybrid particles, temperature-sensitive highly magnetic latex particles have been reported.¹³⁰ The polymerization occurred in the presence of stabilized oil-in-water magnetic droplets by using a hydrophobic monomer as shown in Figure 9.17. This polymerization was performed in two steps. First, the

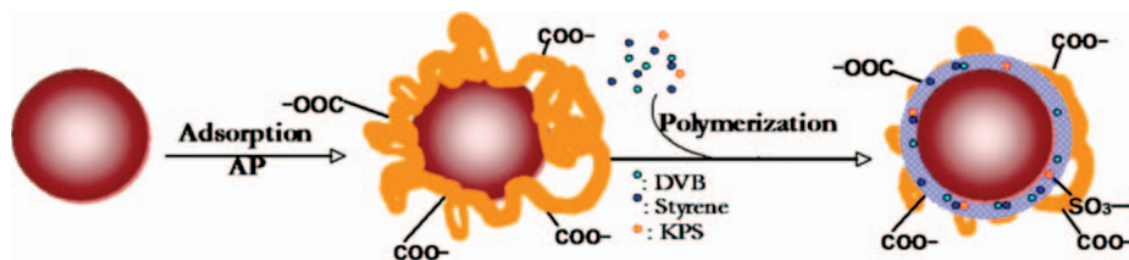


Figure 9.17 Transformation of oil-in-water ferrofluid droplet (composed of highly concentrated iron oxide nanoparticles stabilized *via* surfactant adsorption and dispersed in an aliphatic solvent) into magnetic latex particles using an amphiphilic polymer (AP). Adapted from Ref. 130.

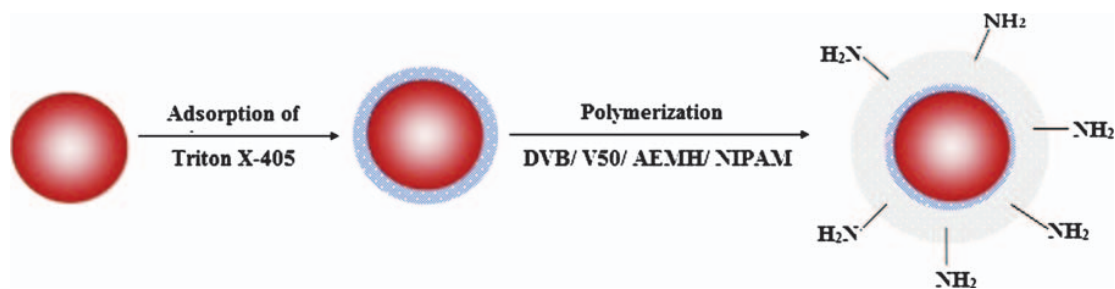


Figure 9.18 Conventional seed radical polymerization using NIPAM, MBA and AEM as a functional monomer to form a shell of cross-linked polymer on a magnetic core. Adapted from Ref. 130.

preparation of seed magnetic latex particles was carried out. Then, functionalized magnetic latexes were obtained through seed polymerization by using water-soluble reactants. Typical reaction conditions involved the preparation of seeded magnetic latexes particles by first washing with Triton X-405. To avoid the formation of water-soluble polymer in order to incorporate NIPAM on the particle surface, two types of cross-linkers, divinylbenzene (DVB) and *N,N*-methylenebisacrylamide (MBA), were used. Encapsulation depended on the water-soluble cross-linker (MBA). Water-soluble polymer formation was reduced by increasing the amount of water-soluble cross-linker (MBA) during polymerization, which led to the formation of a polymer shell.¹³⁰ The composite latexes obtained possessed a shell of cross-linked polymer and a magnetic core as shown in Figure 9.18.

9.3 Biomedical Applications of Soft Hybrid Particles

The soft hybrid colloidal particles are not only designed to control surface functionality, morphology or chemical composition and are not only under evaluation in various biomedical applications, but are also used in practice at various biomedical levels: (i) they are used as solid supports for sample preparation and in bionanotechnology such as in rapid diagnostics; (ii) hairy-like particles bearing end chains and containing functional groups (mainly carboxylic groups in the surface) are generally used for chemical grafting of biomolecules in order to enhance the capture efficiency of a targeted analyte; (iii) charged soft hybrid colloidal particles are used for generic extraction of biomolecules such as adsorption of nucleic acids, proteins and viruses thanks to the highly charged polymer tentacles on the particles, as described in the following.

9.3.1 Extraction of Nucleic Acids

The main purpose in biomedical applications is to enhance sensitivity and specificity, but in the area of nucleic acid probes, problems such as the level of sensitivity are encountered. However, this problem can be solved by increasing the concentration of the target (RNA and/or DNA) in the considered medium. Before specific detection of the target probe, the use of appropriate hybrid

particles for extraction, purification and desorption of already adsorbed nucleic acids would be of great interest.¹³¹ The control of the adsorption and desorption of nucleic acid molecules is effected by interaction between prepared magnetic latex particles and nucleic acid extraction. The adsorption of nucleic acid molecules is performed at acidic pH and low salinity.¹³¹ In *in vitro* biomedical diagnostics, magnetic particles are used for sample manufacture and separation of particles from the aqueous phase. Generally, specific and non-specific processes are used for nucleic acid extraction.

9.3.1.1 Non-Specific Capture of Nucleic Acids

The non-specific capture of nucleic acid molecules using particles is mainly based on electrostatic interactions. Being positively charged, the attractive electrostatic forces lead to rapid and high adsorption. Then, nucleic acid extraction is achieved by using cationic magnetic particles and controlling the pH and salinity of the medium.³⁷ The extracted nucleic acid molecules are subsequently amplified on magnetic beads. After desorption, the magnetic particles are removed by using a polymerase chain reaction (PCR)¹³² in the case of DNA molecules or Reverse Transcriptase (RT)-PCR¹³³ in the case of RNA, as illustrated in Figure 9.19.¹³⁴

9.3.1.2 Specific Capture of Nucleic Acids

The specific capture of nucleic acids^{135,136} using soft hybrid magnetic latex particles is generally performed as follows. First, the captured probe of well-defined sequence is chemically immobilized on the magnetic latex particles.

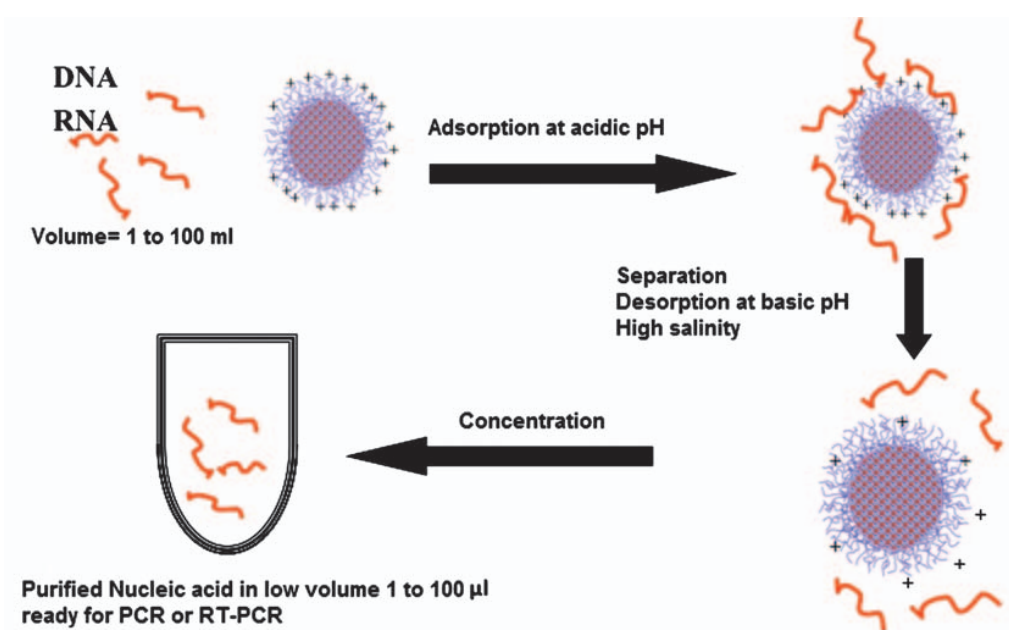


Figure 9.19 Illustration of non-specific capture, purification and concentration of nucleic acid molecules. Adapted from Ref. 134.

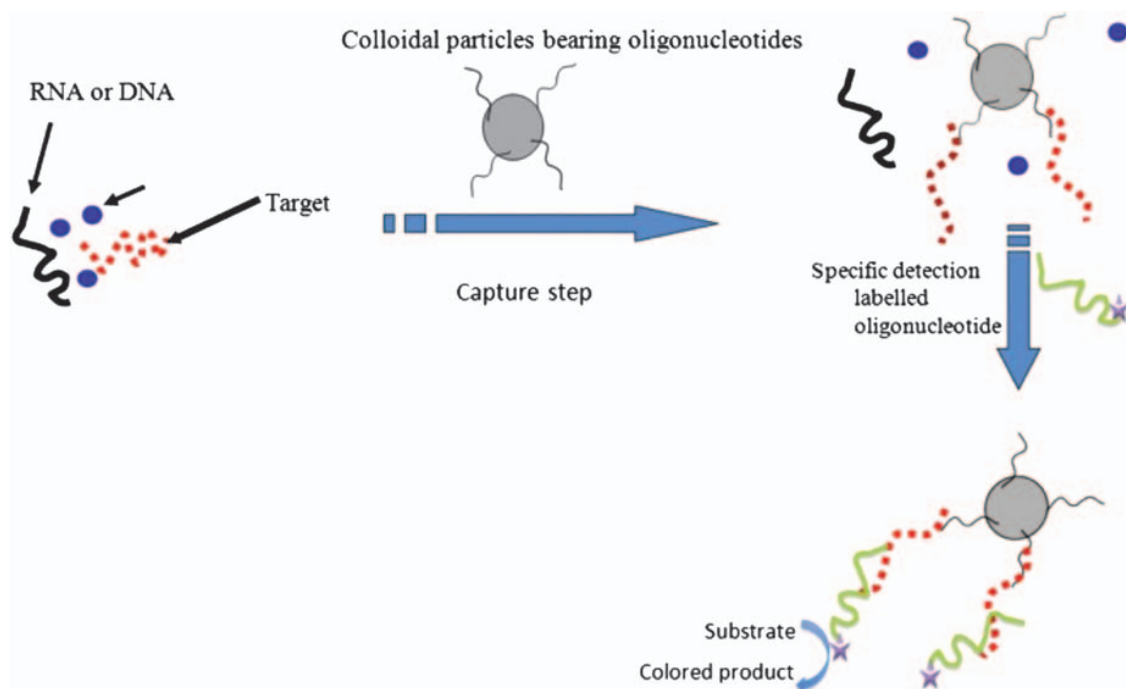


Figure 9.20 Illustration of specific capture and detection of nucleic acids (ODN, oligonucleotide; ssDNA, single-stranded DNA fragment). The intensity of the supernatant due to the presence of coloured product was determined. Specific capture is performed by addition of a substrate that reacts with enzyme in order to form a coloured medium. Adapted from Ref. 138.

Second, the biological sample is mixed with magnetic particle–ODN (ODN = oligonucleotide) conjugates. The specific capture of the target is effected by hybridization (particularly hydrogen bonding). The detection process is performed by adding a detection probe (*i.e.* oligonucleotide labelled with enzyme).¹³¹ Then, the substrate addition is oxidized by the enzyme, which leads to a coloured supernatant as in immunoassay. This specific capture of nucleic acid molecules combined with a well-optimized detection process leads to the enhancement of this molecular biology-based diagnostic method¹³⁷ as illustrated in Figure 9.20.¹³⁸

9.3.2 Extraction of Proteins

In biomedical applications, latex particles have been used as a particulate carrier, so substantial work has been carried out on the preparation of hydrophobic magnetic particles.^{139,140} For protein denaturation and irreversible adsorption, polystyrene has been used as a solid phase when applied in the diagnostics field. The use of thermosensitive microgel particles with low critical solution temperature (LCST) is of great interest in the biomedical field, because their physicochemical properties and the adsorption of proteins can be controlled by changing the pH, the salinity of the medium and the temperature.^{141,142} In addition such particles give non-denaturing support to immobilized proteins, in immunoassays and in protein purification

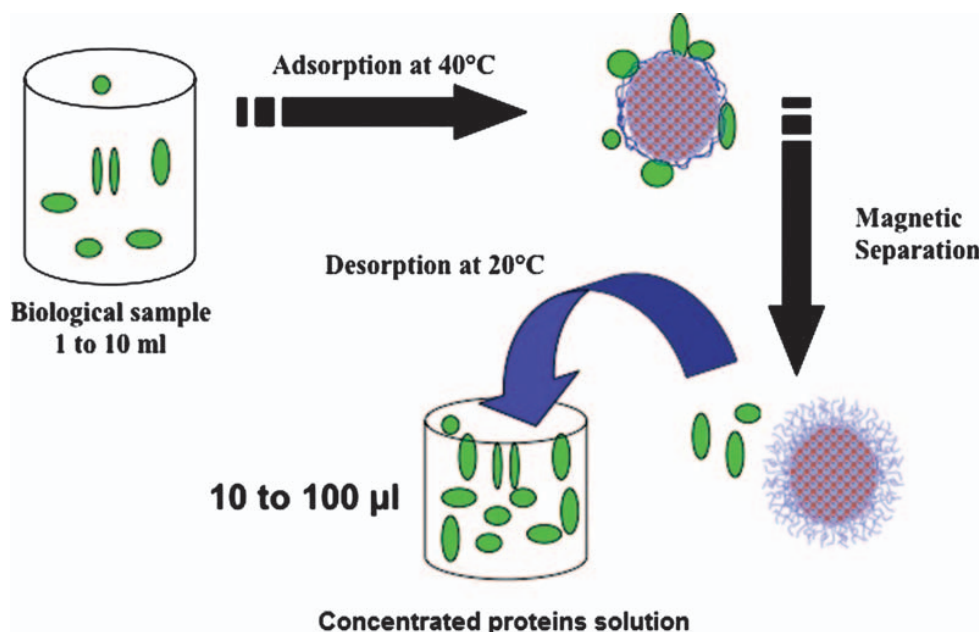


Figure 9.21 Schematic representation of protein concentration using thermosensitive latex particles.
Adapted from Ref. 143.

and concentration. Thermosensitive magnetic latex particles¹⁴³ have been used for protein concentration and purification by controlling both adsorption and desorption processes, as illustrated in Figure 9.21.

The adsorption and desorption of protein on/from thermosensitive magnetic latex particles have been studied using human serum albumin (HSA) as a protein model. Seed precipitation polymerization has been used to prepare thermosensitive core-shell magnetic latex by using magnetic polystyrene particles as a seed, NIPAM as the main monomer, MBA as a cross-linker and potassium persulfate (KPS) as an initiator. The polymerization conversion and water polymer formation have been examined. The adsorption of HSA protein was principally governed by hydrophobic interactions, since high adsorbed amounts of protein were obtained above the LCST of PNIPAM whereas negligible adsorption was evidenced below the LCST. The adsorption kinetics of HSA protein were found to be complete within 10 min at 40 °C. The amount of HSA protein adsorbed on anionic thermosensitive magnetic latex particles at 40 °C (above the LCST) decreased with increase in the pH and the salinity of the medium, reflecting the contribution of electrostatic interactions to the adsorption process. HSA desorption occurred after performing adsorption at acidic pH (~4.5). Various experimental factors, such as incubation time, pH, salinity and temperature of the medium, drastically affected the amount of protein desorbed. The maximum amount of protein desorbed was obtained at basic pH (~8.6), an ionic strength of ~0.1 M and a temperature of 20 °C.¹⁴³

The performance of such thermosensitive magnetic latex particles as soft hybrid material in the purification and concentration of HSA protein was

improved by careful control of both the adsorption and desorption conditions (pH, salinity, incubation time and temperature). The results are quite encouraging, indicating that such particles could serve as an alternative route to other techniques used for purifying and concentrating proteins, *e.g.* precipitation using media of high salt concentration and an ion-exchange column, such as a diethylaminoethyl-Sepharose gel column system.

9.3.3 Extraction of Viruses

The extraction of haemorrhagic fever viruses (such as Lassa and Ebola) is a recent diagnostic method for developing countries. In recent years, only a little work has been carried out using magnetic beads for virus detection and concentration.^{144,145} Moreover, magnetic latex particles have been used for the capture of enveloped viruses.¹⁴⁶ This method is based on the use of functionalized magnetic latex particles for capturing biological samples. After capture, the separation of magnetic particles from supernatant occurred *via* a permanent magnet. The extraction of nucleic acids from the captured viruses was performed by using a commercial kit. Usually, the methodology for the concentration of viruses is used to increase the virus concentration in the sample with no loss of viral activity and infectivity. PCR and RT-PCR were applied in the measurement of the sensitivity of the captured assay. Satoh *et al.*¹⁴⁴ reported that a few RNA and DNA viruses were concentrated more than 100- and 1000-fold, respectively, using polyethylenimine (PEI)-conjugated magnetic beads. Elaissari *et al.*¹⁴⁵ produced functionalized magnetic beads for generic virus extraction and purification. The magnetic colloidal emulsion was functionalized by surface immobilization of polymers. A polycation, PEI, was first adsorbed and then a polyanion, poly(maleic anhydride-*co*-methyl vinyl ether), was either adsorbed or

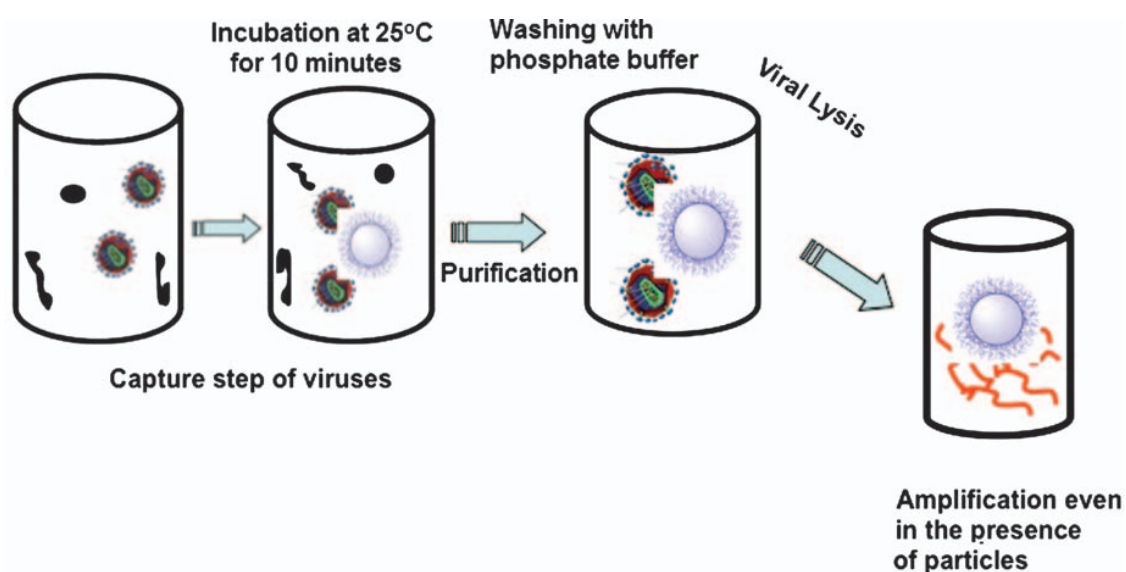


Figure 9.22 Capture of viruses using magnetic particles. Adapted from Ref. 145.

covalently grafted. Negatively charged particles were used as a solid support for generic capture of viruses with yellow fever virus as a model; 90% of the virus could be captured and 10% released after washing. The processes of capture and detection of viral RNA were performed in the same Eppendorf tube. A short incubation of the sample was performed at room temperature and then the particle washing was performed by magnetic separation, supernatant elimination and redispersion. Finally, viral lysis and RT-PCR were carried out, as shown in the Figure 9.22.¹⁴⁵

9.4 Conclusion

The preparation of soft hybrid nanoparticles has attracted considerable attention owing to the potential application of such materials in various fields. Such materials are a combination of both organic and inorganic moieties in well-defined structure and morphology. The softness of such nanoparticles is mainly due to the soft polymer shell. Such materials can be prepared using different processes starting from easy to more complex approaches.

The first and easiest method is basically the adsorption of polymer layers on hybrid nanoparticles. This adsorption can be performed in one step or multiple steps such as random sequential adsorption of oppositely charged polymers. It is interesting that the adsorption process leads to the presence of some aggregated particles due to the bridging flocculation phenomenon. Consequently, this adsorption approach was generally discarded.

In order to avoid the aggregation process, chemical grafting has been widely explored using batch grafting of reactive polymers, 'grafting from' or 'grafting to.' The chemical grafting approach involves the immobilization of preformed polymers or using chemical synthesis approaches, including mainly conventional seeded polymerization processes 'from' or 'to' the colloidal particles. However, conventional polymerization leads to layers of heterogeneous thickness and to an uncontrolled degree of polymerization of the formed brush soft layer.

In order to control the microstructure and the soft shell part, polymerization methods such as atom-transfer radical polymerization (ATRP), reversible addition-fragmentation chain-transfer (RAFT) polymerization and nitroxide-mediated radical polymerization (NMP) have been used. Another interesting polymerization technique based on click chemistry has also been investigated and gave promising results, but RAFT polymerization remains the most interesting approach and leads to a well-controlled soft layer.

Colloidal particles and especially soft hybrid nanoparticles have potential and promising applications, particularly in the biomedical diagnostics domain. The fascinating features of such colloidal particles make them good and suitable candidates for rapid conjugation and sensitive detection of various biomolecules in a very small volume of analyte.

Functionalized soft nanoparticles are used for sample preparation in which the extraction of biomolecules such as proteins, nucleic acids, bacteria and viruses are of paramount importance in order to enhance the sensitivity of *in vitro* biomedical diagnostics. Since the discovery of bionanotechnology, special attention has been dedicated to the elaboration of multifunctionalized and stimuli-responsive soft hybrid nanoparticles for use not only as solid supports for the immobilization of biomolecules, but also for transport and even for detection in microsystems combining microfluidic and lab-on-a-chip technology.

References

1. A. K. Gupta and M. Gupta, *Biomaterials*, 2005, **26**, 3995.
2. S. S. Davis, *Trends Biotechnol.*, 1997, **15**, 217.
3. C. E. Mora-Huertas, H. Fessi and A. Elaissari, *Int. J. Pharm.*, 2010, **385**, 113.
4. A.-H. Lu, E. L. Salabas and F. Schüth, *Angew. Chem. Int. Ed.*, 2007, **46**, 1222.
5. A. V. Bychkova, O. N. Sorokina, M. A. Rosenfeld and A. L. Kovarski, *Russ. Chem. Rev.*, 2012, **81**, 1026.
6. M. M. Rahman and A. Elaissari, *J. Colloid Sci. Biotechnol*, 2012, **1**, 3.
7. P. Boisseau and B. Loubaton, *C. R. Phys.*, 2011, **12**, 620.
8. E. Hübner, J. Allgaier, M. Meyer, J. Stellbrink, W. Pyckhout-Hintzen and D. Richter, *Macromolecules*, 2010, **43**, 856.
9. S. M. Gravano, R. Dumas, K. Liu and T. E. Patten, *J. Polym. Sci.: Polym. Chem.*, 2005, **43**, 3675.
10. L. Bombalski, H. Dong, J. Listak, K. Matyjaszewsk and M. R. Bockstaller, *Adv. Mater.*, 2007, **19**, 4486.
11. L. Zhou, J. Yuan, W. Yuan, M. Zhou, S. Wu, Z. Li, X. Xing and D. Shen, *Mater. Lett.*, 2009, **63**, 1567.
12. Á. Muñoz-Noval, V. Sánchez-Vaquero, V. Torres-Costa, D. Gallach, V. Ferro-Llanos, J. Javier Serrano, M. Manso-Silván, J. P. García-Ruiz, F. del Pozo and R. J. Martín-Palma, *J. Biomed. Opt.*, 2011, **16**, 025002.
13. I. W. Hamley, *Angew. Chem. Int. Ed.*, 2003, **42**, 1692.
14. J. H. Lee, H. H. Ahn, K. S. Kim, J. Y. Lee, M. S. Kim, B. Lee, G. Khang and H. B. Lee, *J. Tissue Eng. Regen. Med.*, 2008, **2**, 288.
15. G. Jiang, K. Park, J. Kim, K. S. Kim, E. J. Oh, H. Kang, S.-E. Han, Y.-K. Oh, T. G. Park and S. Kwang Hahn, *Biopolymers*, 2008, **89**, 635.
16. F. X. Gu, R. Karnik, A. Z. Wang, F. Alexis, E. Levy-Nissenbaum, S. Hong, R. S. Langer and O. C. Farokhzad, *Nano Today*, 2007, **2**, 14.
17. C. J. Sunderland, M. Steiert, J. E. Talmadge, A. M. Derfus and S. E. Barry, *Drug Dev. Res.*, 2006, **67**, 70.
18. J. H. Park, S. Lee, J.-H. Kim, K. Park, K. Kim and I. C. Kwon, *Prog. Polym. Sci.*, 2008, **33**, 113.
19. S. S. Rajan, H. Y. Liu and T. Q. Vu, *ACS Nano*, 2008, **2**, 1153.
20. C. Tekle, B. van Deurs, K. Sandvig and T.-G. Iversen, *Nano Lett.*, 2008, **8**, 1858.

21. J. Yan, M. C. Estévez, J. E. Smith, K. Wang, X. He, L. Wang and W. Tan, *Nano Today*, 2007, **2**, 44.
22. T. T. Hien Pham, C. Cao and S. J. Sim, *J. Magn. Magn. Mater.*, 2008, **320**, 2049.
23. R. Bhattacharya and P. Mukherjee, *Adv. Drug Deliv. Rev.*, 2008, **60**, 1289.
24. C. Sun, J. S. H. Lee and M. Zhang, *Adv. Drug Deliv. Rev.*, 2008, **60**, 1252.
25. X. Song, L. Huang and B. Wu, *Anal. Chem.*, 2008, **80**, 5501.
26. A. Elaissari and H. Fessi, *Braz. J. Phys.*, 2009, **39**, 146.
27. M. Horisberger, *Scanning Electron Microsc.*, 1980, 9.
28. C. Loo, A. Lowery, N. Halas, J. West and R. Drezek, *Nano Lett.*, 2005, **5**, 709.
29. V. Sokolova, A. Kovtun, O. Prymak, W. Meyer-Zaika, E. A. Kubareva, E. A. Romanova, T. S. Oretskaya, R. Heumann and M. Epple, *J. Mater. Chem.*, 2007, **17**, 721.
30. I. W. Bauer, S.-P. Li, Y.-C. Han, L. Yuan and M.-Z. Yin, *J. Mater. Sci. Mater. Med.*, 2008, **19**, 1091.
31. I. I. Slowing, J. L. Vivero-Escoto, C.-W. Wu and V. S.-Y. Lin, *Adv. Drug Deliv. Rev.*, 2008, **60**, 1278.
32. J. M. Singer and C. M. Plotz, *Am. J. Med.*, 1956, **21**, 888.
33. N. G. Portney and M. Ozkan, *Anal. Bioanal. Chem.*, 2006, **384**, 620.
34. M. G. Harisinghani, J. Barentsz, P. F. Hahn, W. M. Deserno, S. Tabatabaei, C. H. van de Kaa, J. de la Rosette and R. Weissleder, *N. Engl. J. Med.*, 2003, **348**, 2491.
35. M. E. Kooi, V. C. Cappendijk, K. B. J. M. Cleutjens, A. G. H. Kessels, P. J. E. H. M. Kitslaar, M. Borgers, P. M. Frederik, M. J. A. P. Daemen and J. M. A. van Engelshoven, *Circulation*, 2003, **107**, 2453.
36. Y. K. Kim, H. S. Kwak, C. S. Kim, G. H. Chung, Y. M. Han and J. M. Lee, *Radiology*, 2006, **238**, 531.
37. A. Elaissari, *Macromol. Symp.*, 2009, **281**, 14.
38. T. A. Taton, C. A. Mirkin and R. L. Letsinger, *Science*, 2000, **289**, 1757.
39. J. Huang, X. Wang and X. Deng, *J. Colloid Interface Sci.*, 2009, **337**, 19.
40. B. R. Sharma, N. C. Dhuldhoya and U. C. Merchant, *J. Polym. Environ.*, 2006, **14**, 195.
41. A. V. Dobrynin and M. Rubinstein, *Prog. Polym. Sci.*, 2005, **30**, 1049.
42. E. Killmann, D. Bauer, A. Fuchs, O. Portenlänger, R. Rehmert and O. Rustemeier, in *Structure, Dynamics and Properties of Disperse Colloidal Systems*, ed. H. Rehage and G. Peschel, Steinkopff, Heidelberg, 1998, pp. 135–143.
43. H. D. Bijsterbosch, *Copolymer Adsorption and the Effect on Colloidal Stability*, thesis, Wageningen Agricultural University, 1998.
44. S. Åkerman, K. Åkerman, J. Karppi, P. Koivu, A. Sundell, P. Paronen and K. Järvinen, *Eur. J. Pharm. Sci.*, 1999, **9**, 137.
45. T.-H. Young, J.-N. Lu, D.-J. Lin, C.-L. Chang, H.-H. Chang and L.-P. Cheng, *Desalination*, 2008, **234**, 134.
46. W. K. Idol and J. L. Anderson, *J. Membr. Sci.*, 1986, **28**, 269.

47. F. Caruso, in *Colloid Chemistry II*, ed. P. D. M. Antonietti, Springer, Berlin, 2003, pp. 145–168.
48. F. Caruso, *Adv. Mater.*, 2001, **13**, 11.
49. Z. Liang, C. Wang, Z. Tong, W. Ye and S. Ye, *React. Funct. Polym.*, 2005, **63**, 85.
50. R. Veyret, T. Delair and A. Elaissari, *J. Magn. Magn. Mater.*, 2005, **293**, 171.
51. M. Lansalot, M. Sabor, A. Elaissari and C. Pichot, *Colloid Polym. Sci.*, 2005, **283**, 1267.
52. M. Okubo, K. Ichikawa, M. Tsujihiro and Y. He, *Colloid Polym. Sci.*, 1990, **268**, 791.
53. R. H. Ottewill, A. B. Schofield, J. A. Waters and N. S. J. Williams, *Colloid Polym. Sci.*, 1997, **275**, 274.
54. F. Sauzedde, A. Elaissari and C. Pichot, *Colloid Polym. Sci.*, 1999, **277**, 846.
55. F. Sauzedde, A. Elaissari and C. Pichot, *Colloid Polym. Sci.*, 1999, **277**, 1041.
56. L. Hu, A. Percheron, D. Chaumont and C.-H. Brachais, in *Microwave Heating*, ed. U. Chandra, InTech, Rijeka, Croatia, 2011, Chapter 12, pp. 265–290.
57. B. Charleux, F. D'Agosto and G. Delaittre, in *Hybrid Latex Particles*, ed. A. M. van Herk and K. Landfester, Springer, Berlin, 2010, pp. 125–183.
58. J. Pyun and K. Matyjaszewski, *Chem. Mater.*, 2001, **13**, 3436.
59. C. J. Galvin and J. Genzer, *Prog. Polym. Sci.*, 2012, **37**, 871.
60. H. C. Kolb, M. G. Finn and K. B. Sharpless, *Angew. Chem. Int. Ed.*, 2001, **40**, 2004.
61. M. Meldal, *Macromol. Rapid Commun.*, 2008, **29**, 1016.
62. M. Meldal and C. W. Tornøe, *Chem. Rev.*, 2008, **108**, 2952.
63. C. W. Tornøe, C. Christensen and M. Meldal, *J. Org. Chem.*, 2002, **67**, 3057.
64. V. V. Rostovtsev, L. G. Green, V. V. Fokin and K. B. Sharpless, *Angew. Chem. Int. Ed.*, 2002, **41**, 2596.
65. W. H. Binder and R. Sachsenhofer, *Macromol. Rapid Commun.*, 2008, **29**, 952.
66. W. H. Binder and R. Sachsenhofer, *Macromol. Rapid Commun.*, 2007, **28**, 15.
67. W. H. Binder and C. Kluger, *Curr. Org. Chem.*, 2006, **10**, 1791.
68. W. H. Binder and R. Sachsenhofer, in *Click Chemistry for Biotechnology and Materials Science*, ed. J. Lahann, Wiley, Chichester, 2009, pp. 119–175.
69. H. D. B. Gacal, *Macromolecules*, 2006, **39**, 5330.
70. J. W. Chan, B. Yu, C. E. Hoyle and A. B. Lowe, *Chem. Commun.*, 2008, 4959.
71. R. Ranjan and W. J. Brittain, *Macromolecules*, 2007, **40**, 6217.
72. M. Kar, P. S. Vijayakumar, B. L. V. Prasad and S. S. Gupta, *Langmuir*, 2010, **26**, 5772.

73. P. Paoprasert, J. W. Spalenka, D. L. Peterson, R. E. Ruther, R. J. Hamers, P. G. Evans and P. Gopalan, *J. Mater. Chem.*, 2010, **20**, 2651.
74. T. Zhang, Y. Wu, X. Pan, Z. Zheng, X. Ding and Y. Peng, *Eur. Polym. J.*, 2009, **45**, 1625.
75. C. Li, J. Hu, J. Yin and S. Liu, *Macromolecules*, 2009, **42**, 5007.
76. N. Li and W. H. Binder, *J. Mater. Chem.*, 2011, **21**, 16717.
77. W. H. Binder, D. Gloger, H. Weinstabl, G. Allmaier and E. Pittenauer, *Macromolecules*, 2007, **40**, 3097.
78. E. Drockenmuller, I. Colinet, D. Damiron, F. Gal, H. Perez and G. Carrot, *Macromolecules*, 2010, **43**, 937.
79. T. Zhang, Z. Zheng, X. Ding and Y. Peng, *Macromol. Rapid Commun.*, 2008, **29**(21), 1716–1720.
80. R. Ranjan and W. J. Brittain, *Macromol. Rapid Commun.*, 2008, **29**, 1104.
81. R. Ranjan and W. J. Brittain, *Macromol. Rapid Commun.*, 2007, **28**, 2084.
82. Y. Tran and P. Auroy, *J. Am. Chem. Soc.*, 2001, **123**, 3644.
83. D. Hritcu, W. Müller and D. E. Brooks, *Macromolecules*, 1999, **32**, 565.
84. O. Prucker and J. Rühle, *Macromolecules*, 1998, **31**, 592.
85. T. von Werne and T. E. Patten, *J. Am. Chem. Soc.*, 2001, **123**, 7497.
86. M. Husseman, E. E. Malmström, M. McNamara, M. Mate, D. Mecerreyes, D. G. Benoit, J. L. Hedrick, P. Mansky, E. Huang, T. P. Russell and C. J. Hawker, *Macromolecules*, 1999, **32**, 1424.
87. R. Jordan, A. Ulman, J. F. Kang, M. H. Rafailovich and J. Sokolov, *J. Am. Chem. Soc.*, 1999, **121**, 1016.
88. M. D. K. Ingall, C. H. Honeyman, J. V. Mercure, P. A. Bianconi and R. R. Kunz, *J. Am. Chem. Soc.*, 1999, **121**, 3607.
89. R. Jordan and A. Ulman, *J. Am. Chem. Soc.*, 1998, **120**, 243.
90. B. Zhao and W. J. Brittain, *Macromolecules*, 2000, **33**, 8813.
91. M. Ejaz, S. Yamamoto, K. Ohno, Y. Tsujii and T. Fukuda, *Macromolecules*, 1998, **31**, 5934.
92. J.-B. Kim, M. L. Bruening and G. L. Baker, *J. Am. Chem. Soc.*, 2000, **122**, 7616.
93. M. Manuszak Guerrini, B. Charleux and J.-P. Vairon, *Macromol. Rapid Commun.*, 2000, **21**, 669.
94. C. Perruchot, M. A. Khan, A. Kamitsi, S. P. Armes, T. von Werne and T. E. Patten, *Langmuir*, 2001, **17**, 4479.
95. K. N. Jayachandran, A. Takacs-Cox and D. E. Brooks, *Macromolecules*, 2002, **35**, 6070.
96. M. Matsuo, Y. Sugiura, T. Kimura and T. Ogita, *Macromolecules*, 2002, **35**, 6070.
97. W. Huang, J.-B. Kim, M. L. Bruening and G. L. Baker, *Macromolecules*, 2002, **35**, 1175.
98. D. M. Jones and W. T. S. Huck, *Adv. Mater.*, 2001, **13**, 1256.
99. D. Bontempo, N. Tirelli, G. Masci, V. Crescenzi and J. A. Hubbell, *Macromol. Rapid Commun.*, 2002, **23**, 417.
100. S. Edmondson, V. L. Osborne and W. T. S. Huck, *Chem. Soc. Rev.*, 2004, **33**, 14.

101. J. N. Kizhakkedathu and D. E. Brooks, *Macromolecules*, 2003, **36**, 591.
102. J. N. Kizhakkedathu, R. Norris-Jones and D. E. Brooks, *Macromolecules*, 2004, **37**, 734.
103. J. N. Kizhakkedathu, K. R. Kumar, D. Goodman and D. E. Brooks, *Polymer*, 2004, **45**, 7471.
104. M. Zhang, L. Liu, H. Zhao, Y. Yang, G. Fu and B. He, *J. Colloid Interface Sci.*, 2006, **301**, 85.
105. D. A. Shipp, *J. Macromol. Sci. Part C: Polym. Rev.*, 2005, **45**, 171.
106. J. Chiefari, Y. K. Chong, F. Ercole, J. Krstina, J. Jeffery, T. P. T. Le, R. T. A. Mayadunne, G. F. Meijs, C. L. Moad, G. Moad, E. Rizzardo and S. H. Thang, *Macromolecules*, 1998, **31**, 5559.
107. C. Schilli, M. G. Lanzendörfer and A. H. E. Müller, *Macromolecules*, 2002, **35**, 6819.
108. G. Moad, E. Rizzardo and S. H. Thang, *Aust. J. Chem.*, 2005, **58**, 379.
109. G. Moad, Y. K. Chong, A. Postma, E. Rizzardo and S. H. Thang, *Polymer*, 2005, **46**, 8458.
110. J. Chiefari, R. T. A. Mayadunne, C. L. Moad, G. Moad, E. Rizzardo, A. Postma and S. H. Thang, *Macromolecules*, 2003, **36**, 2273.
111. Y. K. Chong, T. P. T. Le, G. Moad, E. Rizzardo and S. H. Thang, *Macromolecules*, 1999, **32**, 2071.
112. S. Perrier and P. Takolpuckdee, *J. Polym. Sci.: Polym. Chem.*, 2005, **43**, 5347.
113. A. Favier and M.-T. Charreyre, *Macromol. Rapid Commun.*, 2006, **27**, 653.
114. K. Bridger, D. Fairhurst and B. Vincent, *J. Colloid Interface Sci.*, 1979, **68**, 190.
115. B. Vincent, *Chem. Eng. Sci.*, 1993, **48**, 429.
116. C. Li and B. C. Benicewicz, *Macromolecules*, 2005, **38**, 5929.
117. C. Li, J. Han, C. Y. Ryu and B. C. Benicewicz, *Macromolecules*, 2006, **39**, 3175.
118. P. S. Chinthamanipeta, S. Kobukata, H. Nakata and D. A. Shipp, *Polymer*, 2008, **49**, 5636.
119. P. Espiard and A. Guyot, *Polymer*, 1995, **36**, 4391.
120. H. B. Sunkara, J. M. Jethmalani and W. T. Ford, *Chem. Mater.*, 1994, **6**, 362.
121. S. A. Asher, J. Holtz, L. Liu and Z. Wu, *J. Am. Chem. Soc.*, 1994, **116**, 4997.
122. E. Bourgeat-Lami and J. Lang, *J. Colloid Interface Sci.*, 1998, **197**, 293.
123. C. Barthet, A. J. Hickey, D. B. Cairns and S. P. Armes, *Adv. Mater.*, 1999, **11**, 408.
124. Y. Zhao and S. Perrier, *Macromolecules*, 2006, **39**, 8603.
125. J. Nicolas, Y. Guillaneuf, C. Lefay, D. Bertin, D. Gigmes and B. Charleux, *Prog. Polym. Sci.*, 2013, **38**, 63.
126. V. Ladmiral, T. Morinaga, K. Ohno, T. Fukuda and Y. Tsujii, *Eur. Polym. J.*, 2009, **45**, 2788.
127. Z. Xu, C. Wang, W. Yang, Y. Deng and S. Fu, *J. Magn. Magn. Mater.*, 2004, **277**, 136.

128. Y. Deng, L. Wang, W. Yang, S. Fu and A. Elaissari, *J. Magn. Magn. Mater.*, 2003, **257**, 69.
129. H. Macková, D. Králová and D. Horák, *J. Polym. Sci. Polym. Chem.*, 2007, **45**, 5884.
130. G. Pibre, L. Hakenholz, S. Braconnot, H. Mouaziz and A. Elaissari, *e-Polymers*, 2009, No. 139.
131. A. Elaissari, M. Rodrigue, F. Meunier and C. Herve, *J. Magn. Magn. Mater.*, 2001, **225**, 127.
132. O. Yamada, T. Matsumoto, M. Nakashima, S. Hagari, T. Kamahora, H. Ueyama, Y. Kishi, H. Uemura and T. Kurimura, *J. Virol. Methods*, 1990, **27**, 203.
133. F. Mallet, G. Oriol, C. Mary, C. Verrier and B. Mandrand, *Biotechniques*, 1995, **18**, 678.
134. A. Elaissari, *e-Polymers*, 2005, No. 028.
135. F. Mallet, C. Hebrard, J. M. Livrozet, O. Lees, F. Tron, J. L. Touraine and B. Mandrand, *J. Clin. Microbiol.*, 1995, **33**, 3201.
136. F. Mallet, C. Hebrard, D. Brand, E. Chapuis, P. Cros, P. Allibert, J. M. Besnier, F. Barin and B. Mandrand, *J. Clin. Microbiol.*, 1993, **31**, 1444.
137. M. H. Charles, M. T. Charreyre, T. Delair, A. Elaissari and C. Pichot, *STP Pharma Sci.*, 2001, **11**, 251.
138. A. Elaissari, *Macromol. Symp.*, 2005, **229**, 47.
139. J.-C. Olivier, M. Taverna, C. Vauthier, P. Couvreur and D. Baylocq-Ferrier, *Electrophoresis*, 1994, **15**, 234.
140. P. Van Dulm and W. Norde, *J. Colloid Interface Sci.*, 1983, **91**, 248.
141. H. Kawaguchi, K. Fujimoto and Y. Mizuhara, *Colloid Polym. Sci.*, 1992, **270**, 53.
142. A. Elaissari, L. Holt, F. Meunier, C. Voisset, C. Pichot, B. Mandrand and C. Mabilat, *J. Biomater. Sci. Polym. Ed.*, 1999, **10**, 403.
143. A. Elaissari and V. Bourrel, *J. Magn. Magn. Mater.*, 2001, **225**, 151.
144. K. Satoh, A. Iwata, M. Murata, M. Hikata, T. Hayakawa and T. Yamaguchi, *J. Virol. Methods*, 2003, **114**, 11.
145. R. Veyret, A. Elaissari, P. Marianneau, A. A. Sall and T. Delair, *Anal. Biochem.*, 2005, **346**, 59.
146. A. Arkhis, A. Elaissari, T. Delair, B. Verrier and B. Mandrand, *J. Biomed. Nanotechnol.*, 2010, **6**, 28.

CHAPTER II.3

TGA and magnetization measurements for determination of composition and polymer conversion of magnetic hybrid particles.

Summary:

Particle size, electrokinetic properties and size distribution of magnetic hybrid colloidal particles can be determined using various tools. However, their chemical composition can be accurately evaluated by thermogravimetric analysis (TGA) and interestingly combining this technique with magnetization measurements provides chemical composition as well as the polymer conversion on the seed particles. Therefore, both these techniques act complementarily for characterization of magnetic hybrid colloidal particles. Inorganic nanoparticles have been widely used in variety of technological and biomedical areas due to their unique features and cost effectiveness. Magnetic iron oxide nanoparticles have gained significant attraction recently due to their characteristic supramagnetic properties and their sensitive interaction with external magnetic field. This feature makes them ideal of numerous medical, diagnostic and other technological areas. However, magnetic properties depend upon chemical nature of the material, particle size and size distribution. Controlling these parameters optimally allows their successful use in any intended application. This makes the characterization of magnetic particles a crucial area for their effective employment in any application. Magnetic measurement and thermogravimetric analysis has assumed a paramount role in the elucidation of these particles for their successful application.

Thermogravimetric analysis is a technique in which mass of the substance [and/or its reaction products(s)] is measured as a function of temperature, while the substance is subjected to a controlled temperature. Development in TGA has rendered them to be used in kinetics, thermodynamics, metallurgy, corrosion and polymer characterization. The latter is of great significance can be utilized for kinetic studies, life-time prediction, water absorption and more importantly thermal stability. For Polymer composites containing inorganic particles, TGA is widely used for estimation of polymer amount and subsequently their magnetic content. The results of quantitative analysis can be improved by combining it with chromatography, FTIR and mass spectroscopy. Thermogravimetric curves provide information about the decomposition mechanisms for various materials as change in sample mass during analysis can be observed. TG curves can be differentiated to make derivative of TG (DTG) and are more sensitive to subtle difference in weight loss than TG curves. Vibrating sample magnetometer (VSM) is used to determine magnetization of ferrite based materials upon exposure to external magnetic field. VSM measures magnetization by converting the dipole field of the sample into an electrical signal. When crystals are formed from iron atoms, four different magnetic states can arise that is paramagnetic, ferromagnetic, antiferromagnetic and ferrimagnetic. Changing the size of iron particles significantly alters the magnetic properties and

It is found that iron oxide nanoparticles smaller than 20nm often display supermagnetic behavior at room temperature, a feature very much desired for their successful applications.

Preparation of magnetic latex particles is done by magnetic iron oxide nanoparticles that can be modified using surfactants or polymers. The polymer shell covering the magnetic core can be further functionalized using acryl-amide derivatives resulting in stimuli-responsive highly magnetic submicron latex particles. TGA is good tool for characterization of magnetic latex particles with variety of morphologies like core-shell, Janus and polymeric matrix. It is possible to measure the amount of organic as well as inorganic parts using TGA. Choosing inert or reactive atmosphere is of paramount importance in TGA as the gas employed can affect the thermogravimetric curves. Furthermore, aside from their ability to characterize basic hybrid particles, TGA can be performed for quantitative estimation of complex particles and can gather information about polymerization conversion. Determination of chemical composition of magnetic latex particles by magnetization requires prior determination of chemical nature that can be performed either by using XRD or Mossbauer spectra. Thereafter, magnetic contents can be analyzed by VSM. Although, individual characterization done by TGA and VSM are vital, combination of these two techniques can generate additional characteristic information for magnetic hybrid nanoparticles. For instance, accurate determination of percentage polymerization conversion is possible by the combined TGA and VSM technique. Infact, TGA gives exact amount of organic and inorganic materials while magnetization provides accurate amount of magnetic and non-magnetic contents in the given material.

For employing any magnetic nanoparticle based application, gathering accurate and precise information about the nature, composition and properties is a pre requisite. To achieve this goal, it is necessary to combine various complimentary characterization techniques that not only generate reliable data but also widens the scope of measurements. In fact, most problems faced during end stage applications of magnetic nanoparticles are associated with the type functional groups present on surface and their chemical composition. Although, numerous quality tools are available to elucidate these particles, sometimes, these classical tools no longer remain applicable in some case for instance magnetic hybrid latex particles. In this case, TGA and magnetization measurements are performed simultaneously that not only provide exact chemical composition with ratio between organic and inorganic materials but also determines the changes in organic composition between used seed and the final particles leading to polymer conversion and allows the exact determination of magnetic content of the final particles. Having accurate data in this regards allow for manipulation in the experimental conditions and materials that can be exploited for successful application of these tiny yet powerful particles.

TGA and magnetization measurements for determination of composition and polymer conversion of magnetic hybrid particles

Ernandes Taveira Tenório-Neto^{a,b}, Talha Jamshaid^a, Mohamed Eissa^c, Marcos Hiroiuqui Kunita^b, Nadia Zine^d, Géraldine Agusti^a, Hatem Fessi^a, Abdelhamid Errachid El-Salhi^d and Abdelhamid Elaissari^{a*}

Magnetic hybrid colloidal particles can be characterized using various techniques and numerous tools leading generally to particles size, size distribution, and electrokinetic properties. However, the chemical composition of these hybrid particles can be estimated using thermal gravimetric analysis (TGA). More interestingly, the combination of this quantitative technique with the magnetization measurement leads not only to chemical composition but also to the overall polymerization conversion and more precisely to the polymerization conversion on the seed particles. In fact, the TGA performed on dried magnetic particles leads to exact organic/inorganic chemical composition. Regarding the magnetization, the amount of magnetic material can be deduced, and consequently, the amount of non-magnetic material can be also estimated. Thus, TGA and magnetization measurements are considered as complementary techniques for characterization of magnetic hybrid colloidal particles. Copyright © 2015 John Wiley & Sons, Ltd.

Keywords: magnetic nanoparticles; magnetization; thermal gravimetric analysis; characterization



Ernandes Taveira Tenório Neto is a PhD student at the Department of Chemistry at State University of Maringá, Maringá-PR, Brazil. He has got Bachelor in Chemistry (2010) at Federal University of Mato Grosso, Cuiabá-MT, Brazil, and Master's (2012) at State University of Maringá. Currently, he is doing research at *Laboratoire d'Automatique et de Génie*

des Procédés – LAGEP at Claude Bernard University, Lyon, France. The main focus of his research consists on developing polymeric systems containing magnetic particles for *in vitro* applications. He has expertise in the areas of supercritical fluid, pressure-sensitive adhesive, natural and biodegradable polymers, hydrogels, magnetic particles, and drug release.



Talha Jamshaid is lecturer at the University of Lahore, Lahore, Pakistan. Currently, he is a PhD scholar at LAGEP, University of Lyon-1, France. He received his first degree, Doctor of Pharmacy, from the University of the Punjab, Lahore, Pakistan. He is doing research in the subject of pharmaceutical technology. He is particularly involved in the preparation of magnetic latex particles to be used in microfluidic devices like lab-on-a chip, biosensors, and microfluidics.



Dr. Mohamed M. Eissa is an associate professor in Polymers Department, National Research Centre, Giza, Egypt. He has got Bachelor (1991), Master's (1999), and PhD (2006) from the Department of Chemistry, Faculty of Science, Cairo University, Egypt. His work is focused on polymer synthesis, and preparation of polymer composites and their applications in the

* Correspondence to: Abdelhamid Elaissari El-Salhi, University of Lyon, Université Claude Bernard Lyon-1, CNRS, UMR-5007, LAGEP- CPE; 43 bd 11 Novembre 1918, F-69622, Lyon, Villeurbanne, France.
E-mail: elaissari@lagep.univ-lyon1.fr

a E. T. Tenório-Neto, T. Jamshaid, G. Agusti, H. Fessi, A. Elaissari CNRS, University of Lyon, UMR-5007, LAGEP- CPE; 43 bd 11 Novembre 1918, Villeurbanne, France

b E. T. Tenório-Neto, M. H. Kunita Chemistry Department, State University of Maringá, Av. Colombo 5790 CEP: 87020-900, Maringá, Brazil

c M. Eissa Polymers and Pigments Department, National Research Centre, 33 El Bohouth st. (former El Tahrir st.), Dokki, Giza 12622, Egypt

d N. Zine, A. E. El-Salhi Institut des Sciences Analytiques (ISA), Université Lyon, Université Claude Bernard Lyon-1, UMR-5180, 5 rue de la Doua, F-69100, Villeurbanne, France

industrial and biomedical domains. He has got four post doc scholarships in the period 2010–2013 from the French government in the Engineering Processes and Automatic Laboratory (LAGEP–Lyon), France. Dr. Mohamed M. Eissa is an associate editor in the Journal of Colloid Science and Biotechnology, and he is a reviewer for many international journals.



Dr. Marcos Hiroiqui Kunita is an associate professor at the Department of Chemistry, State University of Maringá, Maringá-PR, Brazil. He has got Bachelor (1998), Master's (2001), and a PhD (2005) from the Department of Chemistry at State University of Maringá. Currently, Dr. Kunita is a fellow researcher from Araucaria Foundation, having experience in physical chemistry with emphasis on materials chemistry. He is acting on the following topics: composites, modification of polymeric surfaces, grafting, metal sulfides, and supercritical fluids.



Dr Nadia Zine received her BS in Chemistry from the University M. Ismail, Meknes, in 1994 and her PhD from the Centro Nacional de Microelectrónica Barcelona in 2005. From 2010, she became a lecturer at the UCBL. Her research interest is the chemical functionalization and the development of unconventional microtechnologies based on microcontact printing and soft lithography.



Geraldine Agusti was born in 1983 in Orange, France. She received her Master's in 2007 from the University of Montpellier I, France. After her graduation, she moved to Lyon to the Engineering Processes and Automatic Laboratory (LAGEP at CPE-Lyon), France. She worked for 2 years on nanoparticles formulations for pharmaceutical applications. Since 2012, she is in charge of instrumentation and analyses; as such, she performs the TEM and SEM observations.



Dr. Hatem Fessi has got Master's and PhD from the Pharmaceutical Sciences of the University of Paris XI. He is a professor of Pharmaceutical Technology at the University Lyon I and an expert member of the scientific committee of the French Medical Agency. He is a head of the joint research unit between the University of Lyon I and the National Center of Scientific Research (CNRS) Chemical Engineering and Automated Process (LAGEP), UMR 5007. Currently, he is the director of LAGEP laboratory.



Professor Abdelhamid Errachid El-Salhi is a full professor at the University Claude Bernard-Lyon 1 since the end of 2008. He has been involved as a principal investigator and team leader in several European projects under fifth, sixth, seventh, and H2020 Framework Programmes. Professor Errachid is the head of the Micro/Nanotechnology group that is one of three groups based in the team SIMS. He obtained top-level results in the field of silicon-based (bio)chemical sensors using field-effect transistors and micro/nanoelectrode structures. His deep knowledge and understanding of the electronic devices structure as well as operation and interplay between (bio)chemical molecules and electronics have resulted in development of new (bio)sensor devices.



Dr. Abdelhamid Elaissari is the director of research at CNRS and received his undergraduate education from Agadir University, Morocco, in 1988. He moved to Louis Pasteur University (ICS), Strasbourg, France, in which he received PhD degree for polymers and colloids in 1991. He got a permanent position in CNRS in 1991 and then he joined CNRS-bioMerieux at ENS-Lyon laboratory, until 2007 in which he has developed colloids for biomedical applications including *in vivo*, *in vitro*, and bionanotechnologies. In 2007, he moved to Engineering Processes and Automatic Laboratory (LAGEP at Lyon) in which he is acting not only as a director of research but also as the vice director of LAGEP.

INTRODUCTION

At the end of the last century, inorganic nanoparticles [e.g. gold, silver, iron oxides, quantum dots, and second harmonic generation nanoparticles] have been widely used in various technological and biomedical applications due to their catchy features emanating from their nano-size and structure, as compared with their bulk counterparts. These features include nonlinear optical properties, superparamagnetic properties, as well as some biological and catalytic activities.^[1] Superparamagnetic properties of magnetic iron oxide nanoparticles and in particular magnetite (Fe₃O₄) and maghemite (γ-Fe₂O₃), which render them easily affected by even low-external magnetic field, have attracted much attention, as reported in the literature.^[2] In addition, their biocompatibility, low toxicity, and ease of preparation at low cost make them suitable candidates for many promising applications in various technological and more particularly in biomedical diagnostic and therapeutic domains.^[3–5]

In addition, magnetic iron oxide nanoparticles cover a broad spectrum of industrial and technological applications such as ferrofluids, magnetic seals in motors, magnetic inks for bank cheques, magnetic recording media, organic and biochemical syntheses, and industrial water treatment.^[3]

In the biomedical domain, the ideal magnetic nanoparticles should have high magnetic properties, sufficient small size with narrow distribution, high surface functionality, and well-defined morphology.^[6,7] Generally, the pristine superparamagnetic iron oxide nanoparticles (SIONPs) tend to make aggregates due to their large surface area-to-volume ratio and dipole–dipole

interaction, leading to the reduction in their intrinsic superparamagnetic properties.

Therefore, surface modification of SIONPs is of paramount importance to enhance their water solubility, biocompatibility, and colloidal stability in aqueous and physiological media and to provide mechanical and chemical stability for SIONPs. In this regard, several approaches for modification or encapsulation of SIONPs have been investigated through physical or chemical processes using various materials starting from low-molecular weight compounds (e.g. ligands and surfactants) to the use of high-molecular weight compounds (e.g. synthetic and natural polymers).^[8–11] More importantly, the polymer coat induces reactive chemical functions capable for immobilizing biological species via chemical interaction (e.g. enzymes, proteins, antibody, antigen, DNA, and RNA), which is highly needed for biomedical applications.^[12–14]

For any application of magnetic nanoparticles, magnetic properties [saturation magnetization (M_s)], which mainly depends on particle size, chemical nature of the used magnetic material and magnetic content are considered as the key factors affecting their successful use. Recently, various techniques have been used for colloidal and physical chemistry characterization of such complex particles, including transmission electron microscopy (TEM), Fourier transform infrared spectroscopy (FTIR), powder X-ray diffraction (XRD) technique, atomic absorption spectroscopy, gel permeation chromatography, differential scanning calorimetric, thermogravimetric analysis (TGA), and electrical conductivity measurement.^[15]

However, because of the presence of magnetic iron oxide, some techniques are automatically discarded (e.g. NMR), which needs to use new roots. Therefore, the most efficient techniques, which are now widely used for their characterization, include magnetization measurements and thermal gravimetric analysis.

The present review is thus important, and various aspects are elaborated including description of TGA technique, description of magnetization, chemical composition measurements by TGA, and magnetization and characterization via combination of both TGA and magnetization measurements as complementary techniques.

DESCRIPTION OF THERMAL GRAVIMETRIC ANALYSIS

According to the International Union of Pure and Applied Chemistry (IUPAC), thermogravimetry (TG) can be classified as a technique in which the mass of a substance [and/or its reaction product(s)] is measured as a function of temperature, while the substance is subjected to a controlled temperature program.^[16]

The development of TGA expands its scope beyond simply confirming gravimetric techniques. Currently, studies in the fields of kinetics, thermodynamics, metallurgy, corrosion, and polymers can be performed using TGA technique.^[17]

Figure 1 shows a simplified diagram describing the thermogravimetric system, which basically constituted a balance, a thermocouple, a gas flow system, and an oven.

Nowadays, thermal gravimetric analysis is a versatile technique used for studying the effect of heat on decomposition characteristics of organic materials and more particularly for polymers.

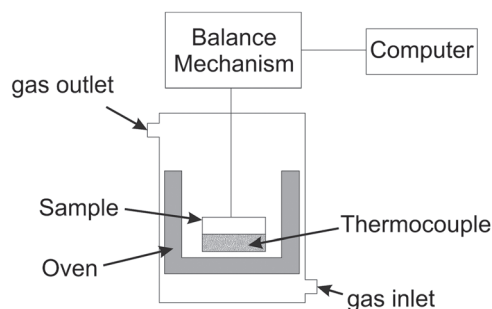


Figure 1. A simplified scheme of the thermobalance used for TG analysis.

Moreover, this technique may be used for polymer characterization, especially on kinetic studies, lifetime prediction, water absorption, and more particularly for thermal stability, which is considered as a basic requirement for some important applications.^[18–20]

For polymer composites containing inorganic particles (e.g. magnetic polymer hybrids), TGA technique is widely used for estimation of the chemical composition (i.e. polymer amount and consequently magnetic content) of the composite. Furthermore, in polymer blends, each polymer shows a characteristic decomposition profile, which may be attributed to different ways of chemical degradation, such as main-chain scission, side group scission, elimination, and depolymerization.^[21] This in turn helps in distinguishing qualitatively one polymer from another, especially in polymer mixtures, using only few milligrams of material. The results of quantitative analysis can be improved if the TGA is coupled with another device, such as gas chromatograph, FTIR, and mass spectrometer.^[22,23]

For quantitative analysis, the thermogravimetric curves provide information about the decomposition mechanisms for various materials, because change in sample mass during analysis could be observed.^[24] If TGA curves do not overlap each other, the mass loss profile of a mixture of materials may be considered as the sum of individual profiles of each of its components providing, easily, quantitative results. Figure 2 shows an example of the thermal behavior of pure polymers and their physical mixtures.

However, when the degradation events from different polymers overlap each other, the simple graph observation for

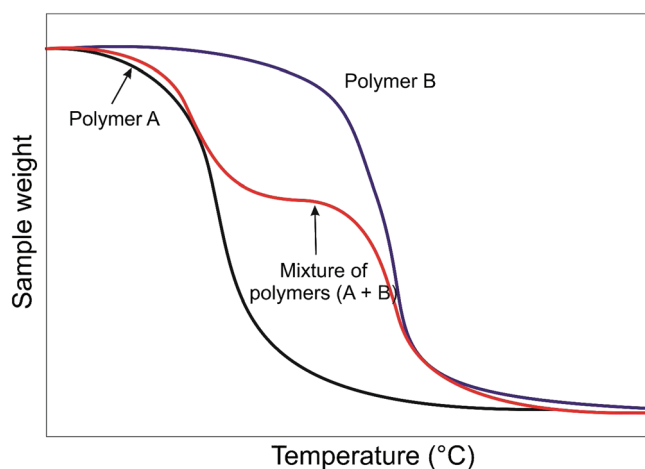


Figure 2. Schematic illustration of TGA curves for hypothetical pure polymers and its physical mixtures (blends). This figure is available in colour online at wileyonlinelibrary.com/journal/pat.

obtaining quantitative results is not possible. In order to overcome this drawback, the TG graphics can be differentiated. Then, the derivative of TG (DTG) curve is sometimes used for determining inflection points on the TG curve. Moreover, DTG is useful in revealing extra details, for example, a hidden degradation event, which would not have been seen on the TG curve itself.^[25] An example for such overlapping can be observed in Fig. 3.

In general, the derivative weight loss curve (DTG) is more sensitive to subtle difference in weight loss than TG curves.^[26] Moreover, by DTG, it is possible to distinguish in which temperature a specific degradation event starts and finishes. Besides identification of an event, the DTG curves may be used to estimate the ratio (%) of polymers in blends. One way consists in plotting a calibration curve, which can be performed through the correlation of peak heights of desired event against a specific temperature or composition.^[26] In order to obtain good consistency on TG experimental, it is important to be careful on the experimental details. The way in which the sample is packed, amount of sample mass analyzed, heating rate, and gas flow rate are some factors that can affect the reproducibility.

DESCRIPTION OF MAGNETIZATION

Various organic and inorganic materials exhibit magnetic properties, which may interest to be explored for well-defined applications. In the last decade, various magnetic materials have been prepared and examined in terms of magnetic properties. Ferrite-based materials and more particularly metallic particles such as iron oxide-based particles have been extensively studied because of their easy chemical preparation (mainly via coprecipitation process) at low cost and the possibility to control their magnetic properties and magnetization.^[27] In order to point out the existence of this property, it is urgent to study their behavior when they are subjected to an external magnetic field. In this regard, vibrating sample magnetometer (VSM) was used.

Vibrating sample magnetometer

Vibrating sample magnetometer is an instrument that measures the magnetization of a small sample of magnetic material placed

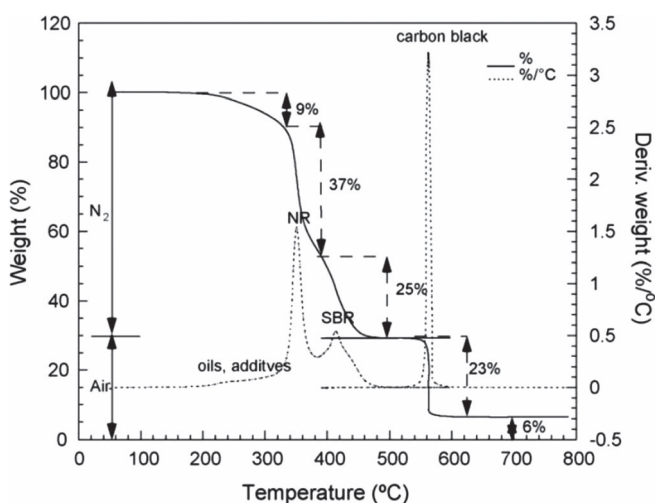


Figure 3. TGA and DTG curves of sample containing natural rubber (NR) 40% (w/w) and styrene-butadiene rubber (SBR) 60% (w/w) vulcanizates.^[25] Reproduced with permission. Copyright © 2006 Elsevier.

in an external magnetizing field by converting the dipole field of the sample into an electrical signal. VSM is based on Faraday's law, which states that an electromagnetic force is generated in a coil when there is a change in flux linking the coil.^[27] In the measurement setup, a magnetic sample is moved in the proximity of two pickup coils as indicated in Fig. 4. The oscillator provides a sinusoidal signal that is translated by the transducer assembly into vertical vibration. The sample, which is fixed to the sample rod, vibrates with a given frequency and amplitude (60 Hz and 1 mm). It is centered between the two pole pieces of an electromagnet that generate a magnetic field H_0 of high homogeneity. Field strengths of several tesla are commonly possible with laboratory VSM systems. Stationary pickup coils are mounted on the poles of the electromagnet. Their symmetry center coincides with the magnetic center of the sample. Hence, the change in magnetic flux originating from the vertical movement of the magnetized sample induces a voltage U_{ind} in the coils. H_0 being constant has no effect on the voltage, but is necessary only for magnetizing the sample. By measuring in the field of an external electromagnet, it is possible to obtain the hysteresis curve of a material.

The measurement setup is sensitive even to very low magnetic moments. Today's VSMs are able to detect magnetic moments down to the μ emu range, which corresponds to approximately 10^{-9} g of iron.^[28]

Magnetic behavior of iron oxide nanoparticles

Iron atom has a strong magnetic moment due to the four unpaired electrons in its 3d orbitals.^[3] As shown in Fig. 5, when crystals are formed from iron atoms, four different magnetic states can arise: paramagnetic, ferromagnetic, ferrimagnetic, and antiferromagnetic (diamagnetic) states. In the paramagnetic state, the individual atomic magnetic moments are randomly aligned with respect to each other, and the crystal has a zero net magnetic moment. If this crystal is subjected to an external magnetic field, some of these moments will align, and the crystal will attain a small net magnetic moment. In ferromagnetic state; all the individual moments in the crystal are aligned even without an external magnetic field (e.g. permanent magnet). In

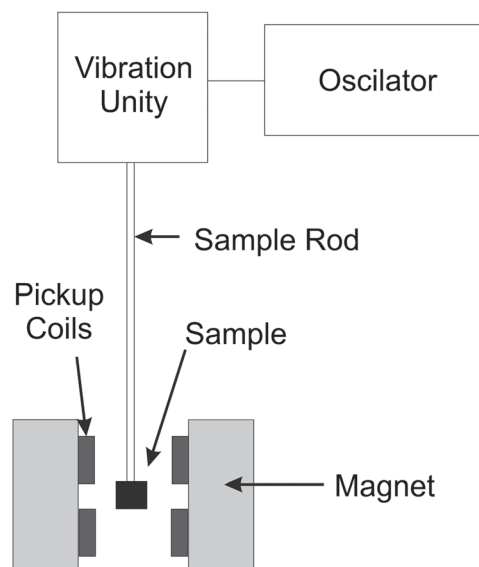


Figure 4. Vibrating sample magnetometer setup.

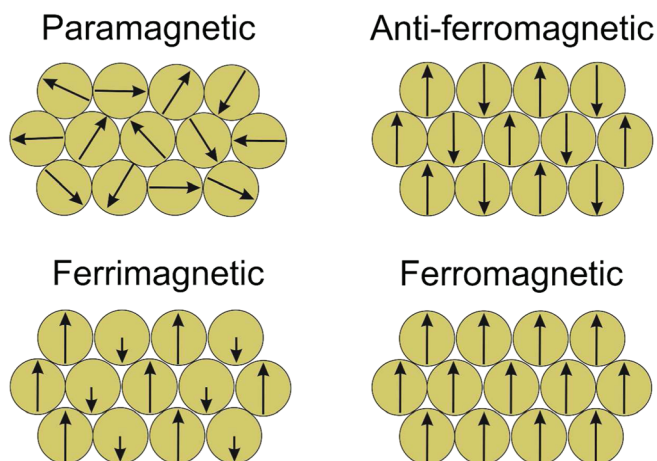


Figure 5. Alignment of individual atomic magnetic moments in different types of materials. This figure is available in colour online at wileyonlinelibrary.com/journal/pat

ferrimagnetic state, the crystal has a net magnetic moment arising from two types of atoms with moments of different strengths that are arranged in an antiparallel fashion. While in antiferromagnetic (diamagnetic) state, magnetic moments are antiparallel and have the same magnitude, then the crystal has no (zero) net magnetic moment.

In the bulk ferromagnetic material, the magnetization M is the vector sum of all the magnetic moments of the atoms per unit volume of the material. The magnitude of M is generally less than its value when all atomic moments are perfectly aligned, because the bulk material consists of domains (Fig. 6). Each domain has its own magnetization vector arising from the alignment of atomic magnetic moments within the domain. The

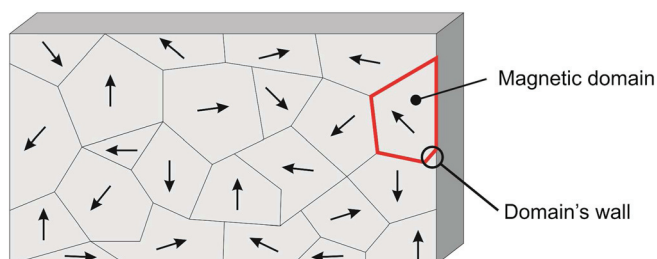


Figure 6. Magnetic domains in a bulk ferromagnetic material. This figure is available in colour online at wileyonlinelibrary.com/journal/pat

regions separating magnetic domains are called domain walls, where the magnetization rotates coherently from the direction in one domain to that in the next domain. Thus, the magnetization vectors of all domains in the material may not be aligned in the same direction, leading to a decrease in the overall magnetization.

If an external magnetic field of strength H is applied to a ferromagnetic material of magnetic strength M [Figure. 7(A)], the magnetization curve is obtained [Figure. 7(B), blue line] showing that M increases with H until maximum saturation magnetization value M_S is reached. The magnetization curve displays a hysteresis loop, because all domains do not return to their original orientations when the magnetic field is removed ($H=0$). Thus, the material will attain a remnant (residual) magnetization M_R , which can only be removed by applying a coercive field H_C in the opposite direction to the initially applied field.

When the size of the material goes down to the submicron or the nanoscale, the number of domains decreases until there is a single domain where the characteristic size of the material is below a critical size (D_c) [Figure. 7(C)]. This single domain describes a region within a magnetic material, which has uniform magnetization, and has no hysteresis loop [Figure. 7(B), red line] and is said to be superparamagnetic. In this case, the individual magnetic nanoparticles have large constant magnetic moment and behave like a giant paramagnetic atom with a fast response to the applied magnetic field without remnant magnetization M_R . It was found that iron oxide nanoparticles smaller than 20 nm often display superparamagnetic behavior at room temperature.^[29,30]

Hybrid magnetic particles

The preparation of magnetic latex particles is incontestably based on the use of magnetic iron oxide nanoparticles. In this direction, modified SIONPs prepared via co-precipitation process are used [Fig. 8(A)].^[34] The iron oxide nanoparticles are first coated with low water solubility surfactant in order to be dispersible in organic phase such as alkane solvent (organic ferrofluid).^[31] Then, the use of this organic ferrofluid in well-appropriate surfactant aqueous solution leads to the formation of oil in water emulsion by using high shearing process or even ultra sound. The obtained oil in water magnetic emulsion can then be used as such to perform mini-emulsion polymerization when the organic solvent is replaced by monomer such as styrene, but the final magnetic latex particles exhibit low magnetic content and then low

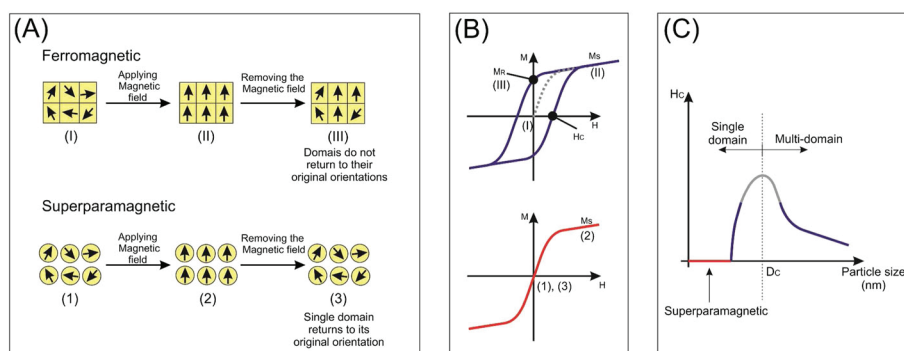


Figure 7. Magnetic properties of ferromagnetic materials as a function of particle size (A and C) and their magnetization curve (hysteresis loop) (B). This figure is available in colour online at wileyonlinelibrary.com/journal/pat.

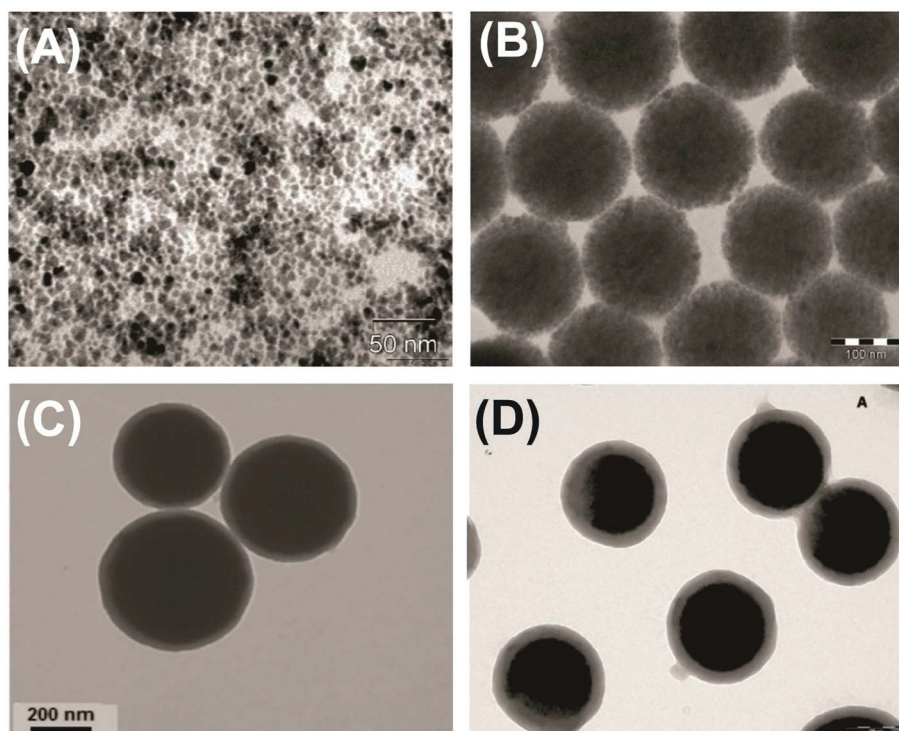


Figure 8. TEM analysis of iron oxide nanoparticles (A),^[34] magnetic emulsion (B),^[32] magnetic poly(divinylbenzene-co-glycidyl methacrylate) colloidal particles (C),^[33] and temperature sensitive poly(NIPAM)-coated magnetic particles (D).^[35] Photos A, C, and D are reproduced with permissions. Copyright © Elsevier. Photo B is reproduced with permissions. Copyright © 2006 American Scientific Publishers.

particles separation under any applied magnetic field. In order to overcome this problem, the prepared magnetic emulsion [Fig. 8(B)] was used as such and as seed in radical emulsion polymerization after avoiding the presence of free micelles in the aqueous phase leading generally to secondary nucleation.^[32] The well-prepared and characterized magnetic emulsion can then be encapsulated using various hydrophobic and/or hydrophilic monomers (mainly styrene monomer or mixture of styrene and functional monomer like glycidyl methacrylate in the presence of divinylbenzene as a crosslinker [Fig. 8(C)].^[33] The polymer shell surrounding the magnetic core can also be further functionalized using acrylamide derivative leading to stimuli-responsive highly magnetic submicron latex particles [Fig. 8(D)].^[35]

CHEMICAL COMPOSITION MEASUREMENTS

Chemical composition by thermal gravimetric analysis

Thermogravimetric analysis may be an interesting tool for characterization of magnetic latex particles with different morphologies (e.g. core-shell, Janus, and polymeric matrix). In general, inorganic oxides do not degrade completely in TG experiment. Based on this fact, it is possible to measure the amount of both organic and inorganic parts.

For estimating the inorganic content, it is important to point out the importance on choosing either inert (e.g. nitrogen) or reactive atmosphere (e.g. air) because the gas employed in TGA measurements can affect the behavior of thermogravimetric curves. For example, in nitrogen (N_2) flow, magnetite (Fe_3O_4) is usually stable up to 600°C, and the TGA data can be used for estimating directly the total

amount of Fe_3O_4 in the sample.^[7,36,37] Moreover, it is well known that FeO is thermodynamically stable above 570°C; for this reason, phase transition from Fe_3O_4 to FeO may be formed when temperature is between 600°C and 800°C. Furthermore, when $T > 800^\circ C$, the deoxidation of FeO may be observed.^[7,38] On the other hand, when TGA curve is obtained under air flow, magnetite is totally converted to Fe_2O_3 in a temperature range between 200°C and 300°C.^[39,40] In such case, the Fe_3O_4 content in the hybrid particles may be estimated by the following chemical equation:



An interesting example on applying the TGA measurement under air flow was reported by Xu and co-workers.^[40] They estimated the amount of Fe_3O_4 in polyacrylamide-coated magnetic particles using Eqn 1. In addition, they could correlate, with reasonable precision, the amount of magnetite with Ms for all samples studied.

In the case of hybrid-based magnetic nanoparticles, TGA under N_2 flow was used to determine the weight percentage of Fe_3O_4 in the Fe_3O_4 /chitosan-polyacrylic acid (PAA) composite microspheres, as shown in Fig. 9.^[41] As clearly seen from the TGA curve (a) of bare Fe_3O_4 nanoparticles, the weight loss is about 3% for the whole temperature range. This might be due to the evaporation of absorbed or crystalline water in the sample. On the other hand, for Fe_3O_4 /chitosan-PAA composites [TGA curve (b)], below 200°C, the weight loss of all the nanocomposites is quite small (7%) due to removal of the absorbed physical and chemical water. Then, the principle chains of chitosan-PAA begin to degrade at about 230°C, and the temperature of final decomposition is at around 500°C, reaching to a weight loss of 68%. In

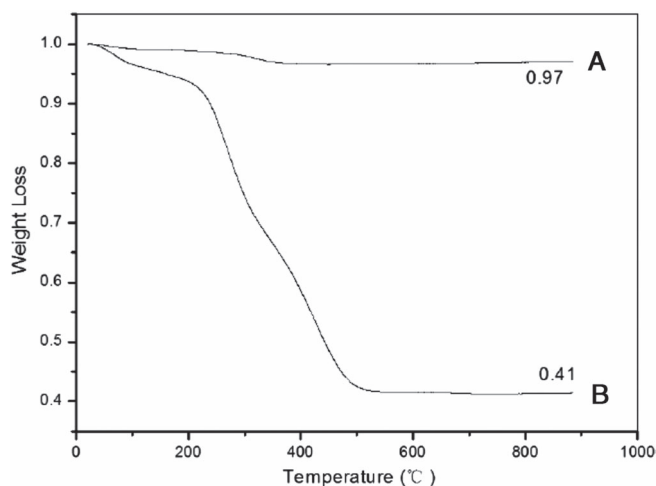


Figure 9. Weight loss curves of (A) bare Fe_3O_4 and (B) Fe_3O_4 /chitosan-PAA magnetic microspheres.^[41] Reproduced from © 2010; licensee MDPI, Basel, Switzerland. Distributed under the terms and conditions of the Creative Commons Attribution license (<http://creativecommons.org/licenses/by/3.0/>).

addition, there is no significant weight change from 500°C to 900°C was observed, implying the presence of only iron oxide. Calculation results showed that the magnetic content of composite microspheres is about 41.3 wt%.

These results are very close to and in conformity with those obtained by magnetization measurements, as can be seen in the Section on Chemical Composition by Magnetization.

Moreover, TGA was used not only for basic hybrid particles but also for more complex ones and principally for quantitative aspect in order to have more information about polymerization conversion. For instance, the amount of inorganic magnetic core of the polymer coated-magnetic particles [MP(NIPAM/MBA/AEMH)] based on N-isopropylacrylamide (NIPAM), N,N'-methylenebisacrylamide (MBA), and aminoethylmethacrylate hydrochloride (AEMH) (Fig. 10) was easily estimated from the percentage of weight loss of the organic part (Fig. 11).

As clearly seen, the major weight loss occurred in the range of 350–450°C and reached a plateau after 500°C. As expected, the amount of residual mass (mostly magnetic content and little amount of ash) about 60% in cross-linked magnetic seed particles is lower than that of magnetic emulsion (82%). This was attributed to the incorporation of polymers on the magnetic seed particles, which lowers magnetic content in the final particles.^[35] Furthermore, the authors also could estimate the percentage of

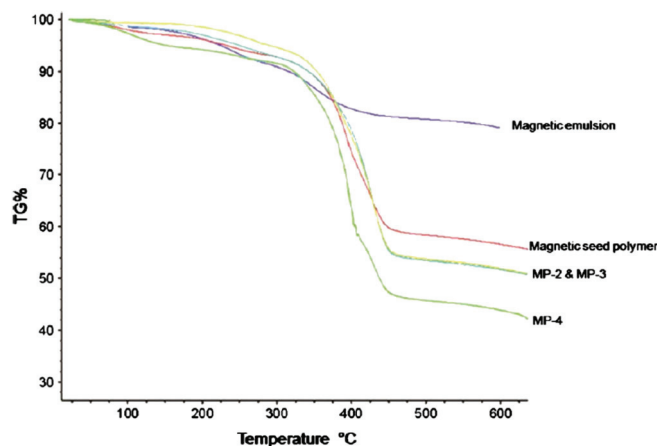


Figure 11. Thermogravimetric curve of magnetic emulsion, magnetic cross-linked polydivinyl benzene particles seed, and magnetic PDVB/P (NIPAM/AEMH/MBA) hybrid composite particles at various seed/monomer ratios (MP-2, MP-3 and MP-4).^[35] Reproduced with permission. Copyright © 2011 Elsevier. This figure is available in colour online at wileyonlinelibrary.com/journal/pat.

temperature-sensitive polymer brushes coated onto magnetic polymer seed by comparing the plateau of the magnetic polymer seed with samples (MP-2, MP-3, and MP-4) after further and successive polymerization. From these observations, it was possible to identify that the sample MP-4 showed the highest encapsulation efficiency. Moreover, their TGA results were in a good agreement with TEM observations.

Chemical composition by magnetization

Chemical structure, physical properties, and the amount of inorganic “magnetic” material in the final particle are the key parameters, which control their physical separation in a magnetic field.^[31] In order to determine the chemical composition of magnetic latex particles via magnetization measurement, it is necessary to know the chemical nature of the used magnetic material, which can be examined by XRD technique and/or Mössbauer spectra. Thereafter, the quantitative analysis (magnetic content) can be performed by using TGA, as mentioned earlier, or by magnetization measurements using VSM.

Generally, Ms of the magnetic particles is highly dependent on the magnetic content and also on the chemical nature of the used magnetic material.^[7,40] Then, this property can be exploited to determine the amount of magnetic part in the final particles

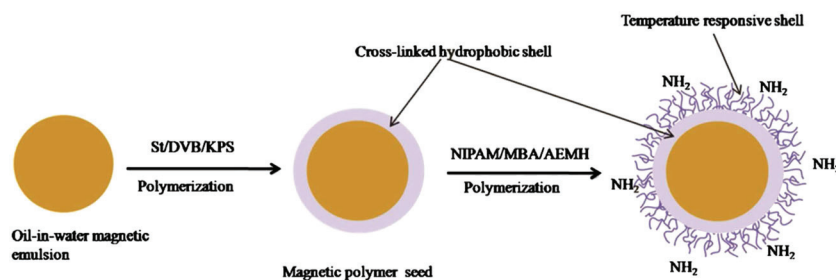


Figure 10. Schematic representation for the preparation of temperature-sensitive amine-containing magnetic poly(DVB)/poly(NIPAM-AEMH) colloidal particles. The starting material is oil-in-water magnetic emulsion, which consisted of oleic acid-coated iron oxide nanoparticles emulsified in aqueous surfactant solution.^[35] Reproduced with permission. Copyright © 2011 Elsevier. AEMH: aminoethyl methacrylate hydrochloride (AEMH), MBA: N,N'-methylenebisacrylamide, DVB: divinylbenzene. This figure is available in colour online at wileyonlinelibrary.com/journal/pat

using magnetization measurements at room temperature. More intensely, this technique is considered as a non-destructive analytical tool as compared with TGA analysis.

Based on the value of M_s of the used initial magnetic nanoparticles and that of dry prepared magnetic hybrid particles, then the magnetic content in the final particles can be measured according to the following equation:

$$\text{Magnetic content (wt\%)} = \frac{M_s}{M_{s_0}} \times 100 \quad (2)$$

where M_s is the saturation magnetization of dry magnetic latex particles, and M_{s_0} is the saturation magnetization of initial magnetic nanoparticles.

In most cases, this technique is complementary and consistent with TGA analysis for determination of magnetic content in the final particles, as previously reported.^[41]

For instance, the magnetization curves of bare Fe_3O_4 particles and Fe_3O_4 /chitosan-PAA composite microspheres recorded with VSM are illustrated in Fig. 12(A) and 12(B), respectively.^[41] As shown in Fig. 12, the magnetization of the samples would approach the saturation values when the applied magnetic field increases to 10,000 Oe. The M_s of bare Fe_3O_4 nanoparticles is 72.5 emu g^{-1} . For the Fe_3O_4 /chitosan-PAA composite microspheres, M_s was about

29.1 emu g^{-1} , which was much less than that of bulk magnetite (84 emu g^{-1}).^[42] The lower value of the measured M_s of bulk Fe_3O_4 nanoparticles was attributed to the presence of the smaller size of maghemite nanoparticles.^[43] In addition, the low M_s of Fe_3O_4 /chitosan-PAA composite microspheres may be attributed to the incorporation of Fe_3O_4 nanoparticles into chitosan-PAA spheres, which added mass of the thick polymer layer on the magnetite nanoparticles. When the magnetic component size of the particles is smaller than the critical size, the particles will exhibit superparamagnetism. A narrow hysteresis loop can be seen in Fig. 12 indicating a small remnant magnetization. It might be that some of the particles are magnetically blocked.

By applying Eqn 2, polymer content could be calculated to be 40.1%, and consequently, polymer or organic content is 59.9%. These values are consistent with those obtained by TGA measurements, as previously mentioned (Fig. 9).

Xu *et al.* have used TGA to measure the magnetite content in magnetic poly(styrene-co-divinylbenzene-co-glycidyl methacrylate) [P(St-DVB-GMA)] latex particles (MLPs).^[44] As shown in Fig. 13(A), the weight loss of the prepared latex was 50 wt% at 400–450°C, which implied that up to 50 wt% of the MLPs consisted of magnetite nanoparticles. On the other hand, the magnetization curve of the prepared latex is plotted in Fig. 13(B).

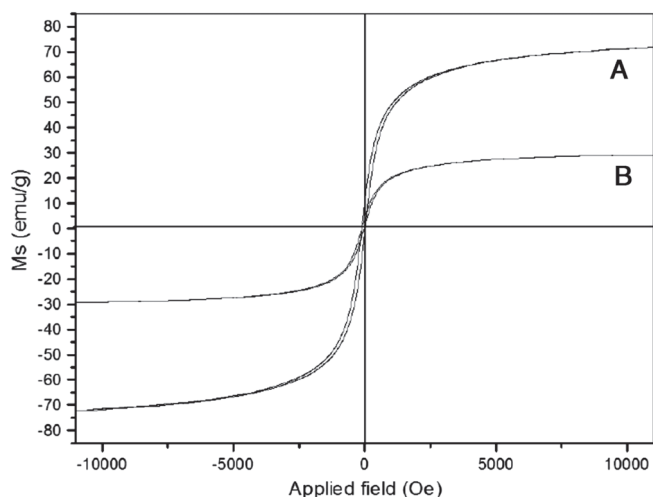


Figure 12. Magnetization curves obtained by vibrating sample magnetometer (VSM) at room temperature: (A) naked Fe_3O_4 ; (B) Fe_3O_4 /chitosan-PAA magnetic microspheres.^[41] Reproduced with permission. Copyright © 2010 John Wiley and Sons.

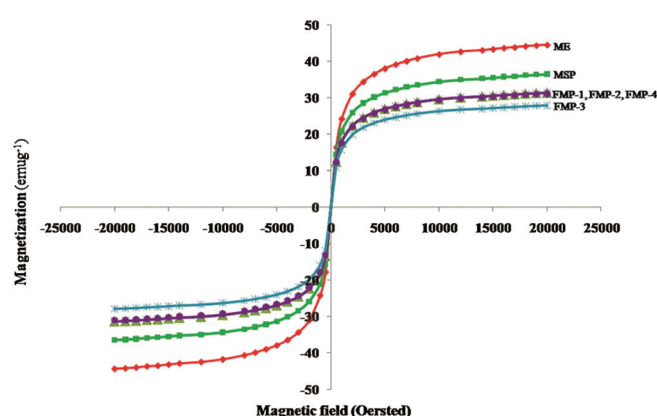


Figure 14. Magnetic hysteresis curve for the oil-in-water magnetic emulsion (ME), magnetic poly(divinylbenzene) seed (MPS), and magnetic@poly(divinylbenzene) @ poly(*N*-isopropyl acrylamide-co-acrylic acid) submicron particles at different AA content, FMP-1, FMP-2, FMP-3 and, FMP-4.^[44] Reproduced with permission. Copyright © 2012 American Scientific Publishers. This figure is available in colour online at wileyonlinelibrary.com/journal/pat.

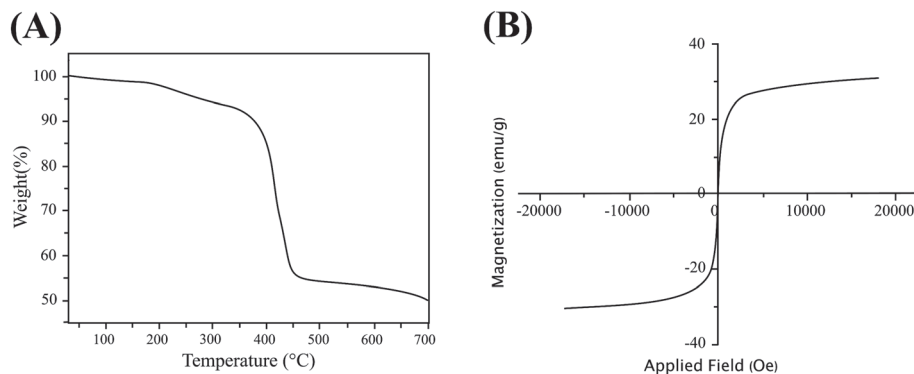


Figure 13. TGA diagram (A) and magnetization curve (B) of MLPs.^[44] Reproduced with permission. Copyright © 2010 John Wiley and Sons.

Table 1. Estimation of magnetic content for dry ME and MP-DVB latexes, which were prepared at various DVB content, based on magnetization and TGA data^[49]

Property	ME	MP-DVB(1) (0.9 ml DVB)	MP-DVB(2) (1.2 ml DVB)
Specific saturation magnetization (emu g^{-1})	51.1	39.6	34.4
Polymer content (wt%) by TGA	0.0	20.2	24.1
Iron oxide content (wt%) by TGA	79.0	67.3	65.2
Iron oxide content (wt%) by VSM	67.2	52.1	45.3
Polymerization conversion (%)	—	64	56

Reproduced with permission. Copyright © 2012, Springer Verlag.

ME, magnetic emulsion; MP-DVB, magnetic poly(divinylbenzene); TGA, thermal gravimetric analysis; VSM, vibrating sample magnetometer.

As shown, the M_s value was 30 emu g^{-1} . Neither remanence nor coercivity was observed, which indicated superparamagnetic property of the MLPs we obtained. The magnetite content calculated from the ratio of the original M_s of Fe_3O_4 nanoparticles (about 60 emu g^{-1}) and that of the synthesized MLPs was 50 wt%; this was in agreement with the result of TGA measurements.

More complex systems have been deeply examined on washed magnetic latex particles after complete removal of any possible secondary nucleation.^[14] As can be easily deduced from Fig. 14, the increase of polymer content in the particles leads to decrease in magnetization. The chemical composition of the used magnetic seed was first determined by TGA and also by magnetization. After polymerization step, the amount of added polymer on the particles can then be determined by magnetization in comparison with the used seed. The obtained results are generally in agreement with the values obtained by TGA analysis.^[14]

As a result, we can say that the combination of TGA and magnetization (as complementary techniques) is good to characterize magnetic latex particles, which cannot be performed by other conventional techniques. If the magnetization of the used seed is well known, the polymerization conversion of monomers to polymer on particles can then be determined even in disperse media after subtracting the diamagnetic property of water only.

COMBINATION OF THERMAL GRAVIMETRIC ANALYSIS AND MAGNETIZATION

Although individual characterization based on TGA and magnetization is vital, however, certain additional characteristics information for magnetic hybrid particles can advantageously be acquired when both these techniques are combined. For example, by combining TGA and magnetization, it is possible to determine the percentage polymerization conversion.

In fact, TGA gives the exact amount of organic and inorganic materials, while magnetization gives the exact amount of magnetic and non-magnetic materials. For instance, in previous work,^[33] M_s of magnetite emulsion (oleic acid-coated Fe_3O_4 nanoparticles) and their corresponding poly(divinylbenzene-co-glycidyl methacrylate) colloidal particles was measured to be 43.85 emu g^{-1} and 35.49 emu g^{-1} , respectively. By assuming that M_s of the magnetite nanoparticles is 60 emu g^{-1} ,^[44] then the amount of magnetic material is 60 wt%, with 40 wt% organic material (oleic acid and surfactant from the seed emulsion and polymer from the polymerization step). These results were very close to that obtained by TGA analysis.^[33]

Similarly, Nguyen and co-authors reported the synthesis of poly(methyl methacrylate)-coated magnetite nanoparticles. For characterizing the samples, TGA data were used for estimating both polymer contents and polymer-shell thickness. Then, the results were correlated with magnetization.^[45] Another interesting work was reported by Chen and co-workers.^[46] Zwitter ionic polymer-coated core-shell magnetic nanoparticles ($\text{Fe}_3\text{O}_4@ \text{SiO}_2@ \text{PMSA}$) were obtained for applying in specific capture of N-linked glycopeptides. For particles characterization, the authors used TGA to calculate both $\text{Fe}_3\text{O}_4@ \text{SiO}_2$ and polymer amounts, then the results could be correlated with magnetization data. Analogous correlations can be found elsewhere.^[47,48]

Moreover, by performing such combined analysis, the amount of polymer induced by polymerization process can be easily deduced and consequently to polymerization conversion as illustrated in Table 1.^[49] Firstly, it is interesting to notice that total polymerization conversions were observed leading to polymer formation on magnetic emulsion and polymer forming secondary nucleation. After subtracting the amount of organic material from the used seed magnetic dispersion and by determining the amount of organic material after polymerization (of washed dispersion), the polymerization conversion leading to polymer on particles can then be estimated and found to be 64% for magnetic poly(divinylbenzene)(1) and 56% for magnetic poly(divinylbenzene)(2).

During the encapsulation of magnetic nanoparticles with polymer, using seeded emulsion polymerization technique, TGA analysis can be used to follow the polymerization conversion as a function of time but cannot point out the presence of any secondary nucleation. In fact, the burned organic material can be directly related to polymerization conversion when crude sample (unclean) is used irrespective of the presence of secondary nucleation. In the same way, the magnetization of dried samples can also be used for estimation of polymerization conversion. In this case, the M_s should decrease as the polymerization conversion increases.

CONCLUSION

Colloids characterization is of great interest, because much information can be deduced such as colloidal properties, chemical composition, intrinsic properties, and then the mechanism of particles formation or modification.

Regarding inorganic or organic particles, various methods are widely used for particles characterization and surface determination including TEM, Scanning electron microscopy, FTIR, XRD technique, atomic absorption spectroscopy, gel permeation

chromatography, differential scanning calorimetric, and electrical conductivity measurement as largely reported in the literature.

Regarding hybrid particles, it is necessary to combine various complementary characterization techniques in order to obtain more information, and various analytical tools can be used. In fact, most problems are related to chemical composition and surface functional groups on the colloidal particles. However, for some hybrid particles, the use of classical methods is not sufficient, and in some cases, these methods cannot be used. This is the case of hybrid magnetic latex particles, which cannot be analyzed by NMR for instance. Then the complete characterization of magnetic latex particles can be, for instance, performed using TGA and magnetization measurements. TGA is used for exact chemical composition by providing the ratio between organic and inorganic materials. The changes in organic composition between the used seed and the final particles lead to polymerization conversion. Regarding magnetization measurement, the amount of magnetic material can be exactly determined. Then, when the polymerization conversion increases, the amount of this magnetic material decreases, and consequently, the polymerization conversion can be deduced.

REFERENCES

- [1] R. Ladj, A. Bitar, M. Eissa, Y. Mugnier, R. Le Dantec, H. Fessi, A. Elaissari, *Journal of Materials Chemistry B* **2013**, *1*, 1381.
- [2] P. E. G. Casillas, C. A. R. Gonzalez, C. A. M. Pérez, *Infrared Spectroscopy of Functionalized Magnetic Nanoparticles, Infrared Spectroscopy*. (Ed.: Prof. Theophanides Theophile), InTech, **2012**. <http://www.intechopen.com/books/infrared-spectroscopy-materials-science-engineering-and-technology/infrared-spectroscopy-of-functionalized-magnetic-nanoparticles>
- [3] A. S. Teja, P.-Y. Koh, *Progress in Crystal Growth and Characterization of Materials* **2009**, *55*, 22.
- [4] M. M. Rahman, A. Elaissari, in *Hybrid Latex Particles: Preparation with (Mini)emulsion Polymerization, Vol. 233* (Eds.: A. M. van Herk, S. A. F. Bon, K. Landfester), Springer, Berlin, **2010**, pp. 237.
- [5] A. Elaissari, H. Fessi, *Macromolecular Symposia* **2010**, *288*, 115.
- [6] J. K. Oh, J. M. Park, *Progress in Polymer Science* **2011**, *36*, 168.
- [7] M. Mahdavi, M. Bin Ahmad, M. J. Haron, F. Namvar, B. Nadi, M. Z. Ab Rahman, J. Amin, *Molecules* **2013**, *18*, 7533.
- [8] R. Ravikumar, S. Kumar, R. Bandyopadhyaya, *Colloids and Surfaces A: Physicochemical and Engineering Aspects* **2012**, *403*, 1.
- [9] K. G. Paul, T. B. Frigo, J. Y. Groman, E. V. Groman, *Bioconjugate Chemistry* **2004**, *15*, 394.
- [10] L. A. Thomas, L. Dekker, M. Kallumadil, P. Southern, M. Wilson, S. P. Nair, Q. A. Pankhurst, I. P. Parkin, *Journal of Materials Chemistry* **2009**, *19*, 6529.
- [11] A. Aqil, S. Vasseur, E. Duguet, C. Passirani, J. P. Benoît, A. Roch, R. Müller, R. Jérôme, C. Jérôme, *European Polymer Journal* **2008**, *44*, 3191.
- [12] A. Andrade, J. Fabris, R. Ferreira, R. Domingues, in *Biomedical Engineering Frontiers and Challenges* (Ed.: R. Fazel), InTech, **2011**, pp. 158. <http://www.intechopen.com/books/mostdownloaded/biomedical-engineering-frontiers-and-challenges>
- [13] H. Macková, D. Horák, S. Trachtová, B. Rittich, A. Spanová, *Journal of Colloid Science and Biotechnology* **2012**, *1*, 235.
- [14] M. M. Rahman, A. Elaissari, *Journal of Colloid Science and Biotechnology* **2012**, *1*, 3.
- [15] J. Carlos, D. O. Mártire, F. S. G. Einschlag, M. C. González, *Water - Treatment Technologies and Recent Analytical Developments*, (Eds.: F. S. G. Einschlag, L. Carlos), InTech, **2013**, pp. 63. <http://www.intechopen.com/books/waste-water-treatment-technologies-and-recent-analytical-developments>
- [16] IUPAC, in *The Gold Book*, 2nd ed. (Eds.: A. D. McNaught, A. Wilkinson), Blackwell Scientific Publications, Oxford, **2006**.
- [17] R. Bud, D. J. Warner, *Instruments of Science: An Historical Encyclopedia*, Science Museum, London, and National Museum of American History, Smithsonian Institution, **1998**.
- [18] S. Mallakpour, M. Taghavi, *Polym. J* **2009**, *41*, 308.
- [19] Z. Dobkowski, E. Rudnik, *Journal of Thermal Analysis and Calorimetry* **2002**, *69*, 693.
- [20] M. Oliveira, L. de Miranda Santos, M. de Gois da Silva, H. da Cunha, E. da Silva Filho, C. da Silva Leite, *Journal of Thermal Analysis and Calorimetry* **2015**, *119*, 37.
- [21] S. Z. D. Cheng, *Handbook of Thermal Analysis and Calorimetry: Applications to Polymers and Plastics, Vol. 3*. Elsevier Science, Amsterdam, **2002**.
- [22] M. Saraji-Bozorgzad, R. Geissler, T. Streibel, F. Mühlberger, M. Sklorz, E. Kaisersberger, T. Denner, R. Zimmermann, *Analytical Chemistry* **2008**, *80*, 3393.
- [23] S. M. Alshehri, A. Al-Fawaz, T. Ahamad, *Journal of Analytical and Applied Pyrolysis* **2013**, *101*, 215.
- [24] P. J. Haines, *Principles of Thermal Analysis and Calorimetry*, Royal Society of Chemistry, Cambridge, **2002**.
- [25] M. J. Fernández-Berridi, N. González, A. Mugica, C. Bernicot, *Thermochimica Acta* **2006**, *444*, 65.
- [26] F. Motiee, S. Taghvaei-Ganjali, M. Malekzadeh, *International Journal of Industrial Chemistry* **2013**, *4*, 16.
- [27] K. H. J. Buschow, F. R. Boer, *Physics of Magnetism and Magnetic Materials*, Vol. 7 Springer, New York, **2003**.
- [28] L. Michalowsky, *Magnettechnik: Grundlagen, Werkstoffe, Anwendungen*, 3rd ed. Vulkan-Verlag, Fachbuchverlag Leipzig, **2006**.
- [29] R. M. Cornell, U. Schwertmann, *The Iron Oxides: Structure, Properties, Reactions, Occurrences and Uses*, 2nd ed. Wiley, Weinheim, **2006**.
- [30] S. R. Dave, X. H. Gao, *Wiley Interdisciplinary Reviews-Nanomedicine and Nanobiotechnology* **2009**, *1*, 583.
- [31] A. Bitar, C. Kaewsaneha, M. M. Eissa, T. Jamshaid, P. Tangboriboonrat, D. Polpanich, A. Elaissari, *Journal of Colloid Science and Biotechnology* **2014**, *3*, 3.
- [32] F. Montagne, S. Braconnot, A. Elaissari, C. Pichot, J. C. Daniel, B. Mandrand, O. Mondain-Monval, *Journal of Nanoscience and Nanotechnology* **2006**, *6*, 2312.
- [33] M. M. Eissa, M. Mahbubor Rahman, N. Zine, N. Jaffrezic, A. Errachid, H. Fessi, A. Elaissari, *Acta Biomaterialia* **2013**, *9*, 5573.
- [34] F. Montagne, O. Mondain-Monval, C. Pichot, H. Mozzanega, A. Elaissari, *Journal of Magnetism and Magnetic Materials* **2002**, *250*, 302.
- [35] M. M. Rahman, M. M. Chehimi, H. Fessi, A. Elaissari, *Journal of Colloid and Interface Science* **2011**, *360*, 556.
- [36] L. Zhang, R. He, H. C. Gu, *Applied Surface Science* **2006**, *253*, 2611.
- [37] L. P. Ramirez, K. Landfester, *Macromolecular Chemistry and Physics* **2003**, *204*, 22.
- [38] S. Y. Zhao, D. K. Lee, C. W. Kim, R. G. Cha, Y. H. Kim, Y. S. Kang, *Bulletin of the Korean Chemical Society* **2006**, *27*, 237.
- [39] H. Zhao, K. Saatchi, U. O. Hafeli, *Journal of Magnetism and Magnetic Materials* **2009**, *321*, 1356.
- [40] Z. Z. Xu, C. C. Wang, W. L. Yang, Y. H. Deng, S. K. Fu, *Journal of Magnetism and Magnetic Materials* **2004**, *277*, 136.
- [41] L. Guo, G. Liu, R.-Y. Hong, H.-Z. Li, *Marine Drugs* **2010**, *8*, 2212.
- [42] M. Yamaura, R. L. Camilo, L. C. Sampaio, M. A. Macêdo, M. Nakamura, H. E. Toma, *Journal of Magnetism and Magnetic Materials* **2004**, *279*, 210.
- [43] Y. Chen, Z. Qian, Z. Zhang, *Colloids and Surfaces A: Physicochemical and Engineering Aspects* **2008**, *312*, 209.
- [44] Y. W. Xu, H. Xu, H. C. Gu, *Journal of Polymer Science Part a-Polymer Chemistry* **2010**, *48*, 2284.
- [45] Q. H. Nguyen, D. H. Quyen, T. K. N. Hoang, *Materials Science-Poland* **2014**, *32*, 264.
- [46] Y. J. Chen, Z. C. Xiong, L. Y. Zhang, J. Y. Zhao, Q. Q. Zhang, L. Peng, W. B. Zhang, M. L. Ye, H. F. Zou, *Nanoscale* **2015**, *7*, 3100.
- [47] X. Q. Liu, M. D. Kaminski, H. T. Chen, M. Torno, L. Taylor, A. J. Rosengart, *Journal of Controlled Release* **2007**, *119*, 52.
- [48] J. Castello, M. Gallardo, M. A. Busquets, J. Estelrich, *Colloids and Surfaces a-Physicochemical and Engineering Aspects* **2015**, *468*, 151.
- [49] S. Braconnot, M. M. Eissa, A. Elaissari, *Colloid and Polymer Science* **2013**, *291*, 193.

CHAPTER II.4

Magnetic particles: From preparation to lab-on-a-chip, biosensors, microsystems and microfluidics applications

Summary

From last ten years, magnetic nanoparticles (superparamagnetism) play an important role in in-vitro and in in-vivo biomedical application. Paramagnetic or superparamagnetic particles, which can respond to an external magnetic field, provide an efficient method of separating samples linked to the magnetic particles from the liquid suspension. Magnetic nanoparticles (superparamagnetism) have been involved in a number of *in-vivo* as well as *in-vitro* operations since last ten years. In order to synthesize homogenous and monodisperse nanoparticles of super paramagnetic iron oxides (SPIONs), different synthetic approaches have been tried for example, thermal decomposition of iron containing precursors in different aqueous or organic media, iron salts precipitation from aqueous solutions or water in oil micro emulsification technique.

Two types of encapsulation processes that is physical and chemical encapsulation are used for surface modification of SPIONs. Physical encapsulation of SPIONs includes direct modification of magnetic nanoparticles with surfactant adsorption, or via layer by layer (LBL) electrostatic adsorption or self-assembly of preformed polymers. Chemical encapsulation of SPIONs includes surface functionalization or modification of magnetic nanoparticles via specific grafting, surface initiated controlled polymerization, inorganic silica/polymer hybridization, or by heterogeneous polymerization in dispersion media. For *in vitro* diagnostic applications, seeded emulsion polymerization technique has been extensively used.

Magnetic nanoparticles especially magnetic colloidal particles have found promising applications in different therapeutic and biomedical diagnostic applications. Magnetic colloidal particles are used as solid support such as in Magnetic Resonance Imaging (MRI) as contrast agents, drug delivery, and hyperthermia biomolecules like bacteria, virus etc in order to enhance the sensitivity of *in-vitro* biomedical diagnosis. Magnetic colloidal particles are commonly used as solid supports (carriers) for the immobilization of biomolecules such as oligonucleotides, peptides, ligands, proteins or antibodies in order to enhance the specific capture of the targeted biomolecules (e.g. bacteria, viruses, etc.).

Microfluidic combined with nanotechnology has played an important role in developing μ TAS or LOC systems. The combination of magnetic nanoparticles and microfluidic system has provided benefits like automation and easy implementation for chemical bonding providing high surface to volume ratio and superparamagnetic nature. For enhancing the mixing and improvement of kinetics of tagging process, magnetic nanoparticles are used. The use of magnetic particles in microfluidic devices provides new possibilities of manipulating molecules in small volume. Different forms of biological applications can be recognized by using magnetic particles in microfluidic systems like sample purification, solid substrate to sample, sample manipulation, labeling, transport, separation and protein-interaction. Purification and capturing of molecules are an important task while performing on-chip nucleic acid analysis. By the use of magnetic microparticles in a microfluidic system, nucleic acid can be brought into contact with particle surface through different means. A preferred solution is the incubation of activated magnetic particles with the sample in a reservoir. Here, purification is done by introducing magnetic field to separate magnetic particles from the sample and nucleic acid capturing is driven by diffusion. An important characteristic of magnetic particles is that they can be suspended in a microfluidic channel by applying

magnetic forces without the use of supporting substrate. However, some solutions used relative velocity between sample and magnetic particles by immobilizing the latter. Mostly, it is based on immobilization of magnetic particles inside a micro channel before or after capture step. Magnetic particles are thus held against a flow through a magnetic field perpendicular to channel while source of magnetic field occurs by integrating electromagnetic element into the chip or by placing permanent magnet at the bottom of the system. Magnetic particles in conjunction with microfluidics can successfully be used for developing micro reactors for proteomic applications. Proteolysis of the proteins occurs through porous magnetic plug when magnetic particles are grafted with enzyme. Magnetic particles when grafted with specific enzymes can very efficiently proteolyse the protein of interest. This can be done by flowing through the protein through the porous magnetic plug.

Molecular processes play a vital role in biomedical field that can be done in particular laboratories with help of various biological tests. These biological tests required multi-step and complex processes like sample collection, preparation and sample identification of biomolecules which needs labor and also these steps required time consumption. A new area in research consist of microfluidic systems that deal with sub-Nano liter volumes of fluids involving miniaturization and the combinations of molecular level biological tests into high performance and ultrafine systems, known as lab-on-a-chip, micro total analytical system or micro fluidic device. These have the ability to incorporate scaled-down lab functions, like isolation and analysis of a mixture's ingredients, on a tiny chip making use of small amount of fluids from nano to pico liters in a properly controlled manner. These devices fulfill all basic needs like they are tiny, easy to handle due to their portable nature, fast in processing, have reduced cost, need minimum amount of sample and the solvent for biomedical research and diagnosis.

Biosensors are being investigated using superparamagnetic particles, nm to μm in size, as labels, which consist of magnetic particles embedded inside a non-magnetic matrix (e.g. natural or synthetic polymers). Recently, magnetic particles have been produced as labels for bio sensing. Different magnetic particles, for example, magnetite nanoparticles and polymer matrix micro beads, have been used for the labeling and detection of biomolecules. It is quite difficult to compare sensitivities of different approaches without taking into account the practical aspects of biosensing, because of differences in magnetic properties and sizes of particles employed. Assay sensitivity combined with detector sensitivity is used to determine the actual sensitivity of a biosensor system based on magnetic bead labeling.

Different biosensors that employ different biosensing principles comprise of different magnetic materials and instrumentation. The first type consists of magnetic relaxation switch assay-sensors which are based on the effects of magnetic particles on water proton relaxation rates. The second type consists of magnetic particle relaxation sensors, which determine the relaxation of the magnetic moment within the magnetic particle. The third type is a magnetoresistive sensor, which detect the presence of magnetic particles on the surface of electronic devices that are sensitive to changes in magnetic fields on their surface. Various sensitive magnetic field devices have been used for purpose of biosensing like giant magnetoresistive (GMR) and spin valves superconducting interference devices (SQUIDS).

At present, magnetic latex nanoparticles have become a basic ingredient for producing fast and sensitive diagnostic devices as well as transportation and even detection in microsystems combining micro-fluidic and lab –on – a chip technology.



Magnetic particles: From preparation to lab-on-a-chip, biosensors, microsystems and microfluidics applications



Talha Jamshaid ^a, Ernandes Taveira Tenório Neto ^{a,d}, Mohamed M. Eissa ^b, Nadia Zine ^c, Marcos Hiroiuqui Kunita ^d, Abdelhamid Errachid El-Salhi ^c, Abdelhamid Elaissari ^{a,*}

^a Université de Lyon, F-69622 Lyon, France, Université Lyon 1, Villeurbanne, CNRS, UMR 5007, LAGEP-CPE, 43 Boulevard 11 Novembre 1918, F-69622 Villeurbanne, France

^b Polymers and Pigments Department, National Research Centre, 33 El Bohouth St. (Former El Tahrir St.), Dokki, Giza 12622, Egypt

^c Institut des Sciences Analytiques (ISA), Université Lyon, Université Claude Bernard Lyon-1, UMR-5180, 5 rue de la Doua, F-69100, Villeurbanne, France

^d Chemistry Department, Universidade Estadual de Maringá, Av. Colombo, 5790 Jardim Univeristário CEP: 87020-900, Maringá, Paraná, Brazil

ARTICLE INFO

Keywords:

Magnetic particles
Functionalization
Sample preparation
Microfluidic
Microsystems
Lab-on-a-chip
In vivo diagnosis

ABSTRACT

Magnetic particles are largely used in various applications and particularly in *in-vitro* biomedical diagnostic and bionanotechnology. In fact, they have been employed for extraction of various biomolecules even from crude samples and as solid support in numerous samples' preparation for *in-vitro* diagnosis. Nowadays, they are also successfully being exploited as a carrier of biomolecules in microsystems, microfluidics, lab-on-a-chip and for detection in specific biosensors. Before any use or any preparation of magnetic hybrid particles, various factors should be considered in order to perfectly target the suitable applications. For instance, in case of nucleic acid, the particles shouldn't induce any inhibition of biological amplification techniques. For microfluidic, these particles should be colloidal stable in order to avoid any jump in the microfluidic canals. Regarding biosensor, these particles need to be chemically well designed generally to enhance specific detection or specific signal.

© 2015 Elsevier B.V. All rights reserved.

Contents

1. Introduction	345
2. Magnetic nanoparticles: from preparation to encapsulation	345
2.1. Magnetic particles preparation	345
3. Magnetic particles as a solid support and as a carrier	345
3.1. Specific capture	346
3.2. Magnetic particles for specific nucleic acids capture	346
3.3. Magnetic particles for immunoassay diagnostic	346
3.4. Magnetic carrier for sample preparation and generic capture	347
3.5. Nucleic acids extraction, concentration and detection	347
3.6. Magnetic particles for detection	347
4. Magnetic particles in Microsystems	347
4.1. Magnetic particles in lab-on-chip	347
4.2. Biomedical applications	349
4.3. Magnetic particles in biosensing	350
4.4. Magnetic particles in microfluidics	354
5. Conclusion	359
Acknowledgment	360
References	360

* Corresponding author. Tel.: +33 472431841; Fax: +33 472431682.
E-mail address: elaissari@lagep.univ-lyon1.fr (A. Elaissari).

1. Introduction

In the last decade, a great attention has been paid to the unique feature of magnetic nanoparticles (superpara-magnetism), which makes them easily guided by an external magnetic field. This unique property has been exploited in fast separation and particularly for *in vitro* biomedical diagnostic domain [1]. Therefore, the development of reactive magnetic nanoparticles for immobilization and fast magnetic separation of biomolecules (e.g. antibodies, proteins, enzymes, etc.) is of great importance nowadays especially for fast diagnostic applications providing early detection of diseases. This in turn helps us to get optimal results in therapy and consequently management and treatment of diseases at early stages of infection. Moreover, magnetic colloidal particles have also been tried in various *in vivo* diagnostic and therapeutic applications such as in Magnetic Resonance Imaging (MRI) [2] as contrast agents, drug delivery, and hyperthermia.

Among magnetic nanoparticles, iron oxides and in particular magnetite (Fe_3O_4) and its oxidized form maghemite ($\gamma\text{-Fe}_2\text{O}_3$) have attracted much attention due to their biocompatibility, low toxicity, and ease of preparation at low cost [3].

More interestingly, the specific optical (fluorescent) or magnetic feature of magnetic nanoparticles are sometimes exploited and integrated in microsystems in order to elaborate medical devices. This provides fast analysis with high sensitivity for low volume analyte, similar to that existing in large-scale analysis equipments. Such systems are called micro-Total Analysis Systems ($\mu\text{-TAS}$) [4] in which all steps are concentrated in one device (e.g. lab-on-a-chip systems(LOC), biosensors, microfluidic systems, etc). These devices and systems (with highly automated operations) are characterized by their small size and robust mechanics. Hence, are important for routine applications and can also be developed as easy-to-use portable devices. In addition, they are not only cost effective but also have low running costs. These are the features that are very much required in biomedical diagnosis, clinical analysis and nanomedicine. Hence, attracting significant attraction from various research groups.

However, in order to be conveniently used in bio-related applications, the control of surface chemistry of superparamagnetic iron oxide nanoparticles (SIONPs) is required. Generally, the pristine SIONPs tend to aggregate into large clusters due to their large surface area-to-volume ratio and dipole-dipole interaction. As a result, this leads to reduction in their intrinsic superparamagnetic properties. Therefore, surface modification of SIONPs is of a paramount importance not only to prevent aggregation of SIONPs, leading to colloidal stability, but also to enhance their water solubility, biocompatibility, bioconjugation, and nonspecific adsorption to cells. Surface modification, therefore, provides them an edge over the other separation techniques (e.g. filtration, centrifugation and sedimentation) that are laborious as well as time consuming. For instance, the coupling of biomolecules (e.g. proteins, enzymes, antibodies, antigens, etc.) to magnetic nanoparticles has been used to achieve simple, fast, inexpensive and highly efficient separation of targeted biomolecules under the effect of an external magnetic field.

Magnetic colloidal particles are commonly used as solid supports (carriers) for the immobilization of biomolecules such as oligonucleotides, peptides, ligands, proteins or antibodies in order to prevent nonspecific adsorption to cell and so enhance the specific capture of the targeted biomolecules (e.g. bacteria, viruses, etc.).

Furthermore, the ideal magnetic nanoparticles should have high magnetic properties, sufficient small size with narrow distribution, high surface functionality and well defined morphology [5]. These characteristics can be achieved by optimizing the synthesis process of SIONPs in order to prepare structured magnetic nanoparticles bearing a reactive shell with well-defined properties [6].

In this regard, several approaches for preparation and modification of SIONPs have been investigated using various materials starting from low molecular weight compounds (e.g. ligands, surfactants, etc) to the use of high molecular weight compounds (e.g. synthetic polymers, synthetic and natural biopolymers like proteins, polysaccharides, polyethylene oxide, dextran, etc.) [7]. The coating or encapsulation of SIONPs with polymers has several advantages in that, they enhance biocompatibility, colloidal stability in aqueous and physiological media, and provide mechanical and chemical stability for SIONPs. More interestingly, they impart functionality to SIONPs to form conjugates with various biomolecules (e.g. enzymes, proteins, antibody, antigen, DNA, RNA, etc), which is highly needed for biomedical applications [8,9]. Recently, there is a great research attempts to use SIONPs in theranostic applications (diagnostic and therapeutic purposes at the same time) [10].

2. Magnetic nanoparticles: from preparation to encapsulation

2.1. Magnetic particles preparation

Main approaches for the preparation of SIONPs include thermal decomposition of iron precursors in organic (or water) media and co-precipitation of iron salts from their aqueous solutions. The latter is attracting much interest due to high yield as well as effectiveness in controlling nanoparticle size and water-in-oil (w/o) microemulsion. Chemical co-precipitation method depends on the type of iron salt as well as pH and ionic strength of precipitating solution. This can be done by either partial oxidation of ferrous hydroxide by different oxidizing agents or by the addition of alkali to an aqueous solution containing mixture of ferrous (Fe^{2+}) and ferric (Fe^{3+}) ions. Iron oxide particles obtained this way are often not stable and hence are stabilized by using low molecular weight legends, surfactants or functionalized polymers. In addition, magnetic nanoparticles are coated with carboxylate surfactants e.g. oleic acid ($\text{C}_{18}\text{H}_{34}\text{O}_2$) during co-precipitation reaction followed by dispersion in organic medium e.g. octane. The obtained magnetic ferrofluids can be used as a template for further encapsulation with various types of polymers.

Surface modification of hydrophilic inorganic nanoparticles has been performed via two main processes namely, physical encapsulation and chemical encapsulation.

Physical encapsulation of SIONPs includes direct modification of magnetic nanoparticles with surfactant adsorption, or via layer-by-layer (LBL) electrostatic adsorption or self-assembly of preformed polymers. LBL assembly method involves controlled synthesis of novel nanocomposites core-shell materials and hollow capsules. By using this strategy, magnetic colloidal particles have been coated with alternating layers of polyelectrolyte, nanoparticles, and proteins that can be utilized for various biomedical applications.

Chemical encapsulation of SIONPs includes surface functionalization or modification of magnetic nanoparticles via specific grafting, surface initiated controlled polymerization, inorganic silica/polymer hybridization, or by heterogeneous polymerization in dispersion media. Inorganic silica/polymer hybridization involves the encapsulation of SIONPs by a cross linked silica shell through hydrolysis/condensation reactions with the hydroxyl groups on the surface of iron oxide nanoparticles. Heterogeneous polymerization is used to prepare well-defined SIONPs-embedded magnetic spheres as well as cross-linked microgels and nanogels. For *in vitro* diagnostic applications, seeded emulsion polymerization technique has been extensively used [11].

3. Magnetic particles as a solid support and as a carrier

Although, polymer and hybrid particles have been used for numerous biomedical applications but magnetic colloidal particles [12]

have advantage over them because they can be used as solid supports for biomolecules in order to enhance the specific capture of the targeted biomolecules (e.g. bacteria, viruses, etc.), specific RNA recognition [13], separation of DNA from probiotic dairy products [14] and as potential solid support for recyclable biocatalysts [15].

3.1. Specific capture

The prepared colloids and their conjugates with biomolecules are assessed in desired biomedical applications like immunology, specific capture of DNA and RNA, cell sorting and identification, bacteria isolation and detection, virus extraction, concentration and detection. Each application is evaluated by scrutinizing the specificity, the stability, and the sensitivity of bare particles and/or particles bearing biomolecules such as antibodies and nucleic acids.

The specificity and the sensitivity of the targeted applications are directly associated to the surface properties of the particles and to the immobilized biomolecules accessibility. The interactions between biomolecules and reactive particles are largely dependent upon the colloidal and surface properties of the dispersion, and the physico-chemical properties of the biomolecules.

The antibody-polymer immobilization is performed via physical adsorption (mainly via hydrophobic interaction) or chemical grafting onto functional reactive groups (Table 1) [16]. The large-sized polymer beads are also extensively used in analytical immun-affinity chromatography for selective isolation of biomolecules. The

desired biomolecules are specifically affixed onto polymer particles and released after purification.

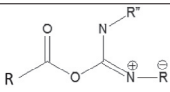
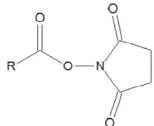
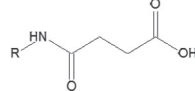
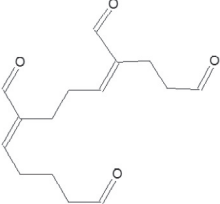
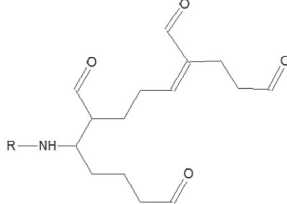
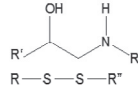
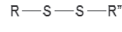
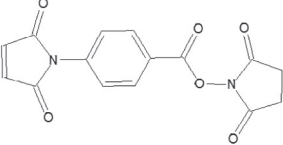
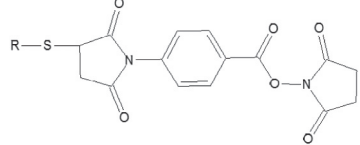
3.2. Magnetic particles for specific nucleic acids capture

The use of magnetic particles for specific capture of nucleic acids is generally performed as follows: The capture probe of well-defined sequence is chemically immobilized on the magnetic latex particles. A test biomolecule sample is mixed with the magnetic particles-ODN conjugates. The biomolecules are then specifically captured via hybridization process (specific hydrogen binding). The detection is done by the addition of oligonucleotide labeled with enzyme, as shown in Fig. 1 [11]. The enzyme oxidizes the substrate and a colored supernatant is produced. This specific capture of nucleic acid molecules combined with well-optimized detection process is the key to improve various biomedical diagnostics.

3.3. Magnetic particles for immunoassay diagnostic

Recently, Eissa et al. [17] have prepared epoxy-functionalized poly(divinylbenzene-co-glycidyl methacrylate) [MPDG] (submicron) colloidal particles using seeded emulsion polymerization technique. The prepared colloidal magnetic particles were chemically immobilized on aminosilane-functionalized silica surface using micro-contact printing technique (μ CP), followed by bio-conjugation with anti-human antibody (Ab). This construction [Ab-MPDG-silica]

Table 1
Examples of chemical grafting onto functional reactive groups [16]

Surface reactive compound	Activating agent	Active derivative
	$R-N=C=N-R^*$ Carbodiimide	
	1-ethyl-3-(3-dimethylaminopropyl) carbodiimine (EDC) / N-hydroxysuccinimide (NHS)	
$R-NH_2$	 Succinic anhydride	
$R-NH_2$	 Glutaraldehyde	
	$R-NH_2$ Primary amine	
$R-S-H$	$H-S-R^*$ Thiol	
$R-S-H$	 3-maleimidobenzoic acid N-hydroxysuccinimide ester	

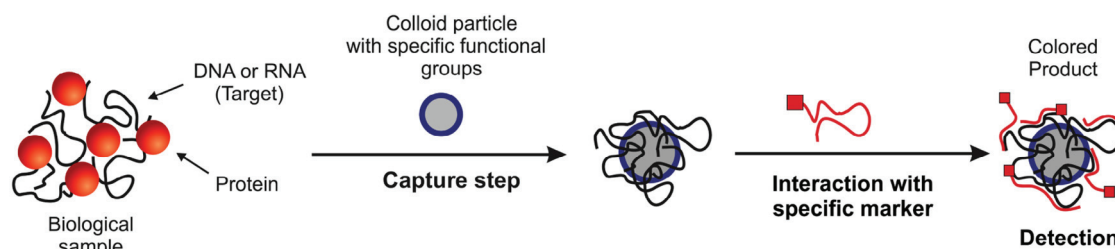


Fig. 1. Schematic illustration of specific capture and detection of nucleic acids (ODN, oligonucleotide; single stranded DNA fragment). The intensity of the supernatant due to the presence of colored product was determined by measuring its absorbance [11].

was used as solid support for immunoassay of the recombinant antigen (Ag). The prepared Ab-MPDG-silica conjugate showed high affinity for specific targeting of the recombinant Ag. This immunoassay was evidenced by fluorescence microscopy using fluorescent-labeled Ab as shown in Fig. 2 [17]. The combination of μ CP and surface functionalization with epoxy-functionalized magnetic MPDG could be integrated into the manufacture of bioelectronic devices such as biosensors, which provide fast analysis with high sensitivity for low analyte volumes.

3.4. Magnetic carrier for sample preparation and generic capture

Magnetic latexes are combination of colloidal polymer particles and magnetic materials i.e., iron oxide nanoparticles. The iron oxide in the polymer particles imparts the magnetic properties to composite latexes [7]. Magnetic latexes are widely utilized in biomedical field as a solid support, in molecular biology, immunoassays, cell sorting, and viruses and bacteria isolation [8]. The magnetic property enables the separation through the use of single magnetic and particle guidance in microsystems. Additionally, the magnetic property also enhances the sensitivity of biomedical diagnostic by enhancing the concentration of biomedical samples. Due to the possible elaboration of well-defined magnetic latexes, several biological tests are automated leading to quick and high sensitivity of biomolecules analysis.

3.5. Nucleic acids extraction, concentration and detection

Due to the polyanion character of nucleic acid molecules, cationic colloidal particles are adsorbed on DNA and RNA via attractive electrostatic interactions. This adsorption is rapid and high at low ionic strength and at acidic medium, and therefore it is controlled by pH and salinity of the incubation medium. After magnetic separation, the supernatant is removed leaving behind the nucleic acids containing magnetic particles. Then the immobilized nucleic acids are washed and desorbed in small volume to increase their concentration. The desorption is principally carried out at basic pH. The purified DNA and RNA are then used to identify the sequence of the target via specific capture of nucleic acid fragments. Before any specific capture, the purified nucleic acids are enzymatically amplified by PCR in case of DNA and by RT-PCR in case of RNA as shown in Fig. 3 [18].

In molecular biology or in the diagnostic world, the magnetic nanoparticles have gained considerable attention as an efficient tool for a fast and easy biomolecule extraction [19]. Numerous types of magnetic particles can be prepared, but only some of them can be adapted to biomolecules analysis. For biomedical diagnostic based on the detection of DNA and RNA, the main complications in the choice of these magnetic colloids are their rapid magnetic separation, demanding a high magnetic oxide content and overall a good compatibility with enzymes for amplification of nucleic acids. In a study, magnetic colloids were prepared from oil in water (o/w) mag-

netic emulsion by a two-step polymer immobilization procedure. First, poly (ethyleneimine) was adsorbed to ensure charge inversion of the emulsion droplets followed by adsorption or chemically grafting of poly (maleic anhydride-co-methyl vinyl ether) subject to its hydrolyzed form. The obtained colloids were evaluated for their surface charge density, colloidal stability, morphology and RT-PCR inhibition test. Selected colloids were used for the nonspecific capture of viruses, with RT-PCR as a means of detection tool. Particle dimension and surface charge studies demonstrated the relevance of these methods. Finally, virus capture tests exhibited 90% capture efficiency with an average detection sensitivity of 103 pfu/ml [19].

3.6. Magnetic particles for detection

Basically, magnetic colloidal particles are mainly used as solid supports for biomolecules in order to enhance the specific capture of the targeted biomolecules. For instance, the individual magnetic nanoparticles were examined in specific capture and isolation of bacteria [8]. In this context, iron oxide nanoparticles were first chemically modified with a specific reactive shell by introducing commonly used functionalized compounds such as carboxylic acid, amines or thiols [7,16]. Then, the selected antibody (e.g. anti-bacteria) was chemically grafted onto the magnetic nanoparticles. These sensitive nanoparticles were then mixed with bacteria containing sample under given buffer conditions (i.e. pH, salinity). The recognized bacteria were then easily extracted using a permanent magnetic field, whereas, the individual magnetic nanoparticles were less sensitive to the applied field, and consequently remained in the supernatant. The extracted bacteria obtained thus can be used for extracting nucleic acid after the bacteria-growing step [20].

Recently, *Salmonella* bacteria in milk were captured by antibody-conjugated magnetic nanoparticles (MNPs) and separated from analyte samples by applying an external magnetic field [21]. The MNP-*Salmonella* complexes were redispersed in a buffer solution followed by their exposure to antibody-immobilized TiO₂ nanocrystals (TNs), which absorb UV light. The assay exhibited high sensitivity toward low concentrations of *Salmonella* bacteria as shown in Fig. 4. The detection limit of *Salmonella* in milk was found to be more than 100 cfu/ml.

4. Magnetic particles in Microsystems

4.1. Magnetic particles in lab-on-chip

Regarding biology of human body, the molecular processes play an important role in biomedical diagnosis [22] that can be performed in specific laboratories with the help of different biological tests. These tests require multi-step and complex processes, including sample collection, preparation, and specific identification of biomolecules necessitating both labor and time [23]. However, more and more biological tests can be performed at the point of

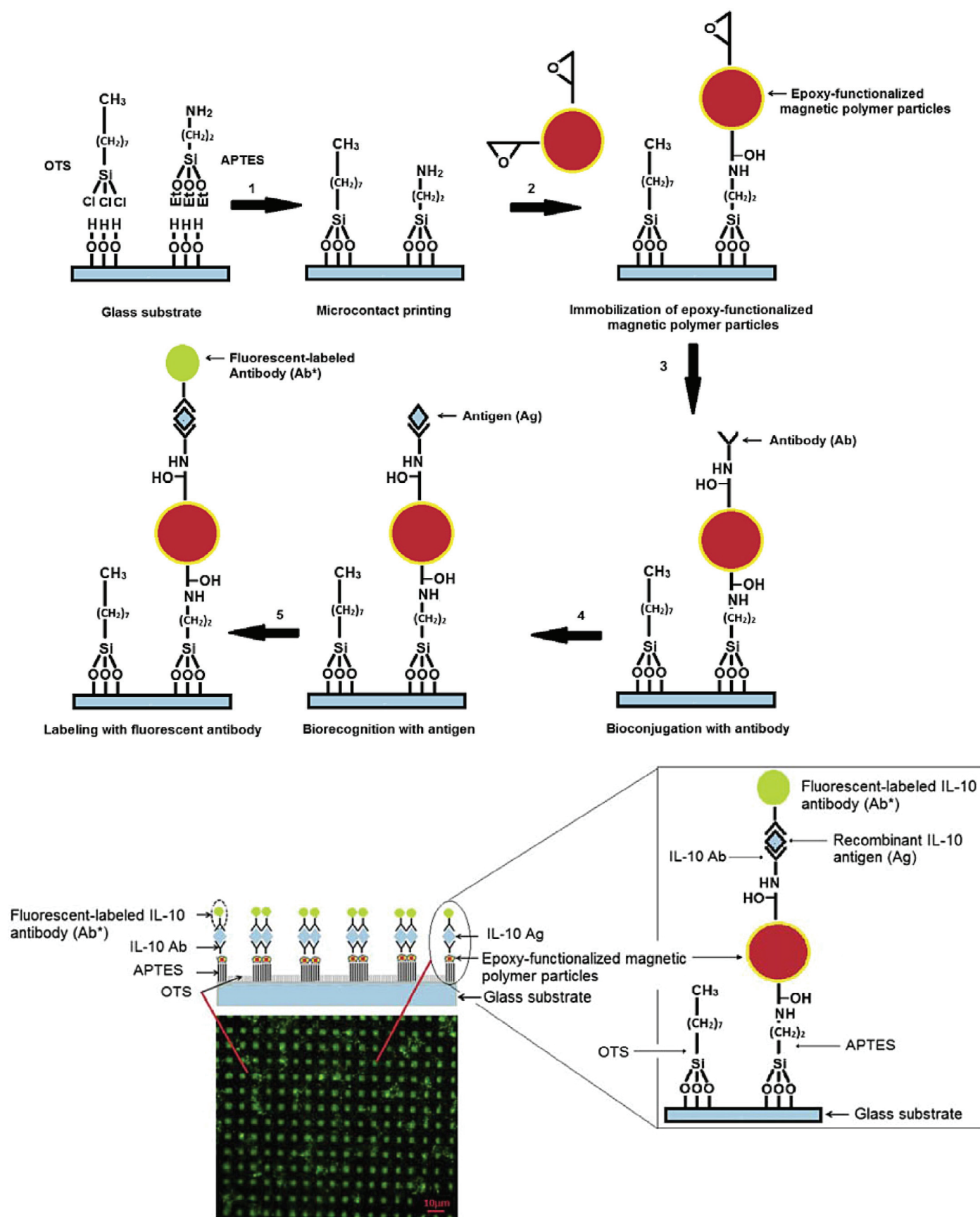


Fig. 2. Epoxy-functionalized magnetic colloidal particles for immunoassay of antigen detection using fluorescent labeled-antibody In figure (OTS) stands for Octadecyltrichlorosilane and 3-aminopropyltriethoxysilane for (APTES) respectively [17].

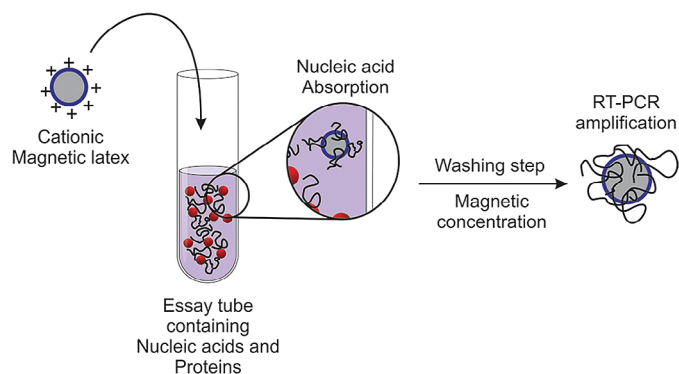


Fig. 3. Schematic illustration of non-specific capture, purification, and concentration of nucleic acid molecules [18].

care [24] i.e. close to the patient allowing smooth testing in the area of medication. In this regard, a new method was developed, dealing with miniaturization and combination of molecular-level biological tests into high-performance and ultrafine systems called Lab-on-a chip [25]. To facilitate the biological tests, magnetic hybrid particles were integrated in these systems in order to facilitate capturing, transportation, labeling and detection of biological molecules from physiological samples [26–28]. In lab-on-chip systems, magnetic separation occurs by binding specific biomolecule to a magnetic particle and then separating it from surrounding matrix by use of magnetic field for manipulating and purification of biological cells or molecules. Magnetic particles, called superparamagnetic particles, are used for such separations. These particles retain no residual magnetism after the field is removed. Bioseparation in microfluidic channel occurs with help of these magnetic particles. In bio separation, first specific antibody is immobilized onto magnetic particles in microfluidic system. The anti-body magnetic particles are then incubated with solution consisting of cells, proteins etc. By collecting the magnetic particles, biomolecules then can be collected in a magnetic field. Magnetic particle-based bioseparation in microfluidic channel is shown in Fig. 5 [29].

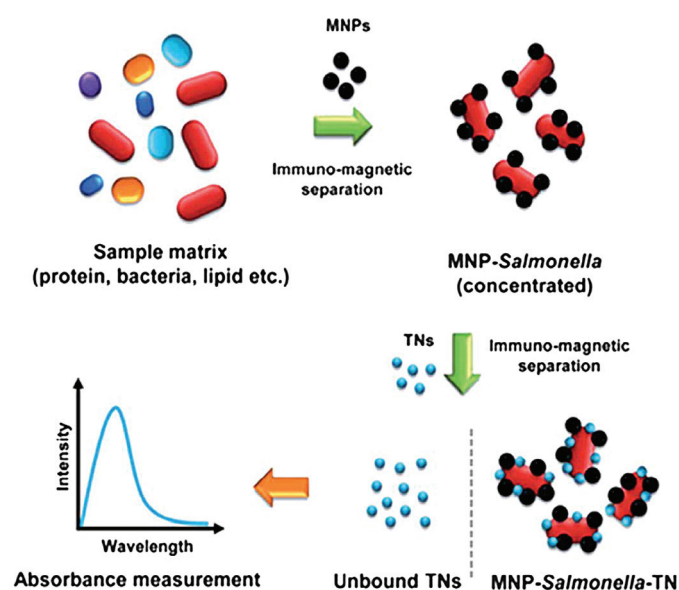


Fig. 4. Schematic illustration for detection of the pathogenic bacteria in milk using magnetic nanoparticles and optical nanoprobes [21].

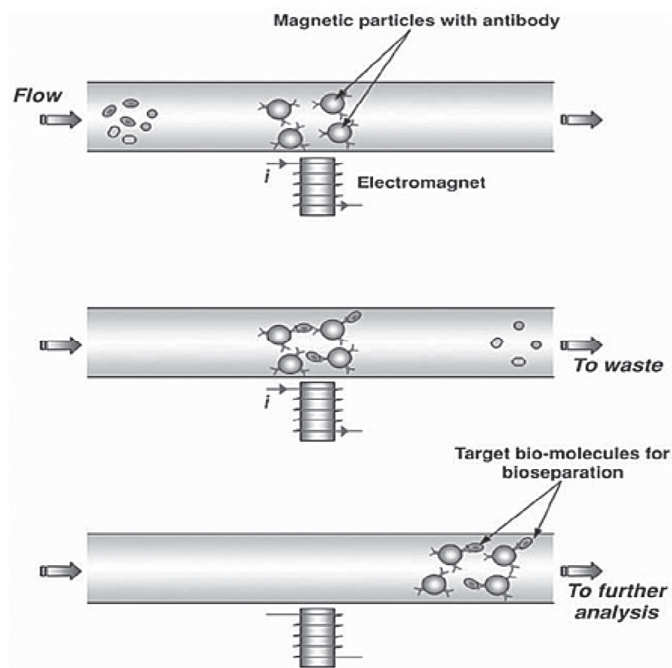


Fig. 5. Magnetic particle-based bioseparation in microfluidic channel [29].

Schematic diagrams of a lab-on-a-chip [30–33] (LOC) device, also known as a μ -TAS or micro fluidics device, and components making up the LOC are shown in Fig. 6 [34] and Fig. 7 [32] respectively. This device can integrate miniaturized laboratory functions (such as separation and analysis of components of a mixture) on a single microprocessor chip using extremely small fluid volumes on the order of nano liters to pico liters.

The LOC was first conceived by Michael Windmer at Ciba-Geigy (now Novartis) in the 1980s, described conceptually in 1990 [35] with a groundbreaking work published in 1992 [36]. Initially, much of the impetus for continued development of LOCs came from the Human Genome Project, a 13-year project coordinated by Department of Energy DOE and the National Institutes of Health (NIH) that began in 1990 and was completed in 2003. Currently, much of the impetus for the continued development of LOCs is being originated from the desire for point-of-care medical diagnostics, whether in the doctor's office, on a spacecraft, or other remote location. Additionally, development research is driven by the continued need for miniaturization, both to reduce the costs and the environmental impacts of research (green analytical chemistry) [37].

4.2. Biomedical applications

The portability, compactness, and parallelization features of lab-on-a-chip devices enhance the emerging trends in point-of-care diagnostics. LOC technology can perform a variety of laboratory tasks on a chip; these include:

- Sizing and quantification of DNA fragments (for example, PCR products or restriction digests) [38],
- Quality analysis and quantification of total or messenger RNA samples,
- Analysis of recombinant protein expression in cell lysates, optimization of protein purification procedures and quality control of antibodies, and
- Analysis of intra- and extracellular protein expression in cells, determination of the transfection status of a cell population and apoptosis studies.

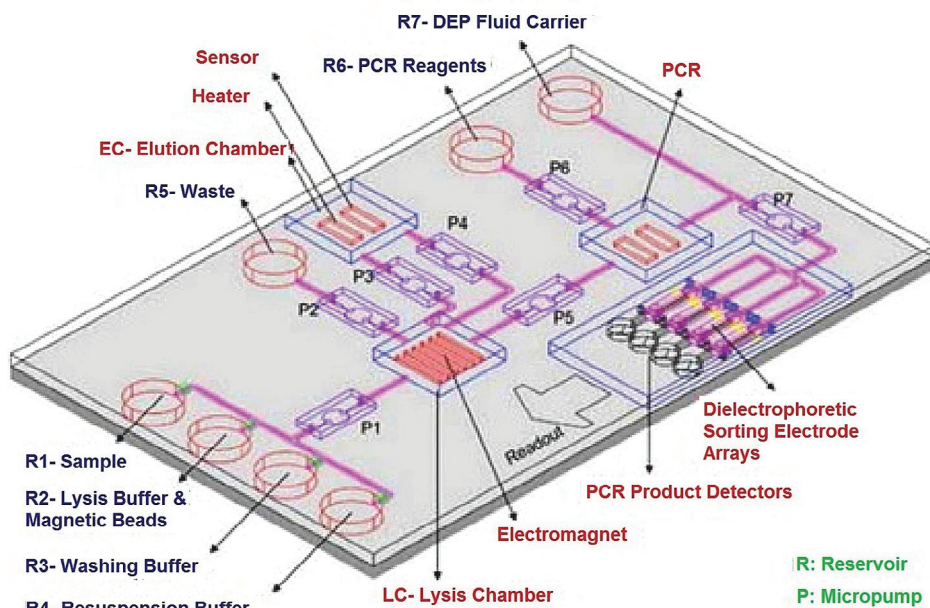


Fig. 6. A Lab-on-a-Chip Device [34].

Arguably, one of the most important and exciting applications of these devices is in the early and accurate diagnosis of infectious diseases in the developing world [38]. The ability to rapidly detect an infection, assess an infected patient's health status and the application of this technology to epidemiological studies in the field are invaluable. In order to be a useful tool in the developing world, several design challenges need to be overcome. The reagents and the chip itself need to be stable at a wide variety of temperatures since refrigeration of the components may not always be feasible in the developing world. The cost of the chips requires to be low. Similarly, the chips need to have a small power source for operation since reliable electrical infrastructure is not found in all parts of the world [25,39].

Research and development work is being undertaken to adapt lab-on-chip technology for the detection of many microorganisms from biological samples including; HIV, malaria, tuberculosis [40,41], diarrheal diseases [42], pertussis [43], and dengue fever [44]. One exciting lab-on-chip application for the detection of enteric infections is the Disposable Enterics Card (DEC) which is able to detect the presence of *Campylobacter jejuni*, *Escherichia coli* O157:H7, *Shigella dysenteriae*, Shiga Toxin producing *Escherichia coli* (STEC) and *Salmonella* from sample of feces, all on one microchip. The DEC lab-on-chip technology combines several laboratory assays to detect the bacteria.

Briefly, a sample of feces is applied to the chip and bacteria from the sample are captured on the chip by using specific antibodies to each bacteria of interest. These antibodies are located in several

different areas of the chip. The bacteria are subsequently lysed using buffers and the bacterial DNA is captured on a silica resin contained within the chip. The purified bacterial DNA is then amplified using a standard molecular biology technique called the polymerase chain reaction (PCR) with DNA primers specific for a gene in each bacterial species of interest. The end of each primer has been designed to contain a fluorescent molecule. After the amplification of the bacterial DNA using PCR, fluorescent molecules are now found at the ends of each amplified molecule of bacterial DNA. The next step in the process is to detect the amplified bacterial DNA. To do this, a laser light is directed at the sample. The fluorophore emits fluorescent light, which can be detected if the sample is positive for the bacteria.

A second application of technology to lab-on-chip capability is the detection of analytes such as electrolytes from a small sample of blood. The iSTAT, a device manufactured by Abbott Diagnostics, has the capability of rapidly analyzing analytes in a few drops of blood. The developers of the iSTAT have miniaturized electrodes by depositing electrode arrays onto silicon cartridges to create a biosensor. A few drops of blood deposited into a sample chamber are able to enter the cartridge by capillary action. Once the sample is in the cartridge it can be treated with chemical reagents prior to analysis. At the analytical stage, the cartridge is inserted into a handheld electromechanical read-out device that provides a power source and controls the temperature of the chip. The electrode arrays deposited on the silicon membrane can then be used to measure the concentration of various blood electrolytes, gases, and other analytes using potentiometry (measuring the electric potential), amperometry (measuring the flow of an electrical current) or conductimetry (measuring the conductance) of the sample [45]. These values are then displayed on a screen. Different chips are used for different analytical applications and each chip is disposed of after one use. All chips use the same handheld electromechanical read-out device.

4.3. Magnetic particles in biosensing

For the purpose of biosensing, different labels can be used like fluorescent molecules, enzymes, radioactive and nano or microparticles [46]. Biosensors are being investigated using

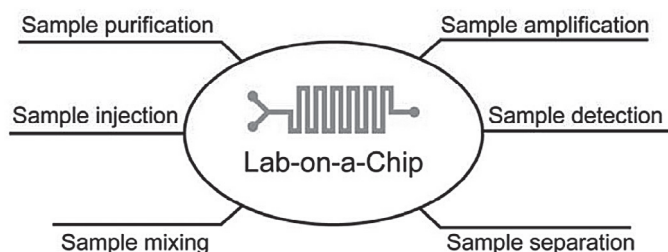


Fig. 7. Components making up the lab-on-a-chip [32].

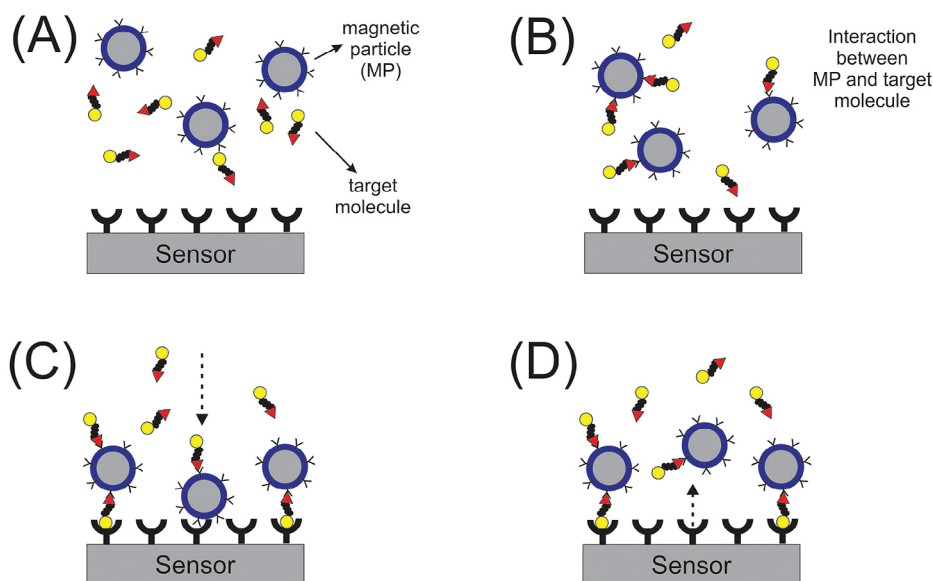


Fig. 8. Schematic representation of biosensor assay [48].

superparamagnetic particles, nm to μm in size, as labels, which consists of magnetic particles embedded inside a non-magnetic matrix (e.g. natural or synthetic polymers) [47]. A schematic representation of biosensor assay is shown in Fig. 8 [48].

Here, (a) and (b) are the target biomolecules sandwiched between the magnetic particles (labels) and sensor surface, which are previously decorated with a specific ligand (e.g. antibodies). Then, the target biomolecule-magnetic particle conjugates were captured and detected by the sensor surface furnished with the recombinant antibody (c). The non-bound particles are discarded from the surface (d) and the bound particles are easily detected which gives the measurement of concentration of target molecules in the solution.

Bio-bar code method provides various advantages over protein detection methods. The system basically depends upon magnetic microparticles probes with antibody that bind to target protein (prostate-specific antigen) [PSA]. This bio-bar code system includes various steps which involves magnetic microparticles probe and fabrication, detection and targeting as shown in Fig. 9 [49].

Biosensor is a compact analytical device or unit incorporating a biological or biologically derived sensitive element associated with a physicochemical transducer [50]. Recently, magnetic particles have been produced as labels for bio sensing. For the biosensing purpose, different types of biosensors have been produced like giant magneto resistive (GMR) sensors and spin valves (SV) [27,51], piezoresistive

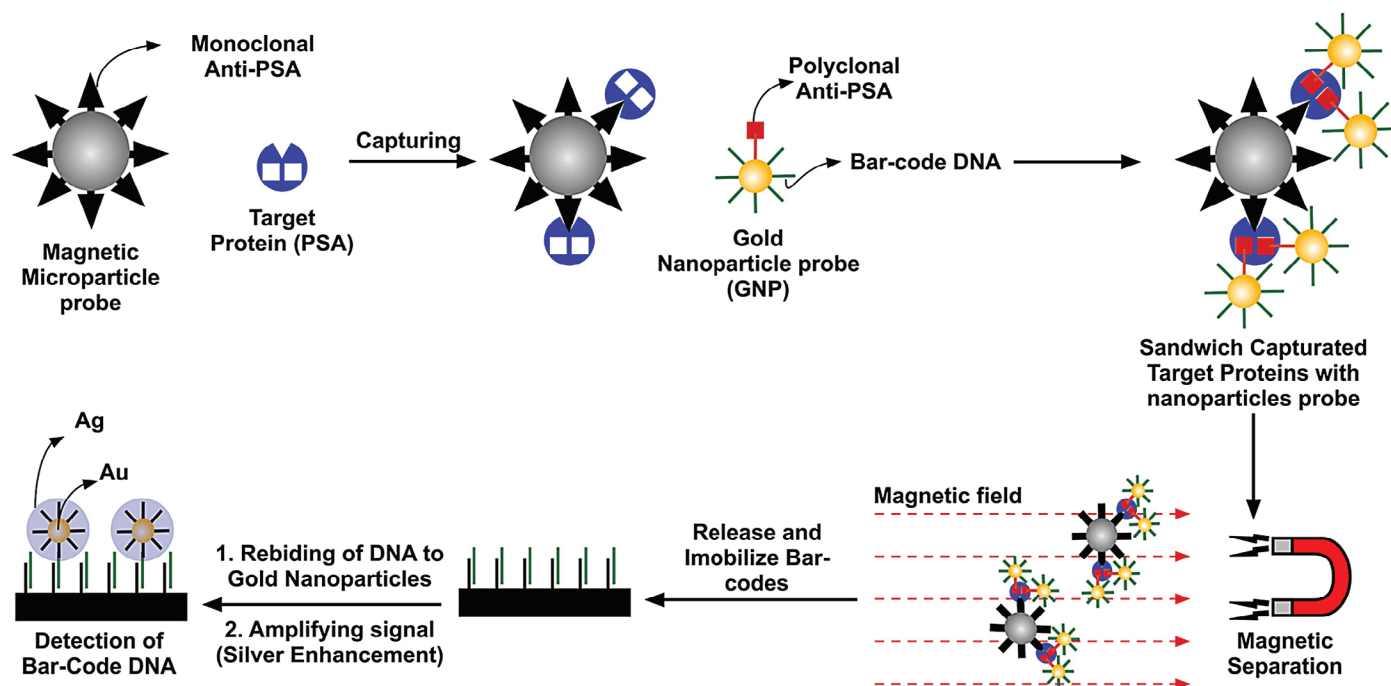


Fig. 9. The bio-bar-code assay method [49].

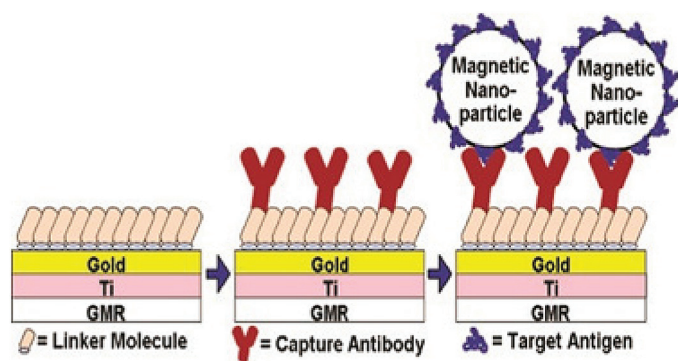


Fig. 10. Immunosorbent assay using magnetic particles with the help of GMR [59].

cantilevers [52], inductive sensors [53], superconducting quantum interference devices (SQUIDs) [54–56], anisotropic magneto resistive (AMR) rings [57], and miniature Hall crosses [58]. Detection of biological molecule is usually achieved by using bimolecular recognition between the target molecule and a specific receptor as for example antibody that is tagged with a label. Fig. 10 shows immunosorbent assay using magnetic nanoparticles [59]. Here, the figure represents that the sensor requires creation of capture antibody surface directly above the GMR sensing and then magnetic nanoparticle is coupled to target antigen. The presence of the particle-labeled antigen is then measured by the change in resistance before and after exposing the capture antibody surface to the labeled sample.

GMR device consists of a pair of magnetic thin films separated by a non-magnetic conducting layer [60]. When an external magnetic field rotates the magnetizations of the magnetic layers towards alignment, spin-dependent electron scattering is reduced at the interfaces within the device, decreasing its electrical resistance. GMR sensors are microscopic in size and they become very sensitive when dealing with micron and smaller sized magnetic particles. With the development of advanced magnetic materials and devices for data storage applications, like magnetic random access memory (MRAM) [61,62], GMR has gained great interest for biosensing.

In past, a biosensor system was produced called as Bead Array Counter (BARC) based on capture and detection of micron-sized paramagnetic beads on chip containing an array of GMR sensors as shown in Fig. 11 [28]. This is the prototype BARC system in which assay is performed inside the flow cell displaced over sensor chip [63,64].

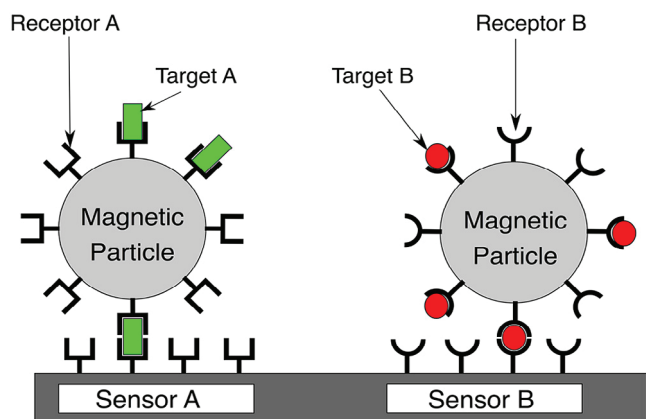


Fig. 11. Magnetic labeling and detection of targets captured onto a solid substrate using specific bimolecular ligand-receptor recognition in a "sandwich" configuration [28].

Table 2
Detection of magnetic particles for biosensing [28]

Detector type	Detection area (μm^2) ^a	Particle	Particle diameter (μm) ^b	Sensitivity (particles)	Area per detectable particle (μm^2)
BARC III	3.1×10^4	Ni ₃₀ Fe ₇₀	3.3	1	3.1×10^4
Resonant coil	2.5×10^7	Dynal M-280	2.8	10^5	2.5×10^2
SQUID	1.7×10^5	Magnetite	35 ^c	4×10^3	42
Spin valve	12	Micromer M	2	1	12
AMR ring	8.0	Ni ₃₀ Fe ₇₀	4.3	1	8.0
Hall sensor	5.8	Dynal M-280	2.8	1	5.8
SQUID	3.1×10^6	Magnetite	50 ^c	1.8×10^6	1.7
SQUID	6.8×10^4	Magnetite	11 ^c	10^8	6.8×10^{-4}

^a Surface area on which particles were captured and detected.

^b Including polymer coating.

^c In nanometer measurement.

Different magnetic particles, for example, magnetite nanoparticles and polymer matrix micro beads, have been used for the labeling and detection of biomolecules. These can be detected with variety of approaches like liquid nitrogen-cooled SQUIDs and Hall cross semiconductor-based electronic devices. It is quite difficult to compare sensitivities of different approaches without taking into account the practical aspects of biosensing, because of differences in magnetic properties and sizes of particles employed. Assay sensitivity combined with detector sensitivity is used to determine the actual sensitivity of a biosensors system based on magnetic bead labeling.

This assay describes about how well target biomolecules are captured from sample into detection zone and labeled with magnetic particle. In assays, where targets are delivered to the capturing surface passively by diffusion or flow, it becomes important to determine the distinction of density of labels within the detection area. This is because the sensitivity of biochemical assay usually drops due to decrease in detection area. Suppose, each particle will label one biomolecule at dilution limit and more target molecules would be captured per unit time for the larger detection area. Then, one sensitivity figure-of-merit would be the sensing area per detectable magnetic particle. Detection of magnetic particles for biosensing is shown in Table 2 [28].

Different types of biosensors use magnetic nanoparticles (5–300 nm) and magnetic particles (300–5,000 nm), which are surface functionalized for recognition of specific molecular target. Three different types of biosensors have been used that utilize various biosensing methodologies and magnetic nanoparticles labeling. These biosensors include; (a) Magnetic Relaxation Switches (MRSws), (b) Magnetic Particle Relaxation Sensors and (c) Magneto resistive Sensors.

MRSws consist of magnetic relaxation switch assay-sensors, which are based on effects of magnetic particles on water proton relaxation rates [41]. Magnetic resonance (MR) contrast agents include superparamagnetic nanoparticles like iron oxide coated with polymer have been used for diagnostic purposes [65,66]. Surface modified nanoparticles (targeted contrast agent) produced a local inhomogeneity upon binding to specific molecules under a magnetic field in tissues, where molecular targets are present. The inhomogeneity leads to a decrease in T_2 (relaxation curve decay) [67] which results in a change in contrast MR images. Recently, MRSws have been used to detect analyte by transitioning between a dispersed phase and clustered state in the presence of an analyte. The aggregated form of nanoparticles diphas the spins of the surrounding protons of water molecules more efficiently than at dispersed phase (not clear). The nanoparticles (30 nm diameter) having monocrystalline core (dark grey circles) coated with cross-linked dextran (grey circles) along with attached molecules are shown in Fig. 12 [67]. The selective binding to target analyte (green triangles) has also been shown in Fig. 12.

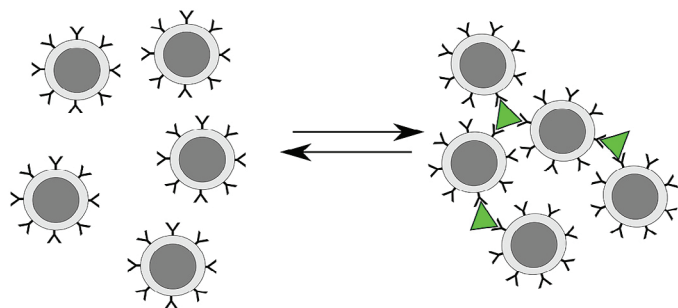


Fig. 12. Magnetic Relaxation Switches (MRSWs) The nanoparticles (30 nm diameter) having monocrystalline core dark grey circles coated with cross-linked dextran (grey circles) with attached molecules that selectively bind to target analyte (green triangles) [67].

Magnetic nanoparticles having surface of cross-linked iron oxide (CLIO) have been used for analytes ranging from small molecules to mammalian cells [68–70]. CLIO possesses good stability in aqueous buffers and blood. Their ability to handle good functionality of amino groups, finds their applications in *in vivo* (MR imaging) [71] and *in vitro* (MRSws assay), respectively [72–74]. However, stability of magnetic particles is an important factor in MRSws assay applications. Stabilization can be achieved by hydrophilic polymer coating which helps in preventing blockage of particle/particle aggregation [75]. Attachment of 10 kDa polyethylene glycol (PEG) diamine on the surface of magnetic particles enhances the initial electrostatic stability of the negatively charged magnetic particles to polymer based stability [76]. Polymeric dextran coating on magnetic nanoparticles, improves the stability of these particles in *in vivo* MR imaging and *in vitro* MRSws assay applications, respectively [77]. Different characteristics of magnetic particles used for biosensing is shown in Table 3 [78].

SQUIDS have been used for significant relaxation of particle magnetic moments. Brownian relaxation is much faster as compared to Néel relaxation. The calculated relaxation time were $t_B \sim 1$ ms and $t_N \sim 1$ s for a 20 nm single domain magnetite particle in a solution. For applications of homogenous immunoassay [79] and bacterial detection [80], the difference in relaxation time has been the principle as shown in Fig. 13.

Fig. 13 shows principle of a SQUIDS-based homogeneous detection of bacteria. The part (a) represents pulse-form magnetic fields orientating the magnetic moments of nanoparticles. Here, magnetic particle (50 nm in diameter) coupled to polyclonal antibody raised

Table 3

Characteristics of magnetic particles used for biosensing R_2 is relaxivity of the particle [78]

Particle	Size (nm)	Composition	Characteristics
CLIO	~ 30	5 nm core, 10 nm dextran coating	MRSw, $R_2 = 50$ ($s \text{ mM Fe}^{-1}$)
Core/shell	16	Fe core, iron oxide shell, 2.5 nm shell thickness	MRSw, $R_2 = 260$ ($s \text{ mM Fe}^{-1}$)
Mn-MNP	16	Mn-doped iron oxide	MRSw, $R_2 = 420$ ($s \text{ mM metal}^{-1}$)
MP	1000	Commercial (Dynabeads)	MRSw, $R_2 = 43$ ($s \text{ mM Fe}^{-1}$)
Iron oxide	56	Commercial (Quantum magnetics, Miltenyi Biotech)	SQUID
Iron oxide	19.5		AC susceptometer
Cubic Fe-Co	12.8	1.5 nm oxidized shell	GMR
SAF	100	Multilayers of ferromagnetic, interlayer of nonmagnetic material	GMR, disk shape
Magnetic bead	130 - 250	Commercial (Micromod Partikeltechnologie)	SQUID

against the bacterial pathogen (*Listeria monocytogenes*). Part (b) represents the Brownian motion that randomizes the magnetic moments of unbound nanoparticles. Nevertheless, the Brownian motion of nanoparticles bound to bacteria is restricted. Bound magnetic nanoparticles undergo Neel relaxation for reorientation of magnetic moments.

Magneto-resistive sensors, which detect the presence of magnetic particles on the surface of electronic devices, are sensitive to change in magnetic fields on their surfaces. Basically, there are two methods by which magnetic particles can be bound to sensor surface; (a) indirect labeling (sandwich type binding) and (b) direct labeling. Indirect labeling follows the method of sandwich in ELISA while direct labeling occurs by using streptavidin-biotin interaction or DNA sequence recognition [78].

Fig. 14 represents the direct and indirect labeling of magnetic nanoparticles as bimolecular labels (nanotags) [60].

Fig. 14 (a) shows the fabrication of SV or MTJ sensor (detector) by optical or e-beam lithography and its binding to a DNA probe.

Fig. 14 (b) represents labeling of unknown DNA target with magnetic nanoparticle as bimolecular labeling (nanotag) which occurs through binding mechanism like biotin-streptavidin. Finally, part(c) shows the labeled DNA target that has been captured by complementary DNA probe and bimolecular labels (magnetic nanotag) is detected by SV or MTJ sensors. This process is called direct

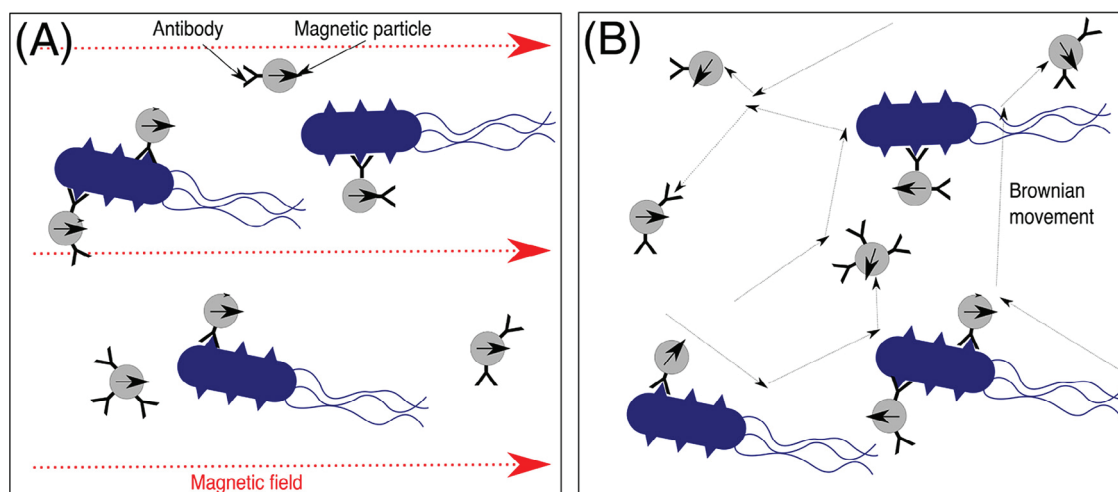


Fig. 13. Principle of a SQUIDS-based homogeneous detector of bacteria [80].

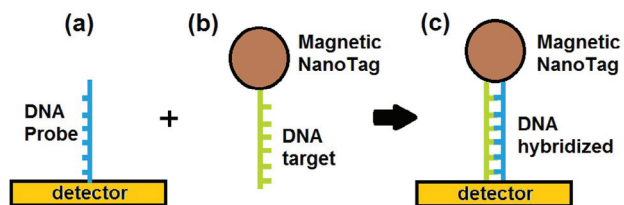


Fig. 14. Direct and indirect labeling of magnetic nanoparticles as bimolecular labels (nanotags) [60].

labeling and earlier one was indirect process. GMR, SV or MTJ sensors have been successfully used to sense MPs. For the attachment of biomolecules, a biologically active molecule can be deposited on gold layer or Silicon dioxide layer to obtain a surface for the attachment of biomolecules [36].

Large size magnetic particles (with diameters between 0.1 and 3 μm) [81] have been used in the past. However, because of good stability in suspension and less binding to particle clustering by applying magnetic field [60,82,83], magnetic nanoparticles have replaced the larger particles. Protein markers have been developed by coating of streptavidin on magnetic particles [84]. In past, 50 nm magnetic cell sorting (MACS) magnetic nanoparticles [83] were used for demonstrating cancer markers in 50% serum at sub Pico molar concentrations. Fig. 15 [83] represents the use of GMR sensor for purpose of ELISA-type protein assay.

Fig. 15 consists of four parts. (A) functionalization of probe surface with specific antibody, while the control surface was obstructed with BSA. (B) a solution was added for a specific binding of analyte proteins to probe surface. (C) a biotinylated antibody bound to the surface-immobilized analytes. (D) streptavidin-coated nanoparticles were added for tagging the probe surface by biotin-streptavidin interaction. Sensitivities of magnetic particles is shown in Table 4 [78].

4.4. Magnetic particles in microfluidics

Microfluidic systems are devices that deal with sub-Nano liter volumes of fluids [85–87]. These devices possess reduced dimensions and together with colloids play an important role in the

Table 4
Configurations and sensitivities reported for magnetic particles based biosensors [78]

	Analyte	Magnetic particle/instrumentation	Sensitivity	Sample volume
MRSw type 1	Nucleotid	CLIO, bench top relaxometer	Low Nm–2pM	300 μL
	Proteins	CLIO, bench top relaxometer	Low nM	300 μL
	Virus	CLIO, MRI	50 viruses/100 μL	100 μL
	Bacteria	Core/shell, DMR ^a	20CFU ^b /100 μL (membrane filtered)	5 μL
MRSw typ2	Cancer cell Antibody	Mn-MNP, DMR MP, bench top relaxation	2 cells/1 μL Less than 1pM	5 μL 300 μL
AC susceptometer SQUID	Antibody	Iron oxide NP	Less than 1 nM	
	Bacteria	Iron oxide NP	1.1×10^5 bacteria/20 μL	
	DNA	Magnetic bead	3–10 pM (Signal amplification)	
GMR	Protein	Cubic FeCo NP	2×10^6 proteins	2 μL
	DNA	Antiferromagnetic NP	10 pM	
	Protein	Iron oxide NP	2.4pM	

(a) DMR: diagnostic magnetic resonance, (b) CFU: colony forming unit.

formation of monodispersed colloidal particles in a continuous mode [88]. Microfluidic reactors [89] are used for the synthesis of nanoparticles. Although, these devices are very useful, but flow process plays a vital role. This flow can be controlled by the use of force motion of colloidal microparticles in microchannels [88]. Some noninvasive techniques are adapted inside the microfluidic devices for sorting and fabrication of particles. It makes them easy to integrate various steps within a lab-on-chip. These techniques include dielectric process [90], optical separation and hydrodynamic phenomenon [91]. For investigation of kinetic and mechanism, microfluidic devices are used as tool when detection techniques are coupled online to microreactors. These microreactors are of two types depending on liquid phases; i.e. single phase and two phases. Recently, microfluidics route are well suited for production of nonspherical nanoparticles having anisotropic particles [92] like Janus

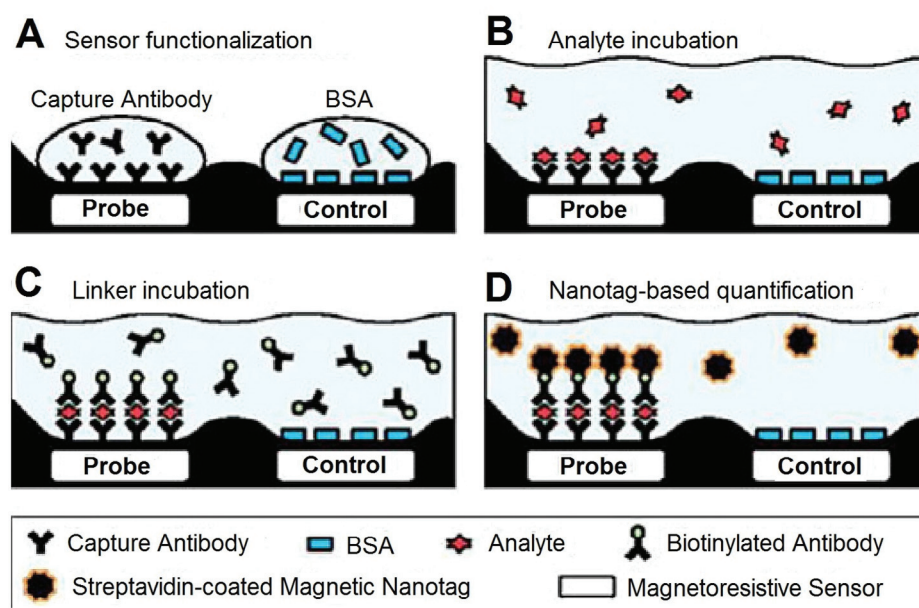


Fig. 15. Representation of the use of GMR sensor for purpose of ELISA-type protein assay [83].

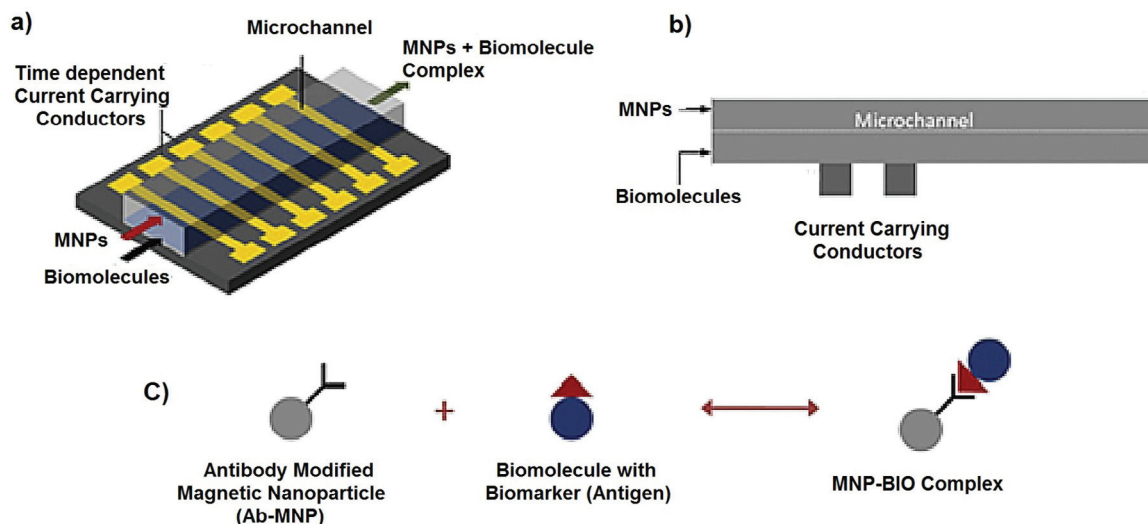


Fig. 16. Schematic representation of time dependent magnetic process with (a) three-dimensional and (b) two-dimensional view (c) binding reaction between MNPs and biomolecule using antigen–antibody [94].

and ternary [93]. Microfluidic combined with nanotechnology has played an important role in developing mTAS or LOC systems. The combination of magnetic nanoparticles and microfluidic system has provided benefits like automation and easy implementation for chemical bonding providing high surface to volume ratio and superparamagnetic nature. For enhancing the mixing and improvement of kinetics of tagging process, magnetic nanoparticles are used together with time dependent magnetic field. Fig. 16 shows a schematic representation of time dependent magnetic process with three-dimensional and two-dimensional views. Magnetic nanoparticles are flowing within microchannel with the help of large magnetic force and magnetic field gradients produced by applying current in electrodes. Flow pattern is set in such a way that biomolecule solution flows from bottom whereas magnetic nanoparticles are loaded from top inlet. A surface modified magnetic nanoparticles containing antibody as receptor were bound with biomolecules [94].

From the synthesis point of view, one important factor involves heat transfer. It allows high surface-to-volume ratio and good control of reaction conditions. Microfluidic devices contain dimensions almost the same as compared to dimensions of various biological cells making it an easy tool for manipulating purposes. The device also enhances analytical performance by reducing consumption of reagents, decrease in analysis time and integration of multiple processes in a single device. Another advantage includes reduction of solvent, sample consumption and mass enhancement [88].

Microfluidic technology has been rapidly developed in recent years and found various interesting applications in pharmaceutical industry, life science and chemical researches. Based on microelectromechanical technology, microfluidic technology integrates and miniaturizes the separating reaction and mixing devices in general laboratories onto a very tiny chip. This microfluidic chip is also called lab on-chip [86]. The use of microfluidic devices with magnetic particles manipulation efficiently implements bioanalytical steps in miniaturized systems [95–97]. The use of magnetic particles in microfluidic devices provides new possibilities of manipulating molecules in small volume [98]. This can be used as solid support for mRNA isolation [4], immunoassay [99], DNA hybridization [100], protein analysis [101] and retaining of magnetic labeled cells [102]. Polymer or silica nanoparticles with embedded iron oxide nanoparticles are most commonly used as magnetic

objects inside the microfluidic devices [103]. Different forms of biological applications can be recognized by using magnetic particles in microfluidic systems. These applications include sample purification, solid substrate to sample, sample manipulation, labeling, transport, separation and protein–interaction which have been found in recent years [4,35,104–106]. Nano and microparticles present large specific surface for chemical binding when applied in microfluidic channel. These particles are generally referred as ‘beads’ in literatures [86]. Manipulations of magnetic beads in microfluidic system is shown in Fig. 17. This figure indicates (a) separation of magnetic beads from flow, which occurs via use of electromagnets, permanent magnets or coils over the channel. (b) Movements: that is magnetic transport is difficult because stronger and comprehensive magnetic force is to be required for the movement of magnetic beads inside liquid without use of microfluidic flow. (c) Labeling: of magnetic beads through magnetic field sensor controlling its stray field when particles are supposed to be an external magnetic induction. An important characteristic of magnetic beads is that they can be suspended in a microfluidic channel by applying magnetic forces without the use of supporting substrate. In this way, such trapped beads are of particular interest when high exposure of the beads to a liquid flow is required [86].

Continuous flow separation systems have been studied in past [107]. Different magnetic particles have been introduced for purpose of purification and immunoassays [108–112]. Separation in a microfluidic capillary occurred without magnetic stationary phase when considering magnetic beads [113]. A quadrupole separator [86] as shown in Fig. 18, possesses macroscopic dimension when considering from magnet point of view. However, with respect to liquid transport point of view, they are called “microfluidic”, because of functionality of laminar flow. Fig. 18 represents that magnetic particles are introduced from top side to inside inner annular flow and buffer solution introduced from outer annular flow channel. When magnetic particles are passed through separator, these magnetic particles are deflected in radial direction. If there is strong deflection, particles are captured in outer annular flow and inner annular flow vice versa.

A system has been suggested for magnetic transportation towards miniaturization and automation, in which liquid movement is substituted with the help of magnetically induced movement of magnetic particles [114]. By arranging electromagnetic actuation in a four-phase scheme in microfluidic channel, magnetic particles

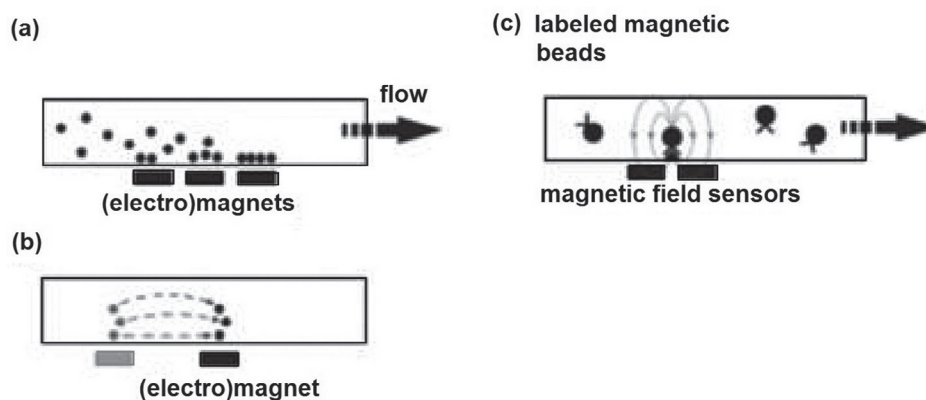


Fig. 17. Magnetic beads in microfluidic system [86].



Fig. 18. Magnetic Quadrupole separator as “microfluidic” because of functionality of laminar flow [86].

have been transported above millimeter distances. The system is also used for transporting alginate microparticles with encapsulated magnetic particles [86]. Apart from these still, “macroscopic” fluidic transport systems have also been proposed for the transport of beads with the advantage of batch *micro fabrication* technologies [86]. Integration of detection, magnetic labeling and combination of sensor chip with microfluidic system have been explained in past [81,115,116].

Droplet microfluidics (also referred as digital microfluidics) deals with small self-enclosed liquid entities [33,117] as compared to continuous flow microfluidics in which large liquid volumes are pumped through the microsystem. Advantage of this system is to reduce sample volumes and possibility of working with diverse samples simultaneously in a common system. It is because of the reason that magnetic droplet manipulation is gaining importance in the development of lab-on-chip system [33]. For performing reactions between various droplets, system requires to complete different

droplet steps for manipulating. These steps are transport, merging, mixing and splitting. Magnetic droplets manipulation provides various advantages like long-range magnetic forces do not depend on intrinsic properties of manipulated medium. It also avoids interaction between biological materials [118], as compared to other solutions having range from electro wetting over dielectrophoresis to acoustic actuation [117]. However, this non interaction needs magnetically responsive material inside droplets for converting magnetic field into force which pulls droplets towards gradient [86]. These types of magnetic particles act as functionalized components in the system like mobile substrate [119] and optical indicators [120]. In anyway, magnetic particle actuation helps in fast droplet manipulation and non labelling in the droplets [86].

There are various commercially cell separation methods which are mainly based on fluorescent flow cytometers and other complicated instruments [121]. Most commonly methods are fluorescence-activated cells (FACS) [121] and MACS [122] as illustrated in Fig. 19.

Cell sorting is performed by using electrostatic deviation of particular fluorescently labeled cell-containing droplets. However, this method is time consuming because of larger amount of reticulocytes, RBCs and platelets in blood samples. FACS methods have also been moved to microfluidic systems with sorting rates less than 100 cells per seconds but this requires good quality with expensive detection optics and electronics. On the other side, MACS method is less expensive and simpler than FACS. But, MACS presents only a first sample-handling step before additional analysis. So, by keeping this in mind, the theme of performing magnetic separation on microfluidic system is attractive as it enhances direct –reading, separation and also counting of cells on a single chip [86]. Berger et al. [123] was first who presented an idea for continuous magnetic separation. The method consists of magnetic force with the help of magnetized stripes at an angle according to hydrodynamic flow direction. The function of these stripes is to create magnetic field gradients that trap magnetic beads and transform their flow direction. A simple schematic representation of microfluidic chip along with magnetic wires is shown in Fig. 20.

Deposition of bacterial cells by magnetic separation finds fast detection of microbial contamination in solutions like industrial water, food and in clinical biology. Recently [124], living *E.coli* bacteria have been separated from fluids in microfluidic system with or without mixed with RBCs. This work shows the separation of *E.coli* cells labeled with magnetic nanoparticles in a 200 μm wide microfluidic channel (Fig. 21).

Another microfluidic system has been used to detect pathogenic bacteria in beef samples [125]. In this system, a gold inter digitated microelectrode array was integrated with 145 nm magnetic nanoparticles-Ab conjugate into an impedance biosensor. Recently,

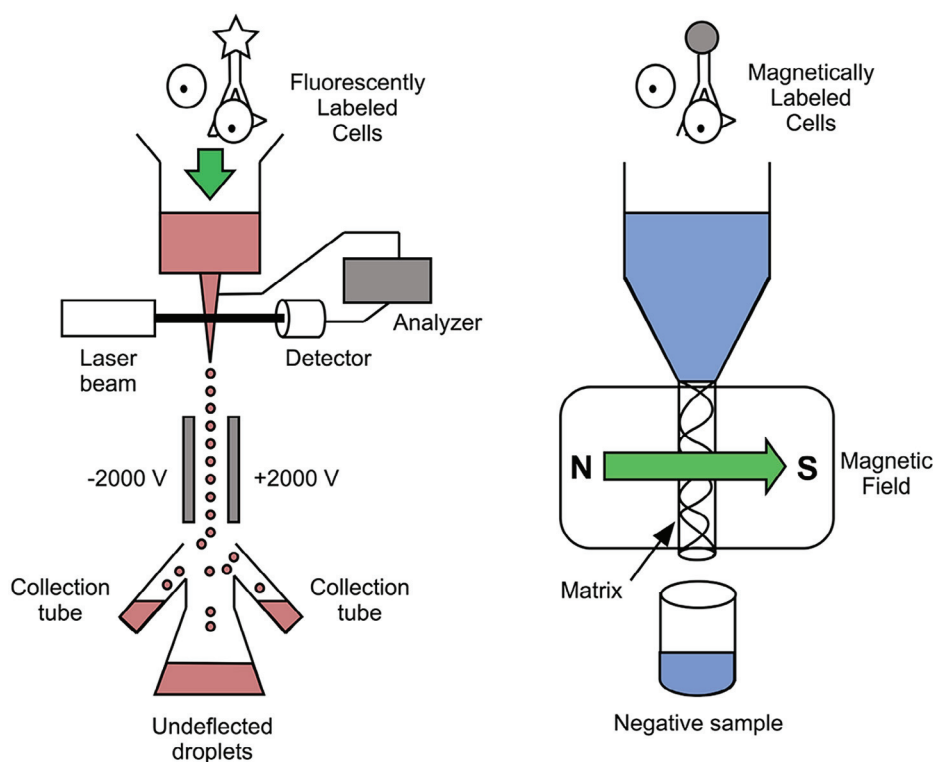


Fig. 19. Fluorescence-activated cells (FACS) [Left] and magnetic activated cell sorting (MACS)[Right] [123].

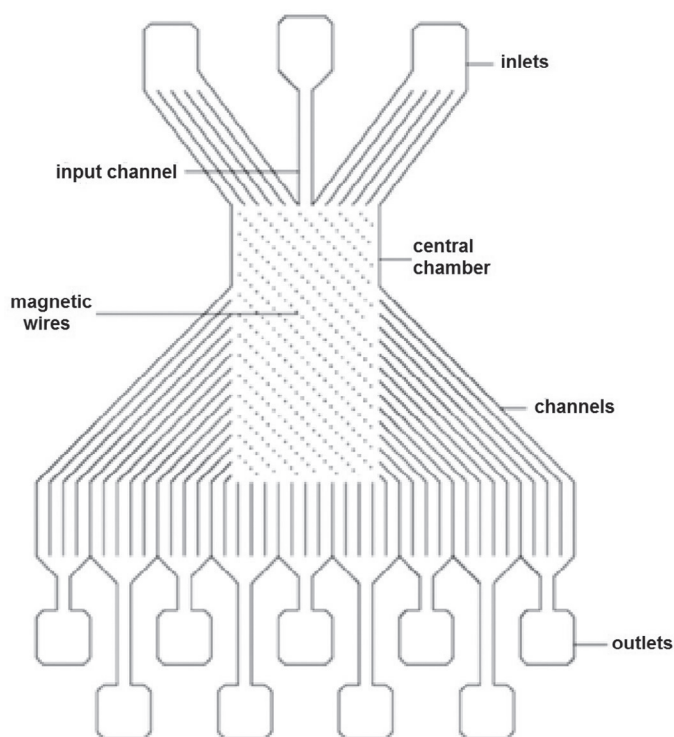


Fig. 20. Microfluidic chip along with magnetic wires [123].

two different magnetic tags were used for labeling two types of *E.coli* cells as shown in Fig. 22 [126]. The device was set up in a way that combined effect of hydrodynamic force (F_d) produced from laminar flow and magnetophoretic force (F_m) created from patterned

ferromagnetic structures inside the microchannel. It resulted in selective purification of differentially labeled target cells into multiple independent outlets.

Breast cancer tumor cells spiked in human [127] or mouse [128] blood were used as target cells, labeled with both fluorescent markers and magnetic nanoparticles for fluorescent microscopy. Besides batch-type magnetic separation systems, continuous flow magnetic separation systems have also been used for removing of rare (skipped) cancer cells from blood samples. Human cervical cancer cells (HeLa) were internally labeled with magnetic nanoparticles following endocytosis pathway and fluorescence was obtained by labeling with Rhodamine albumin [129]. Another type of microfluidic device which consists of micro channels, micro valves and micro pillars was produced for specific capture and sorting of cancer cells as shown in Fig. 23 [129]. Initially, channel was filled with a suspension of superparamagnetic beads and then beads were bio functionalized *in situ* by covalent attachment of specific proteins directly to their surface. This figure shows the *in situ* functionalized superparamagnetic beads in micro channel and to capture A549 cancer cells (human lung carcinoma cell line) from a flow. Due to specific interaction between wheat germ agglutinin and N-acetyl glucosamine on the cell membrane, A549 cancer cells were successfully captured on magnetic particles.

In bioanalytical procedure (nucleic acid assays), magnetic particles play an important role. In macroscopic lab-bench protocols, magnetic particles are used as mobile substrate for capturing and extraction of nucleic acids [130,131]. Different steps followed in an assay, where magnetic particles are applied with different purposes and at different phases of the assay are represented in Fig. 24.

Purification and capturing of molecules are an important task while performing on-chip nucleic acid analysis. By the use of magnetic microparticles in a microfluidic system, nucleic acid can be brought into contact with particle surface through different means. A preferred solution is the incubation of activated magnetic particles

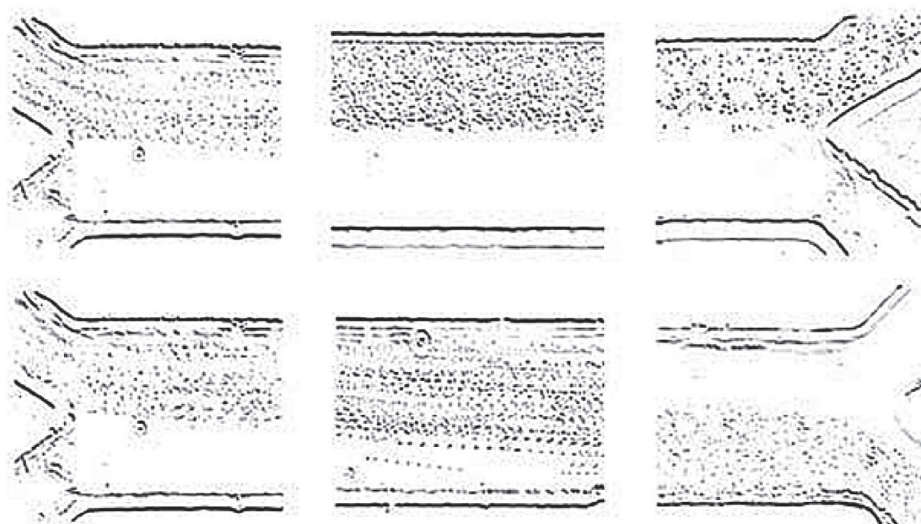


Fig. 21. Separation of *E. coli* cells mixed with magnetic nanoparticles in a flow (from left to right) of PBS in a 200 μm wide channel. The composite bright images were generated by overlaying sequential frames of corresponding movies taken at the beginning, middle, and end (left to right) of the microfluidic channel. In the presence or absence of a neodymium disk magnet placed below the channel (bottom and top images, respectively) [124].

with the sample in a reservoir [132,133]. Here, purification is done by introducing magnetic field to separate magnetic particles from the sample and nucleic acid capturing is driven by diffusion. However, some solutions used relative velocity between sample and magnetic

particles by immobilizing the latter. Mostly, it is based on immobilization of magnetic particles inside a microchannel before or after capture step [97,134,135]. Magnetic particles are herewith held against a flow through a magnetic field perpendicular to

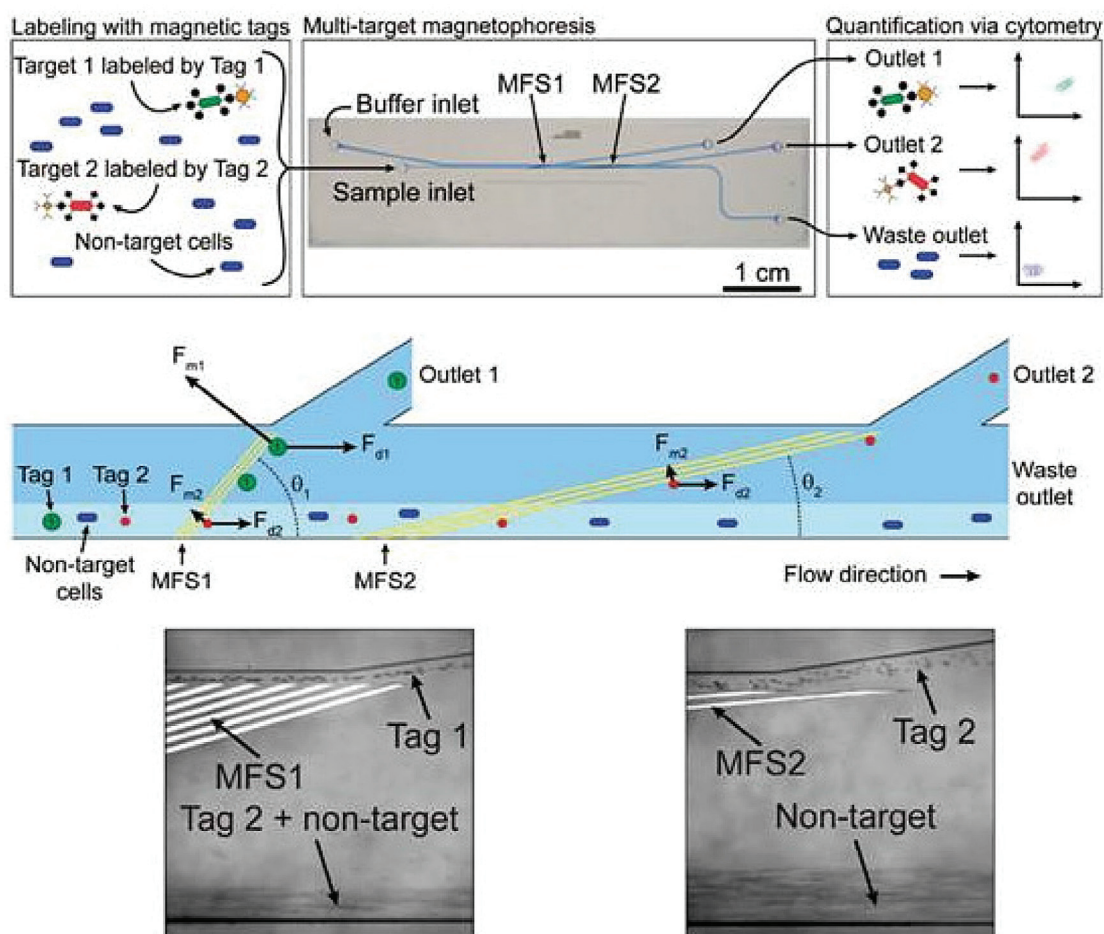


Fig. 22. Multitarget magnetic activated cell sorter separation architecture where MFS stands for Microfabricated ferromagnetic strips [126].

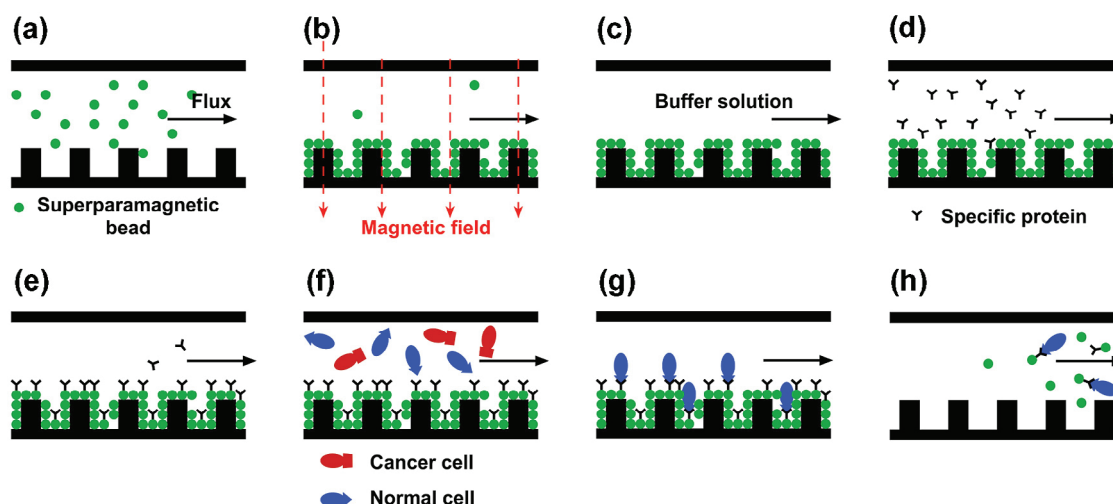


Fig. 23. Schematic representation of the experimental protocol for cell capture and sorting. (a) The channel was initially filled with a suspension of superparamagnetic beads. (b) The external magnetic field was applied and the beads were trapped by the Ni micro pillars. (c) Flow of buffer solution, which activates carboxyl groups on the surface of the beads and washes out any untrapped beads simultaneously. (d) Protein solution was then introduced into the flow stream. (e) Proteins were attached to the beads, and any unbound protein was washed out of the channel. (f) Cells were introduced into the channel. (g) Cancer cells were captured by specific protein-functionalized beads anchored to the nickel micro pillars. (h) The cancer cells captured by the beads were eluted from the channel, when the external magnetic field was removed [129].

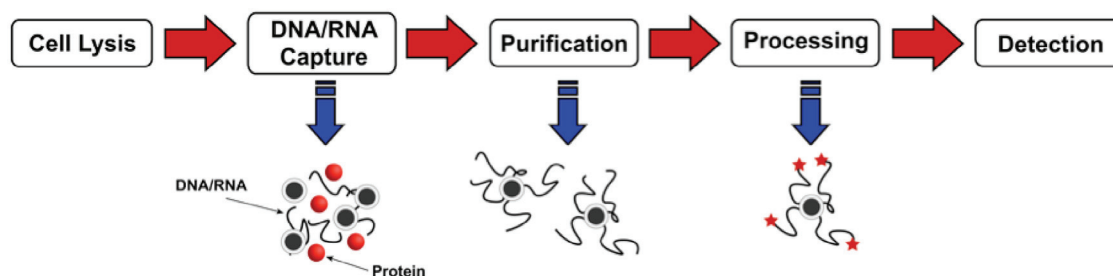


Fig. 24. Different-steps of an on-chip magnetic nucleic acid assay through magnetic particles [86].

channel, while source of magnetic field occurs by integrating electromagnetic element into the chip [97] or by placing permanent magnet at the bottom of the system [133,134].

Proteolysis is the direct degradation of proteins through cellular enzymes called proteases. Magnetic particles in conjunction with microfluidics can successfully be used for developing micro reactors for proteomic applications [136]. Proteolysis of the proteins occurs through porous magnetic plug when magnetic particles are grafted with enzyme. Magnetic particles when grafted with specific enzymes can very efficiently proteolyzed the protein of interest. This can be done by flowing the protein through the porous magnetic plug.

An important advantage of microfluidic magnetic particle based digestion system is the replacement of magnetic matrix by flushing out the old beads and loading new beads into same channel. Another advantage of such system is the reduced cost and better reproducibility due to the fact that grafting on particles can be done *ex situ* in large quantities [86]. Protein digestion inside a microfluidic channel occurs by grafting trypsin on magnetic beads while maintaining self-assembled magnetic particles chain in a microchannel to digest several types of protein samples from flow for subsequent analysis [137].

5. Conclusion

Paramagnetic or superparamagnetic particles, which can respond to an external magnetic field, provide an efficient method for separating samples linked to the magnetic particles from the liquid suspension. Various efficient synthetic approaches have been used

for the preparation of uniform and monodisperse SIONPs in order to be used in biomedical applications. Magnetic particles have been widely used as a universal separation tool to purify nucleic acids (i.e., DNA and RNA), proteins & peptides cells and other biologically active compounds from crude samples.

Micro and nano-sized magnetic particles provide a new technology for their applications in microfluidics, which includes lab-on-chip systems, biosensors and microfluidic systems. Biomolecules labeled with magnetic nanoparticles will be magnetically driven to retain a surface. By combination with precisely engineered microfluidic, flow patterns on-chip will allow to develop and to remove non-specifically adsorbed particle on surface. The use of catalyst immobilized on magnetic nanoparticles for catalytic and separation processes will also be interesting development in microfluidics, especially for chemical and pharmaceutical industries. Numerous of sensitive magnetic field detection devices have been developed to be suitable for biosensing applications. These techniques include GMR sensors and spin valves SQUIDs. Different biosensors that employ different biosensing principles comprise of different magnetic materials and instrumentation. The first type consists of magnetic relaxation switch assay-sensors, which are based on the effects of magnetic particles on water proton relaxation rates. The second type consists of magnetic particle relaxation sensors, which determine the relaxation of the magnetic moment within the magnetic particle. The third type is a magnetoresistive sensor, which detect the presence of magnetic particles on the surface of electronic devices that are sensitive to changes in magnetic fields on their surface. In fact, the integration of magnetic particles in very small devices (e.g. bio-chips, microfluidics and biosensors) have wide

applications and more particularly in the biomedical domain. These devices are characterized by light weight and small size, and provide fast and accurate analysis and can be easily used to perform biological tests at the point of care (i.e. close to the patient) allowing smooth testing in the area of medicament. This in turn will help in the early diagnosis of diseases and thus speed up the chances of treatment at early stages of infection.

Acknowledgment

The authors would like to thank the SMARTCANCERSENS project (FP7-PEOPLE-2012-IRSES) under the grant agreement No. 31805, the SEA-on-a-CHIP project (FP7-KBBE) under the reference 614168, the NATO project, SPS (NUKP.SFP984173) and the HEARTEN under the grant agreement No. 643694

References

- [1] I. Koh, L. Josephson, Magnetic nanoparticle, *Sensors* 9 (2009) 8130–8145.
- [2] A. Ahsan, et al., Smart magnetically engineering colloids and biotin films for diagnostics applications, *J. Colloid Sci. Biotechnol.* 2 (2013) 19–26.
- [3] U. Häfeli, *Scientific and Clinical Applications of Magnetic Carriers*, Springer Science & Business Media, 1997.
- [4] T. Vilkner, D. Janasek, A. Manz, Micro total analysis systems. Recent developments, *Anal. Chem.* 76 (2004) 3373–3385.
- [5] F. Montagne, O. Mondain-Monval, C. Pichot, A. Elaïssari, Highly magnetic latexes from submicrometer oil in water ferrofluid emulsions, *J. Polym. Sci. Part Polym. Chem.* 44 (2006) 2642–2656.
- [6] F. Montagne, S. Braconnot, O. Mondain-Monval, C. Pichot, A. Elaïssari, Colloidal and physicochemical characterization of highly magnetic O/W magnetic emulsions, *J. Dispers. Sci. Technol.* 24 (2003) 821–832.
- [7] A. Elaïssari, F. Sauzedde, F. Montagne, C. Pichot, Preparation of magnetic latexes, in: A. Elaïssari (Editor), *Colloidal Polymers, Synthesis and Characterization*, vol. 115, Marcel Dekker Edition Surfactant Science Series, 2003, pp. 285–318.
- [8] A. Elaïssari, *Colloidal Biomolecules, Biomaterials, and Biomedical Applications*, CRC Press, 2003.
- [9] A. Elaïssari, J. Chatterjee, M. Hamoudeh, H. Fessi, Structure and Functional Properties of Colloidal Systems, CRC Press, 2009, pp. 315–337.
- [10] N. Ahmed, H. Fessi, A. Elaïssari, Theranostic applications of nanoparticles in cancer, *Drug Discov. Today* 17 (2012) 928–934.
- [11] T. Jamshaid, et al., *Soft Nanoparticles for Biomedical Applications*, 2014.
- [12] S.F. Medeiros, et al., Stimuli-responsive and biocompatible Poly(N-vinylcaprolactam-co-acrylic acid)-coated iron oxide nanoparticles by nanoprecipitation technique, *J. Colloid Sci. Biotechnol.* 2 (2013) 180–194.
- [13] M.M. Rahman, A. Elaïssari, Multi-stimuli responsive magnetic core-shell particles: synthesis, characterization and specific RNA recognition, *J. Colloid Sci. Biotechnol.* 1 (2012) 3–15.
- [14] H. Macková, D. Horák, Š. Trachtová, B. Rittich, A. Španová, The use of magnetic poly(N-isopropylacrylamide) microspheres for separation of DNA from probiotic dairy products, *J. Colloid Sci. Biotechnol.* 1 (2012) 235–240.
- [15] H. Ahmad, Preparation and potential applications of magnetically recyclable biocatalysts, *J. Colloid Sci. Biotechnol.* 2 (2013) 171–179.
- [16] V. Dugas, A. Elaïssari, Y. Chevalier, M. Zourob (Editor), *Recognition Receptors in Biosensors*, vol. 1, Springer, New York, 2010, p. 849.
- [17] M.M. Eissa, et al., Reactive magnetic poly(divinylbenzene-co-glycidyl methacrylate) colloidal particles for specific antigen detection using microcontact printing technique, *Acta Biomater.* 9 (2013) 5573–5582.
- [18] A. Elaïssari, Reactive polymer based colloids for biomedical applications, *Macromol. Symp.* 229 (2005) 47–55.
- [19] R. Veyret, A. Elaïssari, P. Marianneau, A.A. Sall, T. Delair, Magnetic colloids for the generic capture of viruses, *Anal. Biochem.* 346 (2005) 59–68.
- [20] R. Veyret, T. Delair, C. Pichot, A. Elaïssari, Amino-containing magnetic nanoemulsions: elaboration and nucleic acid extraction, *J. Magn. Magn. Mater.* 295 (2005) 155–163.
- [21] J. Joo, et al., A facile and sensitive detection of pathogenic bacteria using magnetic nanoparticles and optical nanocrystal probes, *Analyst* 137 (2012) 3609–3612.
- [22] R.E. Banks, et al., Proteomics: new perspectives, new biomedical opportunities, *Lancet* 356 (2000) 1749–1756.
- [23] J. Cheng, P. Fortina, S. Surrey, L. Kricka, P. Wilding, Microchip-based devices for molecular diagnosis of genetic diseases, *Mol. Diagn.* 1 (1996) 183–200.
- [24] A.J. Tüdös, G.A.J. Besselink, R.B.M. Schasfoort, Trends in miniaturized total analysis systems for point-of-care testing in clinical chemistry, *Lab Chip* 1 (2001) 83–95.
- [25] P. Yager, et al., Microfluidic diagnostic technologies for global public health, *Nature* 442 (2006) 412–418.
- [26] F.B. Myers, L.P. Lee, Innovations in optical microfluidic technologies for point-of-care diagnostics, *Lab Chip* 8 (2008) 2015–2031.
- [27] D.R. Baselt, et al., A biosensor based on magnetoresistance technology, *Biosens. Bioelectron.* 13 (1998) 731–739.
- [28] J.C. Rife, et al., Design and performance of GMR sensors for the detection of magnetic microbeads in biosensors, *Sens. Actuators Phys.* 107 (2003) 209–218.
- [29] J.-W. Choi, Fabrication of micromachined magnetic particle separators for bioseparation in microfluidic systems, *Methods Mol. Biol.* 321 (2006) 65–81.
- [30] A.T. Woolley, R.A. Mathies, Ultra-high-speed DNA fragment separations using microfabricated capillary array electrophoresis chips, *Proc. Natl. Acad. Sci. U.S.A.* 91 (1994) 11348–11352.
- [31] M. Kuschel, T. Neumann, P. Barthmaier, M. Kratzmeier, Use of lab-on-a-chip technology for protein sizing and quantitation, *J. Biomol. Tech.* 13 (2002) 172–178.
- [32] N.Y. Lee, Recent progress in lab-on-a-chip technology and its potential application to clinical diagnoses, *Int. Neurobiol. J.* 17 (2013) 2.
- [33] V. Srinivasan, V.K. Pamula, R.B. Fair, An integrated digital microfluidic lab-on-a-chip for clinical diagnostics on human physiological fluids, *Lab Chip* 4 (2004) 310–315.
- [34] I. EnDyna, Potential nano-enabled environmental application for radionuclides, in: M. Nawar (Editor), *Radiation Protection Division, US Environmental Protection Agency, Washington, DC, 2009*, pp. 99–101. 20460.
- [35] A. Manz, N. Graber, H.M. Widmer, Miniaturized total chemical analysis systems: a novel concept for chemical sensing, *Sens. Actuators B Chem.* 1 (1990) 244–248.
- [36] D.J. Harrison, A. Manz, Z. Fan, H. Luedi, H.M. Widmer, Capillary electrophoresis and sample injection systems integrated on a planar glass chip, *Anal. Chem.* 64 (1992) 1926–1932.
- [37] M.A. Unger, H.-P. Chou, T. Thorsen, A. Scherer, S.R. Quake, Monolithic microfabricated valves and pumps by multilayer soft lithography, *Science* 288 (2000) 113–116.
- [38] H. Schulze, G. Giraud, J. Crain, T.T. Bachmann, Multiplexed optical pathogen detection with lab-on-a-chip devices, *J. Biophotonics* 2 (2009) 199–211.
- [39] C.D. Chin, V. Linder, S.K. Sia, Lab-on-a-chip devices for global health: past studies and future opportunities, *Lab Chip* 7 (2007) 41–57.
- [40] R.C. Cooksey, J. Limor, G.P. Morlock, J.T. Crawford, Identifying *Mycobacterium* species and strain typing using a microfluidic labchip instrument, *Biotechniques* 35 (2003) 786–794.
- [41] P.L.A.M. Corstjens, et al., Rapid assay format for multiplex detection of humoral immune responses to infectious disease pathogens (HIV, HCV, and TB), *Ann. N. Y. Acad. Sci.* 1098 (2007) 437–445.
- [42] B.H. Weigl, et al. Fully integrated multiplexed lab-on-a-card assay for enteric pathogens. in 6112, 611202–611202–11 (2006).
- [43] C. De la Rosa, P.A. Tilley, J.D. Fox, K.V.I.S. Kaler, Microfluidic device for dielectrophoresis manipulation and electrodisruption of respiratory pathogen *Bordetella pertussis*, *IEEE Trans. Biomed. Eng.* 55 (2008) 2426–2432.
- [44] N.V. Zaytseva, R.A. Montagna, A.J. Baeumner, Microfluidic biosensor for the serotype-specific detection of dengue virus RNA, *Anal. Chem.* 77 (2005) 7520–7527.
- [45] I.R. Lauks, Microfabricated biosensors and microanalytical systems for blood analysis, *Acc. Chem. Res.* 31 (1998) 317–324.
- [46] M. Keusgen, Biosensors: new approaches in drug discovery, *Naturwissenschaften* 89 (2002) 433–444.
- [47] G. Fønnum, C. Johansson, A. Molteberg, S. Mørup, E. Aksnes, Characterisation of Dynabeads® by magnetization measurements and Mössbauer spectroscopy, *J. Magn. Magn. Mater.* 293 (2005) 41–47.
- [48] D.M. Bruls, et al., Rapid integrated biosensor for multiplexed immunoassays based on actuated magnetic nanoparticles, *Lab Chip* 9 (2009) 3504–3510.
- [49] J.-M. Nam, C.S. Thaxton, C.A. Mirkin, Nanoparticle-based bio-bar codes for the ultrasensitive detection of proteins, *Science* 301 (2003) 1884–1886.
- [50] A.P.F. Turner, Biosensors: sense and sensibility, *Chem. Soc. Rev.* 42 (2013) 3184–3196.
- [51] D.L. Graham, H. Ferreira, J. Bernardo, P.P. Freitas, J.M.S. Cabral, Single magnetic microsphere placement and detection on-chip using current line designs with integrated spin valve sensors: biotechnological applications, *J. Appl. Phys.* 91 (2002) 7786–7788.
- [52] D.R. Baselt, G.U. Lee, K.M. Hansen, L.A. Chrisey, R.J. Colton, A high-sensitivity micromachined biosensor, *Proc. IEEE* 85 (1997) 672–680.
- [53] J. Richardson, A. Hill, R. Luxton, P. Hawkins, A novel measuring system for the determination of paramagnetic particle labels for use in magneto-immunoassays, *Biosens. Bioelectron.* 16 (2001) 1127–1132.
- [54] S. Lee, et al., Magnetic gradiometer based on a high-transition temperature superconducting quantum interference device for improved sensitivity of a biosensor, *Appl. Phys. Lett.* 81 (2002) 3094–3096.
- [55] S. Katsura, T. Yasuda, K. Hirano, A. Mizuno, S. Tanaka, Development of a new detection method for DNA molecules, *Supercond. Sci. Technol.* 14 (2001) 1131.
- [56] K. Enpuku, et al., Detection of magnetic nanoparticles with superconducting quantum interference device (SQUID) magnetometer and application to immunoassays, *Jpn J. Appl. Phys.* 38 (1999) L1102.
- [57] M.M. Miller, G.A. Prinz, S.-F. Cheng, S. Bounnak, Detection of a micron-sized magnetic sphere using a ring-shaped anisotropic magnetoresistance-based sensor: a model for a magnetoresistance-based biosensor, *Appl. Phys. Lett.* 81 (2002) 2211–2213.
- [58] P.-A. Besse, G. Boero, M. Demierre, V. Pott, R. Popovic, Detection of a single magnetic microbead using a miniaturized silicon Hall sensor, *Appl. Phys. Lett.* 80 (2002) 4199–4201.
- [59] R.L. Millen, T. Kawaguchi, M.C. Granger, M.D. Porter, M. Tondra, Giant magnetoresistive sensors and superparamagnetic nanoparticles: a chip-scale detection strategy for immunosorbent assays, *Anal. Chem.* 77 (2005) 6581–6587.

- [60] S.X. Wang, G. Li, Advances in giant magnetoresistance biosensors with magnetic nanoparticle tags: review and outlook, *IEEE Trans. Magn.* 44 (2008) 1687–1702.
- [61] G.A. Prinz, *Magnetolectronics*, Science 282 (1998) 1660–1663.
- [62] J.-G. Zhu, Y. Zheng, G.A. Prinz, Ultrahigh density vertical magnetoresistive random access memory (invited), *J. Appl. Phys.* 87 (2000) 6668–6673.
- [63] R.L. Edelstein, et al., The BARC biosensor applied to the detection of biological warfare agents, *Biosens. Bioelectron.* 14 (2000) 805–813.
- [64] C.R. Tamanaha, L.J. Whitman, R.J. Colton, Hybrid macro–micro fluidics system for a chip-based biosensor, *J. Micromechanics Microengineering* 12 (2002) N7.
- [65] R. Weissleder, M.J. Pittet, Imaging in the era of molecular oncology, *Nature* 452 (2008) 580–589.
- [66] R. Weissleder, Molecular imaging in cancer, *Science* 312 (2006) 1168–1171.
- [67] T.J. Lowery, R. Palazzolo, S.M. Wong, P.J. Prado, S. Taktak, Single-Coil, Multisample, proton relaxation method for magnetic relaxation switch assays, *Anal. Chem.* 80 (2008) 1118–1123.
- [68] J.M. Perez, L. Josephson, T. O’Loughlin, D. Högemann, R. Weissleder, Magnetic relaxation switches capable of sensing molecular interactions, *Nat. Biotechnol.* 20 (2002) 816–820.
- [69] G.Y. Kim, L. Josephson, R. Langer, M.J. Cima, Magnetic relaxation switch detection of human chorionic gonadotrophin, *Bioconjug. Chem.* 18 (2007) 2024–2028.
- [70] H. Lee, E. Sun, D. Ham, R. Weissleder, Chip-NMR biosensor for detection and molecular analysis of cells, *Nat. Med.* 14 (2008) 869–874.
- [71] M.G. Harisinghani, et al., Noninvasive detection of clinically occult lymph-node metastases in prostate cancer, *N. Engl. J. Med.* 348 (2003) 2491–2499.
- [72] J.-H. Lee, et al., Artificially engineered magnetic nanoparticles for ultra-sensitive molecular imaging, *Nat. Med.* 13 (2007) 95–99.
- [73] Y. Jun, et al., Nanoscale Size effect of magnetic nanocrystals and their utilization for cancer diagnosis via magnetic resonance imaging, *J. Am. Chem. Soc.* 127 (2005) 5732–5733.
- [74] J. Park, et al., Ultra-large-scale syntheses of monodisperse nanocrystals, *Nat. Mater.* 3 (2004) 891–895.
- [75] S. Laurent, et al., Magnetic iron oxide nanoparticles: synthesis, stabilization, vectorization, physicochemical characterizations, and biological applications, *Chem. Rev.* 108 (2008) 2064–2110.
- [76] I. Koh, R. Hong, R. Weissleder, L. Josephson, Sensitive NMR sensors detect antibodies to influenza, *Angew. Chem. Int. Ed Engl.* 47 (2008) 4119–4121.
- [77] J.M. Perez, L. Josephson, R. Weissleder, Use of magnetic nanoparticles as nanosensors to probe for molecular interactions, *ChemBiochem* 5 (2004) 261–264.
- [78] I. Koh, L. Josephson, Magnetic nanoparticle sensors, *Sensors* 9 (2009) 8130–8145.
- [79] Y.R. Chemla, et al., Ultrasensitive magnetic biosensor for homogeneous immunoassay, *Proc. Natl. Acad. Sci. U.S.A.* 97 (2000) 14268–14272.
- [80] H.L. Grossman, et al., Detection of bacteria in suspension by using a superconducting quantum interference device, *Proc. Natl. Acad. Sci. U.S.A.* 101 (2004) 129–134.
- [81] D.L. Graham, H.A. Ferreira, P.P. Freitas, Magnetoresistive-based biosensors and biochips, *Trends Biotechnol.* 22 (2004) 455–462.
- [82] A. Fu, et al., Protein-functionalized synthetic antiferromagnetic nanoparticles for biomolecule detection and magnetic manipulation, *Angew. Chem. Int. Ed Engl.* 48 (2009) 1620–1624.
- [83] S.J. Osterfeld, et al., Multiplex protein assays based on real-time magnetic nanotag sensing, *Proc. Natl. Acad. Sci. U.S.A.* 105 (2008) 20637–20640.
- [84] R. De Palma, et al., Magnetic bead sensing platform for the detection of proteins, *Anal. Chem.* 79 (2007) 8669–8677.
- [85] N. Minc, Microfluidic systems of self-assembled magnetic particles; application to DNA separation and protein digestion, *Houille Blanche-Rev. Int. Eau* (2006) 51–54.
- [86] M.A.M. Gijs, F. Lacharme, U. Lehmann, Microfluidic applications of magnetic particles for biological analysis and catalysis, *Chem. Rev.* 110 (2010) 1518–1563.
- [87] Y. Liu, C.P. Hugentobler, H.C. Shum, A millifluidic approach for continuous generation of liquid marbles, *J. Colloid Sci. Biotechnol.* 2 (2014) 350–354.
- [88] A. Elaissari, *Colloidal Nanoparticles in Biotechnology*, John Wiley & Sons, 2008.
- [89] A. Günther, S.A. Khan, M. Thalmann, F. Trachsel, K.F. Jensen, Transport and reaction in microscale segmented gas–liquid flow, *Lab Chip* 4 (2004) 278–286.
- [90] X. Hu, et al., Marker-specific sorting of rare cells using dielectrophoresis, *Proc. Natl. Acad. Sci. U.S.A.* 102 (2005) 15757–15761.
- [91] J. Takagi, M. Yamada, M. Yasuda, M. Seki, Continuous particle separation in a microchannel having asymmetrically arranged multiple branches, *Lab Chip* 5 (2005) 778–784.
- [92] J.-W. Kim, R.J. Larsen, D.A. Weitz, Synthesis of Nonspherical colloidal particles with anisotropic properties, *J. Am. Chem. Soc.* 128 (2006) 14374–14377.
- [93] Z. Nie, W. Li, M. Seo, S. Xu, E. Kumacheva, Janus and ternary particles generated by microfluidic synthesis: design, synthesis, and self-assembly, *J. Am. Chem. Soc.* 128 (2006) 9408–9412.
- [94] A. Munir, Z. Zhu, J. Wang, H.S. Zhou, FEM analysis of magnetic agitation for tagging biomolecules with magnetic nanoparticles in a microfluidic system, *Sens. Actuators B Chem.* 197 (2014) 1–12.
- [95] N. Pamme, Magnetism and microfluidics, *Lab Chip* 6 (2006) 24–38.
- [96] M.A.M. Gijs, Magnetic bead handling on-chip: new opportunities for analytical applications, *Microfluid. Nanofluidics* 1 (2004) 22–40.
- [97] K.-Y. Lien, J.-L. Lin, C.-Y. Liu, H.-Y. Lei, G.-B. Lee, Purification and enrichment of virus samples utilizing magnetic beads on a microfluidic system, *Lab Chip* 7 (2007) 868–875.
- [98] N.Z. Danckwardt, M. Franzreb, A.E. Guber, V. Saile, Pump-free transport of magnetic particles in microfluidic channels, *J. Magn. Magn. Mater.* 323 (2011) 2776–2781.
- [99] N. Pamme, J.C.T. Eijkel, A. Manz, On-chip free-flow magnetophoresis: separation and detection of mixtures of magnetic particles in continuous flow, *J. Magn. Magn. Mater.* 307 (2006) 237–244.
- [100] G.P. Hatch, R.E. Stelter, Magnetic design considerations for devices and particles used for biological high-gradient magnetic separation (HGMS) systems, *J. Magn. Magn. Mater.* 225 (2001) 262–276.
- [101] N. Pamme, R. Koyama, A. Manz, Counting and sizing of particles and particle agglomerates in a microfluidic device using laser light scattering: application to a particle-enhanced immunoassay, *Lab Chip* 3 (2003) 187–192.
- [102] D.P. Schrum, C.T. Culbertson, S.C. Jacobson, J.M. Ramsey, Microchip flow cytometry using electrokinetic focusing, *Anal. Chem.* 71 (1999) 4173–4177.
- [103] N. Pamme, On-chip bioanalysis with magnetic particles, *Curr. Opin. Chem. Biol.* 16 (2012) 436–443.
- [104] P.-A. Auroux, D. Iossifidis, D.R. Reyes, A. Manz, Micro total analysis systems. 2. Analytical standard operations and applications, *Anal. Chem.* 74 (2002) 2637–2652.
- [105] J. West, M. Becker, S. Tombrink, A. Manz, Micro total analysis systems: latest achievements, *Anal. Chem.* 80 (2008) 4403–4419.
- [106] D. Lombardi, P.S. Ditttrich, Droplet microfluidics with magnetic beads: a new tool to investigate drug–protein interactions, *Anal. Bioanal. Chem.* 399 (2011) 347–352.
- [107] N. Pamme, Continuous flow separations in microfluidic devices, *Lab Chip* 7 (2007) 1644–1659.
- [108] P. Dunnill, M.D. Lilly, Purification of enzymes using magnetic bio-affinity materials, *Biotechnol. Bioeng.* 16 (1974) 987–990.
- [109] K. Mosbach, L. Andersson, Magnetic ferrofluids for preparation of magnetic polymers and their application in affinity chromatography, *Nature* 270 (1977) 259–261.
- [110] A. Kondo, H. Kamura, K. Higashitani, Development and application of thermo-sensitive magnetic immunomicrospheres for antibody purification, *Appl. Microbiol. Biotechnol.* 41 (1994) 99–105.
- [111] M. Koneracká, P. Kopčanský, M. Timko, C. Ramchand, Direct binding procedure of proteins and enzymes to fine magnetic particles, *J. Magn. Magn. Mater.* 252 (2002) 409–411.
- [112] V. Kourilov, M. Steinitz, Magnetic-bead enzyme-linked immunosorbent assay verifies adsorption of ligand and epitope accessibility, *Anal. Biochem.* 311 (2002) 166–170.
- [113] A.H. Latham, R.S. Freitas, P. Schiffer, M.E. Williams, Capillary magnetic field flow fractionation and analysis of magnetic nanoparticles, *Anal. Chem.* 77 (2005) 5055–5062.
- [114] S. Østergaard, G. Blankenstein, H. Dirac, O. Leistiko, A novel approach to the automation of clinical chemistry by controlled manipulation of magnetic particles, *J. Magn. Magn. Mater.* 194 (1999) 156–162.
- [115] M. Megens, M. Prins, Magnetic biochips: a new option for sensitive diagnostics, *J. Magn. Magn. Mater.* 293 (2005) 702–708.
- [116] C.R. Tamanaha, S.P. Mulvaney, J.C. Rife, L.J. Whitman, Magnetic labeling, detection, and system integration, *Biosens. Bioelectron.* 24 (2008) 1–13.
- [117] R. Mukhopadhyay, Diving into droplets, *Anal. Chem.* 78 (2006) 1401–1404.
- [118] A.A. García, et al., Magnetic movement of biological fluid droplets, *J. Magn. Magn. Mater.* 311 (2007) 238–243.
- [119] M. Shikida, et al., A palmtop-sized rotary-drive-type biochemical analysis system by magnetic bead handling, *J. Micromechanics Microengineering* 18 (2008) 035034.
- [120] J.R. Dorvee, A.M. Derfus, S.N. Bhatia, M.J. Sailor, Manipulation of liquid droplets using amphiphilic, magnetic one-dimensional photonic crystal chaperones, *Nat. Mater.* 3 (2004) 896–899.
- [121] W.A. Bonner, H.R. Hulet, R.G. Sweet, L.A. Herzenberg, Fluorescence activated cell sorting, *Rev. Sci. Instrum.* 43 (1972) 404–409.
- [122] R. Manz, M. Assenmacher, E. Pfluger, S. Miltenyi, A. Radbruch, Analysis and sorting of live cells according to secreted molecules, relocated to a cell-surface affinity matrix, *Proc. Natl. Acad. Sci. U.S.A.* 92 (1995) 1921–1925.
- [123] M. Berger, J. Castelino, R. Huang, M. Shah, R.H. Austin, Design of a microfabricated magnetic cell separator, *Electrophoresis* 22 (2001) 3883–3892.
- [124] N. Xia, et al., Combined microfluidic–micromagnetic separation of living cells in continuous flow, *Biomed. Microdevices* 8 (2006) 299–308.
- [125] M. Varshney, Y. Li, B. Srinivasan, S. Tung, A label-free, microfluidics and interdigitated array microelectrode-based impedance biosensor in combination with nanoparticles immunoseparation for detection of *Escherichia coli* O157:H7 in food samples, *Sens. Actuators B Chem.* 128 (2007) 99–107.
- [126] J.D. Adams, U. Kim, H.T. Soh, Multitarget magnetic activated cell sorter, *Proc. Natl. Acad. Sci. U.S.A.* 105 (2008) 18165–18170.
- [127] G. Hager, et al., The use of a panel of monoclonal antibodies to enrich circulating breast cancer cells facilitates their detection, *Gynecol. Oncol.* 98 (2005) 211–216.
- [128] A.L. Allan, et al., Detection and quantification of circulating tumor cells in mouse models of human breast cancer using immunomagnetic enrichment and multiparameter flow cytometry, *Cytometry A*. 65A (2005) 4–14.
- [129] Y.-J. Liu, et al., A micropillar-integrated smart microfluidic device for specific capture and sorting of cells, *Electrophoresis* 28 (2007) 4713–4722.

- [130] T. Schuurman, R. de Boer, R. Patty, M. Kooistra-Smid, A. van Zwet, Comparative evaluation of in-house manual, and commercial semi-automated and automated DNA extraction platforms in the sample preparation of human stool specimens for a *Salmonella enterica* 5'-nuclease assay, *J. Microbiol. Methods* 71 (2007) 238–245.
- [131] V. Leeb, et al., Fully automated, internally controlled quantification of hepatitis B Virus DNA by real-time PCR by use of the MagNA Pure LC and LightCycler instruments, *J. Clin. Microbiol.* 42 (2004) 585–590.
- [132] S.-W. Yeung, T.M.-H. Lee, H. Cai, I.-M. Hsing, A DNA biochip for on-the-spot multiplexed pathogen identification, *Nucleic Acids Res.* 34 (2006) e118.
- [133] W. Zhao, S. Yao, I.-M. Hsing, A microsystem compatible strategy for viable *Escherichia coli* detection, *Biosens. Bioelectron.* 21 (2006) 1163–1170.
- [134] G. Jiang, D.J. Harrison, mRNA isolation in a microfluidic device for eventual integration of cDNA library construction, *Analyst* 125 (2000) 2176–2179.
- [135] T. Lund-Olesen, M. Dufva, M.F. Hansen, Capture of DNA in microfluidic channel using magnetic beads: increasing capture efficiency with integrated microfluidic mixer, *J. Magn. Magn. Mater.* 311 (2007) 396–400.
- [136] J. Křenková, F. Foret, Immobilized microfluidic enzymatic reactors, *Electrophoresis* 25 (2004) 3550–3563.
- [137] M. Slovakova, et al., Use of self assembled magnetic beads for on-chip protein digestion, *Lab Chip* 5 (2005) 935–942.

PART III
EXPERIMENTAL PART

Introduction

Colloidal particles showed substantial concern in biomedical area, but these particles require time consuming during separation process, limiting the automation of diagnosis and resulting in delayed in diagnosis procedures. With passage of time, magnetic latex particles (MLPs) have been formulated to overcome all that tedious processes. Pioneer work was described by Ugelstad et al by reporting the synthesis of (MLPs) as well as their applications in diagnosis. While, Elaissari et al have reported synthesis of MLPs using seeded emulsion polymerization that led to submicron MLPs containing high iron oxide content that have been used for various diagnostic applications. Nevertheless, properties of submicron MLPs depend on size as well as shape. Type of initiator, chemical nature of monomer, surfactant stabilizer, polymerization process, amount of internal oil phase in aqueous magnetic emulsion and monomer to magnetic seed ratio, with help of these parameters final morphology of MLPs can be controlled.

Considering all above mentioned parameters, we mainly focused on core-shell like morphology by using our home-made emulsion. Core-shell like morphology plays a vital role in field of biomedical applications because in this type of morphology polymer protects magnetic core and enhances both chemical stability and biocompatibility of MLPs.

In order to evaluate the influence of the main monomer concentrations and also for purpose of obtaining the desired morphology. Initially, different polymerizations experiments with styrene, divinylbenzene as crosslinker, in the presence of hydrophilic initiator potassium persulfate as hydrophilic initiator and well-controlled oil in water magnetic emulsion as a seed, were conducted. Special attention was dedicated to the influence of St/DVB weight ratio on the particle size, morphology, and magnetic properties of the obtained latex particles. The results showed three types of morphologies that is Janus, moon like Janus and the desired perfect core-shell magnetic latex particles. Now, by keeping the concentration of St/DVB at which the desired perfect core-shell like morphology was obtained similar polymerization experiments were conducted with 4, 4'-azobis cyanopentanoic acid (ACPA) under same circumstances as mentioned above. Also by use of second monomer methacrylic acid which enhanced the carboxylic group. Following parameters were evaluated for characterization that includes transmission electron microscopy, particle size measurements, zeta potential measurement, thermo gravimetric analysis, Fourier transform infrared analysis and magnetic properties. Obtained MLPs after functionalization used as solid support in microfluidic, lab-on-chip and microsystems facilitating fast magnetic separation.

A novel capacitance electrochemical biosensor based on silicon nitride substrate (Si_3N_4) combined with a MLPs with carboxylic group functionality was developed. Si_3N_4 is highly stable as it was fabricated by a combination of several layers of Aluminum (Al), silicon p-doped (Si-p), silicon dioxide (SiO_2) and silicon nitride (Si_3N_4). This structure ($\text{Si}_3\text{N}_4/\text{SiO}_2/\text{Si-p}/\text{Al}$) has been administered several advantages as compared with other materials commonly used, and in particular in solid-state physics for electronic-based biosensors. MLPs with terminated carboxylic acid were covalently bonded to Si_3N_4 through a Self-Assembled Monolayers (SAMs) of the silane-amine (3-Aminopropyl) triethoxysilane (APTES). Finally anti-ochratoxin A antibodies were immobilized on MLPs by amide bonding.

Contact angle measurements, atomic force microscopy, scanning electron microscopy and fluorescence microscopy characterizations were performed during the biofunctionalization of the biosensor surface. Electrochemical measurements were carried out using Mott-Schottky analysis for ochratoxin A (OTA) detection. The biosensor was highly sensitive and selective for ochratoxin A antigens, with a limit of detection of 1.845 pg/mL, when compared to other interferences ochratoxin B and aflatoxin G1. The measurements were highly stable and reproducible for detection and interferences. The advanced method is very promising for OTA detection for several agro-food industry applications.

Sensitivity of biosensor by using application of competitive assay through immobilized fixed concentration of antigen (SA2BSA) and antibody (Ab 155) respectively was measured against different concentrations of sulfapyridine (SPY) like 40 μ M, 4 μ M, 2nM and finally only with PBS respectively, with and without use of MLPs with carboxylic group functionality. Using Cyclic voltammetry (CV) and electrochemical impedance spectroscopy (EIS) the microelectrodes were characterized for the bare gold, surface functionalization with 4-aminophenylacetic acid (CMA), immobilized SA2BSA and fixed concentration MLPs that contain immobilized Ab 155 with different concentration of SPY. The Nyquist plot showed a stepwise increase of R_{ct} in both cases (Ab 155 without and with MLPs that contain immobilized Ab 155 with different concentration of SPY). However, after calculations from fitting parameters and drawing graph, it can be clearly observe that there is more linearity while MLPS instead of without use of magnetic nanoparticles, which indicates the increase in sensitivity of biosensor as compared to competitive assay without MLPs. Thus, reported the development of a highly sensitive biosensor for SPY detection using competitive assay, so MLPs applied to increase the sensitivity, limit of detection, and dynamic range for the competitive assay detection of SPY using real conditions for example sea water.

III.1

Preparation and characterization of submicron hybrid magnetic latex particles

Summary

Different types of nanoparticles have been employed for their potential applications in biomedical field, yet most interesting of them are the hybrid particles having both the magnetic properties and the ability to functionalize with important drug moieties and biomolecules. Among the key features of such functional colloidal particles are their soft hybrid core-shell structures, which are engineered in such a way that the core consists of an inorganic material whereas the shell is composed of a soft organic substance. Colloidal particles are of great interest in biomedical field particularly in its diagnostic aspect, for example, immunoassay, nucleic acid capturing and detection and cell sorting. However, these applications require lot of labor and time during their separation, limiting the automation of diagnosis and thus causing delay in diagnosis. Main objective in biomedical diagnosis is to enhance the specificity and sensitivity and to reduce time consumption. One way to solve this problem is to increase the concentration of captured targets like antigen, viruses, bacteria and nucleic acid before detection step. In the last decades, a great attention has been paid to magnetic latex nanoparticles (MNPs) due their superparamagnetic properties emanating from their nano-size. They have found promising applications in various industrial and particularly biomedical diagnostic domains (e.g. fast separation, purification and detection of biomolecules). Magnetic latex particles (MLPs) have been formulated to overcome these problems that provide ease in separation even by applying low magnetic field. Magnetic composites and latexes protect inorganic part to confer reactive chemical functionality that has potential to immobilize biomolecules through chemical reactions. Different approaches have been reported for preparation of MLPs that are based on classical polymerization in dispersed media. The classical work described by Ugelstad et al reported the preparation of MLPs as well as their applications in diagnosis. While, Elaissari et al have reported synthesis of MLPs using seeded emulsion polymerization that led to submicron MLPs containing high iron oxide content that have been used for various diagnostic applications. However, properties of submicron MLPs depend on size as well as shape. Hence, controlling the morphology of these particles is of crucial importance.

Final morphology of MLPs can be controlled by measuring various factors like type of initiator, chemical nature of monomer, surfactant stabilizer, polymerization process, amount of internal oil phase in aqueous magnetic emulsion and monomer to magnetic seed ratio.

The aim of the current study was to evaluate the influence of monomer concentration to obtain desired morphology of MLPs that contained magnetic core and homogenous polymer shell bearing sulphate groups.

For this purpose home-made magnetic emulsion was used. The oil in water magnetic emulsion was prepared in two steps: first iron oxide nanoparticles were prepared in water phase via FeCl_2 and FeCl_3 coprecipitation in concentrated ammonia medium. Then the prepared nanometer size magnetic particles were chemically modified using oil acid in order to be easily compatible with organic solvent (i.e. Octane). The second step consists in emulsification of the prepared octane ferrofluid in water phase containing ionic and non-ionic surfactants mixture. The obtained stable

magnetic oil in water was then purified by removing free surfactants before magnetic particles sorting

Particular attention was paid to evaluate the influence of St/DVB weight ratio on morphology and magnetic properties of MLPs.

These MLPs were prepared by seeded emulsion copolymerization of styrene (St) with divinyl benzene (DVB) crosslinker. Well controlled oil in water magnetic emulsion was used as a seed while potassium persulphate (KPS) as hydrophilic initiator having sulfate group functionality.

The polymerization was carried out in specially designed 60 ml glass reactor. Temperature was maintained at 70⁰ C. The home-made magnetic emulsion stabilized by aqueous solution of SDS was introduced in the reactor. Magnetic emulsion was mixed with nitrogen for 1 hour at 300 rpm for removal of oxygen. Subsequently, total amount of monomers at different St/DVB (volume/volume) ratios were introduced at once in the reactor and was mixed at 300 rpm for 60 min followed by addition of 2 weight % of KPS into the medium. The radical polymerization was carried out at 300 rpm for 18 hours. Finally, the polymerization was terminated by cooling the reactor to room temperature.

In order to evaluate the influence of St Concentration or St/DVB ratio on the final morphology of MLPs, various polymerizations were performed at different concentrations. Following parameters were evaluated for characterization like Transmission Electron Microscopy (TEM) Particle Size Measurements, Zeta Potential measurement, Thermogravimetric Analysis (TGA) Fourier Transform Infrared Analysis (FTIR) and Magnetic Properties.

After the characterization, results showed three types of morphologies that is Janus, moon like Janus and the desired perfect core-shell magnetic latex particles. Core-shell morphology of the magnetic latex nanoparticles is the most favorable for *in-vitro* biomedical diagnostic field. This morphology has an added advantage that it prevents release of ferric, ferrous and magnetic pigments, not suited for any biological based process, in the dispersion medium.

Interestingly, characterizations revealed two remarkable morphologies; Janus-like morphology was obtained with 10% of St and 90 % of DVB. While, perfect core-shell MLPs were obtained by 60 % St and 40 % DVB and no secondary nucleation was observed. Another remarkable characteristic of these MLPs was that they contained about 63.9 % of superparamagnetic iron oxide that is very much desirable for fast magnetic separation.

Furthermore, the obtained MLPs after functionalization can be used as solid support in microfluidic, lab-on-chip and microsystems facilitating fast magnetic separation.

Preparation and characterization of submicron hybrid magnetic latex particles

Talha Jamshaid^{a,b}, Ernandes Taveira Tenório-Neto^{a,c}, Mohamed Eissa^d, Nadia Zine^b, Abdelhamid Errachid El-Salhi^b, Marcos Hiroiuiqui Kunita^c and Abdelhamid Elaissari^{a*}



Micrometer magnetic hybrid particles are of great interest in biomedical field, and various morphologies have been prepared via encapsulation processes. Regarding submicron, only few processes have been investigated and the most recent one leading to highly magnetic submicron magnetic hybrid particles is based on oil in water magnetic emulsion (MES) transformation. The encapsulation of magnetic iron oxide nanoparticles forming oil in water MES was investigated using different styrene/cross-linker divinylbenzene volume ratio in the presence of potassium persulfate initiator. The encapsulation performed in this work is basically conducted by using well-defined oil in water MES as a seed in radical emulsion polymerization. The chemical composition, morphology, iron oxide content, magnetic properties, electrokinetic properties, particle size, and size distribution of the prepared magnetic hybrid particles were examined using various techniques. The desired perfect magnetic core and polymer shell morphology were successfully obtained, and the final magnetic hybrid particles are superparamagnetic in nature and exhibit high iron oxide content (64 wt %). Copyright © 2015 John Wiley & Sons, Ltd.

Supporting information may be found in the online version of this paper.

Keywords: magnetic emulsion; seeded polymerization; hybrids; magnetic latex particles; iron oxide

INTRODUCTION

Colloidal particles are used as solid support in biomedical field, which include immunoassay,^[1] cell sorting,^[2] and nucleic acid capturing and detection.^[3] However, such applications require different tedious and time consuming separation processes, mainly when two kinds of separation processes are used, i.e. (a) filtration and (b) centrifugation.^[4] These processes limit the automation of biomedical diagnosis resulting in loss of time and delay in diagnosis.^[5] Although magnetic latex particles are overcoming these methods, improving the process of automation while also decreases time delay and providing fast particles separation upon applying even low magnetic field.^[5,6] Magnetic latex (ML) is a hybrid material consisting of polymer-encapsulated magnetic particles.^[7] The purpose for the preparation of magnetic composite and latexes in biomedical area is to protect the inorganic part and to induce reactive chemical functionality, which is capable of immobilizing biomolecules through chemical reactions.^[8,9] Furthermore, it is important to mention that the target in the preparation of (MLs) is the elaboration of superparamagnetic magnetic latex particles containing well-defined amount of iron oxide, submicron in size and with narrowly size distribution.^[10,11]

Different approaches have been reported for the preparation of magnetic latex particles for *in vitro* biomedical diagnostic applications. These approaches are based on classical polymerization in dispersed media such as emulsion,^[12] suspension,^[13] miniemulsion,^[14] dispersion,^[15] combination of various polymer-based process,^[16] and inverse emulsion.^[17,18] The pioneer work was described by Ugelstad *et al.*^[19] by reporting not only the preparation of MLs but also their uses for *in vitro* biomedical

diagnosis. On the other hand, Elaissari *et al.*^[6] have reported the synthesis of magnetic latexes using a process called seeded emulsion polymerization. This process leads to submicron ML particles containing high iron oxide content. These prepared functional, submicron, and highly ML particles have been used for nucleic acid extraction and purification,^[20] capturing of biological samples,^[21,22] controlling of protein adsorption and desorption,^[23] molecular imaging,^[24] and specific antigen detection.^[25]

However, the properties of nano/submicron particles are dependent on both size and shape. For this reason, controlling the morphology of the obtained material has a crucial role on its applications. In this sense, core-shell structures – where polymer protects the magnetic core – can enhance both the chemical

* Correspondence to: Abdelhamid Elaissari, CNRS, UMR-5007, LAGEP-CPE, 43 bd 11 November 1918, F-69622 Villeurbanne, France.
E-mail: elaissari@lagep.univ-lyon1.fr

a T. Jamshaid, E. T. Tenório-Neto, A. Elaissari
University of Lyon, CNRS, UMR-5007, LAGEP-CPE, 43 bd 11 November 1918, F-69622, Villeurbanne, France

b T. Jamshaid, N. Zine, A. E. El-Salhi
Institut des Sciences Analytiques (ISA), UMR-5180, Université Claude Bernard Lyon-1, 5 rue de la Doua, F-69100, Villeurbanne, France

c E. T. Tenório-Neto, M. H. Kunita
Universidade Estadual de Maringá, Chemistry Department, Av. Colombo 5790, CEP, 87020-900, Maringá, PR, Brazil

d M. Eissa
Polymers and Pigments Department, National Research Centre, 33 El Bohouth St. (Former El Tahrir St.), Dokki, Giza 12622, Egypt

stability and biocompatibility of the ML. In addition, its surface may be modified for obtaining specific functionalities.^[26]

On the other hand, Janus microparticles, which have anisotropic morphology, offer more possibilities in terms of achievable structure and behavior. The simplest case of Janus particles is achieved by dividing in two distinct hemispheres, such as hydrophobic and hydrophilic parts.^[27,28] This feature is very important in industry, since such material could be applied as stabilizers in emulsions,^[29] biological sciences,^[30] textile industry,^[31] and so forth.

It is well known that the final morphology of the ML nanoparticles can be controlled by adjusting some factors, such as (i) monomer chemical nature, (ii) type of initiator, (iii) surfactant or stabilizer, (iv) polymerization process, (v) monomers/magnetic seed ratio, and (vi) amount of internal oil phase of the used oil in water magnetic emulsion.^[32,33]

In order to evaluate the influence of the main monomer concentrations and also for purpose of obtaining the desired morphology, the aim of this work was to synthesize submicron ML particles with magnetic core and homogeneous polymer shell bearing sulfate surface groups. These magnetic colloidal particles were prepared by seeded emulsion copolymerization of styrene (St) monomer with divinylbenzene (DVB) crosslinker, in the presence of potassium persulfate (KPS) as hydrophilic initiator and well-controlled oil in water magnetic emulsion as a seed. In this study, special attention was dedicated to the influence of St/DVB weight ratio on the particle size, morphology, and magnetic properties of the obtained latex particles.

MATERIALS AND METHODS

Materials

Styrene (99%) and DVB 80% were purchased from Sigma–Aldrich and used after washing with 5% NaOH solution. KPS initiator and sodium dodecyl sulfate (SDS) emulsifier were obtained from Sigma–Aldrich and used without purification. Deionized water was used in all experiments. Home-made magnetic emulsion was prepared according to our previous work.^[34,35]

Methodology

Magnetic latex particles with different morphologies were achieved by using oil in water magnetic emulsion as seed in the emulsion polymerization of St with cross-linker DVB using KPS as initiator.

The polymerization was carried out in a 60 ml three-necked double wall glass reactor made up of glass anchor type stirrer, a reflux condenser, and a nitrogen inlet. The temperature was controlled at 70°C by using a thermal bath. The home-made magnetic emulsion (approximately 50 ml of 4% solid content) was stabilized with 1 g l⁻¹ aqueous solution of SDS (below its critical micelle concentration, CMC) via serum replacement process performing only one time separation/dispersion cycle and introduced in the reactor. Then after, the magnetic emulsion was purged with nitrogen for 1 hr under stirring of 300 rpm for removal of the residual oxygen. The concentration of SDS solution was below the CMC because the excess of surfactants, during polymerization, could increase the amount of particles formed without magnetic seed leading to secondary nucleation.

After that, a total amount of monomers (1200 μl) at different St/DVB (volume/volume) ratios was charged at once into the reactor containing the magnetic emulsion and kept under continuous stirring (300 rpm) for 60 min. This time was necessary in order to favor monomers diffusion into the oil in water magnetic seed droplets. The polymerization temperature was then rapidly increased up to 70°C, followed by the addition of 2 wt % of KPS (with respect to the total weight of monomers) into the polymerization medium. The radical polymerization was then conducted at constant mechanical stirring (300 rpm) and was left overnight for 18 hr. Then after, the polymerization reaction was terminated by cooling to room temperature.

CHARACTERIZATION

Transmission electron microscopy

Transmission electron microscopy (TEM) images were obtained by a Phillips CM120 microscope (CMEABG, University of Claude Bernard Lyon I, Villeurbanne, France) to investigate the morphology and microstructure of the magnetic polymer latex particles. Briefly, a drop of sample diluted in distilled water was deposited on a carbon-coated copper grid and then left to dry at room temperature overnight before TEM imaging.

Particle size measurements

A Malvern Zetasizer (Nano ZS, Malvern Instruments Limited, UK) was used to measure the average hydrodynamic size (D_h) of the magnetic polymer colloidal particles in 10⁻³ M NaCl solution. The average of at least three measurements (10 runs for each colloidal dispersion) was taken into consideration.

Zeta potential measurement

A Malvern Zetasizer (Nano ZS, Malvern Instruments limited) was used to measure the electrophoretic mobility, which is converted to Smoluchowski's zeta potential.^[36,37] The measurements were performed using highly diluted dispersion of the considered colloidal particles in 10⁻³ M NaCl solution at different pH. The pH was adjusted using NaOH or HCl solutions. Each recorded value was the average of at least three measurements.

Thermal gravimetric analysis

Thermo gravimetric analysis (TGA) measurements were carried out on a thermogravimetry analyzer (NETZSCH, model TG 209 F1). The measurements were performed under inert N₂ atmosphere from ambient temperature up to 700°C at a heating rate of 10°C min⁻¹. All samples were washed with distilled water and then dried at 50°C for 24 hr before analysis.

Fourier transform infrared analysis

The investigation of surface properties of the obtained sample was performed using attenuated total reflectance-Fourier transform infrared spectrophotometer (Shimadzu, Japan). All samples were cleaned and dried before analysis. The spectra were scanned over range 4000–400 cm⁻¹.

Magnetic properties

The saturation magnetization and magnetic behavior of the dried magnetic polymer latexes were investigated using a vibrating

sample magnetometer. Magnetization measurements were carried out at room temperature on the automatic bench of magnetic measurements at CNRS-IRC Lyon.

RESULTS AND DISCUSSION

The seeded emulsion polymerization was performed by varying St/DVB (volume/volume) ratio. The influence of St/DVB ratio was investigated in order to point out the relationship between the initial monomers composition and the final morphology of the obtained magnetic hybrid particles. The used initial chemical compositions are summarized in Table 1.

Particle morphology analysis

Figure 1 shows TEM images of various magnetic hybrid particles prepared with different contents of St and DVB. According to the state of the art,^[6,38] it is well known that the final morphology of ML nanoparticles may be controlled by adjusting various factors, such as (i) type of monomer, (ii) type of initiator, (iii) surfactant, (iv) polymerization time, (v) monomers/seed ratio, and (vi) amount of octane in the magnetic-seed emulsion.^[6,21,38] In order to evaluate the influence of St concentration or St/DVB ratio on the final morphology of ML particles, various polymerizations were performed at different St concentrations. The experimental conditions are reported in Table 1. Polymerizations were conducted using KPS as initiator, SDS as surfactant, and the magnetic emulsion as seed. The used magnetic emulsion contains a negligible amount of octane, which was found to be below 10 mg of octane/g of dried emulsion. In fact, the presence of high octane content in the used emulsion leads to the formation of magnetic hybrid particles with heterogeneous morphology (non-core-shell structure).

As shown in Fig. 1A the particles of prepared magnetic emulsion (MES) exhibit a spherical shape with wide size distribution. When emulsion polymerization of DVB was carried out without St (Fig. 1B), surprisingly, Janus nanoparticles were obtained. The formation of submicron particles with this morphology can be explained in terms of chain mobility. During early stage of polymerization, the cross-linked oligomeric DVB radicals which are into the oil droplet cannot diffuse very well. As a consequence, the DVB monomer, which had not been reacted, moves

Table 1. Composition of monomers employed during seeded emulsion polymerization

Sample name	St (% vol)	DVB (% vol)
ML1	0	100
ML2	10	90
ML3	20	80
ML4	40	60
ML5	60	40
ML6	80	20
ML7	90	10
ML8	100	0

Constant polymerization parameters: total monomers (DVB and St) 1200 μ l, total reaction volume 50 ml, potassium persulfate concentration 2 wt% of the total monomers weight, stirring rate 300 rpm, and reaction temperature 70 °C.

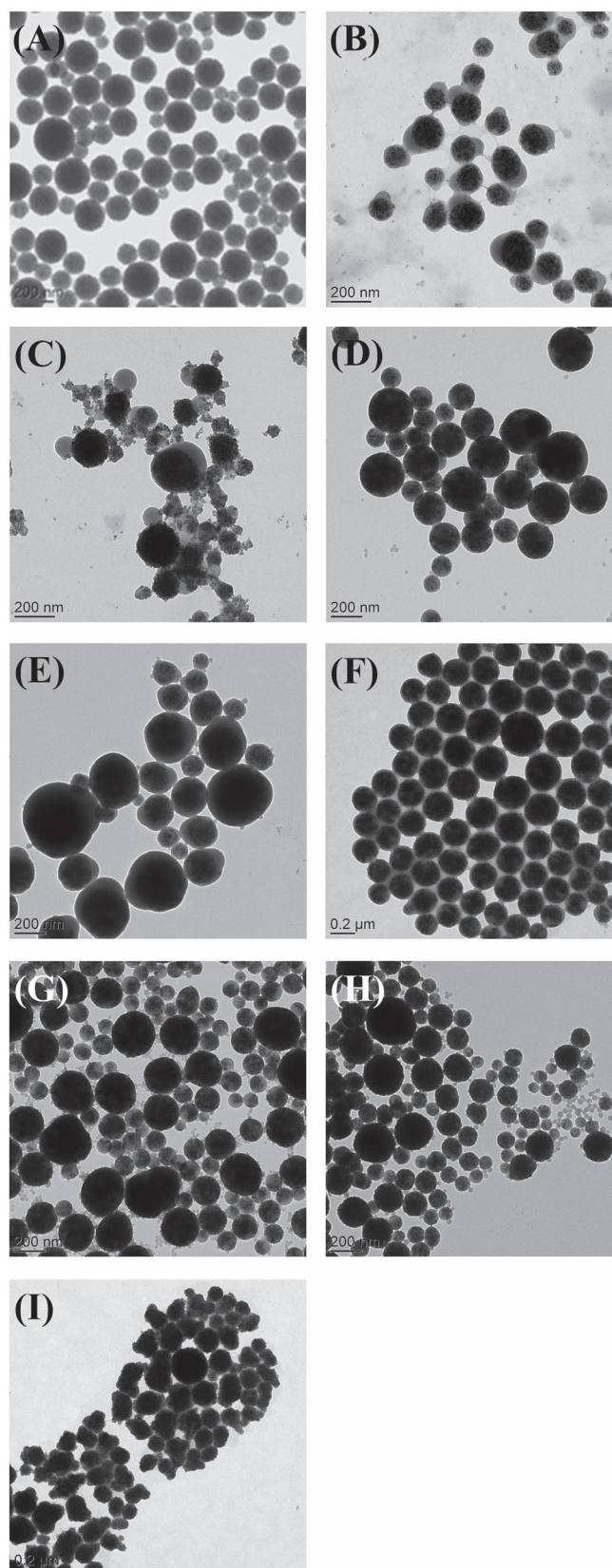


Figure 1. Transmission electron microscopy images of samples (A) magnetic emulsion, (B) ML1, (C) ML2, (D) ML3, (E) ML4, (F) ML5, (G) ML6, (H) ML7, and (I) ML8. Scale bar of images is 200 nm.

near of the cross-linked oligomeric DVB chains, while the iron oxide moves to the opposite side leading to phase separation. Due to this incompatibility, Janus particles were obtained. For sample ML2, which has approximately 10% of St in its composition, the appearance of some particles from secondary nucleation (SN) was observed without any marked changes in the final morphology (Fig. 1C). When St was added in the initial composition, the monomers diffusion, into the oil droplet, was enhanced. Polystyrene oligomers have high chain mobility if compared with oligomers containing DVB. In this case, the styrene oligomer radicals, originating from the water phase, can either enter into the magnetic droplet/particle or undergo homogeneous nucleation, which contributes to the growth of secondary nucleated particles.^[6,33]

By increasing St content (i.e., increasing the St/DVB ratio), the obtained submicron particles were becoming spherical-like, and the SN was reduced as can be seen in Fig. 1D, 1E, and 1F images. The high mobility of St monomer reduces, inside magnetic droplets, phase separation between formed polymer and iron oxide nanoparticles. In addition, polystyrene oligomers (or oligomers rich in styrene) have sulfate-end groups, which in turn contribute to anchor the polymer chains on the particle surface. This effect is similar to the surfactant property (hydrophobic chain and hydrophilic end group). When St concentration increases up to 60%, a perfect-core shell morphology could be obtained as shown in Fig. 1F.

When the amount of styrene was increased to between 80% and 90%, the influence of DVB on polystyrene oligomers mobility was drastically decreased. It can be seen in Fig. 1G and 1H that the prepared samples exhibit a non-uniform size distribution. Furthermore, when the emulsion polymerization was performed using 100% of St, the obtained particles showed small nodules randomly distributed around the magnetic core as shown in Fig. 1I. This morphology may be explained taking in account the high specific surface developed by the presence of small polymer particles compared with large ones. In the early stage of emulsion polymerization, the St monomer is initiated in water phase and not inside the oil droplet because of water-soluble KPS used.^[19] Because the polymerization starts in water phase, the oligomers chain length increases (i.e., increasing polymerization degree). For this reason, the polystyrene oligomers become less and less water soluble (i.e., more hydrophobic). As a consequence, these oligomers are deposited on the magnetic-core surface. Based on these results, the

morphology change versus St/DVB ratio is schematically suggested as shown in Fig. 2.

Chemical composition and size determination

The chemical composition of the magnetic hybrid particles was investigated using TGA. Before analysis, the MLs were separated from the supernatant by applying permanent magnetic field and then washed with deionized water. This procedure was performed three times, in order to remove the non-magnetic material such as surfactant and free polymer particles.

Figure 3A shows the thermogram of MES used as seed during polymerization. In this figure, it can be visualized that degradation of magnetic emulsion could be divided into three steps: (i) 25–150°C, (ii) 150–500°C, and (iii) above 500°C, which corresponds, respectively, to dehydration of physically adsorbed water (1.1%), degradation of organic part (16.6%), and residual inorganic part (82.3%). In the same figure, it can be observed in derivative thermogravimetric graph that the organic content present in the MES showed three peaks, which overlaps each other. These peaks were assigned to the degradation of free oleic acid, SDS, and oleic acid complexed on magnetic nanoparticles.^[8]

Figure 3B shows the thermograms of magnetic particles obtained after emulsion polymerization for samples with different morphologies ML1 (Janus), ML2 (Janus moon-like), ML5 (perfect core-shell), and ML8 (heterogeneous shape). As a general trend, all samples showed higher weight loss than the used seed MES. This is due to polymer being induced during the polymerization process. However, the ML8 prepared using St only showed lower polymer content than sample ML5 (perfect-core shell). The difference of the residual mass can be attributed to the second nucleation favored in the case of ML8. In fact, TEM analysis of crude sample ML8 (data not shown) showed the presence of high amount of submicron polymer based particles. Then, the polymer partition between SN and encapsulation of magnetic particles induced drastic decreases of polymer content in the washed ML8 sample.

Table 2 shows the percentage of both polymer and iron content in the prepared MLs obtained at different St/DVB ratios and the average particle size. In this study, residual mass at 500°C was attributed to percentage of iron oxide content for each sample. This consideration is reasonable, because there

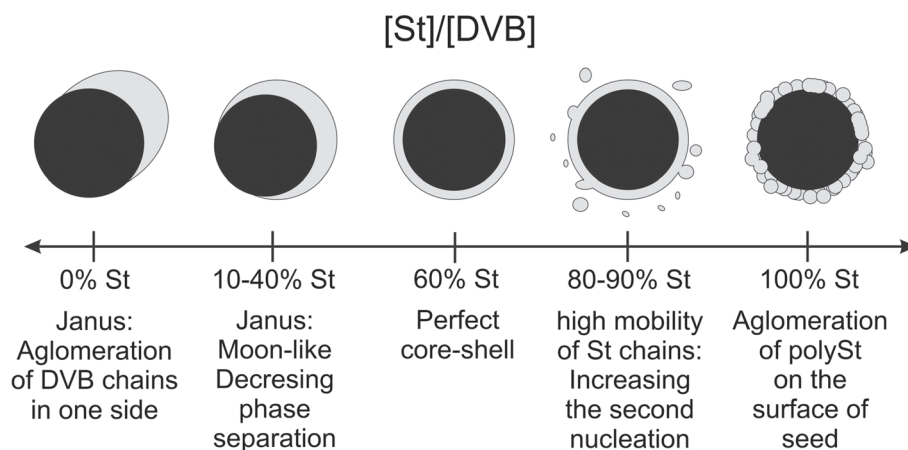


Figure 2. Proposed scheme for controlling the morphology of the prepared magnetic latex particles during the polymerization process depending on styrene/divinylbenzene (St/DVB) ratio. The used magnetic iron oxide emulsion (seed) has low octane content (<10 mg octane /g of dried emulsion).

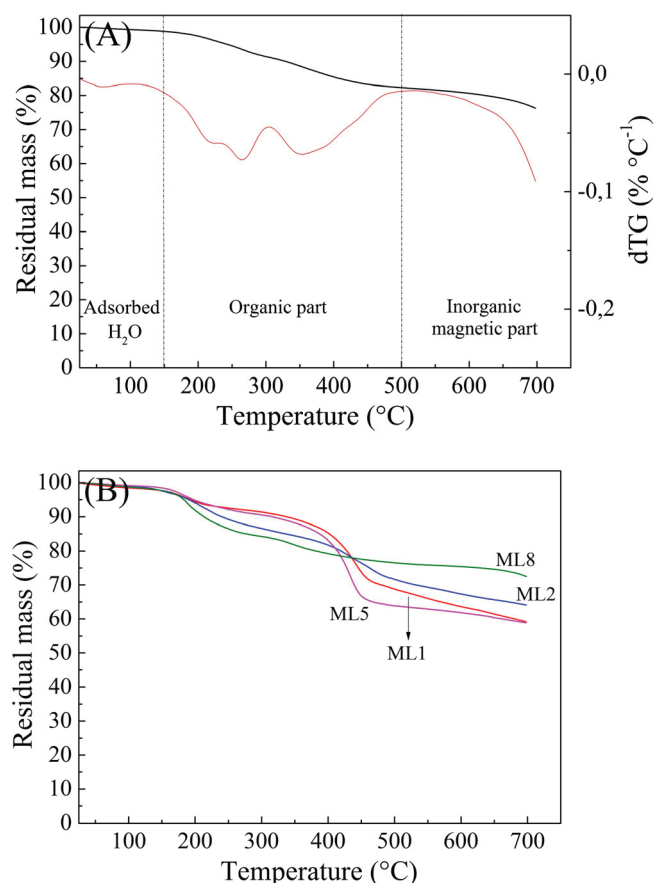


Figure 3. Thermogravimetric curves of samples analyzed in dried state. (A) TGA/dTG of magnetic emulsion seed and (B) TGA of magnetic latexes ML1 (Janus), ML2 (Janus moon-like), ML5 (perfect core-shell), and ML8 (surface polystyrene aggregated). Derivative thermogravimetric, dTG. This figure is available in colour online at wileyonlinelibrary.com/journal/pat

was no increase in weight resulting from oxidation of Fe_3O_4 to Fe_2O_3 , because TGA experiment was carried out under nitrogen atmosphere.^[39,40] The polymer content was calculated by the difference between weights of organic and inorganic part taking into account the amount of organic surfactants (OS). In this work, it is important to mention that OS corresponds to 16.6% of iron oxide content as shown in Fig. 3A (organic part).

As a result, it can be deduced from this study that both polymerization conversions (30–70%) and iron content (50–83%) were not directly correlated to St/DVB ratio. However, St/DVB ratio seems to have a significant role in the particles morphology. Moreover, it was observed that all the synthesized MLs particles ML1 (Janus), ML2 (moon-like Janus), and ML5 (perfect core-shell) are submicron in diameter, because the average particle size is in between 257 nm and 300 nm with near narrow size distribution (Fig. S1, Supporting Information). It can be clearly seen at Table 2 that after polymerization, the particle size of all the synthesized magnetic latex particles with respect to magnetic seed (237 nm) increased irrespective of morphologies. The increase in particle size is attributed to the formation of organic polymer shell upon polymerization of monomers. In addition, the measured sizes and size distribution show that the obtained dispersions are not under aggregated state after polymerization process.

Comparing the size of seed magnetic emulsion with the prepared MLs (ML1 to ML8), it could be observed that the final

Table 2. Percentage of polymer and iron oxide content in the magnetic latexes obtained at different styrene/divinylbenzene ratios

Sample name	Iron oxide content (wt%) ^a	Polymer content (wt%) ^a	Monomers conversion (%) ^b	Particle size (nm)
MES	82.3	—	—	237
ML1	68.8	15.3	35	270
ML2	71.7	11.2	46	295
ML3	63.8	21.6	41	272
ML4	52.7	35.4	44	339
ML5	63.9	21.8	68	269
ML6	71.9	11.7	24	242
ML7	66.2	18.7	56	247
ML8	76.6	6.0	31	300

^aDetermined by thermo gravimetric analysis.
^bPolymerization conversion was calculated based on gravimetric measurements.

particles size as well as the size distribution are not dramatically affected (because the SN is discarded) by both low polymerization conversions and high polydispersity.

Attenuated total reflectance Fourier transform infrared spectroscopy analysis

Figure 4 shows the ATR-FTIR spectra of MES and the sample ML5 (60% St: 40% DVB) after polymerization. The polymer-containing sample was chosen because of its perfect core-shell morphology, as shown in TEM images. For both MES and ML5 samples a common characteristic peak of Fe-O was observed at 580 cm^{-1} . After polymerization, new characteristic C-H aromatic stretching vibration bands of St and DVB were appeared at $3000\text{--}3030\text{ cm}^{-1}$. In addition, the bands at 763 and 698 cm^{-1} were attributed to out-of-plane C-H bending vibrations of styrene aromatic rings. The same vibration for DVB 1,4-disubstituted aromatic ring was observed at 796 cm^{-1} . This in turn proves the formation of crosslinked polystyrene on the surface of magnetic nanoparticles. Furthermore, in the same spectrum, two characteristic bands at 987 and 840 cm^{-1} were observed ascribing to stretching vibrations of SO_4^- and C-O-S, respectively.^[41–43] The presence of $-\text{SO}_4^-$ on the polymeric nanoparticle surface was attributed to sulfate initiator linked to the crosslinked polystyrene organic shell.

Zeta potential measurement

To study the electrokinetic properties of the prepared magnetic latex dispersions, zeta potential was deduced from the measured electrophoretic mobility as a function of pH at constant ionic strength and temperature. The obtained results are shown in Fig. 5.

In order to point out the surface modification after encapsulation of magnetic seed, the zeta potential of all prepared ML particles (ML1 to ML5) was examined as a function of pH and in 1 mM NaCl solution. As can be clearly seen from Fig. 5, magnetic emulsion and ML particles possess negative charges in the investigated pH range (from pH 3 to pH 11). Zeta potential values of the seed MES particles are almost unchanged irrespective of

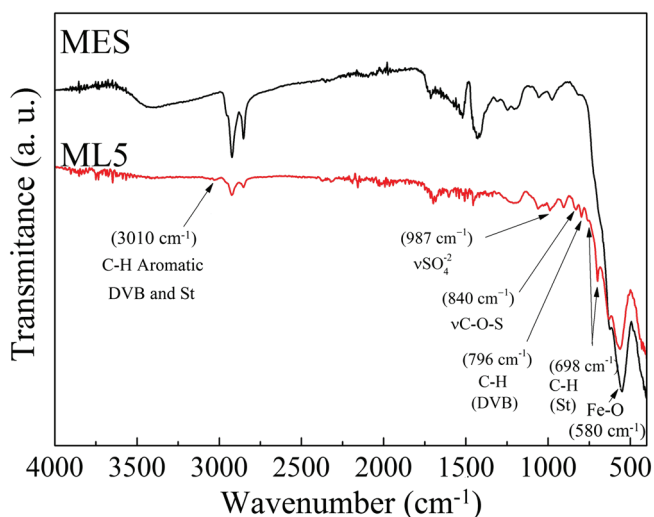


Figure 4. Attenuated total reflectance-Fourier transform infrared spectra of magnetic seed and sample ML5 (after polymerization) in the spectral range of 2000 cm^{-1} to 800 cm^{-1} . DVB, divinylbenzene; St, styrene. This figure is available in colour online at wileyonlinelibrary.com/journal/pat

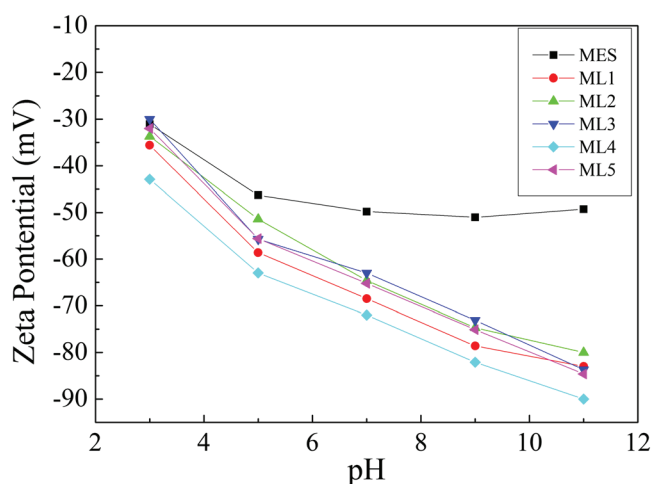


Figure 5. Zeta potential of magnetic emulsion seed (MES) and prepared magnetic latex particles (ML1–ML5). This figure is available in colour online at wileyonlinelibrary.com/journal/pat

pH of the aqueous medium. This behavior can be attributed to the presence of the strong acid sulfate groups ($-\text{SO}_4^-$) emanating from SDS of the stabilizing agent of the magnetic emulsion. On the other hand, zeta potential values of the magnetic latex particles were significantly increased by increasing the pH of the medium due to the possible presence of carboxylic groups originated from oleic acid used in the preparation of organic ferrofluid. The presence of these carboxylic groups is mainly due to the diffusion of oleic acid chain during the swelling process and polymerization step. As a conclusion, this indicates that both magnetic emulsion and all prepared ML particles (ML1 to ML5) possess good colloidal stability over the pH range studied.

Magnetization study

The saturation magnetization (M_s , emu g^{-1}) and magnetic behavior of the dried magnetic polymer latexes were investigated

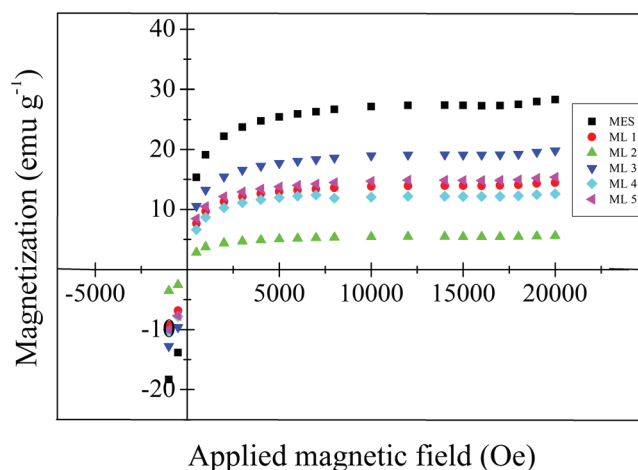


Figure 6. Magnetization curves of the magnetic emulsion (MES) and magnetic latexes ML1, ML2, ML3, ML4, and ML5. This figure is available in colour online at wileyonlinelibrary.com/journal/pat

using a vibrating sample magnetometer. This study was carried out on the automatic bench of magnetic measurements using all dried particles by decreasing the magnetic field (H) strength from $+20,000$ to $-20,000$ oersted at room temperature. Magnetic properties (saturation magnetization and magnetic behavior) of the prepared latex particles mainly depend on amount of inorganic magnetic material in the final particles which control their physical separation in a magnetic field. Therefore, proper control of the magnetic properties before and after polymer encapsulation is of great importance.

Figure 6 shows the magnetization curves for seed MES before and after polymerization (ML1 to ML 5). From this figure, it is clearly obvious that saturation magnetization (M_s) of the seed magnetic emulsion (28.3 emu g^{-1}) decreased to 15.4 emu g^{-1} after polymerization in the case of perfect core shell (ML 5). The other magnetic latex samples (ML1, ML2, ML3, and ML4) also showed similar behavior; their M_s values decreased, respectively, to be 14.5 emu g^{-1} , 5.6 emu g^{-1} , 19.8 emu g^{-1} , and 12.6 emu g^{-1} . The decrease in saturation magnetization after polymerization is attributed to the increase of organic material and consequently the decrease of magnetic content in the prepared latex particles. Importantly, at zero magnetic field ($H=0$), there is no marked residual magnetization revealing negligible remanence of all prepared magnetic particles. So this interesting result indicates that all of the magnetic particles before and after polymerization are superparamagnetic in nature.^[6] The conserved superparamagnetism after polymerization indicates that the polymerization conditions had no effect on the intrinsic magnetic properties of the iron oxide nanoparticles in the used oil in water magnetic emulsion.

CONCLUSION

In order to prepare submicron ML particles bearing high magnetic properties, oil in water magnetic emulsion was first prepared. Characterization of the resulting magnetic dispersion was performed by examining size, size distribution, chemical composition, colloidal stability and magnetic properties. Then the oil in water magnetic emulsion was used as seed of radical

emulsion polymerization of St, cross-linker DVB in the presence of KPS as initiator.

After performing various polymerizations as a function of St/DVB ratio, three types of morphologies were observed; Janus, moon-like Janus and the desired perfect core-shell magnetic latex particles. Core-shell morphology of the magnetic latex nanoparticles is the most favorable for *in vitro* biomedical diagnostic field. In fact, such well-prepared magnetic core-polymer shell prevents the release of ferric, ferrous, and magnetic pigment in the dispersion medium, which is not suitable in any molecular biology based process.

Anyway, the prepared MLs were characterized using various techniques such as TEM for morphology analysis, light scattering for particle size, TGA for chemical composition, magnetization for magnetic property, and zeta potential measurements as a function of pH for possible surface charge modification and surface charge density. Interestingly, two marked morphologies were obtained: (i) Janus-like morphology obtained when 10% of St (90% DVB) was used and (ii) perfect core-shell ML particles was obtained using 60%/40 St/DVB with negligible secondary nucleation. In addition, the obtained core-shell magnetic particles contain a large amount of superparamagnetic iron oxide (approximately 63.9%), which is highly favorable in fast magnetic separation applications. Moreover, such particles after functionalization step are expected to be used as a solid support in microsystems, microfluidic, and lab-on-a-chip in which submicron size and fast magnetic separation are necessary.

Acknowledgements

T.J. is grateful to the University of Lahore, Lahore, Pakistan for funding this project. E.T.T.N. is grateful to the Science Without Borders Program, CNPq, Brazil, for "Sandwich" Ph.D. fellowship.

REFERENCES

- [1] A. Ahsan, A. Aziz, M. A. Arshad, O. Ali, M. Nauman, N. M. Ahmad, A. Elaissari, *J. Colloid Sci. Biotechnol.* **2013**, *2*, 19.
- [2] V. I. Furdul, D. J. Harrison, *Lab Chip* **2004**, *4*, 614.
- [3] M. M. Rahman, A. Elaissari, *J. Colloid Sci. Biotechnol.* **2012**, *1*, 3.
- [4] A. Elaissari, H. Fessi, *Braz. J. Phys.* **2009**, *39*, 146.
- [5] A. Elaissari, H. Fessi, *Macromol. Symp.* **2010**, *288*, 115.
- [6] F. Montagne, O. Mondain-Monval, C. Pichot, A. Elaissari, *J. Polym. Sci. Pol. Chem.* **2006**, *44*, 2642.
- [7] M. Hood, M. Mari, R. Muñoz-Espí, *Materials.* **2014**, *7*, 4057.
- [8] R. Tian, X. Chen, X. Xu, C. Yao, *Anal. Biochem.* **2014**, *463*, 45.
- [9] M. M. Rahman, H. Ahmad, M. M. Islam, *J. Colloid Sci. Biotechnol.* **2013**, *2*, 171.
- [10] J. Thevenot, H. Oliveira, O. Sandre, S. Lecommandoux, *Chem. Soc. Rev.* **2013**, *42*, 7099.
- [11] Y. J. Cui, X. Chen, Y. F. Li, X. Liu, L. Lei, Y. K. Zhang, J. Y. Qian, *Appl. Biochem. Biotech.* **2014**, *172*, 701.
- [12] W. W. Wang, M. J. Liu, J. W. Gu, Q. Y. Zhang, J. W. Mays, *J. Polym. Res.* **2014**, *21*.
- [13] H. X. Liu, C. Y. Wang, Q. X. Gao, X. X. Liu, Z. Tong, *Acta Biomater.* **2010**, *6*, 275.
- [14] S. Chakraborty, K. Jahnichen, H. Komber, A. A. Basfar, B. Voit, *Macromolecules* **2014**, *47*, 4186.
- [15] D. Horak, M. Trchova, M. J. Benes, M. Veverka, E. Pollert, *Polymer* **2010**, *51*, 3116.
- [16] R. A. Ramli, W. A. Laftah, S. Hashim, *RSC Advances.* **2013**, *3*, 15543.
- [17] A. P. Romio, H. H. Rodrigues, A. Peres, A. D. Viegas, E. Kobitskaya, U. Ziener, K. Landfester, C. Sayer, P. H. H. Araujo, *J. Appl. Polym. Sci.* **2013**, *129*, 1426.
- [18] S. F. Medeiros, A. M. Santos, H. Fessi, A. Elaissari, *J. Colloid Sci. Biotechnol.* **2012**, *1*, 99.
- [19] J. Ugelstad, Ø. Olsvik, R. Schmid, A. Berge, S. Funderud, K. Nustad, in *Molecular Interactions in Bioseparations* (Ed.: T. Ngo), Springer, US, **1993**, pp. 229.
- [20] M. M. Rahman, M. M. Chehimi, A. Elaissari, *J. Colloid Sci. Biotechnol.* **2014**, *3*, 46.
- [21] L. Q. Xie, S. H. Ma, Q. Yang, F. Lan, Y. Wu, Z. W. Gu, *RSC Advances.* **2014**, *4*, 1055.
- [22] A. Arkhis, A. Elaissari, T. Delair, B. Verrier, B. Mandrand, *J. Biomed. Nanotechnol.* **2010**, *6*, 28.
- [23] R. X. Gao, X. R. Mu, J. J. Zhang, Y. H. Tang, *J. Mater. Chem. B.* **2014**, *2*, 783.
- [24] N. Naseer, H. Fatima, A. Asghar, N. Fatima, N. Ahmed, A. U. Khan, N. M. Ahmad, *J. Colloid Sci. Biotechnol.* **2014**, *3*, 19.
- [25] M. M. Eissa, M. M. Rahman, N. Zine, N. Jaffrezic, A. Errachid, H. Fessi, A. Elaissari, *Acta Biomater.* **2013**, *9*, 5573.
- [26] K. S. Kumar, V. B. Kumar, P. Paik, *J. Nanopart.* **2013**, *2013*, 24.
- [27] M. Lattuada, T. A. Hatton, *Nano Today.* **2011**, *6*, 286.
- [28] A. Walther, A. H. E. Müller, *Chem. Rev.* **2013**, *113*, 5194.
- [29] A. Walther, M. Hoffmann, A. H. E. Müller, *Angew. Chem. Int. Edit.* **2008**, *47*, 711.
- [30] M. Yoshida, K.-H. Roh, S. Mandal, S. Bhaskar, D. Lim, H. Nandivada, X. Deng, J. Lahann, *Adv. Mater.* **2009**, *21*, 4920.
- [31] A. Synytska, R. Khanum, L. Ionov, C. Cherif, C. Bellmann, *ACS Appl. Mater. Interfaces* **2011**, *3*, 1216.
- [32] S. Xu, W.-F. Ma, L.-J. You, J.-M. Li, J. Guo, J. J. Hu, C.-C. Wang, *Langmuir* **2012**, *28*, 3271.
- [33] S. Braconnot, M. M. Eissa, A. Elaissari, *Colloid Polym. Sci.* **2013**, *291*, 193.
- [34] F. Montagne, S. Braconnot, O. Mondain-Monval, C. Pichot, A. Elaissari, *J. Disper. Sci. Technol.* **2003**, *24*, 821.
- [35] F. Montagne, O. Mondain-Monval, C. Pichot, H. Mozzanega, A. Elaissari, *J. Magn. Magn. Mater.* **2002**, *250*, 302.
- [36] Y.-C. Chang, D.-H. Chen, *J. Colloid Interf. Sci.* **2005**, *283*, 446.
- [37] H. Mouaziz, S. Braconnot, F. Ginot, A. Elaissari, *Colloid Polym. Sci.* **2009**, *287*, 287.
- [38] M. M. Rahman, F. Montagne, H. Fessi, A. Elaissari, *Soft Matter.* **2011**, *7*, 1483.
- [39] G. A. El-Mahdy, A. M. Atta, H. A. Al-Lohedan, *Molecules* **2014**, *19*, 1713.
- [40] S. Lu, J. Ramos, J. Forcada, *Langmuir* **2007**, *23*, 12893.
- [41] M. Machida, K. Kawamura, T. Kawano, D. Zhang, K. Ikeue, *J. Mater. Chem.* **2006**, *16*, 3084.
- [42] W. Grochala, M. K. Cyranski, M. Derzi, T. Michalowski, P. J. Malinowski, Z. Mazej, D. Kurzydowski, W. Kozminski, A. Budzianowski, P. J. Leszczynski, *Dalton T.* **2012**, *41*, 2034.
- [43] L. Li, R. Z. Ma, N. Iyi, Y. Ebina, K. Takada, T. Sasaki, *Chem. Commun.* **2006**, 3125.

SUPPORTING INFORMATION

Supporting information may be found in the online version of this paper.

III.2

Elaboration of Carboxylic magnetic Latex Particles and effect of Methacrylic Acid on prepared latex particles

Summary

Core-shell morphology of the colloidal magnetic nanoparticles is the most favorable for biomedical diagnostic field. In this regard, the current research aims to optimize magnetic latex particles with magnetic core and polymer shell containing carboxylic, starting from a magnetic emulsion which is used as a seed in the emulsion polymerization of styrene (St) with divinylbenzene (DVB). The prepared magnetic particles with carboxylic groups (-COOH) were first characterized using various techniques like , magnetic properties, TEM, TGA, and zeta potential measurements as a function of pH of the dispersion media and then by using this as second seed, for influence of methacrylate acid with different volumes on this prepared latex particles in order to enhance carboxylic groups.

Submicron ML particles bearing high magnetic properties, oil in water magnetic emulsion was first prepared. Characterization of the resulting magnetic dispersion was performed by examining size, size distribution, chemical composition, colloidal stability and magnetic properties. Then the oil in water magnetic emulsion was used as seed of radical emulsion polymerization of St, cross-linker DVB in the presence of ACPA as an initiator. After preparation of magnetic latex particles, the prepared MLs were characterized using various techniques such as TEM for morphology analysis, light scattering for particle size, TGA for chemical composition, magnetization for magnetic property, and zeta potential measurements as a function of pH for possible surface charge modification and surface charge density. Then this magnetic latex was used as second seed for influence of MAA on the prepared latex.

The polymerization was carried out in specially designed 60 ml glass reactor. Temperature was maintained at 70 °C. The home-made magnetic emulsion stabilized by aqueous solution of SDS was introduced in the reactor. Magnetic emulsion was mixed with nitrogen for 1 hour at 300 rpm for removal of oxygen. Subsequently, total amount of monomers at different St/DVB (60%:40% respectively) ratios were introduced at once in the reactor and was mixed at 300 rpm for 60 min followed by addition of 2 weight % of ACPA into the medium. The radical polymerization was carried out at 300 rpm for 18 hours. Finally, the polymerization was terminated by cooling the reactor to room temperature.

In order to evaluate the influence MAA on prepared magnetic latex particles various polymerizations were performed by keeping same Styrene (St) volume constant in all experiments were used with different volumes of MAA respectively by keeping 2wt. % of an initiator ACPA constant in all experiments. Polymerizations were conducted using ACPA as an initiator, SDS as surfactant, and the magnetic emulsion as seed. The used magnetic emulsion contains a negligible amount of octane, which was found to be below 10mg of octane/g of dried emulsion

It was clear from TEM and particle size that there is gradually increase in polymer shell and in size especially, when used high volume of MAA. The prepare magnetic latex particles with carboxylic groups exhibit 58% iron oxide wt .content. Zeta potential measurements clearly indicated the enhancement of polymer shell while using high volume of MAA.

Moreover, such particles after functionalization step are expected to be used as a solid support in biosensors.

Elaboration of Carboxylic magnetic Latex Particles and effect of Methacrylic Acid on prepared latex particles

Talha Jamshaid¹, Mohamed M. Eissa^{1,2}, Quentin Lelong¹, Geraldine Augsti¹, Nadia Zine³,
Abdelhamid Errachid El-Salhi³,
Abdelhamid Elaissari^{1*}

¹University of Lyon, F-69622, Lyon, France; University Lyon-1, Villeurbanne; CNRS, UMR-5007, LAGEP- CPE; 43 bd 11 Novembre 1918, F-69622 Villeurbanne, France.

² Polymers and Pigments Department, National Research Centre, 33 El Bohouth st. (former El Tahrir st.), Dokki, Giza 12622, Egypt.

³ Institut des Sciences Analytiques (ISA), Université Lyon, Université Claude Bernard Lyon-1, UMR-5180, 5 rue de la Doua, F-69100, Villeurbanne, France.

Corresponding author : elaissari@lagep.univ-lyon1.fr

Abstract:

Great attention has been paid to colloidal magnetic nanoparticles (MNPs) due their superparamagnetic properties emanating from their nano-size. They have been found promising applications in various industrial and particularly biomedical diagnostic domains (e.g. fast separation, purification and detection of biomolecules). The structure and morphology of these MNPs play a significant role for their final use. Core-shell morphology of the colloidal magnetic nanoparticles is the most favorable for biomedical diagnostic field. In this regard, the current research aims to optimize magnetic latex particles with magnetic core and polymer shell containing carboxylic, starting from a magnetic emulsion which is used as a seed in the emulsion polymerization of styrene (St) with divinylbenzene (DVB). The prepared magnetic particles with carboxylic groups (-COOH) were first characterized using various techniques like , magnetic properties, TEM, TGA, and zeta potential measurements as a function of pH of the dispersion media and then by using this as second seed, for influence of methacrylate acid with different volumes on this prepared latex particles in order to enhance carboxylic groups.

Keywords:

Magnetic emulsion, Seed emulsion polymerization, Magnetic latex particles, Functionalization.

INTRODUCTION:

Colloidal particles¹ are used as solid support in field of biomedical applications which include immunoassay, cell sorting, and nucleic acid capturing and detection². However such applications require different tedious and time consuming separation processes, mainly two kinds of separation processes are used i.e. a) filtration and b) centrifugation .These processes lead to limit automation of biomedical diagnosis resulting in loss of time and delay in diagnosis³. However, magnetic latexes particles are overcome these methods and improve the process of automation ,also decreasing time delay and providing fast particle separation upon applying even low magnetic field. Magnetic latex is a hybrid material consisting of polymer-encapsulated magnetic particles. Purpose for the preparing of magnetic composite and latexes in biomedical area is to safe inorganic part and to produce reactive chemical functionality which is capable of immobilizing biomolecules through chemical reactions^{1,4}. It is important to mention here that target in the preparation of magnetic latexes is the elaboration of superparamagnetic magnetic latex particles with reasonable amount of iron

oxide, submicron in size and with better size distribution⁵. These prepared functional, submicron, and highly ML particles have been used for nucleic acid extraction and purification⁶, molecular imaging⁷, and specific antibody detection⁸.

Different approaches have been reported for the preparation of magnetic latex particles for diagnostic applications. These approaches are based on classical polymerization in dispersed media like emulsion^{9,10}, suspension¹¹, miniemulsion^{12,13}, dispersion¹⁴, combination of various polymer-based process¹⁵ and inverse emulsion^{16,17}. The pioneer work were reported by Ugelstad⁹ by reporting not only the preparation of magnetic latexes but also their use in biomedical diagnosis. Recently, new process has been reported by Montage et al¹⁸ the process is called seed emulsion polymerization and this process leads to highly magnetic submicron magnetic latex particles

The aim of this paper is to prepare submicron core-shell like magnetic latex particles with carboxylic groups by following same procedure as mentioned in our previous work¹⁹ with functionality group like carboxyl. Then measure effect of methacrylic acid with different volumes in order to enhance carboxylic group on prepared latex particles by considered this as second seed.

Materials and methods

Materials

Styrene (99%) and DVB 80% were purchased from Sigma–Aldrich and used after washing with with 5% NaOH solution. 4, 4'-azobis cyanopentanoic acid (ACPA) as an initiator along with carboxylic group functionality, Methacrylic acid (MAA) and sodium dodecyl sulfate (SDS) emulsifier were obtained from Sigma-Aldrich were used. Deionized water was used in all experiments. Home-made magnetic¹⁹ emulsion was used according to our previous work.

Methodology

Magnetic latex particles with carboxylic group functionality with same concentration of styrene 60%:divenylbenzene40 % and 4, 4'-azobis cyanopentanoic acid (ACPA) with same methodology¹⁹ were prepared according to our previous mentioned work. General representation of prepared magnetic latex particles are shown in figure 1.

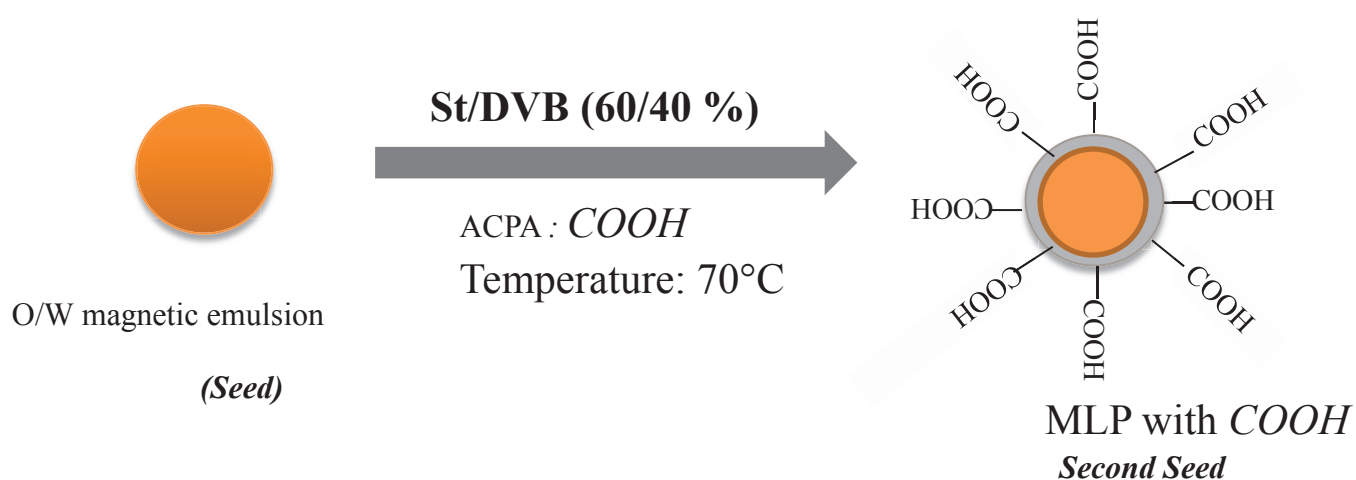


Fig 1: Magnetic latexes particles having carboxylic group.

CHARACTERIZATION

Transmission electron microscopy

Transmission electron microscopy (TEM) images were obtained by a Phillips CM120 microscope (CMEABG, University of Claude Bernard Lyon I, Villeurbanne, France) to investigate the morphology and microstructure of the magnetic polymer latex particles. Briefly, a drop of sample diluted in distilled water was deposited on a carbon-coated copper grid and then left to dry at room temperature overnight before TEM imaging.

Particle size measurements

A Malvern Zetasizer (Nano ZS, Malvern Instruments Limited, UK) was used to measure the average hydrodynamic size (D_h) of the magnetic polymer colloidal particles in 10^{-3} M NaCl solution. The average of at least three measurements (10 runs for each colloidal dispersion) was taken into consideration.

Zeta potential measurement

A Malvern Zetasizer (Nano ZS, Malvern Instruments limited) was used to measure the electrophoretic mobility, which is converted to Smoluchowski's zeta potential. The measurements were performed using highly diluted dispersion of the considered colloidal particles in 10^{-3} M NaCl solution at different pH. The pH was adjusted using NaOH or HCl solutions. Each recorded value was the average of at least three measurements.

Thermal gravimetric analysis

Thermo gravimetric analysis (TGA) measurements were carried out on a thermogravimetry analyzer (NETZSCH, model TG 209 F1). The measurements were performed under inert N₂ atmosphere from ambient temperature up to 700°C at a heating rate of 10°C min⁻¹. All samples were washed with distilled water and then dried at 50°C for 24 hr before analysis.

Fourier transforms infrared analysis

The investigation of surface properties of the obtained sample was performed using attenuated total reflectance-Fourier transform infrared spectrophotometer (Shimadzu, Japan). All samples were cleaned and dried before analysis. The spectra were scanned over range 4000–400 cm⁻¹.

Magnetic properties

The saturation magnetization and magnetic behavior of the dried magnetic polymer latexes were investigated using a vibrating sample magnetometer. Magnetization measurements were carried out at room temperature on the automatic bench of magnetic measurements at CNRS-IRC Lyon.

Results and discussions

Magnetic latex particles with carboxylic group functionality were prepared as mentioned above. Then this magnetic latex was used as second seed for measuring influence of methacrylic acid (MAA).

Particle morphology analysis

The experimental conditions and monomer conversion are reported in Table 1. In order to evaluate the influence MAA on prepared magnetic latex particles (MPSACPA) various polymerizations were performed by keeping same Styrene(St) volume 720 μ L were used with) with different volumes of MAA as 0 μ L,50 μ L,100 μ L,200 μ L and 360 μ L respectively by keeping 2wt.% of an initiator ACPA constant in all experiments. Polymerizations were conducted using ACPA as an initiator, SDS as surfactant, and the magnetic emulsion as seed. The used magnetic emulsion contains a negligible amount of octane, which was found to be below 10mg of octane/g of dried emulsion. In fact, the presence of high octane content in the used emulsion leads to the formation of magnetic hybrid particles with heterogeneous morphology (non-core-shell structure)¹⁹. Figure 2 shows TEM images of (a) magnetic emulsion seed (MES), (b) magnetic latex particles with carboxylic groups (MPSACPA) and MAA with different volumes (c) FM₀ (d) FM₁ (e) FM₂ (f) FM₃ and (g) FM₄.By using higher concentration of St content (i.e., increasing the St/DVB ratio that is 60%:40%DVB), the obtained submicron particles were becoming nearly spherical-like, and the secondary nucleation (SN) was reduced as can be seen in Fig.2b, 2c,2d,2e,2f and 2g images. The high mobility of St Monomer reduces, inside magnetic droplets, phase separation between formed polymer and iron oxide nanoparticles. In addition, polystyrene oligomers (or oligomers rich in styrene) have carboxylic-end groups, which in turn contribute to anchor the polymer chains on the particle surface. This effect is similar to the surfactant property (hydrophobic chain and hydrophilic end group). When St Concentration increases up to 60%¹⁹, perfect-core shell morphology could be obtained as shown in Fig 2b. These magnetic latex particles MPSACPA were then used as second seed for further measuring influence of MAA.

Samples name	Further functionalization with ^d MAA (μ L)	Monomers conversion ^f (%)	Particle Size (nm)
^a MES.....Seed 1	-	-	237
^b MPSACPA.....Seed 2	-	76.3	275
^c [FM ₀]	720 ^e St. + 0 MAA	77.2	358
[FM ₁]	720 St. + 50 MAA	78.6	428
[FM ₂]	720 St. + 100 MAA	79.1	471
[FM ₃]	720 St. + 200 MAA	79.9	480
[FM ₄]	720 St. + 360 MAA	80.40	496

a Magnetic emulsion seed

b Magnetic polystyrene carboxylic particles

c Functional monomer

d Methacrylic Acid

e Styrene

f Polymerization conversion was calculated based on gravimetric measurements .

Table 1. Functionalized with different methacrylic acid to enhance carboxylic group.

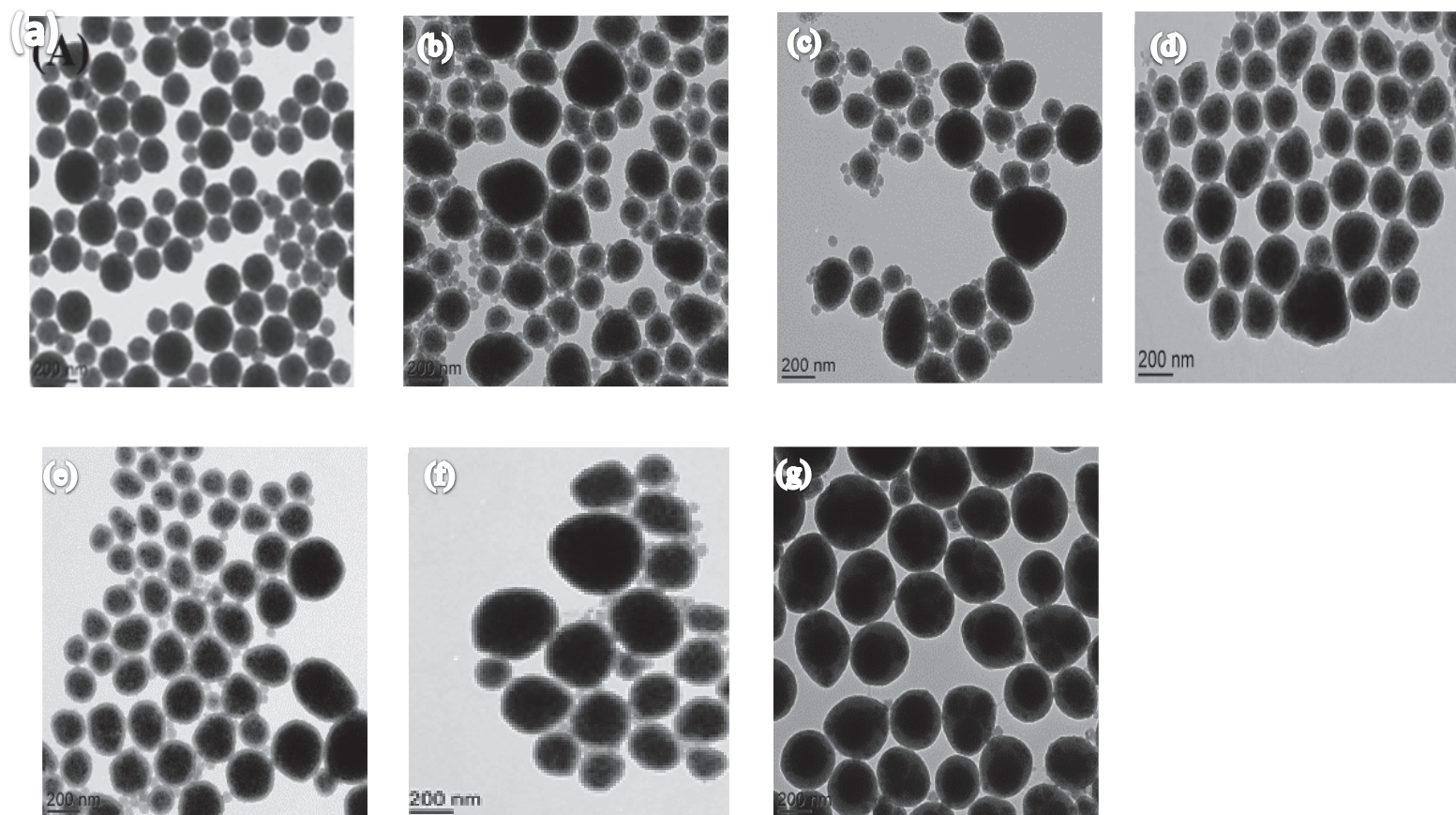


Figure 2. Transmission Electron Microscopy images of samples (a) magnetic emulsion, (b) MPSACPA, (c) [FM₀], (d) [FM₁], (e) [FM₂], (f) [FM₃] and (g) [FM₄]. Scale bar of Images are 200nm.

Chemical composition and size determination

Chemical composition investigated using TGA. Before analysis, all samples (a) MES, (b) MPSACPA and MAA with different volumes (c) FM₀ (d) FM₁ (e) FM₂ (f) FM₃ and (g) FM₄ were separated from the supernatant by applying permanent magnetic field and then washed with deionized water. This procedure was performed three times, in order to remove the non-magnetic material such as surfactant and free polymer particles¹⁹. Figure 3 s hows the thermogram of (a) MES used as seed during polymerization. In this figure, it can be visualized that degradation of magnetic emulsion occurred 150–500°C and above 500°C. Magnetic emulsion MES, reduced weight between 150 to above 500°C mainly assigned to thermal degradation of Oleic acid contained in ferrofluid droplets SDS and oleic acid complexed on magnetic nanoparticles part.

As a general trend, all samples showed higher weight loss than the used seed MES. For magnetic latex (b) MPSACPA and others (c) FM₀, (d) FM₁, (e) FM₂, (f) FM₃ and (g) FM₄ loss occurred in the range of 450°C and tends to almost plateau after 650°C. After degradation of organic part, it was found that remaining content is almost (a) 82.3% in MES. While in (b) 58.42% (c) 57.51% (d) 56.00 % (e) 54.97% (f) 53.45 % and (g) 50.05 % respectively. This degradation in prepared magnetic latex particles is due loss of the organic part (oleic acid and polymer and oleic acid complexed o magnetic nanoparticles).

The magnetic content in the final particles is sufficient to be a very good magnetic sensitive in an external magnetic field and can be separated quickly from the separation medium without difficulties. This is because the produced magnetic polymer particles can be used for

biomedical applications (e.g. antibody, antigen, virus, bacteria, etc). It can be clearly seen at table 1 that after polymerization, the particle size of all the synthesized magnetic latex particles with respect to magnetic seed (237 nm) increased irrespective of morphologies. The increase in particlesize is attributed to the formation of organic polymer shell upon polymerization of monomers. In addition, the measured sizes and size distribution show that the obtained dispersions are not under aggregated state after polymerization process. Average hydrodynamic diameter (D_h) of the particles were measure, at least three readings of each particles were taken. After measuring, it was observed that all the synthesized latexes are submicron in size with almost narrow size distribution as shown in figure 4.

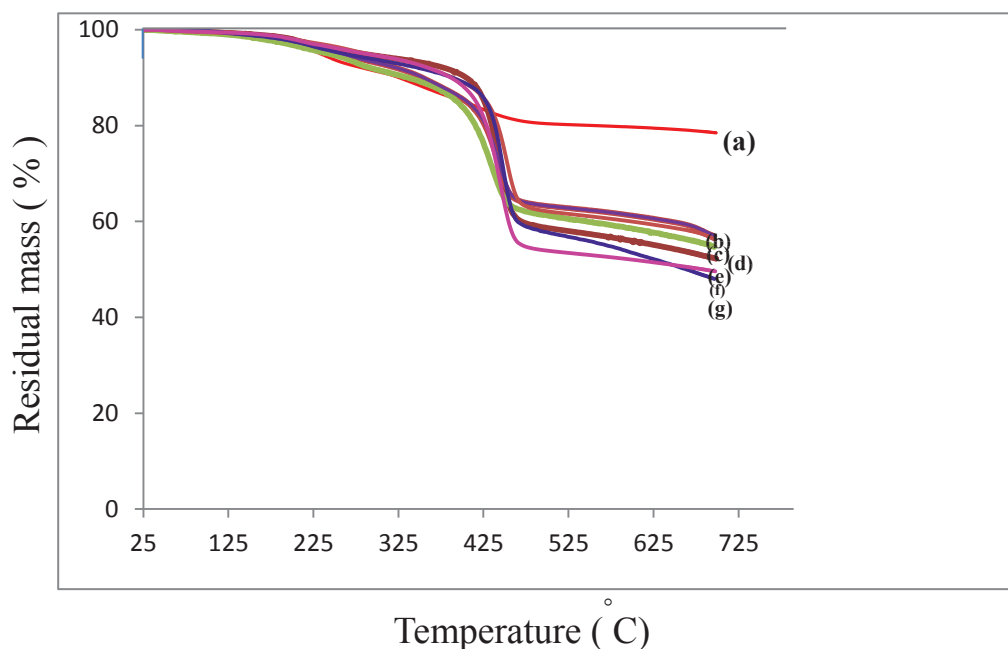


Figure.3 Thermogravimetric curves of samples analyzed in dried state. (a) ■ MES, (b) ■ PSACPA, (c) ■ FM0, (d) ■ FM1, (e) ■ FM2, (f) ■ FM3 and (g) ■ FM4 respectively

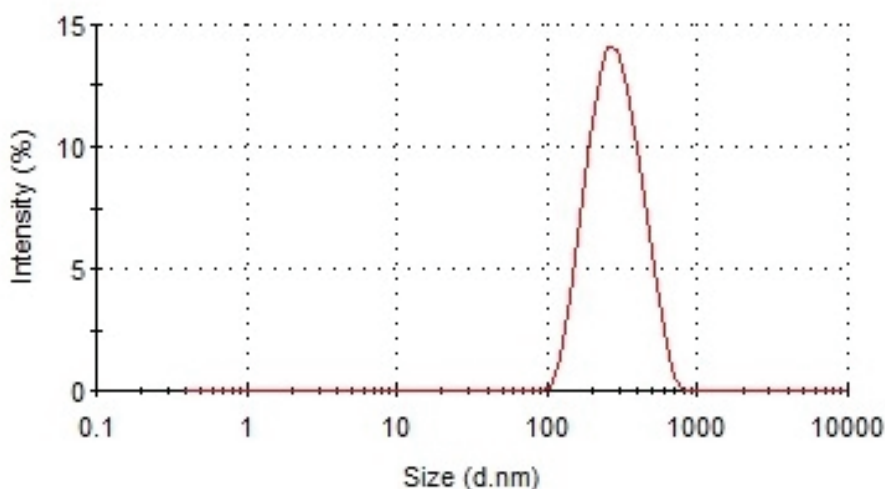


Fig 4. Size distribution of magnetic latex particles MPSACPA and FM₀ FM₁ FM₂ FM₃ and FM₄

Fourier transforms infrared spectroscopy analysis

Figure 5 shows the ATR-FTIR spectra of MES and the second seed MPSACPA (60% St: 40% DVB) after polymerization. The polymer-containing sample was chosen because of its perfect core-shell morphology, as shown in TEM images. For both MES, MPSACPA, FM₀, FM₁, FM₂, FM₃ and FM₄ samples a common characteristic peak of Fe-O was observed at 580 cm⁻¹. After polymerization, new characteristic C-H aromatic stretching vibration bands of St and DVB were appeared at 3000-3030 cm⁻¹. In addition, the bands at 763 and 698 cm⁻¹ was attributed to out of plane C-H bending vibrations of styrene aromatic rings. The same vibration for DVB 1, 4-disubstituted aromatic ring was observed¹⁹ at 796 cm⁻¹. This in turn proves the formation of cross-linked polystyrene on the surface of magnetic nanoparticles. Furthermore, in the same spectrum characteristic bands at 1750 cm⁻¹ were observed ascribing to stretching vibrations of Carboxylic group. The presence of COOH on the polymeric nanoparticle surface was attributed to ACPA initiator linked to the cross-linked polystyrene organic shell.

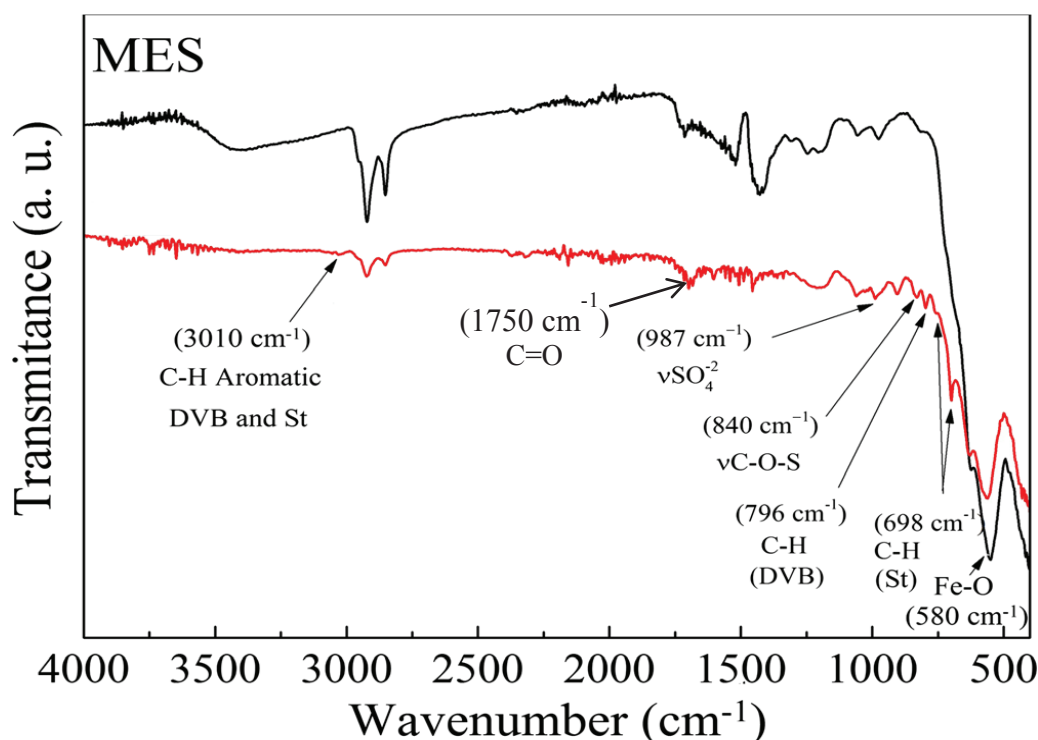


Figure 5. Fourier transforms infrared spectra of MES, MPSACPA, FM₀, FM₁, FM₂, FM₃ and FM₄

Zeta potential measurement

The obtained results of zeta potential of MES, MPSACPA and MAA with different volumes FM₀, FM₁, FM₂, FM₃ and FM₄ are shown in figure 6. In order to point out the surface modification after encapsulation of magnetic seed, the zeta potential of all above prepared ML particles was examined as a function of pH and in 1mM NaCl solution. As can be clearly seen from Fig.6, magnetic emulsion and ML particles possess negative charges in the investigated pH range (from pH 3 to pH 11). Zeta potential values of the seed MES particles are almost

unchanged irrespective of pH of the aqueous medium. This behavior can be attributed to the presence of the strong acid sulfate groups (SO_4^{2-}) emanating from SDS of the stabilizing agent of the magnetic emulsion. On the other hand, zeta potential values of the magnetic latex particles were significantly increased by increasing the pH of the medium due to the possible presence of carboxylic groups originated from oleic acid used in the preparation of organic ferrofluid. The presence of these carboxylic groups is mainly due to the diffusion of oleic acid chain during the swelling process and polymerization step. However zeta potential values of the FM 4 particles were significantly increased by increasing the pH of the medium due to the high amount (360 μL) of MAA used during polymerization.

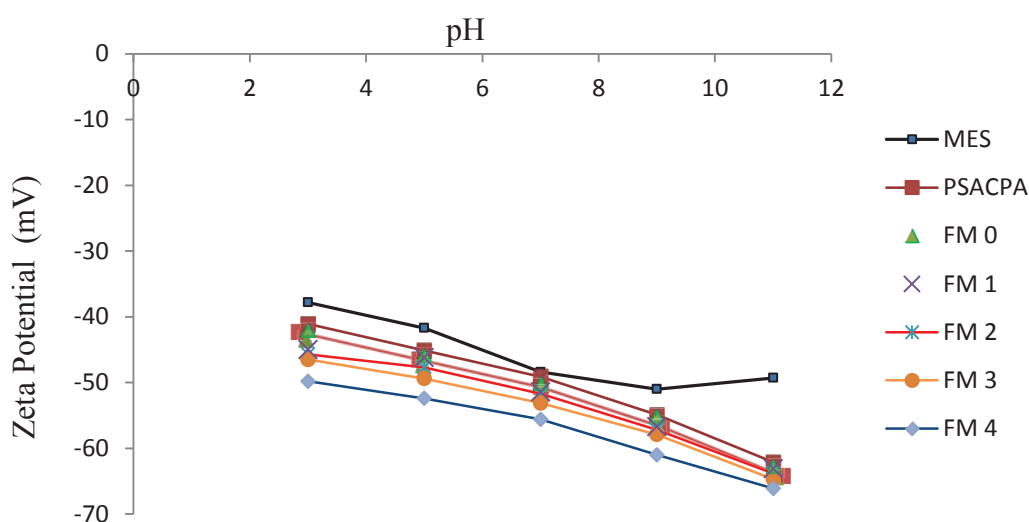


Figure.6. Zeta potential of MES, MPSACPA and MAA with different volumes FM0, FM1, FM2, FM3 and FM4

Magnetization properties

The saturation magnetization (M_s , emu g^{-1}) and magnetic behavior of the dried magnetic polymer latexes were investigated using a vibrating sample magnetometer. This study was carried out on the automatic bench of magnetic measurements using all dried particles by decreasing the magnetic field (H) strength from +20,000 to -20,000 oersted at room temperature. Magnetic properties (saturation magnetization and magnetic behavior) of the prepared latex particles mainly depend on amount of inorganic magnetic material in the final particles which control their physical separation in a magnetic field. Therefore, proper control of the magnetic properties before and after polymer encapsulation is of great importance.

Figure 7 shows the magnetization curves for seed MES before and after polymerization (MPSACPA and MAA with different volumes FM0, FM1, FM2, FM3 and FM4). From this figure, it is clearly obvious that saturation magnetization (M_s) of the seed magnetic emulsion (28.3 emu g^{-1}) show similar behavior; their M_s Values decreased, respectively. The decrease in saturation magnetization after polymerization is attributed to the increase of organic material and consequently the decrease of magnetic content in the prepared latex particles. Importantly, at zero magnetic field ($H = 0$), there is no marked residual magnetization revealing negligible remanence of all prepared magnetic particles. So this interesting result indicates that all of the magnetic particles before and after polymerization are

superparamagnetic in nature¹⁸. The conserved superparamagnetism after polymerization indicates that the polymerization conditions had no effect on the intrinsic magnetic properties of the iron oxide nanoparticles in the used oil in water magnetic emulsion.

Figure 7.

Conclusion

Submicron ML particles bearing high magnetic properties, oil in water magnetic emulsion was first prepared. Characterization of the resulting magnetic dispersion was performed by examining size, size distribution, chemical composition, colloidal stability and magnetic properties. Then the oil in water magnetic emulsion was used as seed of radical emulsion polymerization of St, cross-linker DVB in the presence of ACPA as an initiator. After preparation of MPSACP, the prepared MLs were characterized using various techniques such as TEM for morphology analysis, light scattering for particle size, TGA for chemical composition, magnetization for magnetic property, and zeta potential measurements as a function of pH for possible surface charge modification and surface charge density. Then this magnetic latex was used as second seed for influence of MAA on the prepared latex.

It was clear from TEM and particle size that there is gradually increase in polymer shell and in size especially at when used high volume of MAA. The prepare MPSACPA exhibit 58% iron oxide content. Zeta potential measurements clearly indicated the enhancement of polymer shell while using high volume of MAA.

Moreover, such particles after functionalization step are expected to be used as a solid support in biosensors, microfluidic, and lab-on-a-chip in which submicron size and fast magnetic separation are necessary.

REFERENCES

1. Jada, A. A Special Issue on Inorganic Colloidal Particles, Synthesis, Surface Properties and Applications. *J. Colloid Sci. Biotechnol.* **3**, 1–2 (2014).
2. Rahman, M. M. & Elaissari, A. Multi-Stimuli Responsive Magnetic Core–Shell Particles: Synthesis, Characterization and Specific RNA Recognition. *J. Colloid Sci. Biotechnol.* **1**, 3–15 (2012).
3. Jamshaid, T. *et al.* in *CHAPTER 9: Soft Hybrid Nanoparticles: from Preparation to Biomedical Applications* (2014). at
4. Preparation and Potential Applications of Magnetically Recyclable Biocatalysts. *J. Colloid Sci. Biotechnol.* **2**, 171–179 (2013).
5. Elaïssari, A., Rodrigue, M., Meunier, F. & Herve, C. Hydrophilic magnetic latex for nucleic acid extraction, purification and concentration. *J. Magn. Magn. Mater.* **225**, 127–133 (2001).
6. Rahman, M. M., Chehimi, M. M. & Elaissari, A. Temperature, pH and Diol Tri-Sensing Magnetic Particles for Specific Ribonucleic Acid Recognition. *J. Colloid Sci. Biotechnol.* **3**, 46–57 (2014).
7. Naseer, N. *et al.* Magnetically Responsive Hybrid Polymer Colloids for Ultrasensitive Molecular Imaging. *J. Colloid Sci. Biotechnol.* **3**, 19–29 (2014).
8. Eissa, M. M. *et al.* Reactive magnetic poly(divinylbenzene-co-glycidyl methacrylate) colloidal particles for specific antigen detection using microcontact printing technique. *Acta Biomater.* **9**, 5573–5582 (2013).

9. Yanase, N., Noguchi, H., Asakura, H. & Suzuta, T. Preparation of magnetic latex particles by emulsion polymerization of styrene in the presence of a ferrofluid. *J. Appl. Polym. Sci.* **50**, 765–776 (1993).
10. Hadjira, L., Saïdi-Besbes, S., Elaïssari, A. & Derdour, A. Poly(1,2,3-triazole) Latex Particles: Synthesis and Chelating Properties. *J. Colloid Sci. Biotechnol.* **4**, 64–70 (2015).
11. Daniel, J.-C., Schuppiser, J.-L. & deceased, M. T. Magnetic polymer latex and preparation process. (1982).
12. Ramírez, L. P. & Landfester, K. Magnetic Polystyrene Nanoparticles with a High Magnetite Content Obtained by Miniemulsion Processes. *Macromol. Chem. Phys.* **204**, 22–31 (2003).
13. Moustafa, A. F. Miniemulsion Polymerization of Butadiene: Kinetics Study. *J. Colloid Sci. Biotechnol.* **4**, 14–19 (2015).
14. Ding, X. B., Sun, Z. H., Wan, G. X. & Jiang, Y. Y. Preparation of thermosensitive magnetic particles by dispersion polymerization. *React. Funct. Polym.* **38**, 11–15 (1998).
15. Elaïssari, A. Magnetic Latex Particles in Nanobiotechnologies for Biomedical Diagnostic Applications: State of the Art. *Macromol. Symp.* **281**, 14–19 (2009).
16. Dresco, P. A., Zaitsev, V. S., Gambino, R. J. & Chu, B. Preparation and Properties of Magnetite and Polymer Magnetite Nanoparticles. *Langmuir* **15**, 1945–1951 (1999).
17. Medeiros, S. F., Santos, A. M., Fessi, H. & Elaïssari, A. Thermally-Sensitive and Magnetic Poly(N-Vinylcaprolactam)-Based Nanogels by Inverse Miniemulsion Polymerization. *J. Colloid Sci. Biotechnol.* **1**, 99–112 (2012).
18. Montagne, F., Mondain-Monval, O., Pichot, C. & Elaïssari, A. Highly magnetic latexes from submicrometer oil in water ferrofluid emulsions. *J. Polym. Sci. Part Polym. Chem.* **44**, 2642–2656 (2006).
19. Jamshaid, T. *et al.* Preparation and characterization of submicron hybrid magnetic latex particles. *Polym. Adv. Technol.* **26**, 1102–1108 (2015).

III.3

Development of a novel capacitance electrochemical biosensor based on silicon nitride for Ochratoxin A detection: food analysis

Summary

Ochratoxin A (OTA), is a secondary fungal metabolite produced by various *Aspergillus* and *Penicillium* strains, which was found to be one of the predominant contaminating mycotoxins in a wide variety of food commodities such as cereals, dried fruits, nut, spices, coffee beans. High performance liquid chromatography with fluorescent detection, gas chromatography coupled with mass spectroscopy and enzyme linked immunosorbent assay methods are used for detection of OTA. However these methods lead to some limitations like expensiveness, time –consuming sample preparation steps such as extraction and often analyte derivation in order to enhance sensitivity of detection.

Beside the choose of a good and stable material for biosensor substrates, other spherical nano particles (NPs) have been used as immobilization support in biosensing technology in order to enhance the sensitivity of the biosensors. These NPs are available with a wide variety of surface functional groups and show advantages in the process of immobilization by increasing the surface area, the stability of the surface-bound antibodies, improving orientation of the immobilized antibody as well as achieving faster assay kinetics.

Biosensor is a compact analyte device or unit incorporating a biological or biological derived sensitive element associated with a physicochemical transducer. Nanoparticles have been used as immobilization support in biosensing technology where these particles possesses different functional groups play an important role in immobilization process by increasing surface area. The OTA antigen was detected using Si-p/SiO₂/Si₃N₄ substrate that combined with magnetic latex particles (MLPs) with carboxylic acid groups attached on s urface of particles. For developing sensitive, selective, cost-effective and fast detection of OTA. Mott–Schottky analysis was performed for OTA detection. The biosensor surfaces have been characterized by Contact Angle (CA) measurements, Atomic Force Microscopy (AFM), Scanning Electron Microscopy (SEM), and fluorescence microscopy Microcontact printing (μ CP) was performed to confirm the magnetic latex particles binding onto silicon nitride substrate.

Functionalization of biosensor surface with Self-Assembled Monolayers (SAMs) is most important step for the development of robust and stable biosensors. In recent past, silicon nitride (Si₃N₄) based micro- and nano-fabrication technology has been successfully combined with biochemistry, enabling fabrication of novel biosensing devices with high sensitivity and selectivity. This material offers more advantages when compared to other materials, such as the absence of undesirable impurities and the excellent control of the film composition and thickness. This is especially important for ultra-thin layers used in gate and tunnel dielectrics in the fabrication of biosensor devices with metal-oxide-semiconductor (MOS) technology. The combination of its electronic and mechanical properties makes Si₃N₄ an extremely attractive material for biosensor applications. Thiols group on gold has been explained in past literature based on SAMs on di fferent metals. Though, less work has been devoted to the study of the electronic properties of SAMs deposited on silicon nitride. The surface of this latter is usually modified with organosilanes carrying chemically active groups, to provide a suitable interface between silicon-based transducer and immobilized biomolecules.

Si₃N₄ coated Si substrates were obtained from the Centre Nacional de Microelectrònica (CNM-IMB, CSIC, Spain).

Micro-contact printing (μ CP) technique was used to confirm the MLPs bonding onto silicon nitride surface. An elastomeric stamp based on polydimethylsiloxane (PDMS) was created by replica molding (RM). A mixture of pre-polymer PDMS and curing agent was poured onto a salinized silicon mold which contains micro pillars on relief of its surface. The whole PDMS/silicon-mold degassed to ensure all air bubbles in the PDMS mixture were removed. This avoids the creation of defects on the PDMS stamp surface. The stamp was then brought into immediate and conformal contact with silicon nitride substrate previously activated by piranha. The SAMs of octadecyltrichlorosilane (OTS) were formed on silicon nitride surface which was placed afterward on the oven for 45min in order to enhance OTS adhesion on the surface. Silicon nitride substrate was immersed afterward in ethanol solution containing 1% of (3-Aminopropyl)triethoxysilane (APTES) for 30 min, rinsed with ethanol, dried with a stream of nitrogen and placed again on the oven for 45 min. The APTES silane was bonded onto the remained active silicon nitride surfaces. Finally, the silicon nitride surface was dropped in 500 μ L of MLPs solution mixed with 0.4M EDC and 0.1MNHS for 3hr at 37°C. This allows a covalent bonding of MLPs with amine of APTES.

Afterwards, measured of all characterization parameters it was found a sensitive and selective biosensor based on Si-p/SiO₂/Si₃N₄ structure combined with MLPs for specific detection of OTA. At the end high sensitivity and limitation was found at 0.027 pg/mL and 1.845 pg /mL respectively.



Development of a novel capacitance electrochemical biosensor based on silicon nitride for ochratoxin A detection



Madiha Bougrini^{a,d,e}, Abdoullatif Baraket^a, Talha Jamshaid^b, Abdelhamid El Aissari^b, Joan Bausells^c, Miguel Zabala^c, Nezha El Bari^d, Benachir Bouchikhi^e, Nicole Jaffrezic-Renault^a, Errachid Abdelhamid^{a,*}, Nadia Zine^a

^a Université Claude Bernard Lyon1, UMR 5280, Institut des Sciences Analytiques, 5, rue de la Doua, 69100 Villeurbanne, France

^b Université Claude Bernard Lyon1, LAGEP-CPE, 43 Bd. 11 Nov. 1918, F-69622 Villeurbanne, France

^c Institut de Microelectronica de Barcelona, IMB-CNM (CSIC) Campus UAB, 08193, Bellaterra, Barcelona, Spain

^d Biotechnology Agroalimentary and Biomedical Analysis Group, Department of Biology, Faculty of Sciences, Moulay Ismaïl University, B.P. 11201, Zitoune, 50003 Meknes, Morocco

^e Sensor Electronic & Instrumentation Group, Department of Physics, Faculty of Sciences, Moulay Ismaïl University, B.P. 11201, Zitoune, Meknes, Morocco

ARTICLE INFO

Article history:

Received 9 November 2015

Received in revised form 29 March 2016

Accepted 31 March 2016

Available online 9 April 2016

Keywords:

Capacitive biosensor
Silicon nitride
Magnetic nanoparticles
Mott-Schottky analysis
Ochratoxin A

ABSTRACT

We report in this paper about the development of a novel capacitance electrochemical biosensor based on silicon nitride substrate (Si_3N_4) combined with a new structure of magnetic nanoparticles (MNPs). Si_3N_4 is highly stable as it was fabricated by a combination of several layers of Aluminum (Al), silicon p-doped (Si-p), silicon dioxide (SiO_2) and silicon nitride (Si_3N_4). This structure ($\text{Si}_3\text{N}_4/\text{SiO}_2/\text{Si-p}/\text{Al}$) has provided several advantages compared with other materials commonly used, and in particular in solid-state physics for electronic-based biosensors. The MNPs with terminated carboxylic acid were covalently bonded to Si_3N_4 through a Self-Assembled Monolayers (SAMs) of the silane-amine (3-Aminopropyl) triethoxysilane (APTES). Finally anti-ochratoxin A antibodies were immobilized on MNPs by amide bonding. Contact Angle measurements, Atomic Force Microscopy, Scanning Electron Microscopy and Fluorescence Microscopy characterizations were performed during the biofunctionalization of the biosensor surface. Electrochemical measurements were carried out using Mott-Schottky analysis for ochratoxin A detection. The biosensor was highly sensitive and specific for ochratoxin A antigens, with a limit of detection of 4.57 pM, when compared to other interferences ochratoxin B and aflatoxin G1. The measurements were highly stable and reproducible for detection and interferences. The proposed method is very promising for ochratoxin A detection of several agro-food industry applications.

© 2016 Published by Elsevier B.V.

1. Introduction

Ochratoxin A (OTA), is a secondary fungal metabolite produced by various *Aspergillus* and *Penicillium* strains, which was found to be one of the predominant contaminating mycotoxins in a wide variety of food commodities such as cereals, dried fruits, nut, spices, coffee beans, cocoa, beer, wine, etc [1–3]. In the European Union, some regulatory limits have already been introduced for the levels of OTA in food products such as raw cereal grains (5 $\mu\text{g}/\text{kg}$), dried fruits (10 $\mu\text{g}/\text{kg}$), roasted coffee and coffee products (5 $\mu\text{g}/\text{kg}$), grape juice (2 $\mu\text{g}/\text{kg}$) (EC No. 123/2005) and also

for all types of wines (2 $\mu\text{g}/\text{kg}$) [4]. Currently, the methods commonly used for OTA detection are based on high-performance liquid chromatography (HPLC) with fluorescent detection [5]; the LOD of the proposed method was 0.0025 $\mu\text{g}/\text{L}$. However, HPLC is laborious, time-consuming, and requires sophisticated equipment and qualified personnel. Furthermore, gas chromatography coupled with mass spectrometry (GC-MS) [6] or enzyme-linked immunosorbent assay (ELISA) [7] have also been used for OTA detection and the LOD was around 0.15 ng/mL. Although this technique is used for rapid screening and allows multiple analyses in a short time, it remains limited by using labeled bio reagents which are expensive. To overcome the above limitations, several types of biosensors have aroused the interest of researchers for OTA detection.

In the last years, several optical and electrochemical techniques based on biosensors have been investigated for OTA detection [8–10]. Liu et al. have reported about an ultrasensitive electrochem-

* Corresponding author.

E-mail addresses: abdelhamid.errachid@univ-lyon1.fr, errachid-el-salhi@univ-lyon1.fr (E. Abdelhamid).

ical immunosensor for ochratoxin A using gold colloid-mediated hapten immobilization. The detection limit achieved in this work was 8.2 pg/mL [9]. Biosensors used for this interest in the literature were mainly based on gold or polymer substrate combined with SAMs or cross-linkers for biomolecules immobilization [11]. The functionalization of the biosensor surface with SAMs is the most important step for the development of robust and stable biosensors. Recently, Silicon nitride substrate (Si_3N_4) based micro- and nano-fabrication technology has been successfully combined with biochemistry, enabling the fabrication of novel biosensing devices with high sensitivity and selectivity [12–14]. This material offers more advantages when compared to others, such as the absence of undesirable impurities and the excellent control of the film composition and thickness. This is especially important for ultra-thin layers used in gate and tunnel dielectrics in the fabrication of biosensor devices with metal-oxide-semiconductor (MOS) technology [15]. The combination of its electronic and mechanical properties [13,14,16] makes Si_3N_4 an extremely attractive material for biosensor applications. There is a large work in the literature based on SAMs on different metals [17–20], in particular thiols on gold. However, less work has been devoted to the study of the electronic properties of SAMs deposited on Si_3N_4 . The surface of the latter is usually modified with organosilanes carrying chemically active groups [21,22], to provide a suitable interface between silicon-based transducer and immobilized biomolecules.

Beside the choice of a good and stable material for biosensor substrates, other spherical nano particles (NPs) have been used as immobilization support in biosensing technology in order to enhance the sensitivity of the biosensors [23]. These NPs are available with a wide variety of surface functional groups and show advantages in the process of immobilization by increasing the surface area, the stability of the surface-bound antibodies, improving orientation of the immobilized antibody as well as achieving faster assay kinetics [24–26].

The aim of the present work was to develop a sensitive, selective, cost-effective, and comparatively fast method for quantitative OTA detection. The silicon nitride substrate (Si_3N_4) combined with a new structure of magnetic nanoparticles (MNPs) was used to develop an electrochemical biosensor for OTA detection. Magnetic Nanoparticles (MNP) were composed from a conductive core and carboxylic acid modified shell allowing amid bonding with OTA antibodies. This electrochemical structure using Mott–Schottky analysis was proposed in our knowledge for the first time for OTA detection. In order to control all steps of the biosensing layer, the surface of the biosensor has been characterized by Contact Angle (CA) measurements, Atomic Force Microscopy (AFM), Scanning Electron Microscopy (SEM), and fluorescence microscopy.

2. Experimental

2.1. Chemicals and reagents

Ochratoxin A (OTA), ochratoxin B (OTB), aflatoxin G1 (AFG1), potassium chloride (KCl), hydrogen chloride (HCl), sodium hydroxide (NaOH), sulfuric acid (98%) (H_2SO_4), ethanol (98%), hydrogen peroxide (30%) (H_2O_2), N-hydroxysuccinimide (NHS), 1-ethyl-3-(3-dimethylaminopropyl)-carbodiimide hydrochloride (EDC), (3-Aminopropyl) triethoxysilane (APTES), ethanolamine (ETA), octadecyltrichlorosilane (OTS), styrene (St), divinyl-benzene (DVB), 4,4'-Azobis(4-cyanopentanoic acid) (ACPA) and sodium dodecyl sulfate solution (SDS) were all supplied by Sigma-Aldrich. The monoclonal anti-OTA antibody was purchased from Abcam. Polydimethylsiloxane (PDMS) was purchased from Dow Corning, France. Phosphate buffer saline (PBS) with pH 7.4 was used in Mott–Schottky experiments.

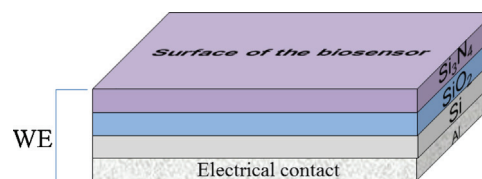


Fig. 1. Schematic illustration of the capacitive biosensor based on $\text{Si}_3\text{N}_4/\text{SiO}_2/\text{Si}/\text{Al}$ substrate.

2.2. Process for Si_3N_4 substrate fabrication

Si_3N_4 coated Si substrates $\langle 100 \rangle$ ($\text{Si-p}/\text{SiO}_2/\text{Si}_3\text{N}_4$) $1.2\text{ cm} \times 1.2\text{ cm}$ in size were obtained from the Centre Nacional de Microelectrònica (CNM-IMB, CSIC, Spain). Silicon wafers were thermally oxidized at 850°C (78 nm thickness) followed by a deposition of a thin layer (100 nm) of Si_3N_4 using low-pressure chemical vapor deposition. The Si-p layer was uniformly doped with boron (dose $1 \times 10^{15}\text{ cm}^{-2}$). An ohmic contact was realized by a deposition of $1\text{ }\mu\text{m}$ of aluminum on the backside of the wafer (Fig. 1).

2.3. Magnetic nanoparticle preparation

Core-shell structure was prepared using a given St/DVB weight ratio (20 wt.% St and 80 wt.% DVB), 2 wt.% ACPA was used as an initiator and solubilized first in 0.1 M NaOH solution. Total amount (1200 μL) of St/DVB respectively was used. The polymerization was carried out in a 60 mL three necked double wall glass reactor made up of glass anchor type stirrer, a reflux condenser and a nitrogen inlet. The temperature was regulated at 70°C by using a thermal bath. The SDS solution was prepared at a concentration below the critical micelle concentration (CMC) 1 gL^{-1} . Magnetic emulsion was finally dispersed in the SDS solution of the boiled and degassed Milli-Q water. First, 50 mL of magnetic emulsion was stabilized with an aqueous solution of anionic surfactant SDS via serum replacement process performing only one time separation/dispersion cycles and introduced in the reactor and purged under nitrogen for 1 h under stirring (300 rpm) for removal of oxygen flux. After that introduced St and DVB at once into reactor for 70 min for swelling of magnetic droplets by monomers, temperature was rapidly increased to 70°C and 2 wt.% ACPA (with respect to the weight of monomer and cross-linker) was added in the monomer swollen magnetic emulsion. The polymerization was run at constant stirring (300 rpm) for 20 h till complete synthesis of magnetic latexes particles which having carboxylic group on surface as shown in Fig. S1 (Supplementary material).

2.4. Contact angles measurements (CAM)

Contact angle measurements were carried out using an Easy drop OCA 20, DataPhysics Instruments (Germany) to characterize silicon nitride substrate after each chemical surface modification. The measurements were analyzed with a droplet of $3\text{ }\mu\text{L}$ of deionized water. Four values of CAM were recorded for each substrate.

2.5. Microcontact printing (μCP)

Micro-contact printing (μCP) technique was used to confirm the MNPs bonding onto modified silicon nitride surface. For this interest, an elastomeric stamp based on PDMS was fabricated by replica molding (RM). Here, a mixture of pre-polymer PDMS and curing agent (10:1 w/w) was poured onto a silanized silicon mold which contains micropillars on relief of its surface (Fig. 2a, b). The whole PDMS/silicon-mold degassed to ensure all air bubbles in the PDMS mixture were removed. This prevents the creation of defects on the

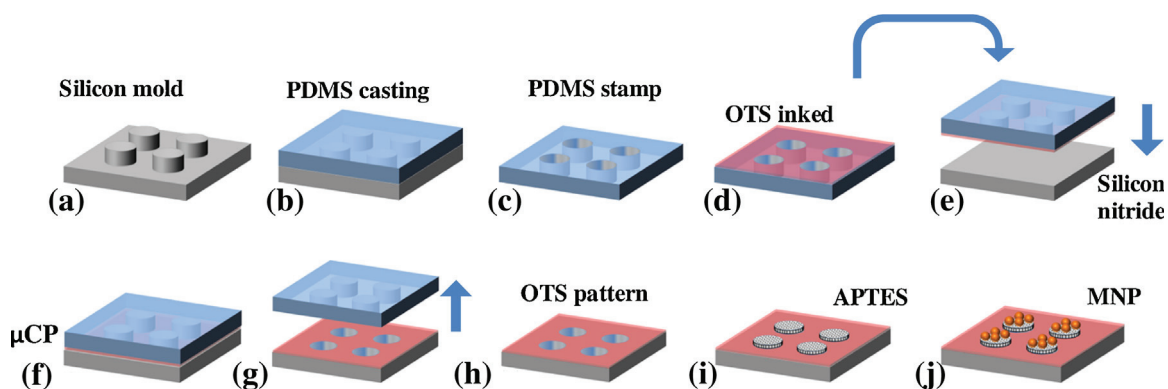


Fig. 2. Micro contact printing (μ CP) process to immobilize MNP onto APTES pattern.

PDMS stamp surface. After polymerization, the PDMS stamp was peeled-off from the silicon mold bearing the microholes on its surface (Fig. 2c). The stamp was then inked by immersion in heptane solution containing OTS ($5 \mu\text{M}$) and carbon tetrachloride (4 mM) for 1 min and dried with stream of nitrogen (Fig. 2d). The stamp was then brought into immediate and conformal contact with silicon nitride substrate previously activated by piranha (Fig. 2e, f). After μ CP, the PDMS stamp was peeled-off from silicon nitride surface (Fig. 2g). Here SAMs of OTS were formed on silicon nitride surface which was placed afterward on the oven for 45 min in order to enhance OTS adhesion on the surface (Fig. 2h). Silicon nitride substrate was immersed afterward in ethanol solution containing 1% of APTES for 30 min, rinsed with ethanol, dried with a stream of nitrogen and placed again on the oven for 45 min. The APTES silane was bonded onto the remaining active silicon nitride surface (Fig. 2i). Finally, the silicon nitride surface was dropped in $500 \mu\text{L}$ of MNPs solution mixed with 0.4 M EDC and 0.1 M NHS for 3 h at 37°C . This allows a covalent bonding of MNPs with amine of APTES (Fig. 2j).

2.6. Fluorescence microscopy

Fluorescence images were taken using a fluorescence microscope (Zeiss Axioplan 2 Imaging apparatus, equipped with $10\times$ and $40\times$ lenses and a monochrome camera). Samples were observed by fluorescent light: OTA sample was excited with a $550 (\pm 25) \text{ nm}$ band-pass filter and fluorescence from the sample was observed with a $605 (\pm 70) \text{ nm}$ band-pass filter.

2.7. Atomic force microscopy (AFM)

Atomic Force Microscopy (AFM) was performed in air under ambient conditions using a Nano observer, CSI Company (France). AFM Nano-Observer has XY scan range $110 \mu\text{m}$ (tolerance $\pm 10\%$), Z range $9 \mu\text{m}$ (tolerance $\pm 10\%$) and XY drive resolution 24 bit control $- 0.06 \text{ \AA}$. Measurements were made using silicon cantilever tip (ScienTec AppNano). The cantilever size L: $125 \mu\text{m}$, W: $35 \mu\text{m}$ and T: $4.5 \mu\text{m}$. The tip radius: $< 10 \text{ nm}$, H: $14\text{--}16 \mu\text{m}$ and with a frequency of $200\text{--}400 \text{ kHz}$ and spring constant of K: $25\text{--}75 \text{ N/m}$. The scanning images were performed at 5 V amplitude, 8 V set point and Tip DC at 477 nV . Measurements were performed in tapping mode with a speed of 0.5 lines per second and 1024 resolution. Samples were analyzed in a $(5 \mu\text{m} \times 5 \mu\text{m})$ area.

2.8. Mott-Schottky analysis

Mott-Schottky analyses were performed in a conventional 1 mL electrochemical Teflon cell containing a three-electrode system (Fig. 3). Measurements were made by a VMP3 potentiostat (Biologic-Science Instrumentation, France). Platinum (Pt) and Calomel

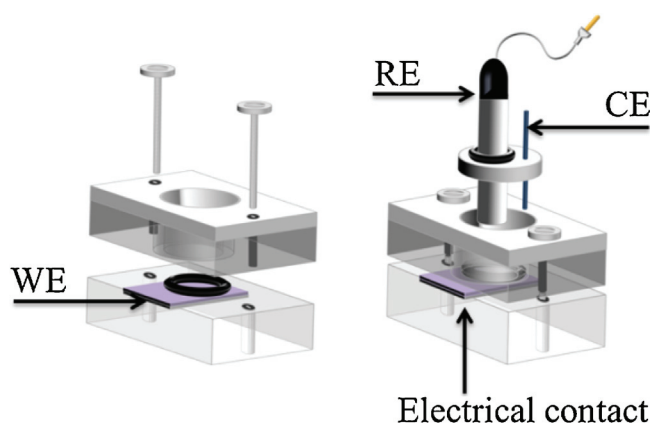


Fig. 3. Teflon electrochemical cell used for electrochemical analysis, with external reference electrode (RE), counter electrode (CE). The working electrode (WE) was sandwiched between the two parts of Teflon cell.

saturated electrode (CSE) were used as counter and reference electrodes, respectively. Silicon nitride electrodes functionalized with monoclonal anti-OTA antibodies acted as working electrodes. The substrate was sandwiched between the two parts of Teflon cell. Electrical contact was realized through the aluminum layer from the back side of the substrate (Fig. 3). Mott-Schottky plots were obtained on the films by sweeping the potential from -1 V/SCE to $+3 \text{ V/SCE}$; at frequency range $2 \text{ kHz}\text{--}70 \text{ kHz}$ and a step rate of 25 mV .

The measurements were carried out in the absence of a redox probe, in PBS at room temperature. The pH was kept constant throughout all the measurements ($\text{pH } 7.4$). All connections were made with coaxial cables to minimize any external electrical noise and the measurements were performed in the dark inside a Faraday cage.

2.9. Antibodies immobilization

Silicon nitride substrates were cleaned by sonication in acetone for 15 min, 3 times and washed with distilled water in order to remove the resin protecting layer. Surface activation of the Si_3N_4 was performed using a Piranha solution ($1:3, \text{ v/v}, \text{ H}_2\text{O}_2:\text{H}_2\text{SO}_4$) for 30 min, and sequential surface chemical treatments in aqueous solutions of NaOH (0.5 M) for 20 min, HCl (0.1 M) for 10 min and a final immersion in NaOH (0.5 M) solution for 10 min [22]. For all these surface chemical treatments, the substrate was floating on the surface and not totally immersed in aqueous solutions. Indeed, silicon nitride was floating and in contact with the solutions leaving the aluminum back side in the air. This procedure was made to protect aluminum layer from all these chemical solutions. After-

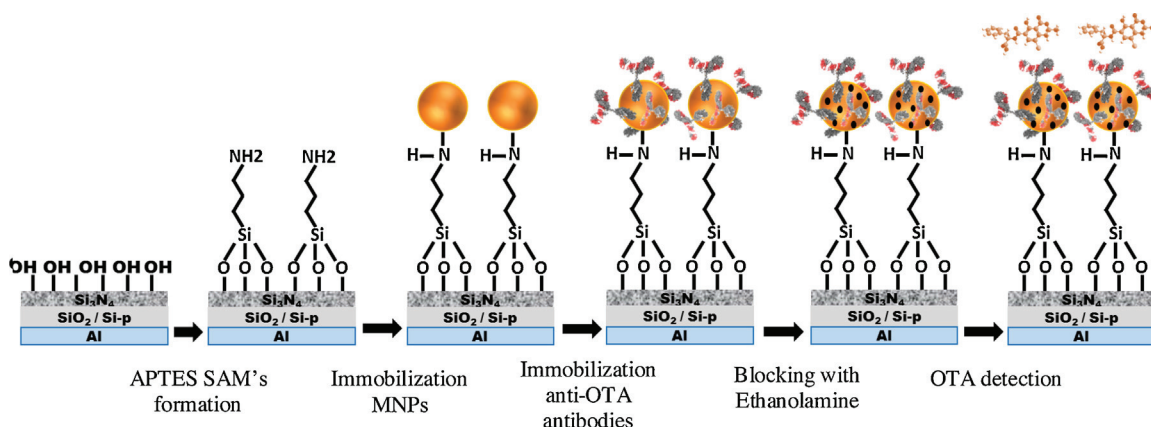


Fig. 4. Schematic representation of the functionalization procedure based on MNPs (●) and anti-OTA antibodies. Ethanol-amine (●) was used after antibodies immobilization to avoid nonspecific adsorption.

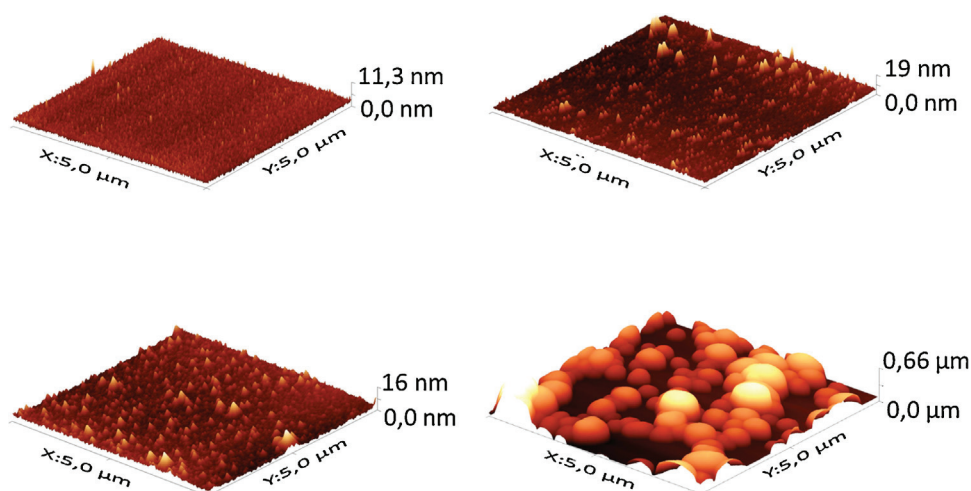


Fig. 5. AFM images of (a) bare (b) Activated, and (c) APTES modified silicon nitride surface. (d) Shows the MNPs distribution onto APTES modified silicon nitride substrate.

Table 1
Contact angle of cleaned substrates, Piranha oxidation, followed by APTES formation on Si_3N_4 .

UV ozone Cleaned Si_3N_4 (60.5°)	After piranha oxidation (8.3°)	After APTES treatment (86.3°)

ward, the samples were then rinsed thoroughly with HCl (0.1 M) and Milli-Q water and dried in an oven at 120°C for 10 min [22].

The Si_3N_4 substrates were functionalized using 1% of APTES in ethanol over night at room temperature. Afterward samples were rinsed with ethanol to remove the unbonded APTES and dried with nitrogen and put in the oven at 100°C for one additional hour. Consequently, SAMs of APTES were formed onto the Si_3N_4 surface with amine terminal groups outward from the surface. These were covalently bonded to carboxylic acid groups of the MNPs which have been previously activated with a mixture of EDC (0.4 M), NHS (0.1 M) and KCl (1 mM) in $500\ \mu\text{L}$ MNPs for 3 h at 37°C [26]. This activation enabled the bonding of amine group of APTES with MNPs. Afterwards the immobilized MNPs were rinsed with HCl (0.1 M) and incubated in anti-OTA solution ($25\ \mu\text{g}/\text{mL}$) for 3 hr at room temperature. The monoclonal anti-OTA antibodies were covalently bonded to MNPs through the acid-amine linkage. The residual activated carboxylic acid groups of MNPs were blocked with 1% of ethanolamine diluted in PBS for 30 min at room temper-

ature. This step is very important to reduce non-specific binding during the detection process. Finally, the biosensor was rinsed with PBS and used for ochratoxin A detection. Fig. 4 depicts the bio-functionalization of the biosensor as detailed in Section 2.

3. Results and discussion

3.1. Contact angle measurements

In order to assess the effectiveness of the functionalization, contact angle measurements were performed on bare Si_3N_4 , before and after activation, and also after its functionalization with APTES. The results in Table 1, demonstrate a slightly hydrophilic nature on bare silicon nitride with a contact angle of 60.5° , which is in agreement with values found in literature [27]. After surface oxidation with Piranha, Si_3N_4 surface becomes highly hydrophilic 8.3° . This was due to the presence of a high amount of hydroxyl groups on the surface. The contact angle has increased again to 86.3° after

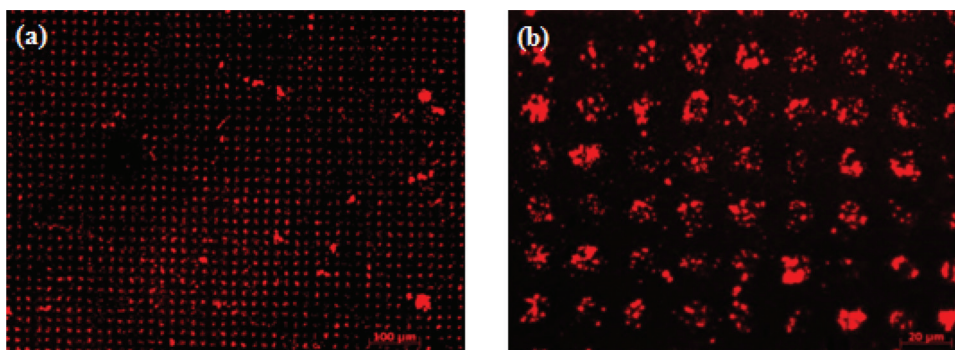


Fig. 6. Fluorescent image of (a) a homogenous pattern of MNP/anti-OTA antibodies after recognition of the corresponding antigen (b) magnification of the positive pattern showing specific detection by the immobilized anti-OTA.

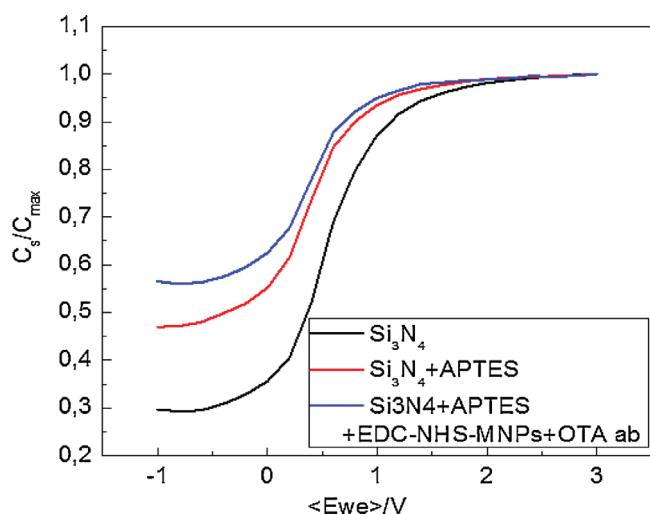


Fig. 7. Mott-Schottky plots of the electrodes: (a) Si_3N_4 , (b) $\text{Si}_3\text{N}_4 + \text{APTES}$, (c) $\text{Si}_3\text{N}_4 + \text{APTES} + \text{EDC-NHS-MNP} + \text{Ab-OTA}$.

the functionalization process with the APTES. This hydrophobic character can be explained by the presence of APTES hydrocarbon chains.

3.2. Atomic force and scanning electron microscopy

Fig. 5 shows the topography of the silicon nitride modified surfaces, observed by AFM compared to bare Si_3N_4 electrode (Fig. 5a). The roughness of the activated Si_3N_4 (0.337 nm) was clearly higher than the bare Si_3N_4 surface (0.152 nm) which confirm the good activation of the surface (Fig. 5b). After the passivation of Si_3N_4 with APTES, the roughness was changed from 0.337 nm to 0.23 nm indicating the good formation of APTES SAMs onto the electrode surface (Fig. 5c). Finally, the AFM image of the MNPs shows good coverage of the surface of the electrode with homogeneous distribution (see Fig. 5d). The MNPs contribute to the high roughness on the modified silicon nitride surface. The layer of MNPs presents a very high textured surface with average depth of $\sim 0.2 \mu\text{m}$ and average roughness of 13.5 nm. This configuration is very important for 3D bio-functionalization (Fig. S2 Supplementary material). This configuration allows the immobilization of a large amount of antibodies which can increase the sensitivity of the biosensor. Fig. S3 in Supplementary material shows a SEM image of MNPs onto silicon substrate and confirms the homogenous distribution of MNPs.

3.3. Fluorescence analysis

Fluorescent imaging is a rapid tool for analyzing bio-layers. This technique is based on the reaction of labeled fluorochrome biomolecules with the corresponding bioreceptor in order to ensure detection or bio-recognition processes. In the present study OTA is on itself fluorescent, and it has an emission maximum at 467 nm in 96% ethanol and 428 nm in absolute ethanol after excitation at 340 nm [28]. The soft-lithographical technique, μCP , facilitates the printing of the required pattern by applying a structured PDMS stamp as mentioned in previous paragraph. Fig. 6 shows fluorescent pattern of OTA. The labeled fluorescent tags formulate positive structures, while the non-fluorescent regions were blocked with OTS. Here well-proportioned positive patterns were shown with perfectly immobilized OTA antigens.

3.4. Mott-Schottky results

Mott-Schottky analyses were performed in order to characterize the semi-conducting behavior of silicon nitride substrate after each step of chemical surface modification (SAMs of APTES and the MNPs/anti-OTA antibodies). Fig. 7 shows the Mott-Schottky plots evolution for bare silicon nitride, APTES modified silicon nitride and after MNPs/anti-OTA antibodies immobilization at the frequency of 70 kHz. This latter has been optimized and chosen as the appropriate frequency, as it gives a better capacitive behavior (Fig. S4 Supplementary material). The capacitance of the substrate (C_s) was normalized by dividing the value of C_s by the maximum value of each curve of $C(V)$ and presented as C_s/C_{max} versus the potential of the working electrode (E_{WE}). Here, the capacitance of the APTES modified silicon nitride has increased when compared to the bare Si_3N_4 due to the formation of new layer onto Si_3N_4 surface. The same behavior of the capacitance increase has been observed after MNPs/anti-OTA antibodies immobilization onto APTES monolayer.

After MNPs/anti-OTA antibodies immobilization, Mott-Schottky analysis has been performed in order to determine blank measurements (Fig. 8a). Then the biosensor was maintained in the electrochemical cell and incubated for 30 min in 1 mL of PBS containing OTA antigens at 4°C . The biosensor was then rinsed with PBS in order to remove any adsorbed proteins and analyzed afterward by Mott-Schottky using 1 mL of PBS as electrolyte. This procedure of the biosensor incubation was made for all OTA concentrations. The detection of OTA antigens at various concentrations is shown in Fig. 8a. Here the C_s/C_{max} shows a shift in the X-direction by increasing OTA concentrations, which confirms a built-in potential difference, equivalent to a flat band voltage variation, and thus an increase in the conduction current value. Based on all these elements, the biosensor sensitivity can be obtained by measuring the potential shift of the flat band of the $C_s = f(V)$ curves.

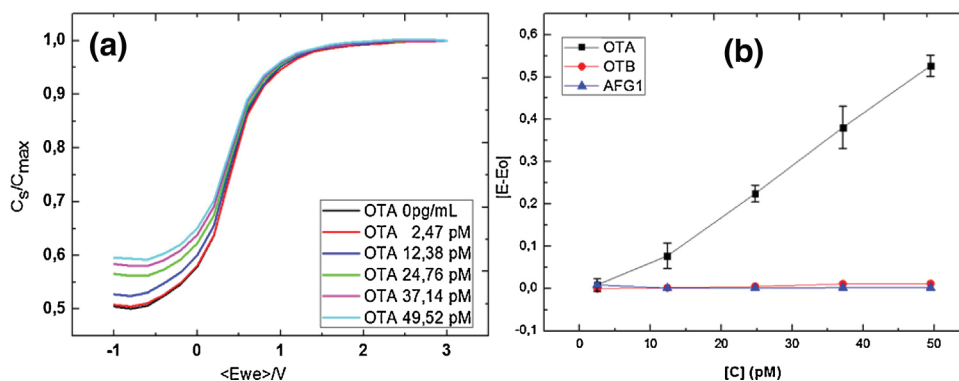


Fig. 8. (a) Mott–Schottky plots for OTA detection using the capacitance biosensor, (b) The Calibration curves of the OTA detection (black curve), and of the two interferences: OTB (red curve) and AFG1 (blue curve). (For interpretation of the references to colour in this figure legend, the reader is referred to the web version of this article.)

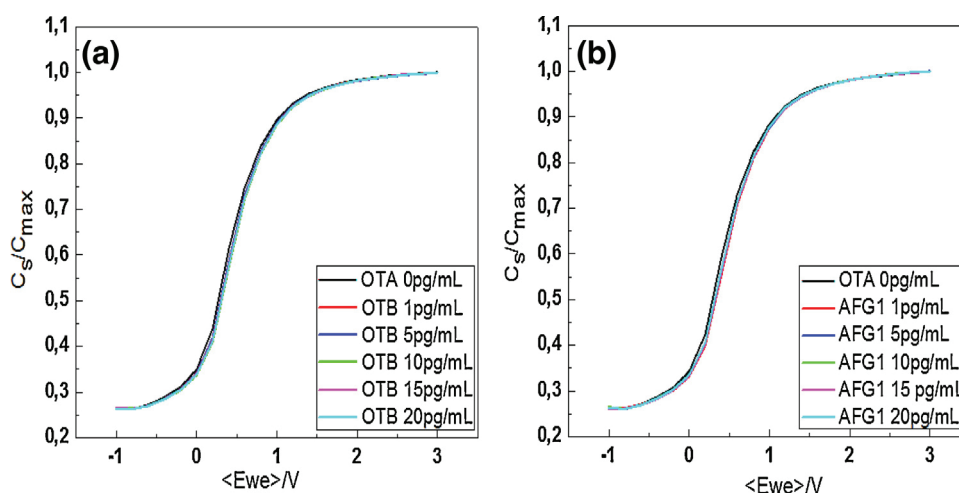


Fig. 9. (a) Mott–Schottky plots for OTB detection and (b) for AFG1 detection using the capacitance biosensor.

Fig. 8b shows the calibration curve of the capacitive biosensor based on silicon nitride in a linear range of 2.47–49.52 pM of OTA. Calibration curve was presented as the absolute value of relative variation of potential $|E-E_0|$ versus concentration of OTA in pM, where E is the potential of different OTA concentrations and E_0 is the potential of the antibodies anti-OTA. The developed biosensor provides a high sensitivity of 0.01 V pM^{-1} , and a good linearity with a correlation coefficient (R^2) of 0.99. The limit of detection of this capacitive biosensor was defined at 4.57 pM.

The specificity of the prepared biosensor was realized using ochratoxin B (OTB) and aflatoxin G1 (AFG1) other compounds with similar structures. Mott–Schottky analyses were carried out, using the same experimental process based on MNPs/anti-OTA antibodies immobilization. The detection of OTB and AFG1 was made in the same linear range of 2.47–49.52 pM. The potential difference of both OTB and AFG1 was negligible when compared to OTA detection Fig. 9. This shows an excellent specificity and sensitivity of the biosensor for OTA antigens (Fig. 8b) and can offer credible results despite the presence of the interfering species.

4. Conclusion

Novel sensitive and selective biosensor based on Si-p/SiO₂/Si₃N₄ structure combined with new magnetic nanoparticles for the specific detection of OTA was developed. Si₃N₄ was chosen for its many attractive physical and chemical properties as well as its stability for long periods. Moreover, making electrochemical analysis using this material provides a stable measurement and rapid response.

Under optimized conditions, the developed biosensor provides a high sensitivity of 0.01 V pM^{-1} , and a limit of detection of 4.57 pM was obtained. The biosensor was highly selective for ochratoxin A antigens, when compared to other interferences ochratoxin B and aflatoxin G1. The proposed method is very promising for OTA detection for several agro-food industry applications. To our knowledge this is the first silicon nitride biosensor reported for the detection of OTA.

Acknowledgments

We acknowledge the funding through the SMARTCANCERSENS project (FP7-PEOPLE-2012-IRSES) under the grant agreement No. 31805, the SEA-on-a-CHIP project (FP7-KBBE) under the reference 614168, the NATO project, SPS (NUKP.SFPP984173) and the HEARTEN under the grant agreement No. 643694.

Appendix A. Supplementary data

Supplementary data associated with this article can be found, in the online version, at <http://dx.doi.org/10.1016/j.snb.2016.03.166>.

References

- [1] A. Jodra, M. Hervás, M. Ángel López, A. Escarpa, Disposable electrochemical magneto immunosensor for simultaneous simplified calibration and determination of Ochatoxin A in coffee samples, *Sens. Actuators B* 221 (2015) 777–783.

- [2] F. Gentile, G.L. La Torre, A.G. Potorti, M. Saitta, M. Alfa, G. Dugo, Organic wine safety: UPLC-FLD determination of Ochratoxin A in Southern Italy wines from organic farming and winemaking, *Food Control* 59 (2016) 20–26.
- [3] F. Dridi, M. Marrakchi, M. Gargouri, A. Garcia-Cruz, S. Dzyadevych, F. Vocanson, J. Saulnier, N. Jaffrezic-Renault, F. Lagarde, Thermolysin entrapped in a gold nanoparticles/polymer composite for direct and sensitive conductometric biosensing of ochratoxin A in olive oil, *Sens. Actuators B* 221 (2015) 480–490.
- [4] European Commission, Commission regulation 472/2002 of 12 March 2002 amending regulation (EC) N. 466/2001 setting maximum levels for certain contaminants in foodstuffs, *Off. J. Eur. Commun. L75* (2002) 18–20.
- [5] J. Mao, S. Lei, X. Yang, D. Xiao, Quantification of ochratoxin A in red wines by conventional HPLC-FLD using a column packed with core-shell particles, *Food Control* 32 (2013) 505–511.
- [6] S. Kirin, B. Skrjanc, N. Kos, B. Kozolc, N. Pirnat, G. Tavcar-Kalcher, Mycotoxins in cereals and cereal products in Slovenia—official control of foods in the years 2008–2012, *Food Control* 50 (2015) 157–165.
- [7] A. Zhang, Y. Ma, L. Feng, Y. Wang, C. He, X. Wang, H. Zhang, Development of a sensitive competitive indirect ELISA method for determination of ochratoxin A levels in cereals originating from Nanjing, China, *Food Control* 22 (2011) 1723–1728.
- [8] B. Prieto-Simon, M. Campàs, J. Marty, T. Noguer, Novel highly-performing immunosensor-based strategy for ochratoxin A detection in wine samples, *Biosens. Bioelectron.* 23 (2008) 995–1002.
- [9] X.P. Liu, Y.J. Deng, X.Y. Jin, L.G. Chen, J.H. Jiang, G.L. Shen, R.Q. Yu, Ultrasensitive electrochemical immunosensor for ochratoxin A using gold colloid-mediated hapten immobilization, *Anal. Biochem.* 389 (2009) 63–68.
- [10] S.H. Alarc on, G. Palleschi, D. Compagnone, M. Pascale, A. Visconti, I. Barna-Vetro, Monoclonal antibody based electrochemical immunosensor for the determination of ochratoxin A in wheat, *Talanta* 69 (2006) 1031–1037.
- [11] M.M. Barsan, M.E. Ghica, C.M.A. Brett, Electrochemical sensors and biosensors based on redox polymer/carbon nanotube modified electrodes: a review, *Anal. Chim. Acta* (2015) (accepted manuscript).
- [12] K. Awsiuk, A. Bernasik, M. Kitsara, A. Budkowski, P. Petrou, S. Kakabakos, S. Prauzner-Bechcicki, J. Rysz, I. Raptis, Spectroscopic and microscopic characterization of biosensor surfaces with protein/amino-organosilane/silicon structure, *Colloids Surf. B* 90 (2012) 159–168.
- [13] N.H.Z. Ariffin, H. Yahaya, S. Shinano, S. Tanaka, A.M. Hashim, Fabrication of conical micropore structure on silicon nitride/silicon using focused ion beam milling for biosensor application, *Microelectron. Eng.* 133 (2015) 1–5.
- [14] Q. Liu, X. Tu, K.W. Kim, J.S. Kee, Y. Shin, K. Han, Y.-J. Yoon, G.-Q. Lo, M.K. Park, Highly sensitive Mach-Zehnder interferometer biosensor based on silicon nitride slot waveguide, *Sens. Actuators B* 188 (2013) 681–688.
- [15] P.M. Levinea, P. Gong, R. Leviskyb, K.L. Sheparda, Real-time, multiplexed electrochemical DNA detection using an active complementary metal-oxide-semiconductor biosensor array with integrated sensor electronics, *Biosens. Bioelectron.* 24 (2009) 1995–2001.
- [16] J.Y. Kim, K. Choi, D. Moon, J.H. Ahn, T.J. Park, S.Y. Lee, Y.K. Choi, Surface engineering for enhancement of sensitivity in an underlap-FET biosensor by control of wettability, *Biosens. Bioelectron.* 41 (2013) 867–870.
- [17] A. Szwarzja, J. Wei, M.I. Schukfeh, M. Tornowa, Self-assembled monolayers of alkyl-thiols on InAs: a Kelvin probe force microscopy study, *Surf. Sci.* 633 (2015) 53–59.
- [18] F.C. Fernandes, A. Santos, D.C. Martins, M.S. Góes, P.R. Bueno, Comparing label free electrochemical impedimetric and capacitive biosensing architectures, *Biosens. Bioelectron.* 57 (2014) 96–102.
- [19] M.S. Góes, J.J. Davis, P.R. Bueno, Label free redox capacitive biosensing, *Biosens. Bioelectron.* 50 (2013) 437–440.
- [20] J. Lehr, F.C. Bedatty, P.R. Bueno, J.J. Davis, Label-free capacitive diagnostics: exploiting local redox probe state occupancy, *Anal. Chem.* 86 (2014) 2559–2564.
- [21] K. Awsiuk, A. Bernasik, M. Kitsara, A. Budkowski, J. Rysz, J. Haberko, P. Petrou, K. Beltsios, J. Raczowska, Protein coverage on silicon surfaces modified with amino-organic films: a study by AFM and angle-resolved XPS, *Colloids Surf. B* 80 (2010) 63–71.
- [22] D. Caballero, J. Samitier, J. Bausells, A. Errachid, Direct patterning of anti-Human serum albumin antibodies on aldehyde-Terminated silicon nitride surfaces for HSA protein detection, *Small* 5 (13) (2009) 1531–1534.
- [23] C. Jianrong, M. Yuqing, H. Nongyue, W. Xiaohue, L. Sijiao, Nanotechnology and biosensors, *Biotechnol. Adv.* 22 (2004) 505–518.
- [24] W.M. Hassen, L. Angnes, A. Abdelghani, F. Bessueille, D. Leonard, N. Jaffrezic-Renault, Under flow impedimetric measurements using magnetic particles for label-free detection affinity target, *Mater. Scie. Eng. C* 28 (2008) 820–825.
- [25] R. Rawal, S. Chawla, C.S. Pundir, An electrochemical sulfite biosensor based on gold coated magnetic nanoparticles modified gold electrode, *Biosens. Bioelectron.* 31 (2012) 144–150.
- [26] L.G. Zamfir, I. Geana, S. Bourigua, L. Rotariua, C. Bala, A. Errachid, N. Jaffrezic-Renault, Highly sensitive label-free immunosensor for ochratoxin A based on functionalized magnetic nanoparticles and EIS/SPR detection, *Sens. Actuators B* 159 (2011) 178–184.
- [27] D. Caballero, E. Martinez, J. Bausells, A. Errachid, J. Samitier, Impedimetric immunosensor for human serum albumin detection on a direct aldehyde-functionalized silicon nitride surface, *Anal. Chim. Acta* 720 (2012) 43–48.
- [28] K. Biró, L. Solti, I. Barna-Vetró, G. Bagó, R. Glávits, E. Szabó, J. Fink-Gremmels, Tissue distribution of ochratoxin A as determined by HPLC and ELISA and histopathological effects in chickens, *Avian Pathol.* 31 (2) (2010) 141–148.

Biographies

Madiha Bougrini is currently a PhD student in the Institute of Analytical Sciences at the University of Lyon and in the Laboratory of Electronics, Automatic and Biotechnology, University Moulay Ismail, Faculty of Sciences in Meknes, Morocco. Her research interests include sensors networks based electronic noses/tongues for food analysis and the design of electrochemical biosensors.

Abdoulatif Baraket received his B.S. in physics and M.S. in scientific computing in physics and experimental high energy from Hassan 2 University in 2006 and 2008 respectively. He also received a M.S. in physics and nanomaterial from the University of Maine in 2009. He obtained his Ph.D at the Université de Lyon in 2013 and afterwards he was a postdoctoral researcher at the Commissariat à l'énergie atomique (CEA) Grenoble. He is now a postdoctoral researcher in the group of Prof. Abdelhamid Errachid.

Joan Bausells was born in Barcelona, Spain, in 1957. He graduated in physics in 1980, and received M.S. (1982) and Ph.D. (1986) degrees in solid-state physics, all from the University of Barcelona. From 1981 to 1986 he worked as an R&D engineer in the semiconductor industry. In 1986 he joined IMB-CNM, where he is a permanent researcher since 1988 and Research Professor since 2002. At IMB-CNM he was manager of the Sensor and Actuator Group (1990–1995), the Microsystems Department (1999–2002) and the Nanotechnology Group (2002–2006). From 2008 to 2012 he was Deputy Director of IMB-CNM, and Acting Director from January to June 2012. He has published more than 90 papers in international journals, and has contributed more than 220 papers to Conferences. He has participated in 14 projects funded by the EC Framework Programmes in the micro- and nano-systems field, and has coordinated two of them. His current research interests include micro- and nano-electromechanical structures and nanoelectronic devices, and their applications to micro/nano (sensor) systems based on silicon.

Miguel Zabala graduated in telecommunications engineering at the Universitat Politècnica de Catalunya, Barcelona, in 1994. In 1995, he joined the Centro Nacional de Microelectrónica (CNM) where he is currently working. His main area of interest is thermal process engineering for nano-microelectronic technologies and analog circuitry for microsystems.

Nazha El Bari received her PhD degree in 1989 from the University of Nancy (France). She joined the University of Moulay Ismail in 1990, and she was a wanted a Doctor of Sciences degree in 1995 in this university. She has been Professor since 1999, and she created a Biotechnology research group in 2005. Her research interests include quality control of milk and their products.

Benachir Bouchikhi received his PhD degree in 1982 from the University of Aix Marseille (France). He joined the University of Nancy I in the same year, and he award a Doctor of sciences degree in 1988. In 1994, he has been Professor at the Faculty of Sciences of Moulay Ismail University (Morocco), and he created a Sensors, Electronics and Instrumentation Group in 2005. His current major research interests involve electronic nose and characterization of thin film chemical sensors.

Abdelhamid Errachid is a Full Professor in Claude Bernard University-Lyon 1 since the end of 2008. He has been involved as a principal investigator and team leader in several European Projects under 5th, 6th, and 7th Framework Programmes: FP6 (DVT-IMP, MAPTech, Nano2Life, Cell-PROM, ARES, VECTOR, SPOT-NOSED) and FP7 (SensorART, BOND, SEA-on-a-CHIP) as well as NATO, INTAS and TEMPUS International Projects, and Spanish national projects (MICROMENCE, MINAHE I, MINAHE II, and PETRI). Prof. Errachid is a head of the SIMS (Surface-(bio) Interfaces-Micro/nano Systems) group from 2010 to 2014. Papers: 130, Congress: 322, h-index: 219, Patents: 3 (1 PTC), Publications: Books: 8. His current research activity is focused in BioElectronics, Biofunctionalization, and NanoBiotechnology.

Nadia Zine received her B.S. in chemistry from the University M. Ismail, Meknes in 1994 and her Ph.D. from the Centro Nacional de Microelectrónica (CNM) Barcelona in 2005. Currently, she is a lecturer/researcher at the Université Claude Bernard Lyon 1. Her research interests are within chemical characterization of silicon chemical sensors, and specially, of ISFET devices.

III.4

Development of Novel magneto-biosensor for
Sulfaperidine detection.

Summary

At current time, main objective in biomedical diagnosis is to enhance the specificity and sensitivity and to reduce time consumption. One way to solve this problem is to increase the concentration of captured targets like antigen, viruses, bacteria and nucleic acid before detection step. Different magnetic particles, for example, magnetite nanoparticles and polymer matrix micro beads, have been used for the labeling and detection of biomolecules. These can be detected with variety of approaches like liquid nitrogen-cooled SQUIDs Hall cross semiconductor-based electronic devices. It is quite difficult to compare sensitivities of different approaches without taking into account the practical aspects of biosensing, because of differences in magnetic properties and sizes of particles employed. Assay sensitivity combined with detector sensitivity is used to determine the actual sensitivity of a biosensor system based on magnetic particles labeling. Magnetic colloidal particles are mainly used as solid supports for biomolecules in order to enhance the specific capture of the targeted biomolecules. For instance, the individual magnetic nanoparticles were examined in specific capture and isolation of bacteria. In this context, iron oxide nanoparticles were first chemically modified with a specific reactive shell by introducing commonly used functionalized compounds such as carboxylic acid. From last ten years, a great attention has been paid to magnetic latex nanoparticles (MLPs) due their superparamagnetic properties emerging from their nano-size. They have found promising applications in various industrial and particularly biomedical diagnostic domains for example fast separation upon applying even low magnetic field, purification and detection of biomolecules.

Gold working electrodes (WEs) having silicon were cleaned first by rinsing them with ethanol and then completely rinsed with deionized water. They were then dried under stream of nitrogen gently. The device was connected to the potentiostat (VMP3, EC-Lab, France.) Cyclic voltammetry (CV) and electrochemical impedance spectroscopy (EIS) were made. An external reference electrode and counter electrode was applied. CV and EIS measurements were made. For checking the sensitivity of biosensor, magnetic latex particles with carboxylic groups (MLPs-COOH) were immobilized on silicon nitride (Si_3N_4) surface using micro-contact printing (μCP) technique. $\text{Si}_3\text{N}_4/\text{SiO}_2/\text{Si-p}/\text{Al}$ substrate was used as biosensor surface. Briefly, this surface was functionalized with amino-reactive groups by chemical immobilization of the salinizing agent 3-Aminopropyl triethoxysilane (APTES) on the silicon substrate. MLPs with terminated carboxylic acid groups were then covalently bonded to Si_3N_4 via the reaction with amino groups on the SAMs of APTES using EDC activation chemistry. Finally anti-ochratoxin A (amine-containing) antibodies were immobilized on MNPs by covalent bonding through amide bonding.

Electrochemical measurements were carried out using Mott-Schottky analysis for OTA detection. The biosensor was highly sensitive and selective for ochratoxin A antigens, with a limit of detection of 1.845 pg/mL a high sensitivity of 0.027 pg/mL were observed, when compared to other interferences ochratoxin B and aflatoxin G1. The measurements were highly stable and reproducible for detection and interferences. The proposed method was very promising for OTA detection for several agro-food industry applications.

Finally, MLPs were used through application of competitive assay in order to increase sensitivity of biosensor and for detection of sulfapyridine (SPY). This assay was performed

in two ways; one without the use of MLPs and second with MLPs.

Immobilization of the coating antigen (SA2BSA) was done onto separate microelectrodes first. Fixed concentration of antibody (Ab155) with different concentration of antigen (SPY) was performed. In case of high concentration of SPY, all Ab155 were saturated with SPY and there was no response in EIS. However, in case of weak concentration of SPY, the Ab155 was shared with SPY and also SA2BSA which gave weak EIS response. Finally in the absence of SPY, all Ab155 will be detected by SA2BSA and the EIS response was high. The same principle of competition detection was applied again, but this time Ab155 were immobilized onto MLPs which was helpful to increase the sensitivity of the biosensor.

Nyquist plot was performed which showed a stepwise increase of R_{ct} in both cases (without and with MLPs immobilized Ab 155). However, it was clearly observed that there was more linearity with MLPs. This linearity was indicated the increase in sensitivity of biosensor.

Development of Novel magneto-biosensor for Sulfaperidine detection.

Talha Jamshaid ^{a,b}, Abdoullatif Baraket ^a Abdelhamid Elaissari ^b, Abdelhamid Errachid ^{a*}

and Nadia Zine ^a

^aUniversité Claude Bernard Lyon1, UMR 5280, Institut des Sciences Analytiques, 5, rue de la Doua, 69100 Villeurbanne, France

^bUniversité Claude Bernard Lyon1, LAGEP-CPE, 43 Bd. 11 Nov. 1918, F-69622 Villeurbanne, France.

*Corresponding author:

AbdelhamidErrachid

Tel.:+33472431444;fax:+334724489.

E-mail [address:abdelhamid.errachid@univ-lyon1.fr](mailto:abdelhamid.errachid@univ-lyon1.fr)

Abstract:

In this article, we report on the development of a highly sensitive biosensor for SPY detection. In this interest, magnetic latex particles have been used to create 3D architecture to increase sensitivity of biosensor. Microelectrodes, which consist of 4 working electrodes (WEs), a platinum counter microelectrode (CE) and reference electrode (RE) was used in all experiments. The microchip was cleaned and then 4-aminophenylacetic acid 98% (CMA) was electro dressed onto individual gold electrodes. The carboxylic acid functionalization of the diazoted aromatic amine was activated by carbodiimide chemistry and the coating antigen SA2BSA was immobilized onto the transducers surface. First, immobilized fixed concentration of SA2BSA with electrochemical impedance spectroscopy (EIS) with increasing concentrations of Ab 155. Subsequently, the optimized concentration of Ab 155 was analyzed as a competitive assay with different concentrations of sulfapyridine (SPY) and finally with phosphate buffer solution (PBS) using EIS. From data fitting calculation and drawing graph it can be clearly observe that there is more linearity while using magnetic latex particles instead of without use of magnetic nanoparticles, which indicates the increase in sensitivity of biosensor as compared to competitive assay without magnetic latex particles.

Keywords:

Biosensor, Antigen (SA2BSA), Antibody (Ab 155), magnetic latex particles(MLPs), electrochemical impedance spectroscopy (EIS) and cyclic voltammetry (CV).

1. Introduction

Increasing attentions have been paid to antibiotics as aquatic micropollutants with their environmental fate and impact to be understood (**Rosi-Marshall and Kelly, 2015**). Sulfonamide antibiotics (SAs), as one of the most important classes of antibiotics, are widely used in aquaculture, livestock husbandry, and human medicine. Recently, SAs have been detected ubiquitously in the aquatic environment, which may pose risks toward organisms. Among the SAs, sulfapyridine that is commonly used in aquaculture, was frequently detected in various environmental waters (e.g. wastewater effluents and receiving water bodies, as well as fish farms and adjacent water bodies (**Yan et al., 2013**)). For the detection of Sulfapyridine various methods have been used such as chromatographic methods likely high-performance liquid chromatography coupled with mass spectrometric detection (HPLC-MS) have been applied due to their sensitivity and compound quantification data. Sample preparation is required using commercially available cartridges for solid-phase extraction (SPE). Also gas chromatography (GC), thin layer chromatography, GC-MS , LC-MS and radio- active immune receptor for purpose of foodstuffs have been employed (**Pang et al., 2003**). However, the above mentioned techniques require complex sample-preparation procedures, expensive laboratory equipment and skilled professional required to handle these techniques which requires time consuming. Biosensor is a compact analytical device or unit incorporating a biological or biologically derived sensitive element associated with a physicochemical transducer .Recently, magnetic particles have been produced as labels for bio sensing. For the biosensing purpose, different types of biosensors have been produced like giant magnetoresistive (GMR) sensors and spin valves (SV) cantilevers, inductive sensors, superconducting quantum interference devices (SQUIDs), anisotropic magneto resistive (AMR) rings, and miniature Hall crosses. Detection of biological molecule is usually achieved by using bimolecular recognition between the target molecule and a specific receptor as for example antibody that is tagged with a label.

Magnetic latex particles are promising candidates to improve automation avoid time consumption and also enhancing sensitivity of diagnosis by increasing the concentration of the captured targets (**Jamshaid et al., 2014**)

In this work, we present the magneto-biosensor for Sulfapyridine detection by optimization fixed concentration of coating antigen SA2BSA and Ab 155 by application of competitive assay that is with magnetic latex particles and without these particles. Simple representation is shown in figure1.



(a)

(b)

Fig 1. (a) No increase in sensitivity of biosensor (b) while there is increase in sensitivity with Magnetic latex particles combined with antibody Ab 155 (MLP-Ab 155).

2. Materials and Methods

All chemicals were purchased from Sigma-Aldrich, France apart from 4-aminophenylacetic acid 98% which was purchased from *Acros Organics*, France, sodium nitrite from *Fisher Scientific*, France, phosphate buffer saline tablet from Sigma, Ethanolamine from *Fluka analytical* and hydrochloric acid 37% from *VWR*, France.

Cotig antigen (SA2BSA), antibody (Ab155), sulfapyridine were supplied from *R&D system*. Magnetic particles with functionality of carboxylic groups were produced in *LAGEP laboratory under university Lyon1*, France.

2.1. Cleaning of chips and microelectrodes

Gold WEs based on silicon substrate were cleaned by rinsing them with ethanol for 5 minutes and then properly rinsed with deionized water. They were then dried under steam of nitrogen. The surface WEs was then cleaned from organic contaminants by using UV/O₃ (UV/ Ozone Pro Cleaner TM, Bio Force Nano sciences) for 30 minutes. The device was connected afterward to the potentiostat (VMP3, EC-Lab, France). Analysis was then monitored and modeled using the EC-Lab software. Cyclic voltammetry (CV) and electrochemical impedance spectroscopy (EIS) were applied to characterize the surface of WEs before and after bio functionalization, using K₃[Fe(CN)₆]/K₄[Fe(CN)₆] (5 mM) as electrolyte in phosphate buffered saline (PBS, pH 7.4). CV measurements were made at potential of 0.5 V to -0.3 V, scan rate at 80mV/s and minimum 3 cycles taken. EIS measurements were made at potential of 0.228 V, frequency at 200 kHz to 200 mHz and sinus amplitude of 25 mV.

2.2. Deposition of 4-aminophenylacetic acid (CMA)

electrochemical deposition of 4-aminophenylacetic acid 98% (CMA) was made by using 5 mM of CMA in water with 15 mM of sodium nitrite and 15 mM of hydrochloridric acid. Both sodium nitrite and hydrochloride solutions were added to solution of CMA solution and kept in ice bath for 15 minutes. This is a modification of the electrode preparation reported by (Allongue et al., 1997). The final solution was kept at 0°C and immediately used. Figure 2 shows a schematic illustration of CMA deposition onto gold WEs.

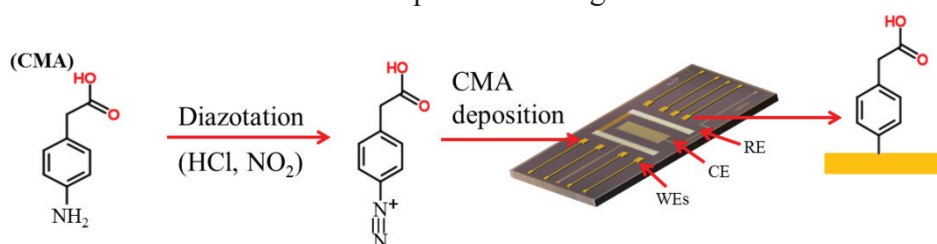


Fig 2. Schematic illustration of CMA deposition onto gold WEs.

The reductive adsorption of the salt onto the electrode was achieved by four repetitive scans of CV between 0.3 and -1.0 V at 200 mV/s. The initial cycle in Figure 3(i) shows a broad and irreversible cathodic wave with a peak potential at -0.9 V that indicates diazotised CMA attachment onto the gold surface by diazonium salt reduction. The cathodic current was remarkably weakened in the successive scans. These were attributed to the large passivation

area of the microelectrode. Here, the results were confirmed by CV with before and after gold WEs modification **Figure 3(ii a)**. Here, an important decrease in peak-to-peak of the CV cycle was seen when compared to the bare gold microelectrodes **Figure 3(ii b)**.

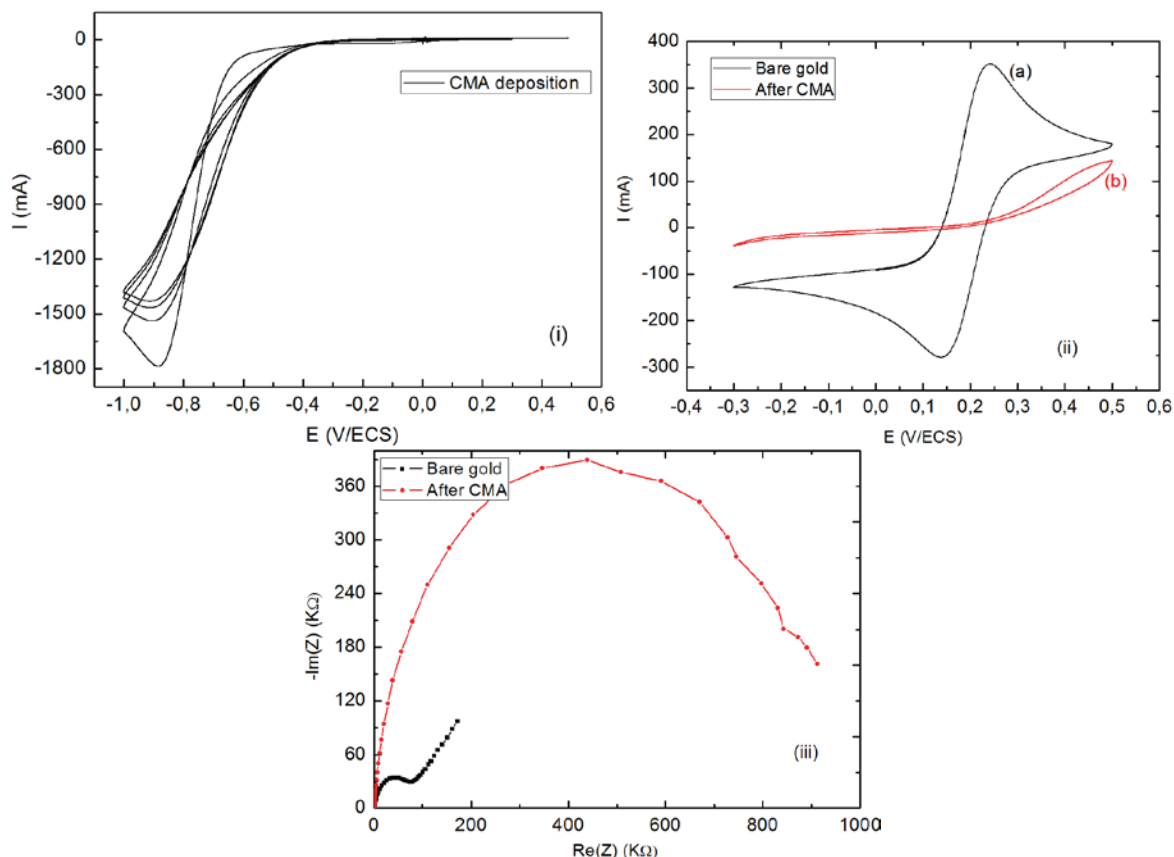


Fig 3. (i) CV for electro deposition of CMA. Four repetitive potential cycles from 0.3 V to -1 V with a scan rate of 0.2 V/s were applied in 5mM of CMA with 15mM of HCl and 15mM of NaNO_2 . (ii) A CV scan for: (a) bare gold WEs and (b) CMA immobilized onto the WEs and (iii) EIS analysis of bare gold and CMA modified WEs.

These results were confirmed by EIS analysis before and after CMA deposition **Figure 3 (iii)**. Therefore, the first semi-circle of Nyquist plot image correspond to impedance of gold WEs which is too weak when compared to CMA modified WEs. This was related to the passivation of WEs with CMA layer which increase the transfert charge resistance (R_{tc}) between the modified WEs and the electrolyte solution.

2.3. Carboxylic group activation

A solution of N-(3-Dimethylaminopropyl)-N ethylcarbomide hydrochloride (EDC) of 0.4 M and N-Hydroxysuccinimide (NHS) of 0.1 M respectively was made up in 1ml of anhydrous ethanol and the device was incubated in a 2 mL eppendorf for 1hr at room temperature. After this time, the device was rinsed with 0.1M HCl and dried with nitrogen stream carefully. Immediately, the CMA modified WEs were incubated in 60 μL of SA2BSA antigens at 100 $\mu\text{g}/\text{mL}$ for 1hour at room temperature. Then, the microelectrodes were rinsed with PBS and incubated in 0.1% solution of ethanolamine (ETA) in PBS for 20 m in at room temperature. This deactivates all remaining carboxylic activated sites. This step is very necessary in order to prevent no-specific binding. At this stage the Biosensors is ready for antibodies detection.

2.4. Detection of antibodies Ab155.

Electrochemical impedance spectroscopy (EIS) was made for the coating antigens SA2BSA (Figure 4). Here the first semi-circle of Nyquist plot correspond the coating antigens without any detection. Afterword, the biosensors was rinsed with PBS and incubated in 60 μ L of antibodies Ab155 at 1 μ g/mL for 30 min, then rinsed with PBS and analyzed with EIS. The second Nyquist plot semi-circle was shifted from the first showing thus an increase of the transfer charge resistance (R_{tc}). The shift between Nyquist plot semi-circles continue to increase by increasing the concentration of antibodies Ab155.

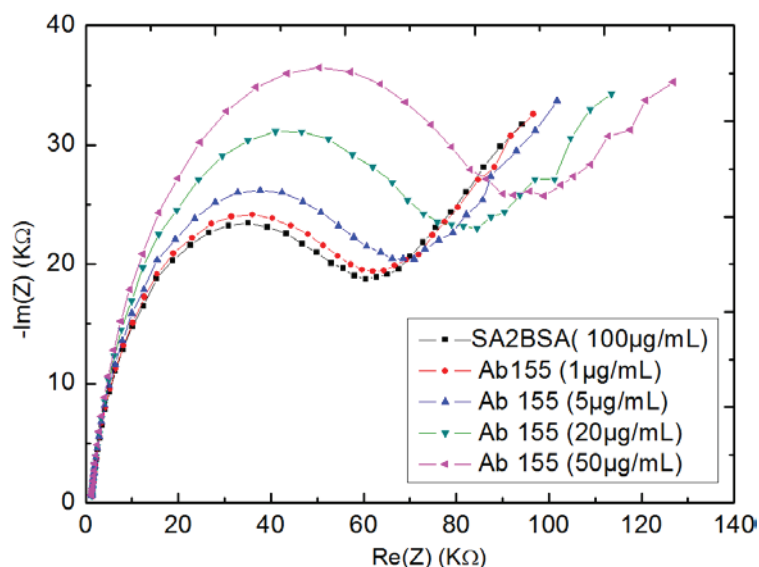


Fig. 4. EIS measurements of different concentratons of Ab 155 (1, 5, 20 and 50 μ g/mL respectively) with fixed concentration of SA2BSA.

2.5 Competitive assay with SPY

After showing the interactivity of the coating antigens with different concentrations of Ab155 antibodies, the same principle of EIS detection will be applied in this section by using Ab155 antibodies with another antigen sulfapyridine (SPY) which is also specific to Ab155 antibodies. Here a mixture of 20 μ L of fixed concentration of Ab155 antibodies (50 μ g/ml) was added to 20 μ L of different concentrations of SPY 40 μ M, 4 μ M, 2nM and finally 0M (only PBS) respectively. For each concentration the two solutions (20 μ L of Ab 155 and 20 μ L of SPY) were then allowed to incubate the SA2BSA modified biosensor for 30 min and kept at 4°C. After each incubation, the surface of microelectrodes was rinsed with PBS and analyzed by EIS measurements. Here there will be a competition between SPY and SA2BSA to detect Ab155 antibodies.

Figure 5 shows the Nyquist plot image for all SPY concentrations. The first and second semi-circles correspond to the bare gold and the the coating antigens SA2BSA respectively. After the first incubation of the biosensor within 40 μ L of (Ab155 and 40 μ M of SPY), the third Nyquist plot semi-circle has shifted showing a detection of SA2BSA by Ab155 antibodies. Here the concentration of SPY is too high which means a big amount of Ab155 has been reacted with SPY and the rest was attached to the coating antigens SA2BSA. By decreasing the concentration of SPY, there more antibodies Ab155 free in the solution of incubation which react with SA2BSA. This was confirmed by the increase of Nyquist plot semi-circles. Finally, when the biosensor was incubated only in Ab155 antibodies with PBS, the totality of the antibodies has reacted with the coating antigen thus giving big shift between Nyquist plot semi-circles.

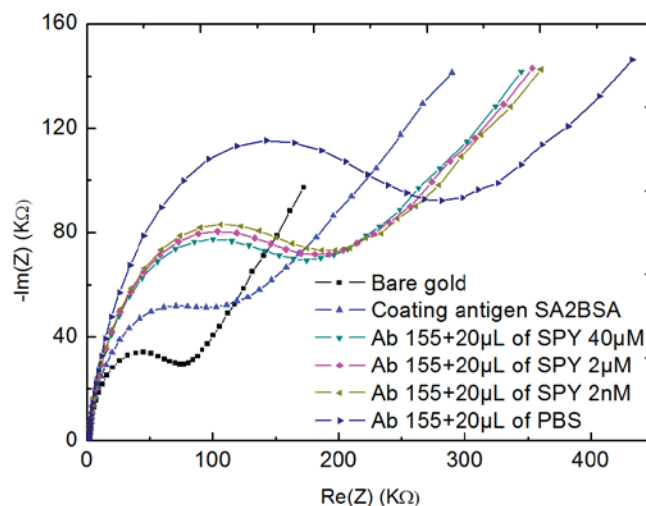


Fig.5. EIS measurements of Ab 155 with different concentrations of SPY (40µM, 4µM, 2nM) and PBSS only

2.6 Biofunctionalization of magnetic latex particles

In order to increase the sensitivity of the biosensor, the antibodies Ab155 has been immobilized onto spherical magnetic nanoparticles with carboxylic acid function. These magnetic latex particles have been fabricated by (Jamshaid et al., 2015). MLPs were firstly washed with PBS in order to maintain pH of medium constant and also for an optimal binding capacity. Therefore, a vial of 1mL of MLPs was placed in a magnetic rack to immobilize the MLPs and to remove the support solution. Afterward, the magnetic rack was removed and 1mL of PBS was added in order to wash MLPs. This operation was repeated three times to insure that all surfactants were removed.

The carboxylic acid function was activated by adding MLPs in solution of NHS 100mM and EDC 100mM during 90 minutes with stirring continuously at 500 rpm and at room temperature. MNP were washed then 3 times to remove EDC/NHS by using magnetic rack with cold HCl 1mM in order to keep the activity of carboxylic acid. Immediately a 500 µL of a purified antibody Ab155 (100µg/ml in PBS10mM) was added to the activated MLPs with stirring continuously at 500 rpm and at room temperature during 2-3 hours. Finally the vial of Ab155 modified MLPs was washed with PBS for three times using the magnetic rack and stored in PBS at 4°C.

2.7 Immobilization of Ab 155 with magnetic latex particles and competitive assay with SPY

Firstly, the immobilization of the coating antigen with 100 µg/mL solution of SA2BSA was made onto WEs surface as explained previously. Afterward, the Ab155 modified MLPs with fixed quantity of 20µL are mixed with different concentrations of SPY that is 40 µM, 4 µM, 2nM and finally only with PBS respectively. Here the same principle of competitive detection between SPY and SA2BSA was applied (Figure 6). Always by decreasing the concentration of SPY the shifted between Nyquist plot semi-circle increase. Here the shift is more important for the concentrations 40µM, 2µM and 2nM when compared to the competitive detection without MLPs. This was due to the high amount of antibodies present onto the MLPs surface.

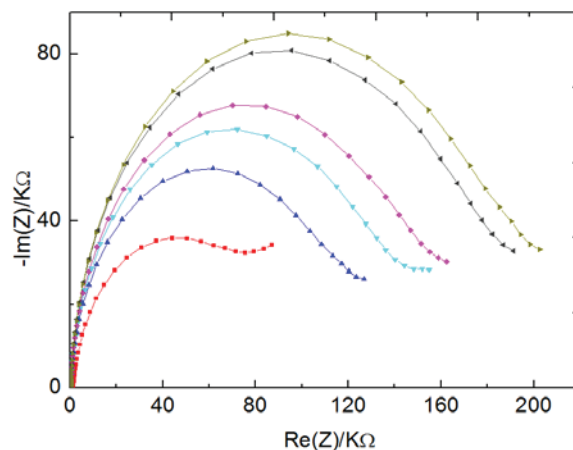


Fig.6. EIS measurements of fixed concentration of magnetic latex particles (20 μ L) with Ab 155 (60 μ L) against different concentrations of SPY (40 μ M, 4 μ M, 2nM) and PBS only Bare gold (■) SA2BSA (▲) MLPs-Ab 155+40 μ M Spy ▼ MLPs-Ab155+ 4 μ M SPy ◆ MLPs-Ab 155+2nM ◀ MLPs-Ab 155+Only PBS(▶)

Nyquist plots were fitted for both figures 5 and 6 concerning the detection of Ab155 with and without MLPs by using the equivalent circuit in figure 7 (i) (inset) (Baraket et al., 2013). Here R_1 indicates electrolyte solution resistance; Q_2 is the constant phase element which corresponds to the charge distribution at the interface electrode/electrolyte. This latter is in parallel with R_2 which the resistance of charge transfers. Finally W corresponds to Warburg resistance which is related to the diffusion phenomenon at the interface electrode/electrolyte.

After calculating fitting parameters from the applied equivalent circuit it is observe that there is more linearity for biosensor with ab155 modified MLPs (Figure 7 (ii)) when compared to competitive detection without magnetic nanoparticles (Figure 7 (i)). This is very important to increase the sensitivity of the biosensor and to understand the behavior of the interaction of Ab155 antibodies in the presence of SA2BSA and SPY in the same time. When response of the biosensor is too weak this means that there is an important concentration of SPY that has saturated all the antibodies Ab155. We are in the case of sample contaminated with SPY. On the other hand, if the response of the biosensor is too high, this means that all the antibodies are collected with the coating antigens SA2BSA. We are in the presence of sample without contamination or it contains a weak amount of SPY.

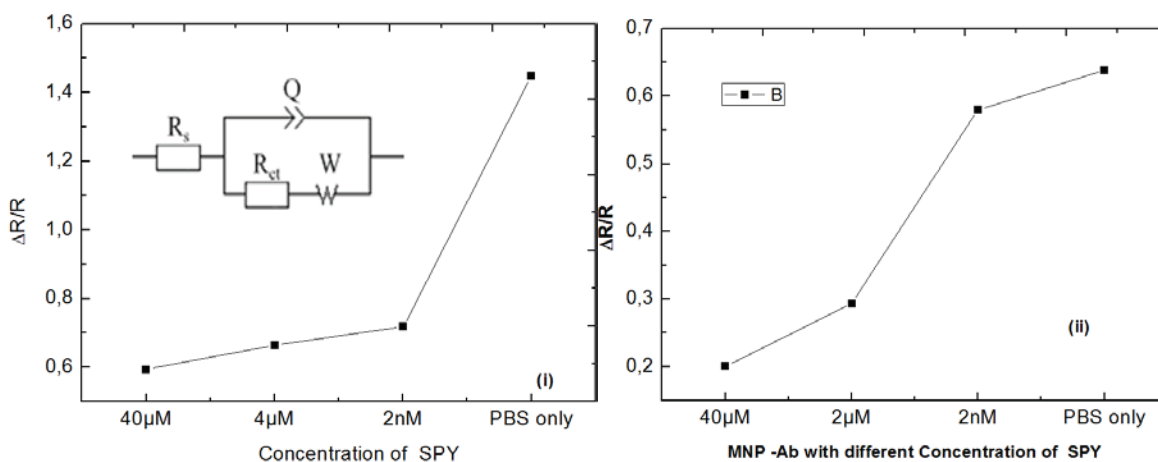


Fig .7. (i) Graphical representation of fixed concentration of SA2BSA and Ab155 without magnetic particles, (ii) Graphical representation of fixed concentration of SA2BSA and Ab155 with magnetic particle

3. Results and discussion

After the cleaning procedure of microelectrodes, the devices were connected to a potentiostat and electrochemical properties were measured. Fig. 3 (ii a) the bare gold microelectrode shows characteristic CV peak currents for the redox reaction with ferri /Ferro cyanide solution. After diazotation, of CMA onto the gold microelectrode surface, the peak currents decreased fig 3 (ii b) because of blocking behaviour of the CMA on the modified gold microelectrode (**Baraket et al., 2013**) which indicates the functionalization of the gold surface with a self-assembled monolayer (SAM) of CMA. For EIS measurements bare gold Fig.3 (iii) charge transfer resistance (R_{ct}) was measure at 68.031 k Ω , however after CMA electrodepositing, the R_{ct} increased to 901.185k Ω which clearly indicates that the gold microelectrode surface was functionalized with CMA.

After the immobilization of the SA2BSA, there was decreased in R_{ct} through carbodiimide cross-linker at 56.048 k Ω which indicates that the coating antigen was successfully hitch on the surface figure 4, also shows Nyquist plots for the detection of Ab155 with increasing concentrations against the immobilized coating antigen (SA2BSA) at 100 μ g/mL. After measuring EIS the results indicate the detection of the antibody was made against fixed concentration of coating antigen SA2BSA. From Nyquist plot it can be observed that there is stepwise increasing R_{ct} of Ab 155 which clearly represents the strongly biorecognition of the Ab-Ag complex.

The Nyquist plot figure 5 and 6 respectively shows a stepwise increase of the R_{ct} which represents that the biosensor was sensitive for the competitive assay measurements. However, after calculating fitting parameters from the applied equivalent circuit for detection of SPY by using fixed concentration of SA2BSA and Ab155 without and with magnetic particles in figure 7 (i and ii respectively) that there is more linearity while using magnetic latex particles which increase the sensitivity of biosensor as compared to competitive detection without magnetic latex particles.

4. Conclusion

In this article, we reported the sensitivity of the biosensor by using the application of competitive assay by immobilized fixed concentration of SA2BSA (100 μ g/mL) and fixed concentration of Ab 155 (50 μ g/mL) against different concentrations of SPY like 40 μ M, 4 μ M, 2nM and finally only with PBS respectively, with and without use of magnetic nano particles. Using CV and EIS the microelectrodes were characterized for the bare gold, surface functionalization with CMA, immobilized SA2BSA and fixed concentration of magnetic nanoparticles that contain immobilized Ab155 with different concentration of SPY.

The Nyquist plot showed a stepwise increase of R_{ct} in both cases (Ab 155 without and magnetic particles that contain immobilized Ab 155 with different concentration of SPY). However, after calculations from fitting parameters and drawing graph, it can be clearly observe that there is more linearity while using magnetic nanoparticles instead of without use of magnetic nanoparticles, which indicates the increase in sensitivity of biosensor as compared to competitive assay without magnetic nanoparticles Thus, reported the

development of a highly sensitive biosensor for SPY detection using competitive assay, so in this interest magnetic nanoparticles have been used to create 3D architecture to increase sensitivity of biosensor.

Acknowledgements:

The authors acknowledge the financial support from the projects NATO (CBP.NUKR.SFP 984173) and European Communities Seventh Framework Programmes: SensorART-IP (FP7/2007-2013) under the grant agreement No. 248763 and SEA-on-a-CHIP (FP7-OCEAN-2013) under the grant agreement No.614168 and funding from the European Union's Horizon 2020 research and innovation programme entitled HEARTEN under grant agreement No 643694". T.J. is grateful to university of Lahore, Lahore, Pakistan for funding.

References

- Allongue, P., Delamar, M., Desbat, B., Fagebaume, O., Hitmi, R., Pinson, J., Savéant, J.-M., 1997. Covalent Modification of Carbon Surfaces by Aryl Radicals Generated from the Electrochemical Reduction of Diazonium Salts. *J. Am. Chem. Soc.* 119, 201–207. doi:10.1021/ja963354s
- Baraket, A., Lee, M., Zine, N., Sigaud, M., Yaakoubi, N., Trivella, M.G., Zabala, M., Bausells, J., Jaffrezic-Renault, N., Errachid, A., 2013. Diazonium modified gold microelectrodes onto polyimide substrates for impedimetric cytokine detection with an integrated Ag/AgCl reference electrode. *Sens. Actuators B Chem., Selected Papers from the 26th European Conference on Solid-State Transducers* 189, 165–172. doi:10.1016/j.snb.2013.02.088
- Jamshaid, T., Eissa, M., Zine, N., El-Salhi, A.E., Ahmad, N.M., Elaissari, A., 2014. CHAPTER 9 Soft Hybrid Nanoparticles: from Preparation to Biomedical Applications, in: *Soft Nanoparticles for Biomedical Applications*.
- Jamshaid, T., Tenório-Neto, E.T., Eissa, M., Zine, N., El-Salhi, A.E., Kunita, M.H., Elaissari, A., 2015. Preparation and characterization of submicron hybrid magnetic latex particles. *Polym. Adv. Technol.* 26, 1102–1108. doi:10.1002/pat.3541
- Pang, G.-F., Cao, Y.-Z., Fan, C.-L., Zhang, J.-J., Li, X.-M., Li, Z.-Y., Jia, G.-Q., 2003. Liquid chromatography-fluorescence detection for simultaneous analysis of sulfonamide residues in honey. *Anal. Bioanal. Chem.* 376, 534–541. doi:10.1007/s00216-003-1883-4
- Rosi-Marshall, E.J., Kelly, J.J., 2015. Antibiotic Stewardship Should Consider Environmental Fate of Antibiotics. *Environ. Sci. Technol.* 49, 5257–5258. doi:10.1021/acs.est.5b01519
- Yan, C., Yang, Y., Zhou, J., Liu, M., Nie, M., Shi, H., Gu, L., 2013. Antibiotics in the surface water of the Yangtze Estuary: Occurrence, distribution and risk assessment. *Environ. Pollut.* 175, 22–29. doi:10.1016/j.envpol.2012.12.008

IV
DISCUSSION, CONCLUSION

Discussion and Conclusion

Various types of nanoparticles were employed for their potential applications in biomedical field, yet most interesting of them was hybrid particles having both the magnetic properties and the ability to functionalize with important drug moieties and biomolecules. Among the key features of such functional colloidal particles were their soft hybrid core-shell structures, which were engineered in such a way that the core consists of an inorganic material whereas the shell is composed of a soft organic substance.

Magnetic nanoparticles (magnetite and maghemite) and their polymer dispersion (magnetic latexes) were used in various applications. In addition to their biocompatibility (low toxicity) and their superparamagnetic properties which make them easily affected even by low magnetic field, their high specific area was important for immobilization of large amount of biomolecules. Furthermore, the narrow size distribution allows a homogeneous particle behavior. Additionally, the magnetic content was high enough to obtain magnetic latex nanoparticles with high saturation magnetization which was critical criterion for their application in fast magnetic separation and to avoid contact with biomolecules and alteration of their biological properties.

The (o/w) magnetic emulsion was first prepared in two steps: first iron oxide nanoparticles were prepared in water phase via coprecipitation method by using ferrous chloride (FeCl_2) and ferric chloride (FeCl_3) solutions in concentrated ammonia medium. Then the prepared magnetic nanoparticles were chemically modified using oleic acid in order to prevent their aggregation, to maintain their particles size and to be easily compatible with organic solvent (i.e. Octane) forming organic ferrofluid. The second step consists of high shear emulsification of the prepared organic ferrofluid in water phase containing a high concentration of the anionic surfactant SDS. The obtained stable o/w magnetic emulsion was then purified by removing free surfactants before magnetic particles sorting through consecutive magnetic separations.

The prepared (home-made) oil-in-water (o/w) magnetic emulsion was (used as seed) successfully transformed to submicron magnetic polymer latex particles using seed emulsion polymerization technique. The final physico-chemical properties of magnetic latex particles (MLPs) was controlled during their preparation by adjusting various factors such as (i) type of monomer, (ii) type of initiator, (iii) surfactant, (iv) polymerization time, (v) monomers/seed ratio, and (vi) amount of octane in the magnetic-seed emulsion.

The emulsion polymerization of styrene (St) and divinylbenzene (DVB) with different ratios in the presence of (o/w) magnetic emulsion and potassium persulfate (KPS) initiator conferred three distinct morphologies (a) Janus, (0% St :100% DVB) (b) Moon like Janus (10% St:90%DVB) and (c) desired core-shell. The desired core-shell morphology was obtained by the use of St and DVB at the ratio (60/40, v/v %).

After optimization of the reaction conditions at this monomers ratio, the same seed emulsion polymerization method was performed, but in presence of carboxylic acid initiator 4,4-azobiscyanopentonic acid (ACPA) leading to the formation of core-shell magnetic latex particles with magnetic core and carboxylic group functionality on polymer shell. The obtained submicron (275 nm) magnetic latex particles possessed superparamagnetic properties with narrow size distribution, and high magnetic content (58 wt %).

In order to point out surface modification after encapsulation zeta potential was examined as a function of pH. Zeta potential values of the prepared magnetic latex particles were significantly increased by increasing the pH of the medium, due to the possible presence of carboxylic groups originated from oleic acid used in the preparation of organic ferrofluid. The presence of these

carboxylic groups is mainly due to the diffusion of oleic acid chain during the swelling process and polymerization step and also ACPA as an initiator moreover because of MAA. The influence of methacrylic acid (MAA) was also observed on the prepared magnetic latex particles. For this purpose, various polymerizations experiments were performed with different volumes of MAA. Polymerizations experiments were conducted using ACPA as an initiator, SDS as surfactant, and the magnetic emulsion as seed. The used magnetic emulsion contains a negligible amount of octane, which was found to be below 10mg of octane/g of dried emulsion.

After experiments, it was observed that the MAA helpful to enhance the carboxylic acid groups on the surface of magnetic latex particles. TEM and particle size measurements clearly indicated the enhancement of carboxylic groups on the surface of magnetic latex particles as indicated from the increase in size from 275 nm to 496 nm at maximum concentration of MAA. Moreover, these reactive magnetic particles could be easily immobilized on solid surfaces in order to be suitable for biosensor applications.

For checking the sensitivity of biosensor, magnetic latex particles with carboxylic groups (MLPs-COOH) were immobilized on silicon nitride (Si_3N_4) surface using micro-contact printing (μCP) technique. $\text{Si}_3\text{N}_4/\text{SiO}_2/\text{Si-p}/\text{Al}$ substrate was used as biosensor surface. Briefly, this surface was functionalized with amino-reactive groups by chemical immobilization of the silanizing agent 3-Aminopropyl triethoxysilane (APTES) on the silicon substrate. MLPs with terminated carboxylic acid groups were then covalently bonded to Si_3N_4 via the reaction with amino groups on the SAMs of APTES using EDC activation chemistry. Finally anti-ochratoxin A (amine-containing) antibodies were immobilized on MNPs by covalent bonding through amide bonding.

Electrochemical measurements were carried out using Mott-Schottky analysis for OTA detection. The biosensor was highly sensitive and selective for ochratoxin A antigens, with a limit of detection of 1.845 pg/mL a high sensitivity of 0.027 pg/mL were observed, when compared to other interferences ochratoxin B and aflatoxin G1. The measurements were highly stable and reproducible for detection and interferences. The proposed method was very promising for OTA detection for several agro-food industry applications.

Finally, MLPs were used through application of competitive assay in order to increase sensitivity of biosensor and for detection of sulphapyridine (SPY). This assay was performed in two ways; one without the use of MLPs and second with MLPs.

Immobilization of the coating antigen (SA2BSA) was done onto separate microelectrodes first. Fixed concentration of antibody (Ab155) with different concentration of antigen (SPY) was performed. In case of high concentration of SPY, all Ab155 were saturated with SPY and there was no response in EIS. However, in case of weak concentration of SPY, the Ab155 was shared with SPY and also SA2BSA which gave weak EIS response. Finally in the absence of SPY, all Ab155 will be detected by SA2BSA and the EIS response was high. The same principle of competition detection was applied again, but this time Ab155 were immobilized onto MLPs which was helpful to increase the sensitivity of the biosensor.

Nyquist plot was performed which showed a stepwise increase of R_{ct} in both cases (without and with MLPs immobilized Ab155). However, it was clearly observed that there was more linearity with MLPs. This linearity was indicated the increase in sensitivity of biosensor.

V
Perspectives

Perspectives

Desired morphology with perfect core-shell having sulfate and carboxylic functionality on the surface of particles were obtained by using oil in water (o/w) magnetic emulsion. However, by using this emulsion as seed, in future further functionalization will be possible with different functional groups like amine, aldehyde, ester, epoxy.

Tremendous interest for preparation of magnetic nanocomposites has been observed due to their potential applications in various biomedical and microelectronics (e.g. biosensors) areas. Recent developments in both inorganic nanoparticles and polymer chemistry provide extensive techniques to prepare novel hybrid materials that can find wide applications in these areas.

Multifunctional latex particles are highly needed, which combine not only magnetic, but also photonic properties, etc. Regarding to *in vitro* diagnosis, nowadays, various applications need to combine various aspects, such as sample preparation consisting of specific biomolecules extraction, purification and then local concentration in well-designed microfluidic system for analysis on sophisticated biosensors. Such new technologies need the use of well-defined magnetic particles in order to avoid *in vitro* aggregation in the microfluidic systems. The encapsulation of iron oxide is well recommended in order to avoid the release of iron oxide nanoparticles or ferric and ferrous salts which may affect the sensitivity of the molecular diagnosis. In addition, such particles should have high capture efficiency and also good release of adsorbed or specifically capture biomolecules in order to enhance the diagnostic efficiency after pre-concentration step.

These magnetic latex particles (MLPs) can be used in specific RNA extraction evaluation using automated and microsystems. Because of ability of covalent bonding, these particles will chemically graft for well-defined antibody. Furthermore, these particles can be used to create photonic crystals in a photocurable resin, with optical properties that can be handled with external magnetic field. Heterodimer or core-shell type magnetic latex particles will use in not only combining the properties of their single constituents but also enhance material properties.

MLPs can be used to express their activities in a desired process (e.g. immobilized enzymes), or as affinity ligands to capture or to modify the target molecules or cells (e.g. antibodies or their fragments, streptavidin, lectins, oligonucleotides, aptamers, oligo- and polysaccharides, metal chelate binding groups, etc.). MLPs with immobilized antibodies form the basis of immunomagnetic procedures, especially used in microbiology and cell biology for selective capture of target cells. MLPs can be used by activation of 3-aminopropyltriethoxysilane for the immobilization of various enzymes, antibodies and protein A after glutaraldehyde treatment. Extremely inexpensive magnetic microparticles for large scale biotechnology applications (E.g. separation of biologically active compounds from agricultural wastes or removal of

xenobiotics from waste water) are necessary. In vivo and analytical applications require specific MLPs covered by appropriate biocompatible molecules in a precisely predefined way (quantity, orientation, geometric arrangement). Introduction of a biotin molecule at the oligonucleotide will use in combination with MLPs coated with streptavidin.

In future, MLPs will be used in different process steps of a lab-on-a-chip diagnostic assay. Actuated by applied magnetic fields, these particles can be used in to mix fluids, to selectively capture specific analytes, to transfer analytes to another fluid, to label particles for detection, to form clusters for detection, to induce surface binding for detection, and to apply stringency forces in order to improve the signal-to-noise ratio. MLPs will use as a fundamental tools for studying in development of miniaturized biosensing systems and allow a range of unique stationary-fluidic system concepts.

PART VI
Publication

1. Talha Jamshaid, Mohamed Eissa, Nadia Zine, Abdelhamid Errachid El-Salhi, Nasir Ahmad and Abdelhamid Elaissari Chapter 9: Soft Hybrid Nanoparticles for Biomedical applications in **Royal Society of Chemistry (RSC)** 2014.
2. Bitar Ahmad, Kaewsaneha, Chariya, Eissa, Mohamed M., Jamshaid, Talha, Tangboriboonrat Pramuan, Polpanich, Duangporn, Elaissari, Abdelhamid From Preparation to Biomedical Applications in **Journal of Colloidal Science and Biotechnology (JCSB)** 2014.
3. Ernandes Taveira Tenorio-Neto, Talha Jamshaid, Mohamed Eissa, Marcos Hiroiuqui Kunita, Nadia Zine, Géraldine Agusti, Hatem Fessi, Abdelhamid Errachid, Abdelhamid Elaissari TGA & Magnetization Measurements for Specific Characterization of Magnetic Hybrid Particles in **Polymer for Advanced Technologies. (PAT)** 2015.
4. Talha Jamshaid Ernandes Taveira Tenório Neto, Mohamed M. Eissa Nadia Zine, Marcos Hiroiuqui Kunita Abdelhamid Errachid El-Salhi, Abdelhami Elaissari Biomedical applications of magnetic particles in microfluidic and microsystems in **Trends in Analytical Chemistry (TrAC)** 2015.
5. Talha Jamshaid, Ernandes Taveira Tenorio-Neto, Mohamed Eissa, Nadia Zine, Abdelhamid Errachid, Marcos Hiroiuqui Kunita, Abdelhamid Elaissari, Preparation and characterization of submicron hybrid magnetic latex particles in **Polymer for Advanced Technologies. (PAT)** 2015.
6. Madiha Bougrini, Abdoullatif Baraket, Talha Jamshaid, Abdelhamid Elaissari, Joan Bausells, Nezha El Bari, Benachir Bouchikhi, Nicole Jaffrezic-Renault, Abdelhamid Errachid and Nadia Zine Development of a novel capacitance electrochemical biosensor based on silicon nitride for Ochratoxin A detection: food analysis in **Sensors and Actuators and Actuator B: Chemicals** . 2016
7. Talha Jamshaid, Abdoullatif Baraket, Abdelhamid Elaissari, Abdelhamid Errachid and Nadia Zine Development of Novel magneto-biosensor for Sulfaperidine detection ready to submit in **Biosensor and bioelectronics. 2016 (Accepted)**
8. Talha Jamshaid, Mohamed M. Eissa, Nadia Zine, Abdelhamid Errachid El-Salhi, Abdelhamid Elaissari Elaboration of Carboxylic magnetic Latex Particles and effect of Methacrylic Acid on prepared latex particles **(In progress)**